To the Graduate Council:

I am submitting herewith a thesis written by Thomas Frank Zondlo entitled "Identification of Subaqueous Groundwater Discharge to Large Scale Surface Water Bodies, East Tennessee Technology Park Site, DOE Oak Ridge Reservation, Oak Ridge, Tennessee". I have examined the final copy of this thesis for form and content and recommend it be accepted in partial fulfillment of the requirements for the degree of Master of Science, with a major in Geology.

Larry D. McKay, Major Professsor

We have read this thesis and recommend its acceptance:

Accepted for the Council:

Associate Vice Chancellor and
Dean of the Graduate School

Identification of Subaqueous Groundwater Discharge to Large Scale Surface Water Bodies, East Tennessee Technology Park Site, DOE Oak Ridge Reservation, Oak Ridge, Tennessee

A Thesis
Presented for the
Master of Science Degree
The University of Tennessee, Knoxville

Thomas Frank Zondlo
May 1998

ACKNOWLEDGMENTS

I am grateful to the following individuals who have provided considerable support in conducting the field effort: Dennis Crumby, Clell Ford, Rick Goeltz, Chris Lane, Dan Levine, Scott Martin, and the late Tom Stephens. Many thanks to the seaworthy crew of the SSS *Springseeker*.

I am also grateful for the financial support of this research, provided by the Lockheed-Martin Energy Systems Environmental Restoration Program and the Department of Energy who ultimately funded this work. I'd also like to extend my appreciation to my advisor, Dr. Larry McKay, and to Dr. Claudia Mora and Dr. James Smoot for serving on my thesis committee.

Finally, I am most grateful to my wife Kathy and son Zachary for their patience and continual support of my effort at completing this milestone.

ABSTRACT

In East Tennessee, the Tennessee River and its tributaries cut across many of the sub-parallel strike valleys in the Valley and Ridge several times, including the karstic carbonate strike belts within them. The construction of dams along the Tennessee River and it's tributaries, including the Clinch River, has increased the river stage between 5 and 20 m, which caused inundation of considerable areas. This also raised the baselevel for drainage, thus altering the groundwater regime within the valleys intersected by these rivers. The study area addressed in this research includes an industrial facility situated on karstic carbonate bedrock which is bounded by a Tennessee Valley Authority-controlled run-of-the-river surface impoundment, the Clinch River, and Poplar Creek, a large first order tributary to that impoundment. Surface water flow and stage conditions in these water bodies are dictated by reservoir operations at upstream and downstream dams. Surface water stage plays a major role in regulating overall groundwater flow from the facility.

Typically, the master surface water drains represent baselevel for groundwater discharge and it was expected that large springs, reflecting the karstic nature of the bedrock underlying the site, would occur along these surface water bodies. However, a comprehensive inventory of springs and seeps within the study area identified only a few small seeps near the impoundment, most of which are transient in nature. Consequently, it was expected that much of the groundwater discharges to surface water via subaqueous springs possibly related to pre-impoundment baselevel conditions. Remote methods such as infrared thermography were attempted in order to locate potential zones of subaqueous groundwater discharge but proved unsuccessful.

This study documents an attempt to identify direct subaqueous discharge of groundwater to a flowing surface water body on the basis of inherent differences in temperature and specific conductance between groundwater and the receiving surface

water. This approach was applied to a study area which includes the East Tennessee Technology Park (ETTP) located within the Department of Energy Oak Ridge Reservation in east Tennessee. The site is bounded by the Clinch River, a run-of-the-river impoundment and Poplar Creek, a large first order tributary to that impoundment. The geology at this site is highly complex, reflecting structural and stratigraphic controls on groundwater flow, all of which have been overprinted by karst dissolutional processes and the effects of reservoir impoundment and operation.

In this effort, a multi-parameter probe was suspended below a small boat and trolled along the bottom of a run-of-the-river impoundment in water depths ranging from ~1 to 16 m. Temperature, specific conductance, dissolved oxygen, head, bathymetry, and boat/probe position were continuously recorded along multiple survey runs oriented roughly parallel to shoreline at 1-10 m spacings. Real-time corrected Global Positioning System (GPS) technology was used to provide sub-meter resolution of probe and bota position. Water quality and GPS data were integrated and recorded using onboard portable computers.

Field work was completed over an 18-day period in late January to early March 1996. A total of 152 survey runs were performed over nearly 12 km of surface water, yielding more than 157,000 records. From this data, a total of 198 anomalies were identified. Anomalies ranging up to 0.74 °C and 38 uS/cm were identified, the majority of which were detected in shallow water < 3 m deep. The magnitude of the anomalies identified are within the range predicted using simple mixing models. These models also indicate that given the high ambient flow rates in the river, many low volume subaqueous springs may be below the resolution for detection.

The locations of anomalies identified in this effort were found to coincide with a number of key hydrogeologic features and trends where groundwater discharge was expected to occur. The location and character of the anomalies detected appears to represent two distinct modes of groundwater discharge. Where the surface water bodies

intersect flowpaths in the saturated overburden above bedrock or, where the creek bottom is mantled with thick alluvium, groundwater appears to discharge as diffuse seepage zones or as a continuous seepage face. In contrast, anomalies were more frequently detected where bedrock is exposed along the river/creek bottom. Further, these anomalies were typically of higher magnitude and discrete, representing groundwater discharge along primary bedrock flowpaths. These include solutionally enlarged fractures, faults, and conduits.

The dynamic nature of the bounding surface water bodies in this study area results in highly variable and transient patterns of groundwater discharge. It is likely that subaqueous springs inferred from the anomalies are part of a highly complex, interconnected distributary network that functions differently in response to the highly transient surface water boundary conditions.

The results of this study support the findings of a previous water balance study, indicating that the majority of groundwater discharge from the ETTP site is occurring through subaqueous discharge to the Clinch River and Poplar Creek. The results further support the contention that there is little potential for significant underflow of these surface water bodies. Direct investigation of subaqueous spring discharge, possibly involving divers and the installation of river bottom seepage meters is recommended to confirm the spring locations identified in this study and to evaluate their role in the overall hydrogeology of the site.

TABLE OF CONTENTS

CHAPTER	PAGE
1. INTRODUCTION	1
Statement of the Problem	1
Objectives of the Study	5
2. HYDROGEOLOGIC SETTING	6
Study Area Description	6
Geologic Framework of the Study Area	6
Surface Water Hydrology	16
Groundwater Hydrology	25
Conceptual Model	37
Identification of Key Target Areas for Subaqueous Groundwater Discharge	39
3. METHODS	43
Review of Available Methods	43
Previous Investigations	44
Method Description and Procedures	48
4. RESULTS	54
Overview of Results	54
Representative Examples	66
5. DISCUSSION AND IMPLICATIONS	80
Heat Transfer Hydrodynamic Implications	80
Hydrogeologic Significance	99
6. SUMMARY AND CONCLUSIONS	109
REFERENCES	112
APPENDICES	118
VITA	258

LIST OF FIGURES

No.	Title	Page
2.1	Map of the East Tennessee Technology Park Study Area.	7
2.2	Stratigraphic column for bedrock formations within the study area.	9
2.3	Geologic map of the East Tennessee Technology Park Study Area	10
2.4	Karst features within the East Tennessee Technology Park Study Area	14
2.5	Regional surface water hydrologic setting.	17
2.6	Mean seasonal range of surface water and groundwater temperatures and river stage	20
2.7	Compound hydrograph showing typical surface water hydrologic conditions within the study area.	23
2.8	Potentiometric map representing low pool stage, wet season conditions typical of the study period.	26
2.9	Composite hydrographs for select Chickamauga Group and Knox Group bedrock wells that monitor karst solution cavities (upper), Clinch River stage (middle), and precipitation (lower), 1993-1994	32
2.10	Composite hydrograph for wells and springs in the Knox Group within the study area showing aquifer response to stage and rainfall	34
2.11	Map of key hydrogeologic targets, trends and features where groundwater discharge is expected to occur.	41
3.1	Schematic diagram of field data acquisition system	49
3.2	Schematic diagram of the principal electronic data acquisition components	51
4.1	Map showing survey coverage	56
4.2	Survey results for February 20, 1996, Run 7 (Anomaly 220R07-1)	60
4.3	Simple two-component mixing model (upper); flow and ambient river temperature impacts on mixed temperatures (lower)	61
4.4	Anomaly location map	65

LIST OF FIGURES (Continued)

No.	Title	Page
4.5	Comparison of anomalies in areas of overlapping surveys for February 29, 1996 and March 12, 1996	69
4.6	Map showing the location of anomalies identified on overlapping survey runs on February 27th and February 29th, 1996.	72
4.7	Mixing of Poplar Creek and Clinch River waters near the mouth of Poplar Creek, March 4, 1996.	75
4.8	Composite hydrograph showing the complex relationships between river stage changes, rainfall, hydraulic gradient, changing aquifer water levels and flux.	78
5.1	Conceptual diagram showing the significance of geologic structure and the angle of incidence of a river bottom spring relative to ambient river flow directions on heat dissipation and thermal plume geometry	88
5.2	Spatial patterns of calculated subaqueous spring discharge	91
5.3	Plot of identified temperature anomalies as a function of ambient river discharge.	93
5.4	Plot of identified temperature anomalies as a function of ambient river temperature at the time of detection	94
5.5	Plot of identified temperature anomalies as a function of the water depth in which they occur (opposing hydrostatic head)	95
5.6	Plot of identified temperature anomalies as a function of R, the ratio of ambient river discharge to calculated spring discharge	96
5.7	Plot of identified temperature anomalies as a function of calculated spring discharge rate	97
5.8	Plot of identified temperature anomalies as a function of river stage	98
5.9	Locations of identified anomalies with respect to expected areas of groundwater discharge	101

LIST OF TABLES

No.	Title	Page
4.1	Summary of field data	55
4.2	Summary of field data for February 20, 1996	58
4.3	Anomaly classification system	64
4.4	Distribution of Anomaly Classes	67
4.5	Overlapping anomaly comparison, February 29, 1996 and March 12, 1996.	70
4.6	Overlapping anomaly comparison, February 27, 1996 and February 29, 1996	73
5.1	Summary of anomalies potentially related to expected areas of groundwater discharge associated with karst features or trends	102
5.2	Summary of anomalies potentially related to expected areas of groundwater discharge associated with key structural features	103
5.3	Summary of anomalies related to potential stratabound flow zones	104

1. INTRODUCTION

Statement of the Problem

Groundwater flowpaths in a karst aquifer are represented by a continuum ranging from flow along discrete bedrock fractures in the "diffuse" zone to large conduits or networks of conduits which integrate all flow within the system. Although the exact groundwater flowpaths between two points are seldom defined with certainty in karst aquifers, groundwater ultimately emerges at springs which represent focused points of groundwater discharge from the overall catchment area. While the locations of springs are determined by the hydrogeologic framework of the aquifer, some of the largest springs in a karst terrain are located along master streams or other surface water bodies which represent baselevel for groundwater discharge through integrating conduits as well as fractures in the diffuse zone. However, not all groundwater discharge occurs at the land surface. Karst springs also occur below the water level of the receiving surface water body, whether it be a river, surface impoundment, or the sea.

High volume fresh water subaqueous springs, or *vruljes,* have been documented in coastal areas worldwide, including the Persian Gulf, along the coast of Florida, New York, and California in the USA, Cuba, Mexico, Chile, Hawaii, and in the Mediterranean Basin (Drogue and Razack, 1984; Bonacci, 1987). Most of these subaqueous springs occur at depths of 10 m or less (Alfaro and Wallace, 1994) although a few have been reported at depths ranging up to 50 m along the sea floor (Milanovic, 1981). Other workers (Cherkauer and Nader, 1989; Bogle and Loy, 1995; and Milanovic, 1986 for example) have identified subaqueous groundwater discharge in fresh water lakes, rivers, and impoundments.

Alfaro and Wallace (1994), Bogli (1976), and Bonacci (1987) describe four principal origins of subaqueous springs. The first three represent natural geologic processes and are formed over longer geologic timescales. These include subaqueous

springs formed: i) as baselevel springs associated with prior lower sea level conditions but which are now inundated, ii) formed due to submergence of former karst valley springs as a result of morphological or tectonic processes, or, iii) formed where groundwater heads in the underlying aquifer exceed the hydrostatic head in the existing surface water body, typically in response to either evolving watersheds or receding surface water bodies. In contrast, a much more rapid mode of subaqueous spring formation stems from, iv) inundation of existing baselevel springs as a result of reservoir construction and impoundment of contributing rivers.

Milanovic (1981) and Bonacci (1987) describe many examples of subaqueous springs in man-made lakes caused by impoundment of master drains in the Dinaric karst region of the former Yugoslavia. In many of these cases, an increase in river stage related to the construction of surface impoundments has been documented to have significantly altered not only the flow regime of the now drowned springs but also the groundwater flow regime in the surrounding karst aquifer within the catchment area of the springs. Milanovic (1986) cites one example of a large spring zone along the Trebisnjica River in Yugoslavia which was inundated by over 75 m of water following construction of a downstream dam to form the Bileca Reservoir. It was observed that spring flow and karst aquifer hydrodynamics were dependent on the reservoir stage and precipitation within the catchment area of the spring zone. The effects of reservoir impoundment on this well developed karst system could be observed at distances up to 30 km from the springs

Milanovic (1986) reports that prior to construction of the Grancarevo Dam and during low pool reservoir stage conditions thereafter, individual springs in this zone were observed to flow at rates up to 2 m^3/sec. With the reservoir at full pool stage, the spring zone was still manifested at the surface of the reservoir by a large circular boil several 10's of meters in diameter. However, reservoir stage was shown to regulate the rate of groundwater discharge from the aquifer and thus, impacts the manner in which the

aquifer system responds to recharge loading. In particular, the submergence of these primary discharge features affected the drainage of the aquifer after a rainfall event. Hydraulic gradients and thus groundwater discharge rates to the reservoir declined with increasing reservoir stage. Consequently, the recession times following storms were extended as the aquifer drains more slowly. Additionally, while the submerged springs still functioned as discharge points during high stage periods, additional groundwater discharge zones were observed to emerge depending on recharge within the watershed and local hydrogeology .

In east Tennessee, the Tennessee River and it's tributaries cut across many of the subparallel strike valleys in the Valley and Ridge several times, including the karstic carbonate strike belts within them. Since the early 1900's, the Tennessee Valley Authority (TVA) has constructed a number of dams along the Tennessee River and its major tributary rivers. Water levels in the resulting impoundments have been raised between 5 and 20 m, inundating considerable area and, altering the overall flow systems along valleys which are intersected by these surface water bodies.

The study area addressed in this research involves a karstic carbonate aquifer bounded by a TVA run-of-the-river surface impoundment and a large first order tributary stream to that impoundment. Much like the case presented by Milanovic (1986) for the Trebisnjica River, the impoundment of the Clinch and Tennessee rivers by Watts Bar Dam raised the Clinch River stage approximately 6 m within the study area, inundating former springs located along or within the former channels and altering the groundwater regime in the adjacent aquifer. Available hydrogeologic information (DOE 1996, DOE, 1997a) documents the interrelationship between groundwater discharge and surface water stage and further suggests the river serves as boundary to groundwater flow. However, while potentiometric maps indicate groundwater flow towards the adjacent surface water bodies, spring and seep occurrences at the surface along the banks of the river or creek are sparse. Therefore, it is hypothesized that most of the groundwater discharge occurs as

subaqueous seepage within the surface water bodies. It is expected that now inundated pre-impoundment springs may still function as points of focused groundwater discharge to some degree, governed by temporal relationships between the hydraulic heads in the aquifer and the opposing hydrostatic heads imposed by the impoundment.

Although large subaqueous springs such as those described by Milanovic (1986) in the Trebisnjica River impoundment are manifested by large boils at the water surface, not all subaqueous springs are as obvious. Bogle and Loy (1995) identified more subtle subaqueous springs identified in an embayment of a Chickamauga Reservoir, another large surface impoundment in east Tennessee. In this case, the springs were identified as thermal anomalies evident from thermal infrared imagery and apart from small ice-free areas noted when the embayment froze over, showed no surface manifestations of discharge.

Where pre-impoundment spring locations are unknown or are not manifested at the water surface, other methods have been applied to locate them. These methods include exploratory diving and direct or indirect measurement of differences in physical and chemical characteristics (chiefly temperature and specific conductance) between groundwater and the receiving surface water body. Infrared thermography and multispectral remote sensing are two examples of the latter that have proven effective when conditions are favorable (typically in shallow, stagnant water situations). Dye tracer studies are often applied to confirm suspected subaqueous spring locations but are of limited use as an exploratory tool where the area of potential groundwater discharge in question is large or in surface water bodies with high flow rates (Milanovic, 1981).

The water depth, transient stage and flow conditions, and large surface area in the Clinch River within the study area limit the application of these methods. Therefore, an alternative approach is required to identify points of direct subaqueous groundwater discharge to this large, flowing surface water bodies where prior knowledge of pre-impoundment springs is unavailable.

Objectives of the Study

The objectives of this research are twofold: 1) development of an improved system for identifying direct subaqueous groundwater discharge to large surface water bodies on the basis of water quality anomalies and, 2) application of this methodology to identify anomalies within the ETTP site study area in east Tennessee to test a conceptual model that assumes that most of the groundwater discharge from the site still occurs as direct, subaqueous discharge to surface water following impoundment of the river. Since pre-impoundment springs are unknown in the study area, the results of this research are evaluated and discussed relative to expected locations of subaqueous spring occurrences based upon an existing understanding of site hydrogeology. Consequently, subaqueous springs inferred from this study can be used to evaluate: i) the role of key structural or stratigraphic features and suspected karst conduit flowpaths in focusing groundwater discharge; and, ii) the impacts of surface impoundments on groundwater flow and discharge to surface water.

2. HYDROGEOLOGIC SETTING

The following section describes the key elements of the hydrogeologic framework of the study area in order to provide a basis for discussion of the results obtained in this research. The reader is directed to the references provided, principally DOE, 1996, for a more thorough treatment of the hydrogeologic setting.

Study Area Description

The East Tennessee Technology Park (ETTP), formerly known as the K-25 site, is an approximately 1000-acre industrial facility located ~45 km northwest of Knoxville, Tennessee on the Department of Energy (DOE) Oak Ridge Reservation (ORR). The ETTP site, shown in Figure 2.1, is located within East Fork Valley between Pine Ridge to the southeast, McKinney Ridge to the northeast, and Blackoak Ridge to the northwest. The site is further bounded by the Clinch River and a large first order tributary to the Clinch, Poplar Creek. Poplar Creek meanders through the site, and in conjunction with the Clinch River, dissects the ETTP site into several discrete land areas such as the Main Plant area, located east of Poplar Creek, and the K-33, Duct Island and Powerhouse areas as noted on Figure 2.1. This research focuses on groundwater discharge from the ETTP site to the adjacent surface water features. Consequently, the study area for this research is defined by those reaches of Poplar Creek and the Clinch River highlighted on Figure 2.1.

Geologic Framework of the Study Area

The geology within the study area is complex, reflecting lithologic diversity (carbonate, clastics) and structural complexity at different scales, all of which have been overprinted by karst solution processes to varying degrees. Numerous workers have contributed to the current understanding of the geology of the site (Rodgers, 1953; McMaster, 1962; Hatcher *et al.*, 1992), but perhaps the most thorough mapping was performed by Lemiszki (1994, 1995) whose work forms the basis for the geologic

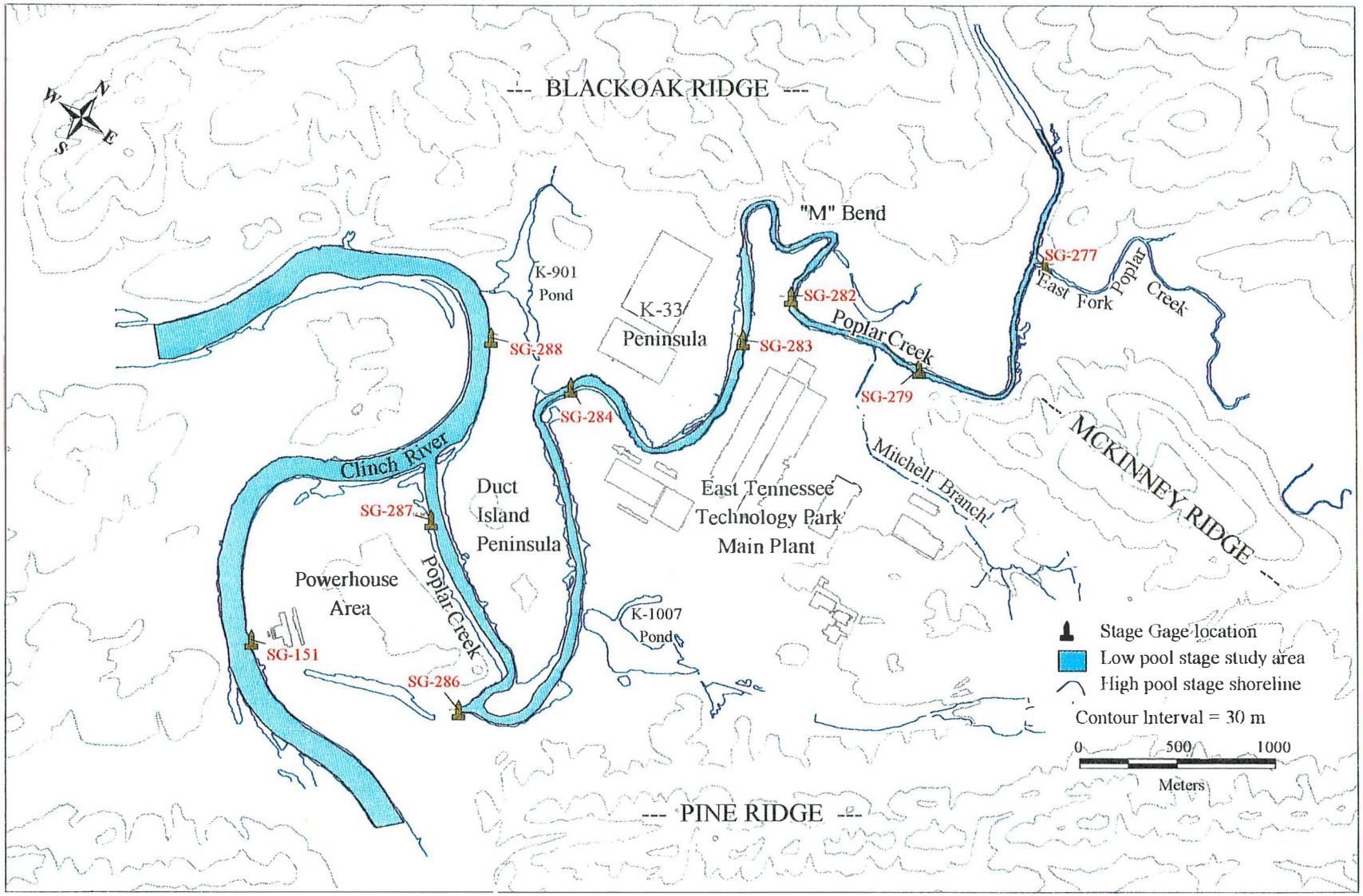


Figure 2.1. Map of the East Tennessee Technology Park Study Area.

description to follow.

The ETTP site is situated on the trailing edge of the Kingston thrust sheet adjacent to the Whiteoak Mountain Fault and is underlain by bedrock that can be broadly classed as either carbonate (Cambro-Ordovician Knox Group and Ordovician Chickamauga Supergroup) or clastic (Cambrian Rome Fm). Within the ETTP study area, bedrock is largely mantled by a veneer of unconsolidated overburden ranging up to 20 m thick. However, with the exception of point bar deposits along the inside meander bends in the river, bedrock is exposed along nearly the entire shoreline and bottom of the Clinch River. Conversely, sediment accumulations are quite thick (up to several meters) in Poplar Creek such that bedrock is only exposed in isolated outcrops along the shore, and perhaps in deep holes along the bottom.

Figure 2.2 presents a stratigraphic column of bedrock units present at the site; Figure 2.3 is a geologic map of the study area. Chickamauga Supergroup carbonates (including the Nashville and Stones River groups) occupy the valley bottom, and underlie the majority of the ETTP study area. The Cambrian Rome Fm clastics underlie Pine Ridge and part of McKinney Ridge on the hanging wall of the Whiteoak Mountain and K-25 thrust faults, respectively. The Knox Group carbonates underlie Blackoak Ridge. The contact between the Chickamauga Supergroup and underlying Knox Group carbonates, marked by a regional unconformity, occurs near the base of Blackoak Ridge and trends through the northern third of the study area

The Knox Group carbonates consist of stacks of fractured and solutioned, thick to massively bedded dolostone that is highly siliceous. The Chickamauga Supergroup, on the other hand, is composed primarily of limestone although there are also distinct calcareous shale beds, mud rich limestones, and thin mud seams and stringers. Argillaceous limestones and calcareous shale within several formations in the Chickamauga, such as in the Pond Springs Fm, Ridley Ls, Carters Ls, and Hermitage Formation appear to have the least well developed fractures and often serve as fracture

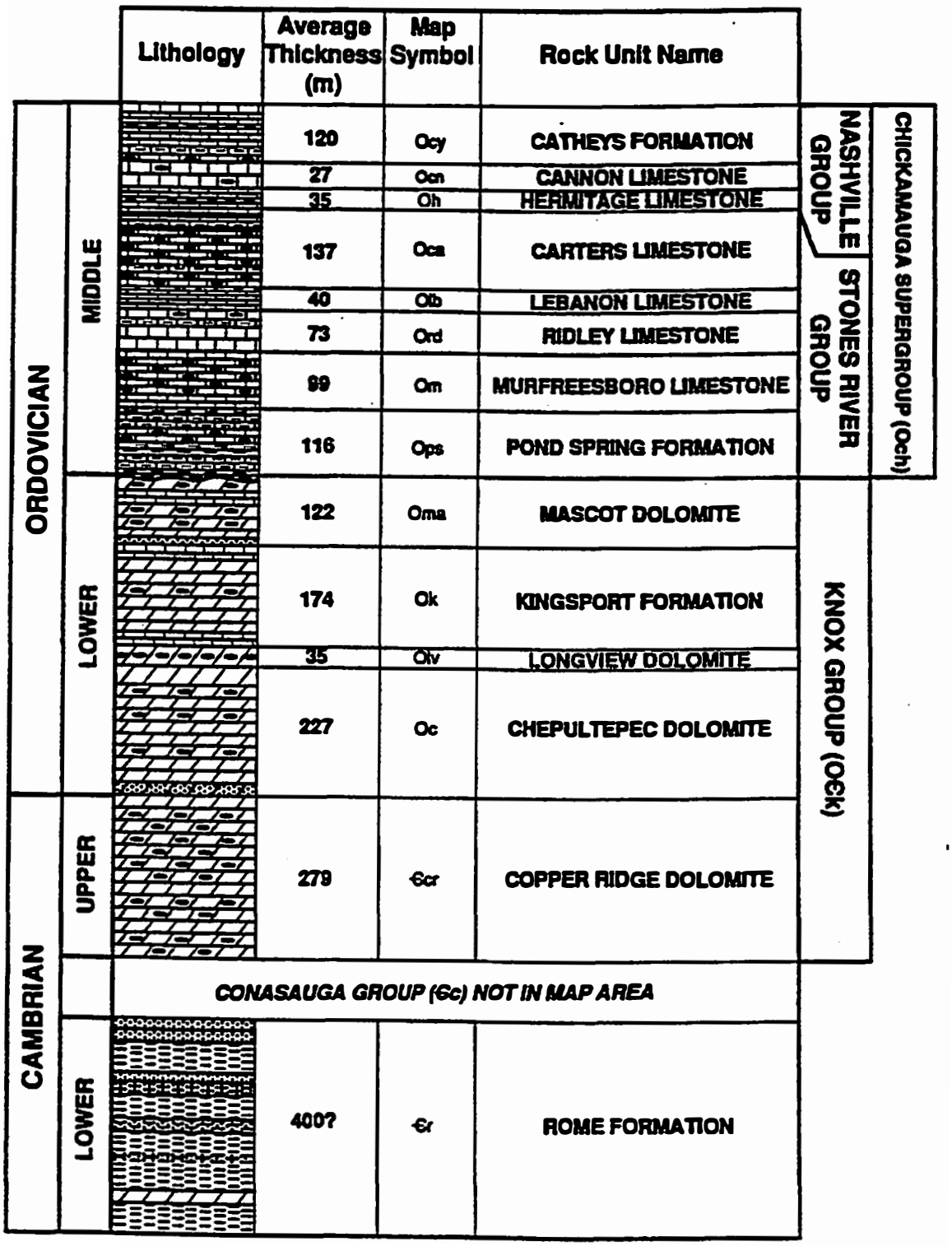


Figure 2.2. Stratigraphic column for bedrock formations within the study area. (Source: Lemiszki, 1994)

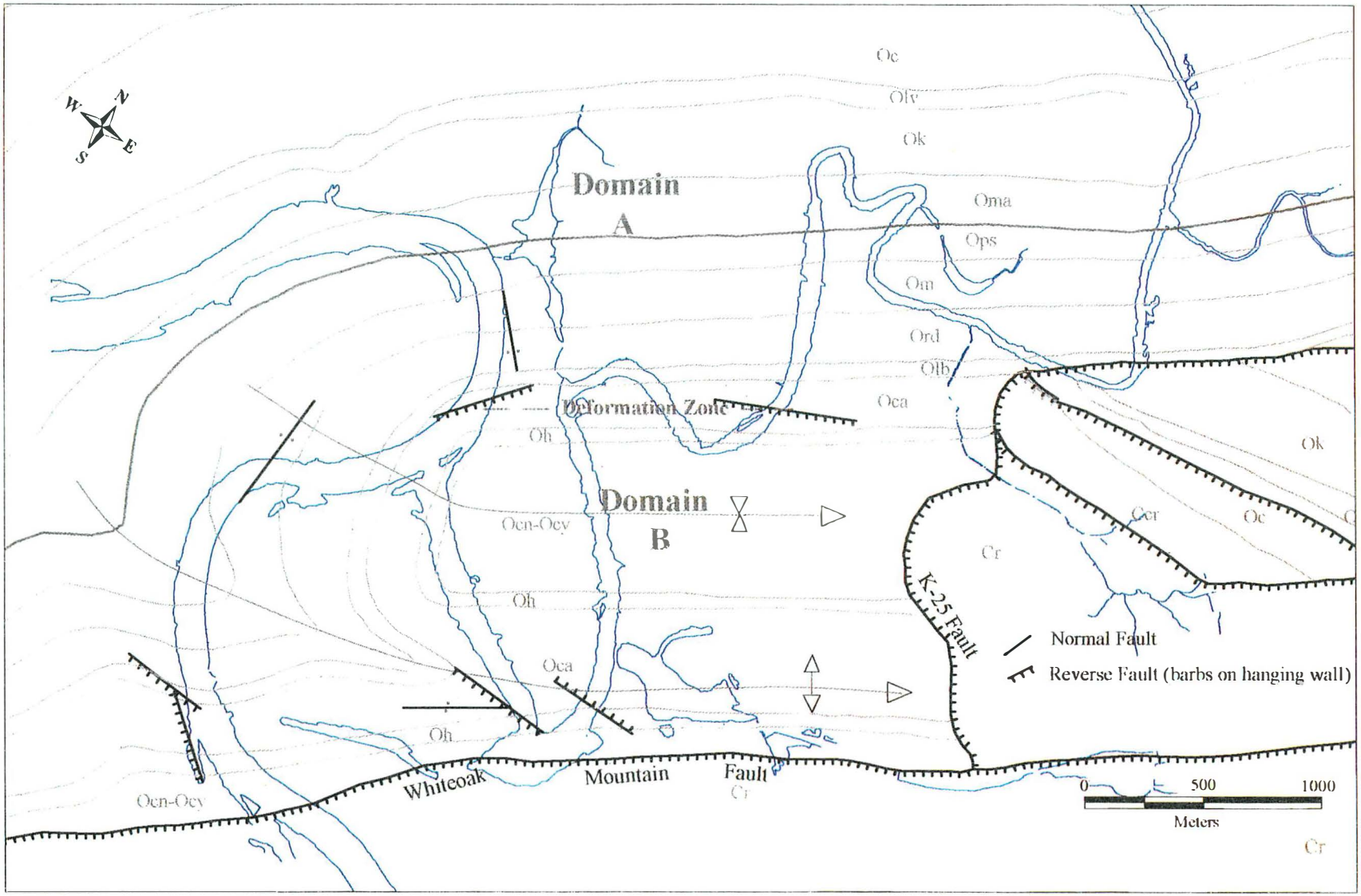


Figure 2.3. Geologic map of the East Tennessee Technology park Study Area (after Lemiszki, 1995)

termination points for the fractures developed in the adjacent, cleaner limestones. Because of their lack of fracturing, these lithologies can potentially constrict flow along the more intensely fractured limestone intervals, creating stratabound flow conditions (Ketelle and Lee, 1992). Key potential stratabound flow zones could include: a) along the basal Hermitage Fm calcareous shale zone; b) along the metabentonites which occur in the middle of the Carters Ls; c) along the bed-parallel chert lenses in the massive micritic limestones within the middle of the Pond Springs Fm; d) along the calcareous shales in the middle of the Ridley Limestone, and; e) along the Knox-Chickamauga unconformity which is marked by a zone of jasperoidal chert.

The structural geology within the study area includes macroscopic folds and faults as well as mesoscopic fractures, folds, and faults. Major faults in the study area (shown on Figure 2.3) include the aforementioned Whiteoak Mountain Thrust Fault, and the K-25 Fault. The K-25 Fault is a steeply northeast-dipping thrust fault that places Rome Fm bedrock over Chickamauga carbonates. In the footwall, the fault cuts obliquely through northeast trending folds in the Chickamauga group, truncating these structures to at least the Carters Ls (Lemiszki, 1995). The K-25 Fault is significant to this research only 1) as a potential conduit for groundwater discharge where intersecting the upper reaches of Poplar Creek and 2) because of it's role in potentially limiting the along-valley extent of recharge available to the Chickamauga carbonates and thus, limiting the degree of karstification in those units. Other macro- and mesoscopic reverse and normal faults have been mapped by Lemiszki (1994, 1995) in outcrops along Poplar Creek and the Clinch River, as shown on Figure 2.3. Generally displacement along these structures is minor, ranging from 0 to 1.5 m. Faults are oriented both parallel and perpendicular to the axes of macroscopic structural features.

One of the most conspicuous structural features evident on Figure 2.3 is a macroscopic anticline-syncline pair in the middle to upper Chickamauga carbonates. These structures plunge to the northeast, presumably beneath the K-25 fault, intersecting

the Clinch River and Poplar Creek at several points along the fold axes. Other mesoscopic folds, some of which are overturned, have been mapped by Lemiszki (1994, 1995) in outcrops along the river and creek.

Based upon outcrops along Poplar Creek and the Clinch River, Lemiszki (1995) identified a narrow, linear deformation zone within the middle of the Carters Ls that appears to extend across the study area. This trend, marked by numerous macroscopic normal and reverse faults exposed along Poplar Creek and the Clinch River, apparently separates two distinct structural domains characterized by monoclinally dipping Knox and lower Chickamauga bedrock to the northwest (Domain A on Figure 2.3) and the more complexly folded and faulted middle and upper Chickamauga carbonates to the southeast (Domain B). This zone of deformation has been interpreted by Lemiszki (1994, 1995) as a surface manifestation of a thrust fault at depth, possibly linked to the K-25 fault.

Lemiszki (1994, 1995) observed at least two primary and as many as 5 distinct extensional fracture sets. The primary, regional fracture set consists of bedding strike parallel and bedding strike perpendicular fractures, which form an orthogonal network. The geometric relationships between fracture sets and bedding are maintained, and rotate accordingly along with changes in bedding strike. A number of additional (shear) fracture sets related to local deformation are superimposed on the regional set; the auxiliary fractures are commonly perpendicular to bedding, at angles of 30 to 45° clockwise or counterclockwise to the bedding strike parallel set.

Although many of the fractures observed in outcrop are healed or calcite filled, Lemiszki (1995) observed that bedding strike parallel fractures sets appear to reflect a higher percentage of open fractures. The preferential weathering of this set suggests its importance in controlling groundwater flowpaths parallel to the valley and ridge topography. Further, Lemiszki (1995) observed that within massively bedded limestones, long, bed-normal fractures appear to be preferentially open and host considerable solution cavity development. In Chickamauga Group outcrops along the Clinch River, widened

cavities were commonly found where fractures terminated against beds of different, commonly more argillaceous lithology, thus limiting further downward solution development. In other instances, a planar zone of dissolution was observed along a bedding plane contact between two dissimilar lithologies within a given formation, resulting in a stratabound flowpath.

It is important to note that both Poplar Creek and the Clinch River transect bedding strike and consequently, intersect countless shallow, bedding-strike parallel flowpaths, including fractures, solutionally widened fractures and cavities, and potential stratabound flow intervals. In study reaches along the Clinch River where the river turns to the southwest to roughly follow geologic strike in the Kingsport Dolomite, the bedding strike perpendicular fractures appear solutionally enlarged. These likely reflect groundwater flowpaths towards the river that are oriented both downdip and in the direction of steepest hydraulic gradient.

A karst inventory was conducted for the study area by the author and reported in DOE (1996). Karst features of interest include surficial evidence of subsurface karst (sinkholes, sinking streams, springs, enterable caves) as well as cavities encountered in subsurface penetrations. These features are summarized graphically in map form on Figure 2.4. From examination of Figure 2.4, it is clear that there is abundant evidence of karst within the carbonate bedrock underlying the study area. However, the degree and style of karstification varies between the Knox and Chickamauga carbonates at least in part as a function of lithologic and mechanical characteristics of each, but also as a result of structural and hydrologic variables.

In the subsurface, cavities have been encountered in 39% of all bedrock penetrations within the study area (DOE, 1996). Cavity heights observed in boreholes range up to 11.5 m, though the larger cavities are generally restricted to the Knox Group carbonates. Chickamauga carbonate cavities are typically smaller, on the order of 1 m or less and often mud filled. Of the cavities identified, nearly 60% were mud filled.

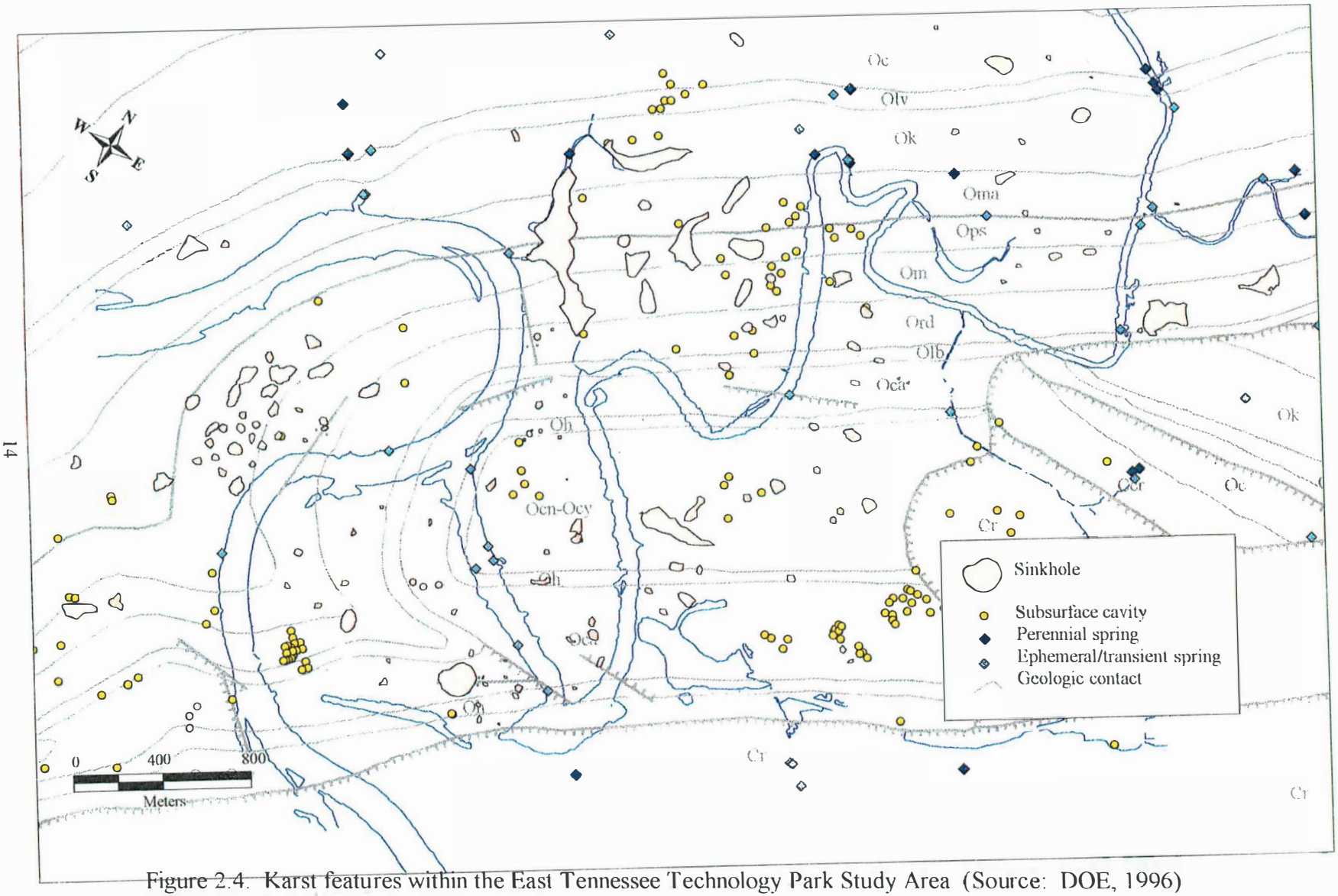


Figure 2.4. Karst features within the East Tennessee Technology Park Study Area (Source: DOE, 1996)

From Figure 2.4, it is clear that sinkholes appear more abundant and typically larger in the Knox Group and lower Stones River Group Chickamauga carbonates than in the upper Chickamauga. Further, there is an obvious linear trend of large sinkholes that occur in the Chickamauga Pond Springs Fm, parallel to the Knox-Chickamauga unconformity contact, extending both upvalley from the study area and downvalley on the opposite side of the Clinch River. Considering that the Pond Springs is largely a thin-bedded argillaceous limestone with some shale partings, it is likely that the sinkholes in this formation reflect collapse of this weaker unit into cavities developed in the underlying Mascot Dolomite of the Knox Group. Whereas the baselevel for cavity development in the Chickamauga is represented by the current baselevel, the upper Knox contact is marked by a regional unconformity reflecting the fact that the upper Knox was a subaerial exposure surface prior to deposition of the overlying Pond Springs Fm. Regionally, there is abundant evidence of paleokarst development in the upper 100 m of the Knox Group (Montanez and Read, 1992; Mussman et al, 1988; Palmer and Palmer, 1989) . Consequently, larger cavities can also be observed at depths considerably below the current baselevel in the Knox, parallel to the unconformity surface.

The sparsity of sinkholes and larger subsurface cavities in the Chickamauga carbonates along the valley floor in the study area may be attributed to the K-25 Fault. Whereas the Knox and lower Stones River Group Chickamauga carbonate rocks extend uninterrupted upvalley along strike, the Chickamauga carbonates are truncated by the K-25 fault. Thus in the Knox, there is the potential for development of a large through-going network of conduits that originated well upvalley of the study area and continues through it to the intersection with the river. It is likely that the trend of large sinkholes paralleling the contact are evidence of a large conduit network in the underlying Knox. This is supported by microgravity anomalies identified at two separate points along this trend (Figure 2.4). The magnitude of these anomalies dwarfed other microgravity anomalies that have been correlated to cavities on the order of 7 m in height encountered

in exploratory drilling (DOE, 1996; DOE, 1997a).

Enterable caves developed in the Chickamauga carbonates are rare within the study area as well as regionally. Bedrock is exposed at the surface over much of the Duct Island Peninsula and there are numerous small, open sinks and swallets that rapidly channel rainfall to the subsurface. There are several enterable caves within the study area within the Knox Group bedrock. Caves are located within the Copper Ridge Dolomite in the Blackoak Ridge water gap along Poplar Creek. Potentially enterable Knox cavities have been noted in the Mascot in the bluff along the "M"-bend of Poplar Creek, although these have not been explored to date.

Surface Water Hydrology

The study area is bounded by the Clinch River and Poplar Creek which flows through the ETTP site. Groundwater and surface water at the ETTP site interact in a complex manner, with surface water conditions dramatically influencing groundwater flow and discharge. Therefore, an understanding of the hydrodynamics of these two surface water bodies is integral to evaluating the results of this research.

The Clinch River in the vicinity of the ETTP site is a run-of-the-river impoundment forming a portion of the greater Watts Bar Reservoir. The study area is located approximately 45 km upstream of Watts Bar Dam and 17 km downstream of Melton Hill Dam. Watts Bar Dam, located on the Tennessee River below the confluence with the Clinch River, was constructed by TVA in 1942. The resulting impoundment increased the Clinch River and Poplar Creek stage in the study area by approximately 6 m (Tennessee Synfuels Assoc., 1981) and inundated considerable land area.

From a regional perspective, the Clinch River flows along East Fork Valley to a point above Oak Ridge (roughly 22 km upvalley of the study area), where it abruptly cuts across strike to leave the valley (point "A" on Figure 2.5). Stage height in this reach of the river upvalley of the study area is controlled by reservoir operations at upstream Melton Hill Dam. Below Melton Hill Dam, the Clinch River reenters East Fork Valley

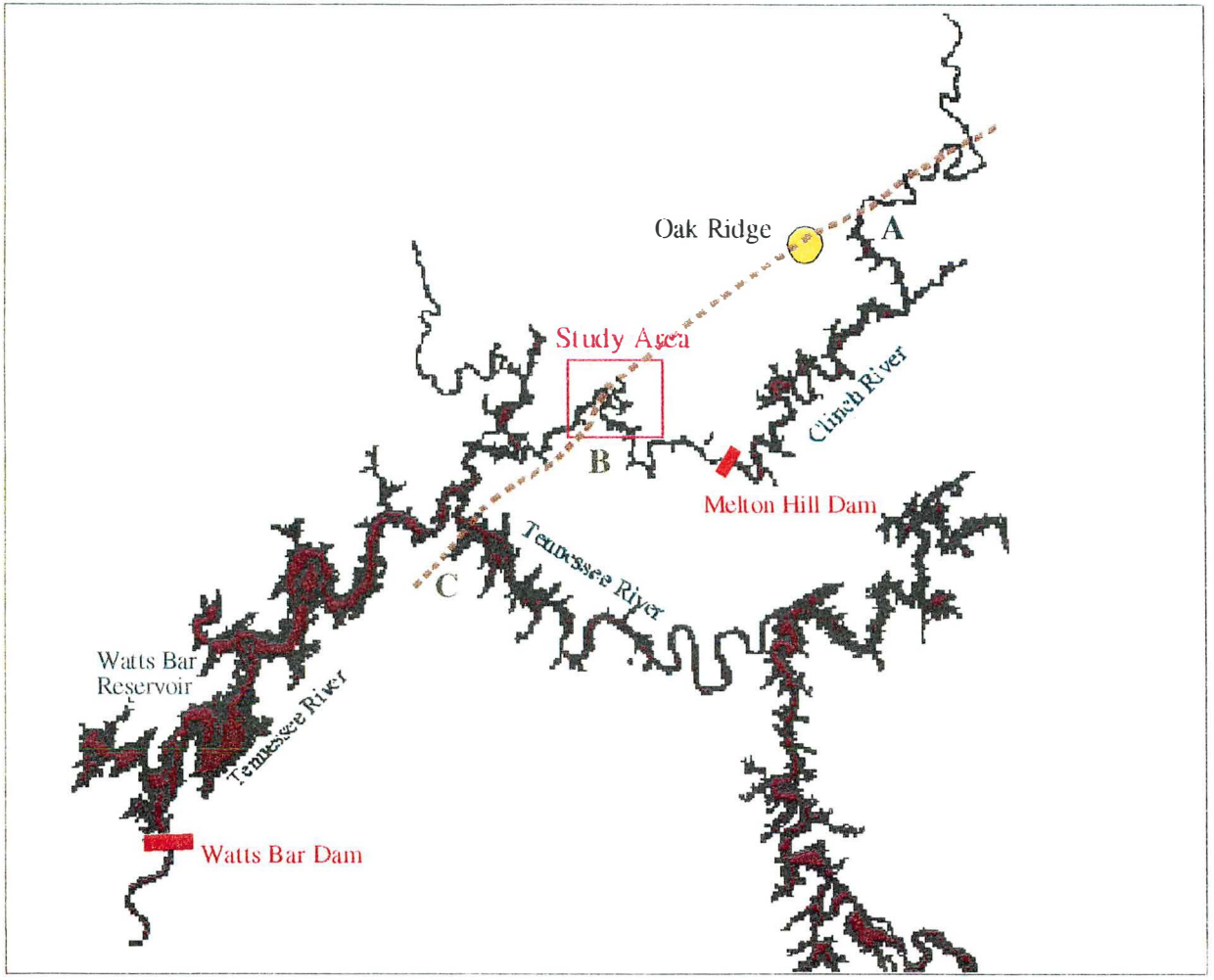


Figure 2.5. Regional surface water hydrologic setting. Dashed line indicates the Knox-Chickamauga Group formation contact.

through the water gap in Pine Ridge, flows across the valley floor, directly across geologic strike, then turns towards the southwest to flow along the valley towards Watts Bar Dam (point "B" on Figure 2.5). Roughly 6 km further downstream, the river turns to cut through Blackoak Ridge into the next valley before joining the Tennessee River further downstream. The Tennessee River is the next major master drain to cut across East Fork Valley which it does roughly 12 km further downvalley along strike (point "C), paralleling the course of the Clinch River within the valley. The stage elevation in the Tennessee River in this reach below Ft. Loudoun Dam is also maintained by Watts Bar Dam and thus, is effectively the same as in the Clinch River in the study area. In contrast, the Clinch River stage upvalley of the study area above Melton Hill Dam is consistently 12.5 m above the Clinch River adjacent to the ETTP Site. Therefore, from a regional perspective there is an overall downvalley hydraulic gradient from above Oak Ridge towards the ETTP site. However, the Clinch River represents the lowest possible heads from this point further downvalley for the next 12 to 40 km. The implication is that the Clinch River is expected to serve as a discharge boundary to groundwater flow in the vicinity of the study area. Further, stage conditions in the Clinch River have a regulating influence on groundwater discharge to surface water in the vicinity of the study area.

In the study area, the Clinch River is up to 150 m wide and 16 m deep, though on average, the depth is less than 10 m. Water depths are greatest within the pre-impoundment river channel. The deepest reach of the Clinch River encountered in the study area is located downstream of the confluence with Poplar Creek, within the outcrop belt of the Chickamauga Pond Springs Fm. Deep, strike-parallel "holes" related to bedding exposed along the river bottom were encountered in several locations. For example, water depths were observed to increase suddenly to nearly 16 m along a bedding plane hole that extends out into the river within the lower Pond Springs outcrop belt on the Clinch River, near the K-901 Pond outfall.

River bottom water temperatures are monitored daily at the DOE K-1503 water

intake facility located just upstream of the study area on the Clinch River. Figure 2.6 (middle panel) depicts the long term seasonal patterns of surface water temperatures in the Clinch, based on data from 1993-1996. Temperatures fluctuate on a seasonal basis with average water temperatures ranging from a high of ~22.5 °C in July-August to 6-8 °C in January-March period (Bowman, 1996). River temperatures can also fluctuate several degrees over the course of a day. This is related to the hydraulic detention time of the river (the time required to flush and replace the entire river volume with fresh water) which ranges from around 7 hours to ~ 3 days, depending on the prevailing discharge rates (Tennessee Synfuels, 1981; DOE, 1996) as controlled by reservoir operations. Thus, the entire river volume in the study area is replaced over a short period of time and the observed variability of temperatures reflects the continually changing stored water volume.

Poplar Creek originates in adjacent Sugar Grove Valley and enters East Fork Valley through a water gap cut through Blackoak Ridge at which point it is joined by East Fork Poplar Creek, which drains East Fork Valley above the study area. The creek then meanders for ~8.9 km through the ETTP site, from the upstream confluence with East Fork Poplar Creek to the confluence with the Clinch River. As it flows through the ETTP site, additional flow is contributed by Mitchell Branch and an unnamed tributary which discharges through the K-1007 holding pond. At high pool stage, Poplar Creek ranges up to 70 m wide with water depths ranging up to 7 m though most of the time is less than 5 m deep. During low pool stage, the creek is on the order of 30-40 m wide, largely restricted to the pre-impoundment channel. Periodic upstream flow reversals have been observed from the mouth of Poplar Creek upstream to above the Blackoak Ridge water gap, though the magnitude of the flow reversals decreases progressively upstream. Water in Poplar Creek is commonly more turbid than in the Clinch River while water temperatures are somewhat warmer, ranging from 6-12 °C, but averaging 9 °C during the winter months.

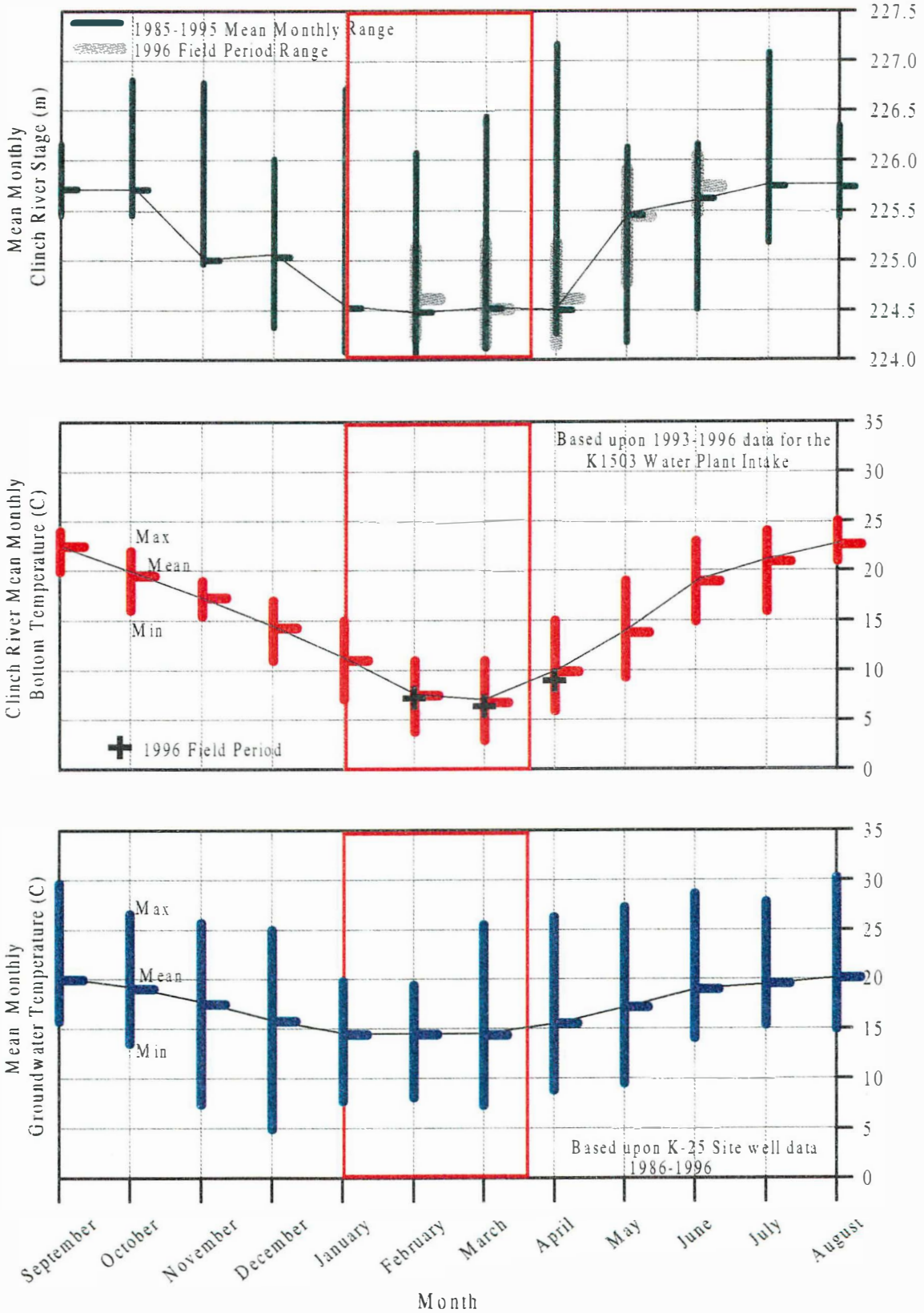


Figure 2.6. Mean seasonal range of surface water and groundwater temperatures and river stage.

Stage levels in both the Clinch River and Poplar Creek have been monitored continuously (and synchronously) at 15-minute intervals at nine stage gages for several years, including the period of this research. The stage gage locations are shown on Figure 2.1. Two of the gages are located on the Clinch River above and below the confluence with Poplar Creek while the remaining seven gages are located at points along Poplar Creek. Headwater stage data is also collected hourly by TVA at Melton Hill and Watts Bar dams (TVA, 1996). An integrated analysis of this data (Zondlo, reported in DOE, 1996) reveals that stage height is directly related to reservoir operations at upstream Melton Hill and downstream Watts Bar dams although discharges from Melton Hill dominate the hydrographs.

Patterns of stage fluctuations are observed at three scales: seasonal, diurnal, and storm-related. TVA maintains the Watts Bar stage at a low pool stage elevation of approximately 224.0 m during the winter months from early December through early April, and a high pool stage (226.0 m) during the summer months. This is shown on Figure 2.6 which displays the seasonal stage component based upon long term mean monthly stage data for the Clinch River in the study area. The diurnal fluctuations consist of 0.3 to 0.5 m increases which last for a few hours twice daily. These fluctuations are the result of discharge at Melton Hill dam. Finally, high intensity or long duration winter storms have been observed to cause short term (lasting several days to a week) increases of up to 2.5 m, which are superimposed on the normal reservoir operation fluctuations.

There are currently no provisions for measuring flow in either Poplar Creek or the Clinch River due to the size of these water bodies. Discharge is recorded hourly at Melton Hill and Watts Bar dams (TVA, 1996). However, both dams are too far removed from the study area to yield site specific flow information. Consequently, as part of this study, flow rates for Poplar Creek and the Clinch River were determined for different reaches using the Manning equation, bathymetric data obtained in this research, and stage data from the existing stage gages. This analysis yields flow data at 15-minute

increments. The methodology and calculations are presented in Appendix B. During the study period (late January to mid-March 1996) flow in the Clinch River was typically ~200 m^3/sec (~7,000 cfs) downstream but ranged from a maximum of 474 m^3/sec (16,714 cfs) downstream to 435 (15,361 cfs) m^3/sec upstream (though the latter flow reversals are short-lived). Poplar Creek flow rates were determined at two locations representing the lower part of the creek near the mouth (at stage gage SG-287) and the upstream reach removed from the Clinch River (at stage gage SG-282). Poplar Creek flow at the mouth of the creek ranges from 92 m^3/sec (3,251 cfs) downstream to 67 m^3/sec (2,366 cfs) upstream, with an average downstream flow of 27 m^3/sec (952 cfs). By contrast, Melton Hill Dam discharge ranges from 0 to 596 m^3/sec (21,000 cfs), averaging 228 m^3/sec (8,063 cfs). Watts Bar discharge ranges from 0 to 1,287 m^3/sec (45,455 cfs), averaging 1,037 m^3/sec (36,615 cfs) during the study period.

Examining both the dam discharge and stage response patterns, it is clear that reservoir operations at the two dams determine the flow conditions in the study area at any time, resulting in an extremely transient and variable boundary condition. This is demonstrated in Figure 2.7 which is a composite hydrograph that relates precipitation, dam discharge, calculated river/creek discharge, and stage conditions for a seven day period in January 1996. Note that this period was selected to demonstrate both storm and non-storm responses as well as varying reservoir operational patterns typical of conditions encountered throughout the study period. These variable, transient conditions are significant relative to the results of this study as will be described later.

From Figure 2.7, the diurnal discharge cycles at Melton Hill dam are clearly shown to impact downstream stage and flow conditions, with stage fluctuations in the study area lagging behind dam discharge by approximately 1 hr. Note that during non-storm periods there is an initial sharp-peaked response in stage and flow in the study area which then subsides towards an equilibrium level that is maintained until Melton Hill discharge is terminated, at which point stage and flow decline dramatically. The highest

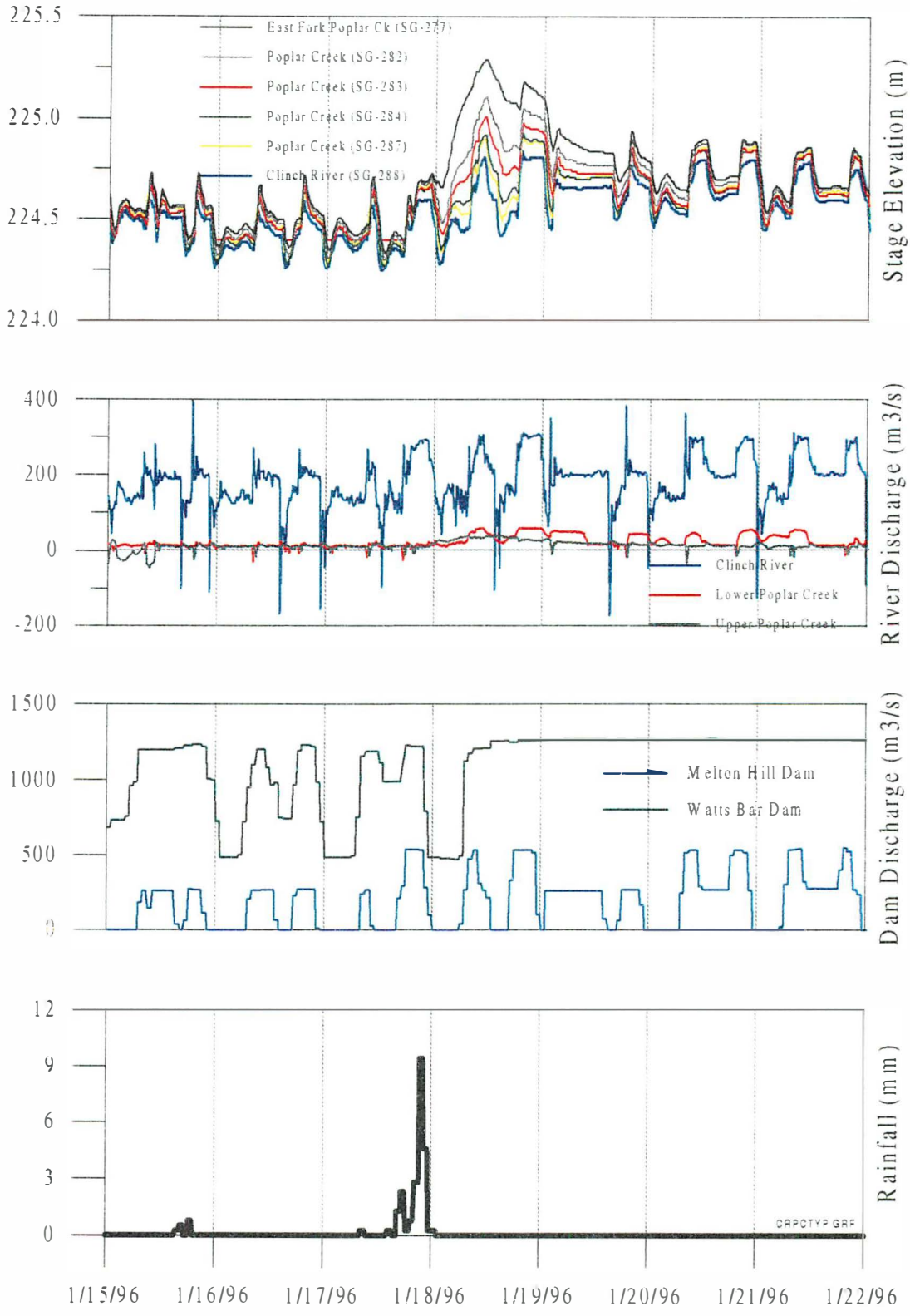


Figure 2.7. Compound hydrograph showing typical surface water hydrologic conditions within the study area.

calculated flow rates in the Clinch River correlate to the initiation of dam discharge and are evidenced by a sharp increase in stage height on Figure 2.7. The initial stage peak in Poplar Creek represents a temporary flow reversal into Poplar Creek caused by the sudden increase in Clinch River stage and flow volume. Stage increases can even be observed at upstream Poplar Creek gages as normal downstream flow is interrupted. However, the momentum of the flow reversal in Poplar Creek appears to carry the stage elevation in the creek past the equilibrium point so that the stage elevation declines in downstream reaches. When the tidal energy is dissipated, flow reverses again this time marked by an initial downstream surge in flow rate followed by normal outflow from Poplar Creek to the river. The return to normal outflow causes a second peak in the Clinch River flow rate, although this peak is of lesser magnitude than the initial surge following the beginning of the Melton Hill discharge cycle. The creek stage then again seeks equilibrium and a smaller peak is seen in the creek stage data associated with a minor flow reversal. When Melton Hill Dam discharge is terminated (sharply to zero typically), the creek and river stage in the study area drop suddenly, with short periods of upstream backflow observable in the Clinch River before it again rebounds. However, the rebound flow rates in the river are less than previously observed when the dam was discharging. This rebound again causes a secondary short term flow reversal in Poplar Creek.

From Figure 2.7 it is also clear that while Melton Hill discharge cycles dominate the hydrograph, the stage and flow responses are also a function of discharge patterns at downstream Watts Bar dam. When Watts Bar discharge is cyclic, the flow in the river is damped (especially when Melton Hill and Watts Bar are out of synch). When Watts Bar is discharging at a constant rate, as indicated by the right half of the hydrograph shown in Figure 2.7, the profiles clearly reflect Melton Hill influences only and the overall flow rates from Poplar Creek and the Clinch River in the study area are higher overall. Further, discharge at Watts Bar results in elevated flow rates within the study area even

during non-discharge periods at Melton Hill dam. Finally, precipitation impacts Poplar Creek flows and stage dramatically but appears to have little impact on the Clinch River. However, this is not unexpected since river flows are managed by TVA for flood control as well. Note that minor storms of low intensity or duration have virtually no impact on stage or flow.

Sediment flux modeling performed by Garrett and Evers (1997) support these conclusions. These workers generated an animated model which incorporated surface water flow hydrodynamics in order to evaluate patterns of discharge of potentially contaminated sediments from Poplar Creek to the Clinch River. The simulation was based upon output of a 3D, time-dependent finite difference code (ALGE), calibrated with stage data, field ground-truthing data (temperature and turbidity profiling) and remote sensing imagery. Their results document mixing between Poplar Creek and the Clinch River in the vicinity of confluence between the two. Thermal IR data indicated plumes of warmer (or colder) Poplar Creek waters projecting out into the river a distance of nearly two thirds of the width of the Clinch River during period of flow rebound from the creek. Conversely, thermal IR data also document actual movement of Clinch River water back up into Poplar Creek during flow reversals. Mixing of the two water bodies can be expected to complicate the identification of groundwater anomalies in the vicinity of the confluence as will be discussed later.

Groundwater Hydrology

Within the study area, the groundwater flow system can be considered unconfined. Figure 2.8 is a potentiometric surface (water table) map representing winter high base conditions (in this case, February 1995). The water table occurs at depths ranging from 0.5 to 5 m below land surface within the unconsolidated zone above bedrock, where the unconsolidated zone is present. Figure 2.8 shows where the water table occurs above (unshaded area) versus below the top of bedrock (shaded areas). In general, the water table reflects surface topography, indicating flow from the higher

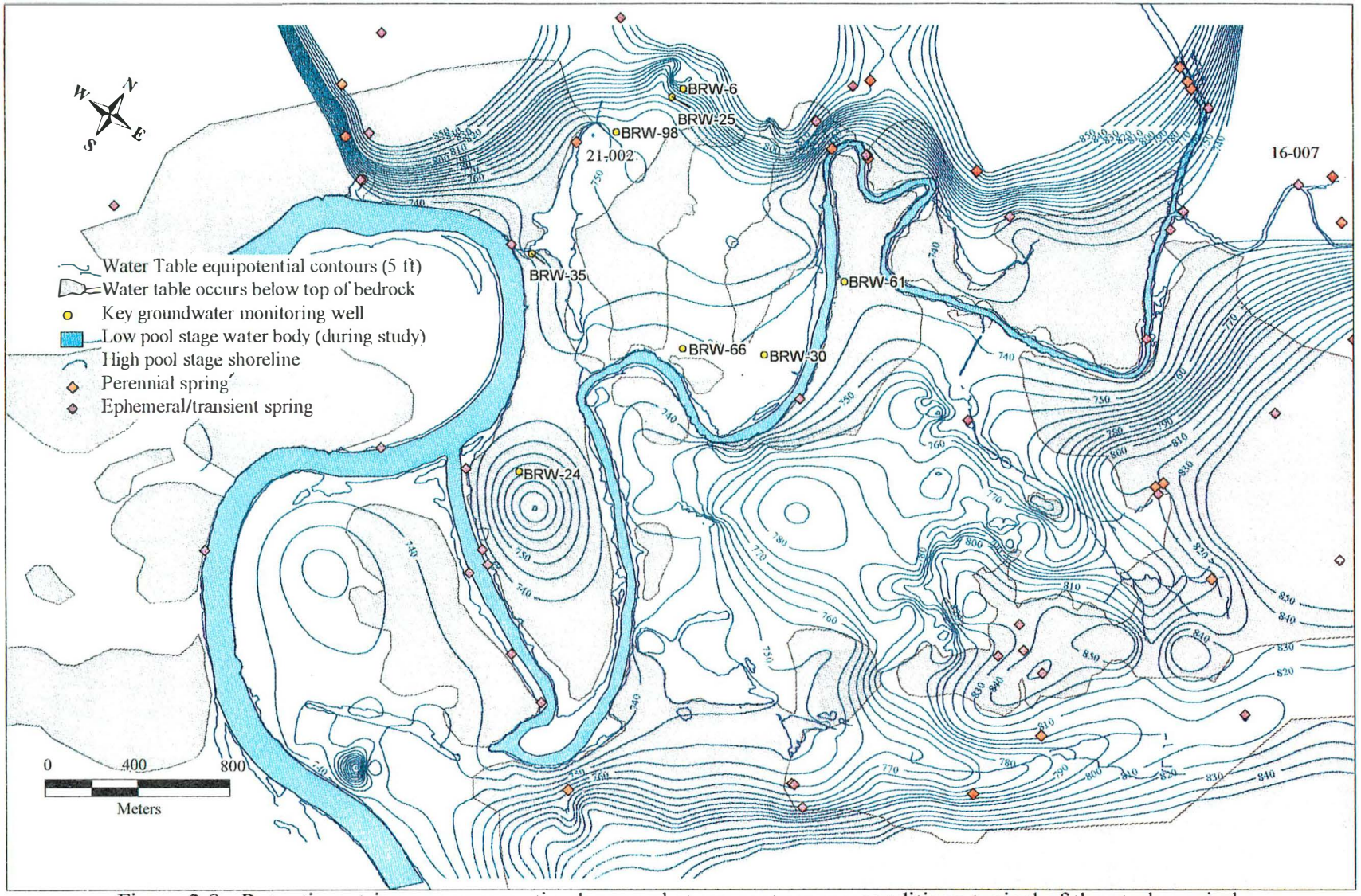


Figure 2.8. Potentiometric map representing low pool stage, wet season conditions typical of the study period.

elevation areas towards the river and creek. Heads in wells on the opposite side of the Clinch River are as much as 18 m higher than the Clinch River, thus indicating flow back towards the river from that side (Tennessee Synfuels Assoc., 1981). Water levels in deep and shallow well pairs near the river indicate upward hydraulic gradients, even from great depths below the base of the river (DOE, 1996, Tennessee Synfuels Assoc., 1981). The vertical gradients, in conjunction with the uniform baselevel heads created the by reservoir all along the valley, suggests that the river serves as a hydrologic boundary to groundwater flow. A water balance completed for the ETTP Main Plant area suggests groundwater discharge is to Poplar Creek with little potential for underflow (DOE, 1996).

Within the Knox carbonates on the flanks of Blackoak Ridge, chert-rich beds weather to form cherty gravel intervals which retain the original bedding orientation. These higher permeability relict bedding features have been documented to serve as preferential groundwater flowpaths in the unconsolidated zone above Knox bedrock (DOE, 1997a). In contrast, the overburden above the Chickamauga carbonates weathers to a silty clay with little or no relict bedding features. Groundwater flow in the unconsolidated zone above the Chickamauga along the valley bottom is believed to follow the direction of the steepest hydraulic gradient, effectively, perpendicular to the equipotential contours shown on Figure 2.8. This assumption is supported by the geometry of mapped plumes in the Main Plant area (DOE, 1996; DOE, 1997b).

Groundwater flow in the bedrock occurs mainly along the higher permeability flowpaths such as fractures, solutionally enlarged fractures and conduits. Map scale structural features such as the Whiteoak Mountain Fault, smaller features associated with the aforementioned deformation zone, and solutionally enlarged axisymmetric fractures associated with mapped anticlines and synclines likely serve as primary bedrock flow paths within the Chickamauga carbonates. Karst conduits dominate groundwater flow in the Knox Group carbonates. The direction of groundwater flow in bedrock is controlled by the governing hydraulic gradient and the orientation of such features relative to that

gradient. In general, strike-parallel flowpaths predominate in the Valley and Ridge (Swain *et al.*, 1991), particularly where the hydraulic gradient is parallel to bedding strike.

The meandering nature of Poplar Creek creates several isolated peninsulas, such as the Duct Island and Power Plant areas of the site. Due to the limited surface area within these isolated tracts, recharge to groundwater is limited and the flow, as indicated in Figure 2.8, is clearly towards the surrounding surface water bodies. Within the Main Plant area, the high degree of impervious cover (paved areas, building roof areas) and an extensive network of storm drains increase the runoff from the site thus limiting groundwater recharge from rainfall. However, it has been demonstrated (DOE, 1996) that leaking water supply lines represent a significant source of perennial recharge to groundwater within the industrialized portions of the study area. The recharge area for groundwater in the Knox Group carbonates along Blackoak Ridge is clearly constrained by topography, in particular by Poplar Creek which cuts through the ridge. However, considering the cavernous nature of the bedrock, the linear trend of sinkholes extending along the valley paralleling the Knox-Chickamauga contact and the large (yet untested) microgravity anomalies identified along this trend, it is possible that the catchment area for any springs occurring in the river or creek along this trend may be much larger than indicated by topographic watersheds. Karst watersheds commonly differ from those suggested by topography (Ford and Williams, 1989)

Swain *et al.* (1991) observed that within the Valley and Ridge province, the master drains which cut across the ridges and valley floors serve as baselevel drains. The majority of groundwater discharges to one or more large springs along or directly to the master streams. Hence, it was expected that large springs would occur along both Poplar Creek and the Clinch River within the study area. However, a thorough, multi-season inventory of springs was conducted by the USGS (reported in DOE, 1996) which revealed a number of ephemeral seeps, typically encountered at higher elevations, but few perennial springs along the river or creek. Springs are shown on Figure 2.8. Those that

were encountered are small, with flow rates typically < 0.001 m^3/sec (5 gpm). The largest spring (16-007 on Figure 2.8) is located along East Fork Poplar Creek, just upstream of the confluence with Poplar Creek and occurs within the upper Mascot Dolomite near the Knox-Chickamauga contact (DOE, 1996). Spring 16-007 discharge ranges between a maximum of 0.04 m^3/sec (550 gpm) and a minimum of 0.006 m^3/sec (95 gpm).

Within the study area, other key perennial springs include springs 8-900 and PCTZ-1 and -2 located along the north shore of Poplar Creek along the "M"-shaped bend, and spring 21-002 which feeds the K-901 Pond. A group of ephemeral springs located slightly upgradient of spring 21-002 have been observed to function as overflow springs when the discharge capacity at 21-002 is exceeded (DOE, 1997a). Continuous monitoring data for these springs (Zondlo, 1997, unpublished) reflects an interdependence with the adjacent surface water body; spring flow varies in response to stage changes.

A number of large springs occur along the Knox-Chickamauga contact outside the study area along East Fork valley (DeBuchananne and Richardson, 1956). Hollyday and Smith (1990) present data for one such spring, Crystal Spring, which is located roughly 2.5 km upvalley of spring 16-007. This spring flows at rates ranging from 0.009 to 0.09 m^3/sec (0.32 to 3.2 cfs). The nearest spring within East Fork valley on the opposite side of the Clinch River for which there are flow records is located 4 km away along strike. The discharge rate for this spring has been documented as 0.0003 m3/sec (0.01 cfs) by DeBuchananne and Richardson (1956). Hollyday and Smith (1990) compiled data on large springs within the Valley and Ridge in Tennessee. The highest reported spring discharge rate was 1.23 m^3/sec (43.7 cfs) for Cave Spring near Hixson, Tennessee. Very few springs are documented as occurring in the Chickamauga along the entire East Fork Valley. Those few that have been reported occur in the lowermost Chickamauga Group outcrop belt.

While large perennial springs were not identified within the study area, a number

of large boils have been observed along the exposed banks of the Clinch River and Poplar Creek under low pool stage conditions. Often these develop with "potholes" up to a meter in diameter in the bank sediments, discharging to the river/creek at rates of up to ~0.002 m^3/sec (25 gpm). However, upon revisiting these locations many times over the past two years, it is clear that these points of groundwater discharge are highly transient and tend to shift from location to location depending on ambient hydrologic conditions (antecedent recharge, stage). This highlights the transient nature of overall patterns of groundwater discharge in the study area. Many of the springs identified within the study area appear to function as overflow springs that flow only during or following recharge events that exceed the capacity of lower (presumably subaqueous) springs to discharge groundwater.

Given the industrialized nature of the study area, not all groundwater flowpaths are natural in origin. For example, several key storm drains which discharge to Poplar Creek in the industrialized Main Plant and K-33 Peninsula areas have been observed to flow perennially, even during periods of extreme drought (DOE, 1996). Portions of these drains are situated below the water table, particularly at lower elevations adjacent to Poplar Creek and are discharging infiltrating groundwater directly to Poplar Creek. Storm drain video surveys have shown many of these submerged areas to be gaining reaches (i.e., groundwater is infiltrating into the drains). Consequently, the storm drains serve as focused points of groundwater discharge. The magnitude of the influence of these drains on local groundwater flow is unknown, but it may be sufficient to preclude the possibility of other direct groundwater discharge points within the capture zone associated with the drains.

Groundwater temperatures fluctuate seasonally following trends in mean monthly air temperature. The perennial springs display a range of temperatures between 12.5 and 15 °C. This is consistent with the long term range of groundwater temperatures or record from the 250 wells at this site (Figure 2.6, bottom panel). Based upon ten years of data,

the long term mean monthly groundwater temperature for February and March is approximately 14.5 °C.

As described previously, stage conditions in the Clinch River and Poplar Creek are highly transient, creating constantly changing boundary conditions throughout the year. Seasonal stage patterns represented by low pool stage in the winter and high pool stage in the summer combine with seasonal patterns of groundwater recharge (dictated by rainfall and evapotranspiration) to yield two distinct flow regimes. In summer months, the water table declines in higher elevation areas of the site due to evapotranspiration while the water table at lower elevations adjacent to the surface water bodies tends to increase in response to high pool stage. This results in significantly reduced hydraulic gradients and consequently, reduced groundwater flux. In contrast, in the winter months, low pool stage conditions, a lack of evapotranspiration, and the occurrence of high intensity, longer duration winter rainfall all combine to create the steepest hydraulic gradients and consequently, the highest groundwater flux.

In addition to seasonal components of flow, the transient nature of bounding surface water features has been shown to have a significant effect on groundwater flow (Energy Systems, 1995; DOE, 1996). Continuous water level data for nearly all shallow unconsolidated zone wells and deeper bedrock wells proximal (within 100-200 m) to the river and creek show that water levels fluctuate directly in response to changes in stage. Stage impacts have also been observed in wells nearly 700 m removed from the river and in bedrock wells completed nearly 30 m below the bottom of the Clinch (Tennessee Synfuels Assoc., 1981) although the responses are attenuated with distance from the surface water body. Stage induced water level fluctuations are most apparent during high pool stage conditions in summer and but are less noticeable in winter when masked by rainfall events which dominate the hydrographs (Energy Systems, 1995). This is shown in Figure 2.9, which presents continuous water level data for select Chickamauga and Knox bedrock wells in 1993-94. Nonetheless, these "tidal effects" demonstrate the close

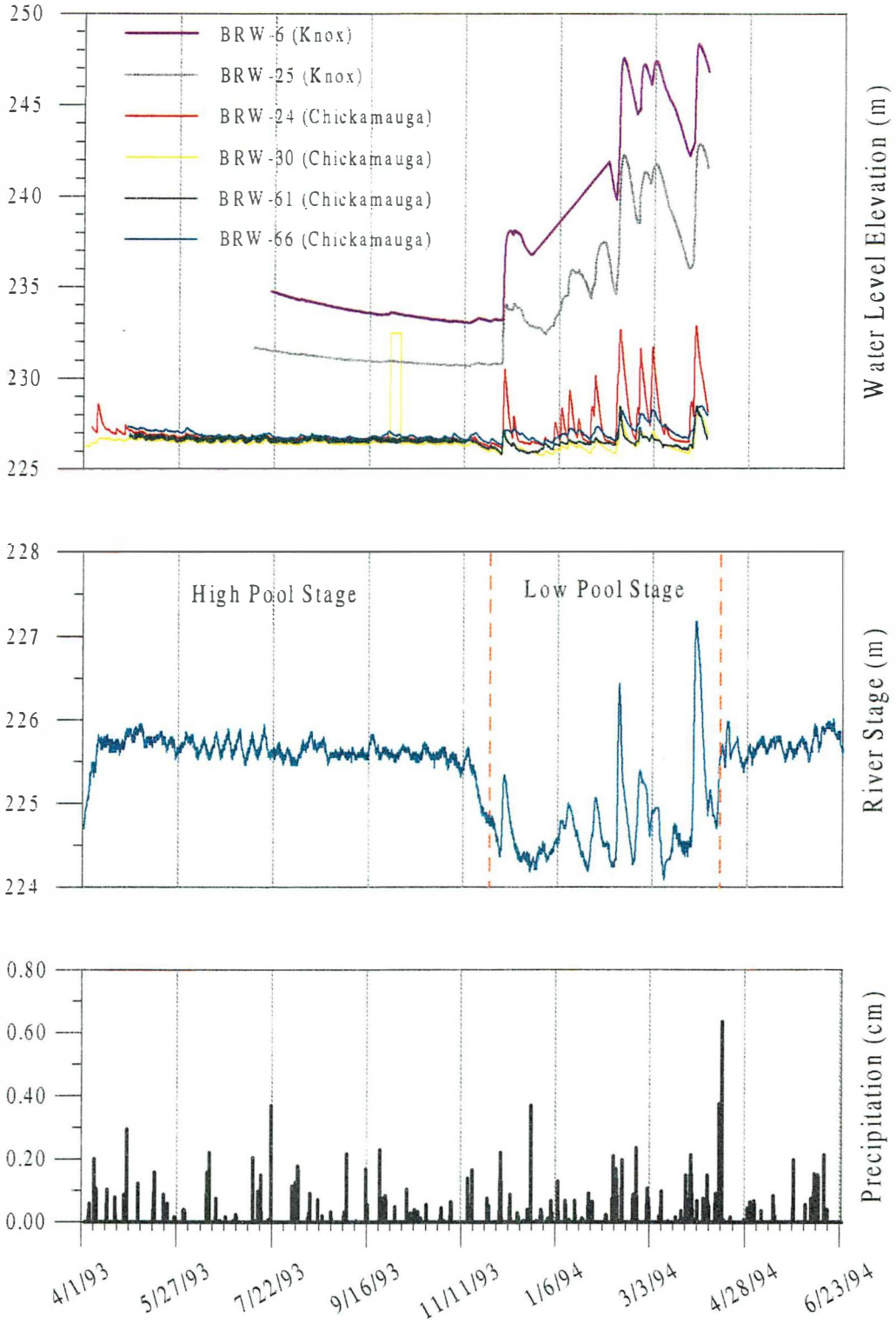


Figure 2.9. Composite hydrographs for select Chickamauga Group and Knox Group bedrock wells that monitor karst solution cavities (upper), Clinch River stage (middle), and precipitation (lower), 1993-1994.

hydraulic connection between surface water and groundwater.

Figure 2.9 also reveals a difference in response to rainfall between the Chickamauga along the valley bottom and the Knox and lower Chickamauga Group carbonates along the flanks of Blackoak Ridge. Bedrock wells in the upper Chickamauga carbonates along the valley bottom, including those which monitor cavities (lower panel of Figure 2.9), show a flashy response to rainfall events in the winter months (DOE, 1996, Energy Systems, 1995). The lag between onset of rainfall and peak water levels is approximately 1-3 days; recessions to pre-storm levels commonly last 4-7 days. In contrast, wells completed in cavities in the Knox carbonates (Figure 2.9, upper panel) display a larger range in water level increase and the lag to peak water levels follows rainfall by 4-7 days. Additionally, rather than receding to pre-storm baseflow levels between recharge events as in the Chickamauga, the water levels in the Knox Group bedrock wells only recede slightly but continue to increase throughout the winter months. The slight recessions coincide with decreases in river stage but never achieve pre-storm initial water levels.

While river stage clearly impacts groundwater levels and flux in the summer months, as shown on Figure 2.10, hydrographs developed from continuous water level data for wells in the Knox along the flanks of Blackoak Ridge (Zondlo, 1997 unpublished) suggest that river stage regulates the rate of groundwater discharge and thus the heads in the aquifer adjacent to it in winter months as well. Although small scale stage fluctuations are not discernible in the well hydrographs during the wet season, the storm responses in wells appear to be superimposed on the broader stage responses, mimicking the broader stage patterns. Similar to the Trebisnjica River impoundment example of Milanovic (1986) discussed earlier, increased river stage decreases the hydraulic gradient which in turn reduces the discharge rate and extends the recession period following a storm.

It is expected that during high stage and high intensity recharge events, the

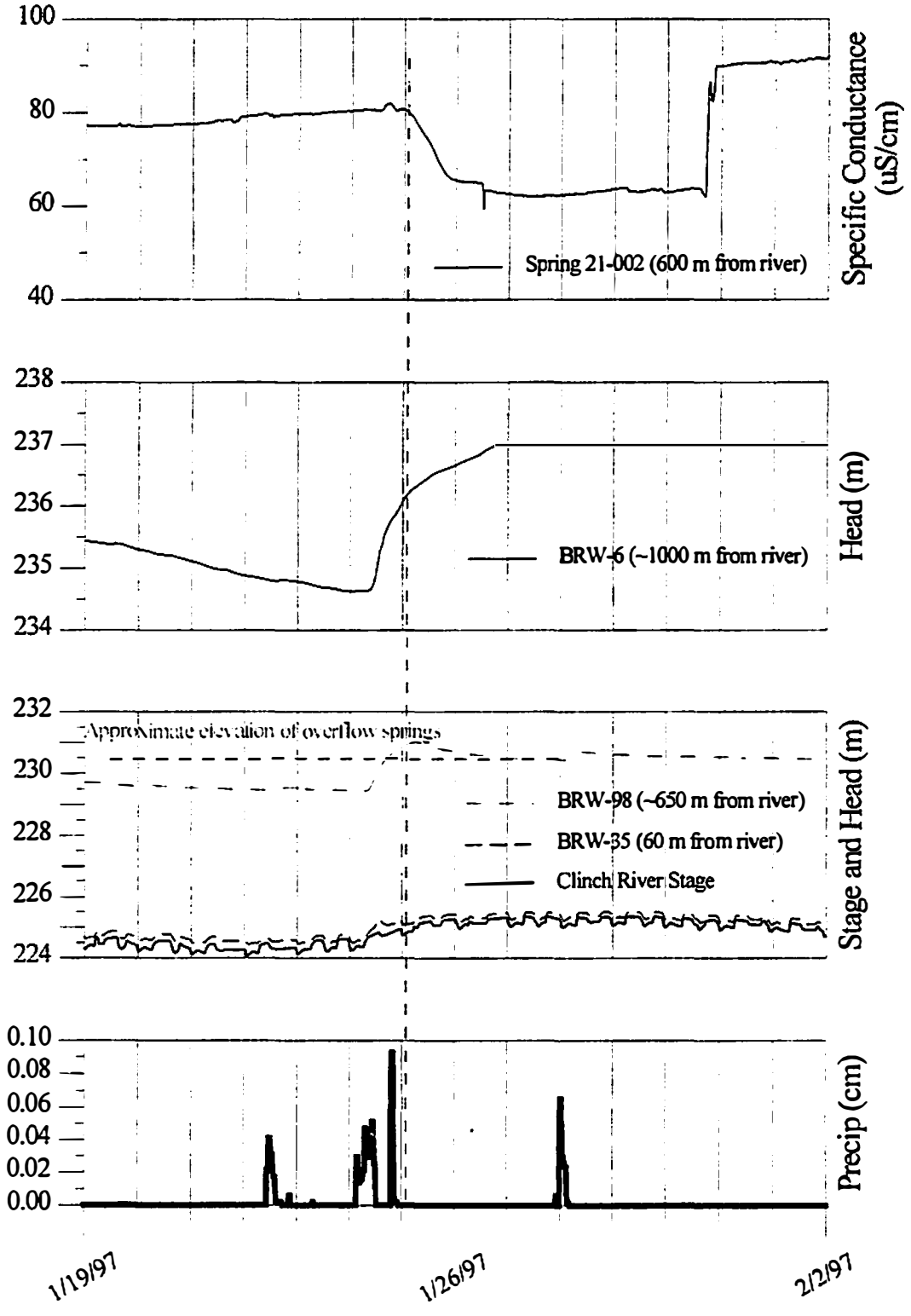


Figure 2.10. Composite hydrograph for wells and springs in the Knox Group within the study area showing aquifer response to stage and rainfall.

capacity of subaqueous springs in the Clinch River to discharge groundwater is exceeded and causes groundwater to "back up". Bedrock wells such as BRW-35 (shown on Figure 2.10) located 60 m from the river show strong stage control on water levels but little recharge response. BRW-98, the next upgradient cavity well, begins to respond shortly after stage increases begin. The water levels in this well which is located ~650 m inland from the river but only 9 m above the river level rise to a peak elevation of 230 m triggering discharge at nearby spring 21-002. Spring 21-002 discharge is evidenced by a sharp change in specific conductance that coincides with the peak in BRW-98. Eventually, the discharge capacity of the 21-002 spring is exceeded, which triggers discharge at upgradient "overflow" springs. As the capacity of these springs is exceeded, water levels continue to rise within the aquifer, progressively filling upper cavities and the unconsolidated zone. Well BRW-6 is located approximately 1000 m inland from the river at an elevation of 248 m, but is screened across a large cavity positioned at an elevation equivalent to the base of the Clinch River. Comparing the shape of the hydrograph for upgradient cavity well BRW-6 (Figure 2.9, 2.10) to stage suggests that water levels in the aquifer are controlled by stage.

As stage recedes (due to flood control management by TVA), heads in the aquifer away from the river begin to recede, but the rate of recession is slower than the surface water recession. Consequently, the bulk of the groundwater flux occurs during the recession following storms when stage is low or being lowered and hydraulic gradients to surface water are greatest. In the absence of additional rainfall events in the interim, the groundwater recession for a single high intensity rainfall event may last for several weeks, though periods of high groundwater flux are of shorter duration within the recession limb of the hydrograph.

Overall, the storm hydrograph for Knox Group cavity wells BRW-6 and -25 in the Knox, although displaying considerable range, are much less flashy than would be typically expected for large conduits with low storage capacity. Consequently, this is

interpreted as evidence that the recharge area to the conduit network in the Knox is much greater than implied by topographic watersheds, and possibly extends a great distance upvalley along strike.

This model of stage controlled groundwater flow is supported by results of a multi-dye tracer test conducted during the winter of 1996 which delineated a flowpath between wells located approximately 1000 m upgradient of the river and downgradient overflow springs at elevations slightly above the river (DOE, 1997a). Several different dyes were injected in wells (including BRW-6) constructed to monitor cavities in the Knox Group Longview Dolomite and Chepultepec Fm at depths equal to or lower than the bottom of the Clinch River (i.e., dye was injected into conduits at an elevation of approximately 213 m). The bulk of the dye mass appeared in the 21-002 spring, located downgradient above the K-901 Pond (see Figure 2.8 for location), at an elevation of approximately 228 m. The river stage during the time period immediately following dye injection was approximately 224.9 m.

While some dye must have been discharged directly to the river, the emergence of the bulk of the dye mass at this elevation above the river from an injection elevation well below river stage supports the hypothesis that the river is not only a boundary to offsite flow, but also impacts flow in the aquifer adjacent to it. Dye was not detected at any of the perennial springs monitored on the opposite side of the river. This adds additional confirmation of the role of the river as a boundary condition to flow from the ETTP site.

Although the primary karst pathway was to the 21-002 spring, over the next several months, with subsequent rainfall events, the dye began to appear in other wells (including the unconsolidated zone wells). This indicates a well developed network of conduits and solutionally enlarged fractures in the Knox which function as a *dis*tributary system as recharge and discharge boundary (stage) conditions change.

Given that a large number of karst features are evident within the study area, karst flow must have been significant at one time to have formed the features observed.

However, similar to the case presented by Milanovic (1986) for the Trebisnjica River impoundment in Dinaric karst, the impoundment of the Clinch River in 1939 may have dramatically altered the dynamics of the karst system in the vicinity of the study area and potentially, all along this strike valley within the Knox and lower Chickamauga formations. Whereas the pre-impoundment river levels were 6-7 m lower than at present and decreased progressively downstream, but now the controlling baselevel stage is effectively the same all along the valley from the study area downstream. The increase in baselevel may have inundated previous springs and "backed up" the flow system due to the reduction in gradient and thus discharge from groundwater. This also resulted in the formation of overflow springs further upgradient along the karst network, such as spring 16-007 where the Knox unconformity contact intersects East Fork Poplar Creek.

Consequently, although there is likely a large conduit network associated with the Knox-Chickamauga contact microgravity anomalies, these are likely flooded and do not act as groundwater sinks. In fact, both East Fork Poplar Creek and Poplar Creek cross this trend several times without apparent loss of flow. These surface water bodies are likely discharge points for the underlying subsurface conduit system and it is expected that there may be gaining reaches along them.

Conceptual Model

In summary then, differences between lithology (carbonate versus clastic), stratigraphy, and structural style define three principal hydrogeologic regimes, two of which are relevant to this research since they are encountered along the Clinch River and Poplar Creek. These regimes can be related to the structural domains (A and B) noted previously on Figure 2.3 as defined by Lemiszki (1995) and can further be distinguished on the basis of degree of karst development, groundwater recharge, and groundwater flow.

The first hydrogeologic regime encompasses the monoclinally southeast-dipping Knox Group carbonates and the overlying lower Chickamauga (Stones River Group)

carbonates extending from Blackoak Ridge to the aforementioned deformation zone. This domain is laterally extensive, trending unimpeded all the way up East Fork Valley above the study area as well as continuing downvalley on the opposite side of the Clinch River. Karst features are well developed within this regime, possibly related to paleokarst development in the Knox and likely represents a large catchment area for recharge, potentially extending from the Clinch River within the study area to the city of Oak Ridge. Groundwater flow is expected to be dominated by a series of well developed and interconnected roughly strike parallel conduits which integrate flow along smaller fractures in the diffuse zone.

The second hydrogeologic regime of interest includes the structurally deformed middle to upper Chickamauga Group carbonates that occupy the bulk of the valley bottom in the Main Plant area, extending from the deformation zone in the middle Carters Ls to the Whiteoak Mountain Fault. Karst development in this regime is less well developed, possibly due to a limited area of groundwater recharge imposed by the truncation of these formations by the K-25 fault. Groundwater occurs in the unconsolidated overburden above bedrock, where present and unconsolidated flow is expected to follow hydraulic gradients inferred from maps of the potentiometric surface. Flow in bedrock is controlled by a combination of hydraulic head and geologic strike and is expected to be dominated by fractures, solutionally enlarged fractures and small karst conduits developed along macroscopic and mesoscopic faults and folds.

In all regimes, hydraulic gradients are greatest during winter months when Poplar Creek and Clinch River stage are maintained at low pool stage, evapotranspiration is non-existent, and thus recharge related to winter rainfall is at a maximum. The net result is that groundwater flux is highest during winter months, particularly, during recession periods following high intensity, longer duration rainfall events.

Because the Clinch River represents the lowest possible hydraulic head in the valley, both upgradient and downgradient for some distance, the river serves as a

discharge boundary for groundwater. Further, because the Clinch River (and to some degree Poplar Creek) cut directly across strike, these surface water features potentially intersect all possible shallow flowpaths from the ETTP site, as well as integrating deeper local or regional flowpaths. The sparsity of groundwater springs along the shore of the Clinch River and Poplar Creek suggests that most of the groundwater discharge to surface water occurs through subaqueous springs, possibly along the pre-impoundment channels. Further, since the Clinch serves as the master drain for the valley and is incised more deeply than Poplar Creek, groundwater may be discharging as upgradient overflow springs in the creek along strike. All groundwater discharge is controlled by opposing heads related to river stage, which in turn is highly variable and transient in response to TVA reservoir operations and rainfall. A key attribute of all subaqueous springs is that they only rarely function as perennial springs and characteristically display a wide range in discharge rates over time when functioning (Milanovic, 1981). Bonacci (1987) observed that individual subaqueous springs are often components of a larger, more complex springs system acting as a distributary system rather than a single conduit discharge point. All of these springs function differently, either independently or collectively, under differing ambient hydrologic conditions (stage, season, recharge). Similar distributary systems have been described in the Mammoth Cave system by Conlon and Ewers (1989), and are expected to occur within the study area.

Identification of Key Target Areas for Subaqueous Groundwater Discharge

Considering the conceptual model and current understanding of the hydrogeologic framework of the study area, there are a number of reaches within the Clinch River and Poplar Creek where groundwater discharge as subaqueous springs may be expected to occur. Basically, these "target" areas combine intersections of surface water with key stratigraphic, structural, and karst features or trends. Structural features increase fracture density which in conjunction with changes in lithology create stratabound flow intervals which further focus karst dissolution. These features or trends are therefore expected to

focus groundwater discharge within the Chickamauga along the valley bottom (hydrogeologic regime B).

Given the hydrogeologic conditions within the study area, it is also expected that groundwater discharge may occur along the shoreline as a continuous seepage face where the river or creek truncate flowpaths in the unconsolidated zone. In areas where the water table occurs below the top of bedrock or bedrock is exposed along the surface water boundary, groundwater discharge is expected to occur as either discrete subaqueous springs related to key flowpaths or as a spring "zone" associated with interconnected, interdependent flowpaths along a distributary conduit or fracture network.

It is expected that bedrock groundwater discharge would be focused at the first, upgradient-most intersection with the creek or river and the key features and trends. These locations would serve as "knick-points" representing the first intersection of the lowest possible local hydraulic heads along strike dominated flowpaths. Cherkauer and McKereghan (1991) observed a similar phenomenon in studying groundwater seepage into Lake Michigan where it was noted that nearly 60% of the groundwater discharge was focused in embayments along the shore which penetrate further upgradient into the groundwater system and cause convergence of equipotentials towards them.

Key target areas where subaqueous groundwater discharge would be expected to occur are shown in map form on Figure 2.11. Assuming that groundwater springs would have been present along the pre-impoundment river/creek channel, subaqueous groundwater discharge may still be evident along or above the former channel where it intersects the following features and trends:

- reactivated paleokarst features associated with the regional unconformity marking the contact between Knox and Chickamauga carbonates (map locations A1 through A4);
- within the middle to lower Pond Springs Fm related to the conspicuous trend of surficial karst features (sinkholes) extending up and down valley on both sides of the river (map locations B1-B4);

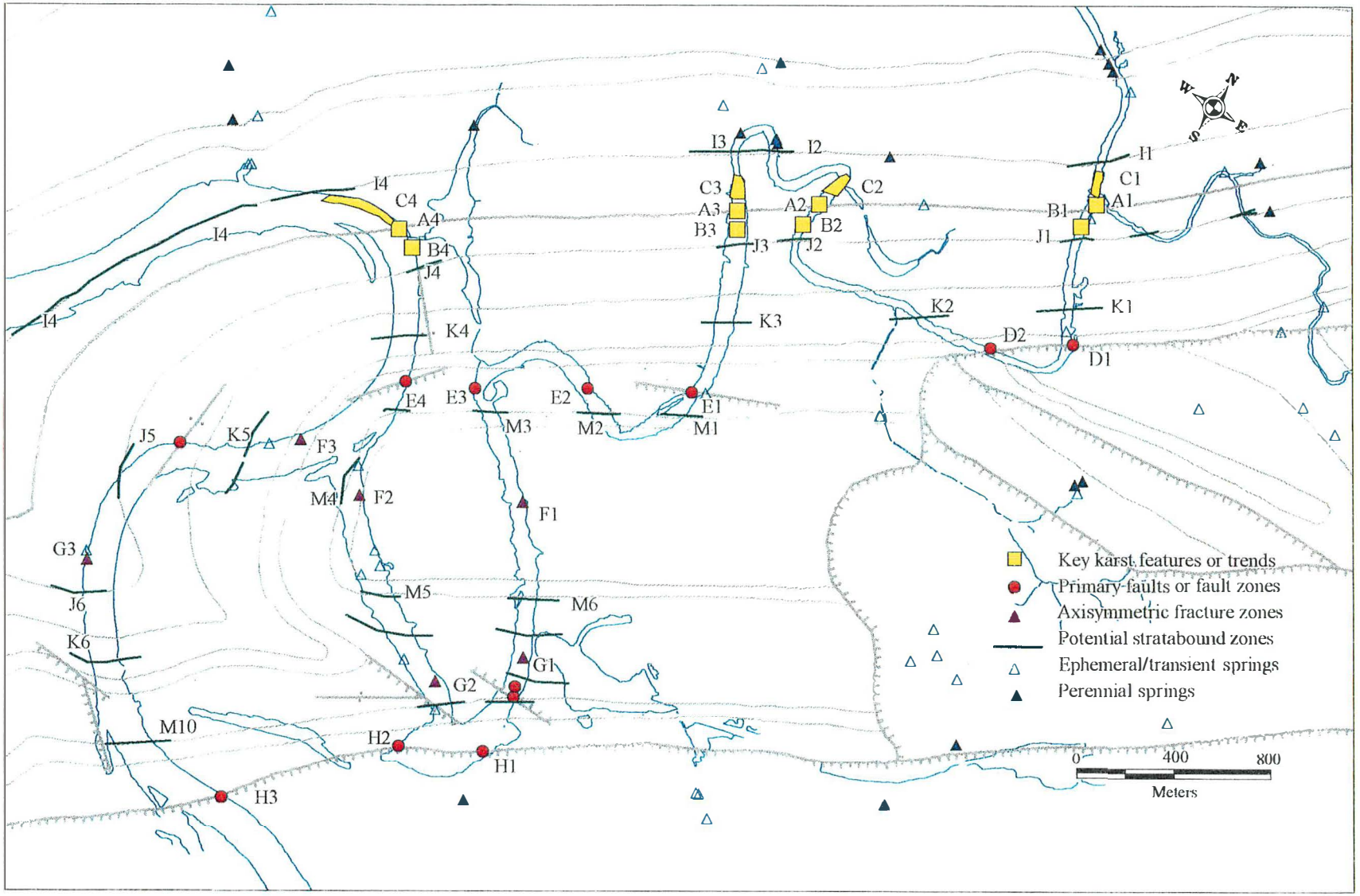


Figure 2.11. Map of key hydrogeologic targets, trends, and features where groundwater discharge is expected to occur.

- within the Mascot Dolomite of the Knox group, associated with the trend of large microgravity anomalies coupled with subsurface cavity and surface cave opening occurrence (map locations C1-C4);
- in the vicinity of faults, either related to the fault itself or the zone of intensified fracturing bounding the faults in the hanging and footwall:
  - the K-25 fault where it intersects Poplar Creek (map locations D1, D2);
  - the Whiteoak Mountain fault where intersecting the Clinch River (map locations H1-H3);
  - mesoscopic and macroscopic normal and reverse faults identified along both the creek and river associated with the deformation zone and/or the map scale anticlinal structure (map locations E1-E4);
- along the axis of macrocopic structural features, notably the map-scale anticline-syncline pair within the Chickamauga Group in the Main Plant area (map locations F1-F3 and G1-G3);
- related to potential stratabound flow zones resulting from changes in lithology within or between formations of the Chickamauga and Knox, some of which may include:
  - along the Mascot-Kingsport contact, marked by a zone of jasperoidal chert (map locations I1-I4);
  - within the middle Mascot Dolomite associated with an increase in bedded chert
  - within the middle Pond Springs Fm where bed parallel chert pods are interbedded with massive micritic limestone;
  - near the contact of the argillaceous Pond Springs Fm and the micritic limestones of the overlying Murfreesboro Ls (map locations J1-J4);
  - related to the calcareous shale in the middle of the Ridley Ls (map locations K1-K6);
  - along metabentonites (and table-top chert beds underlying them) in the middle of the Carters Ls (map locations L1-L8);
  - above the basal calcareous shale in the Hermitage Fm (map locations M1-M12)

3. METHODS

Review of Available Methods

Zektser and Meskheteli (1988) provide a summary of hydrogeologic methodologies that can be applied to locating subaqueous discharges. In general, there are four methods that are commonly employed, most of which focus on identification of temperature or other physical anomalies: 1) remote sensing (thermal infrared and multispectral imaging); 2) profiling of water and sediment columns; 3) use of diving equipment to physically explore and map bottom features; and 4) continuous profiling for anomalies along the bottom-water interface. Zektser and Meskheteli (1988) further suggest a phased approach leading from remote sensing to reconnaissance anomaly mapping (2 and 4 above) to diving/physical exploration. The latter phase is intended to confirm and quantify discrete groundwater discharges and may include point-dilution and seepage meters for determining discharge rates..

There are numerous examples demonstrating application of infrared thermography and multispectral scanning imagery to detection of groundwater discharge both on land and underwater. Recent studies performed by Banks *et al.* (1996) and Bogle and Loy (1995) illustrate the feasibility of remotely detecting thermal anomalies indicative of subaqueous discharge. In the latter case, Bogle and Loy applied these methods at a site where the impoundment of the Tennessee River by Chickamauga dam resulted in the inundation of smaller tributaries and embayments proximal to their study site, creating a setting very similar to that found at the ETTP study area. TVA pre-impoundment maps indicated the existence of 5 distinct springs now inundated in this quiescent embayment at water depths of up to 6.1 m. Use of low altitude, infrared thermography was successful in locating 9 submerged springs, though none of the original five TVA springs were detected. In general, those springs that were identified were found in shallow waters ranging from 1.5-3 m deep discharging from solution cavities and joints in bedrock

exposed along the bottom. Several of these were physically identified through diving and were manifested as ice-free areas when the embayment later froze over.

A local resident provided the exact location of a pre-impoundment spring not previously noted on the TVA surveys. Diving showed the spring to be emanating from a now submerged cave opening roughly 0.5 m^2 located 6 m below the surface. This feature was not detectable at the surface using thermal IR methods.

Infrared thermography was attempted within the ETTP study area as part of a corollary project. Multispectral analysis was applied to pre-dawn thermal IR flyover data from March 1992 and March 1994. Limited ground truthing data was applied to the imagery in order to calibrate the spectral responses to temperature. This work was performed by ORNL with results reported in DOE, 1996. However, apart from several bank springs or springs located along tributary feeder channels, the method was unable to distinguish discrete springs in either the Clinch River or Poplar Creek. The data did however clearly illustrate temperature differences between Poplar Creek and the Clinch River (Poplar Creek being somewhat warmer), and the active channel in the river (denoted by colder water). The 1994 survey, which was of higher resolution, was apparently performed during a period when flow rates were relatively high in both the Clinch River and Poplar Creek. Given the flow conditions and greater water depth, it appears the applications of infrared thermography in this setting are limited.

Vroblesky *et al.* (1991) describes an intrusive method that involves the use of driven creek-bottom samplers to detect groundwater discharge to surface water. In this case, contaminants analyzed in vapor samples collected from the bottom samplers were successfully used to identify contaminated groundwater discharge in a shallow coastal application.

Previous Investigations

Although various papers suggest the potential of for mapping subaqueous discharge of groundwater using thermal or other methods, there are relatively few

documented cases of actual application of this approach in the literature. Those that were identified share some common elements with the approach applied in this research. The following is an overview of the previous studies that utilized similar methods to address a common objective of identifying groundwater discharge to surface water bodies on the basis of temperature and/or specific conductance anomalies.

The work of Hess *et al.* (1974) on identifying karst springs along the Green and Barren Rivers in the vicinity of Mammoth Cave, Kentucky represents a rudimentary approach to finding springs from a technological standpoint. In that effort, the river banks were floated in a small boat and a thermistor and specific conductance (SC) probe was trolled along the boat in order to identify anomalies indicative of springs. The surveys were purposefully conducted during a period of the year (in this case, summer to early fall) representing the maximum contrast between groundwater and surface water temperatures and the minimum river stage. A total of 105 springs were identified and in general, showed a temperature or specific conductance signature indicative of groundwater discharge. Most of the springs that were found were identified based on visual features such as small subtle notches under trees along the river bank, spring resurgence channels, or discrete cave openings. Only a very small percentage of the springs were actually located on the basis of temperature or SC changes. One observation of note from that study was that the flow conditions at the springs were clearly related to the difference between the hydrostatic head caused by the river stage and heads in the aquifer and recharge in the catchment area at any given time . Consequently, at different times and under differing hydrologic conditions, springs were noted as either discharging to the river, serving as sinks recharging the aquifer, or in null flow mode. The nature of the springs varied as the boundary conditions changed.

In the 1970's there was considerable interest in the ecological impacts of nuclear and other utility plant cooling water effluent on receiving water bodies. Staff from Argonne National Laboratory (Frigo and Frye, 1972; Madding *et al.*, 1975) developed a

system for delineating the extent of thermal plumes and applied this to study power plant effluent plumes along the shores of Lake Michigan. In many respects, the setup they used closely resembles that developed for this effort with the exception that, at that time, those workers did not have access to advanced technologies, including the portable computer, digital equipment, and Global Positioning Systems (GPS), that are commonplace today. Further, they were focused on surface temperature anomalies rather than lake or river bottom anomalies.

The system used by the Argonne researchers consisted of a 2-channel digital thermometer that was connected to a series of thermistors set on a downrigger arm attached to a small boat; thermistors were set at 0.5 m intervals along the downrigger arm. Initially, measurements were made by manually switching a selector between the thermistors and then manually recording the data. Later designs eliminated the manual interrogation and recording and used a digital mainframe thermometer with a thermistor plug-module. Analog temperature data was subsequently digitized and then visually displayed and recorded on magnetic cassette tape. Digital time from a separate clock and the three channels of temperature data were output to an onboard plotter to record the data. In early applications, locations of discrete measurements were crudely determined in the field by interpolating boat speed and elapsed time between pre-established buoys. Later, a microwave rangefinder system was employed using two fixed, shore-based transponders and an on-board receiver/transmitter and range console. The range data was later translated using trilateration into boat position in a subsequent computer processing step. Digital depthfinder data was output in binary form for subsequent integration with other data streams.

Most recently, Lee and Dal Bianco (1994) developed a system for delineating and measuring groundwater seepage into the Onaping River in Ontario. In this case, a specially-developed bottom contacting probe was towed along the river bottom behind a small boat in water depths up to 3.5 m. The technique provided continuous recordings of

specific conductance along the sediment-water interface that were used to identify mining-related contaminated groundwater discharge. Similar to this thesis research, Lee and Dal Bianco employed a three-man crew to perform the surveys. A portable computer and paper chart recorder provided for data recording and visual display of the data, respectively. Custom software was developed for this application to later link the probe data with positional data. The positioning system consisted of a shore-based tripod and theodolite (for angle and elevation), a small computer, a radio-telemetry unit and a laser range finder. This approach proved quite successful in detecting seepage locations (where SC was found to be several orders of magnitude higher than background) in a river system with flow rates on the order of 0.2 -0.3 m/sec. However, since the probe is towed behind the boat, the location of the probe and thus the anomalies, was poorly controlled (~3 m spatial accuracy). Further, there was no capability to track position in the field. It should be noted that seepage confirmation required the subsequent installation of piezometers and seepage meters placed in the river bottom in areas of the SC anomalies. Piezometer and seepage meter indicated groundwater heads ranging from 0 - 75 cm above the river stage, with seepage rates on the order of 0.005 to 0.008 m/sec (the ratio of ambient river to seepage flows was ~ 40).

In 1995, a system was developed to identify springs in the Clinch River adjacent to the ETTP site by the author. The equipment was field tested on the Clinch River within the study area over a five day period in early spring of 1995, following a very warm winter. The results of that effort (reported in Zondlo, 1995a, 1995b) were encouraging in that a temperature anomaly of approximately 0.96°C was encountered and confirmed by multiple passes. A number of smaller anomalies were also identified but considered questionable at the time since the surface water temperatures were rising during the study period and were approaching the range of expected groundwater temperatures. The field testing period also highlighted the need for more detailed bathymetry information in order to more effectively complete survey runs. The

bathymetric data was obtained for the Clinch River and Poplar Creek in June and July of 1995 and consisted of nearly 23,000 measurements of water depth.

Method Description and Procedures

Although designed independently of the systems described previously, the method used in this research is conceptually similar to the approaches of Hess *et al.* (1974) and Lee and Dal Bianco (1994) but utilizes state-of-the-art technologies and equipment not available to previous workers. The method is briefly summarized below and a detailed description of the components and design are provided in Zondlo (1996).

With this system, shown schematically in Figure 3.1, a Hydrolab multi-parameter water quality monitoring device was suspended from a small boat and trolled along the bottom of Poplar Creek and the Clinch River. As shown in Figure 3.1, the Hydrolab is housed in a perforated, protective PVC sleeve fitted inside a stainless steel cage which is dragged along the river bottom. The cage is attached to a hand-operated winch system via three cables which in turn are connected to three worm gear winches. A single crank and series of belt-driven pulleys allow all three winches to be operated simultaneously, thus raising or lowering the cage directly below the boat. This winch system is capable of operating in water up to 15 m (50 ft) deep but, since the winch system is hand-operated, it functions best where either water depths are relatively consistent or bathymetric information is available to select a course that minimizes the need for rapidly changing the probe depth. A three-person crew was required to operate the electronic equipment, navigate, and operate the winch works.

Temperature, specific conductance, dissolved oxygen, and pressure (head/water depth) data was collected continuously at 1 second intervals along multiple traverses oriented roughly parallel to the shoreline. A digital depth finder and transducer mounted at the bow of the boat was used to monitor water depth and bottom configuration so as to allow for rapid vertical positioning of the Hydrolab cage with respect to the bottom. An on-board GPS receiver provided continuous information on the position of the boat. The

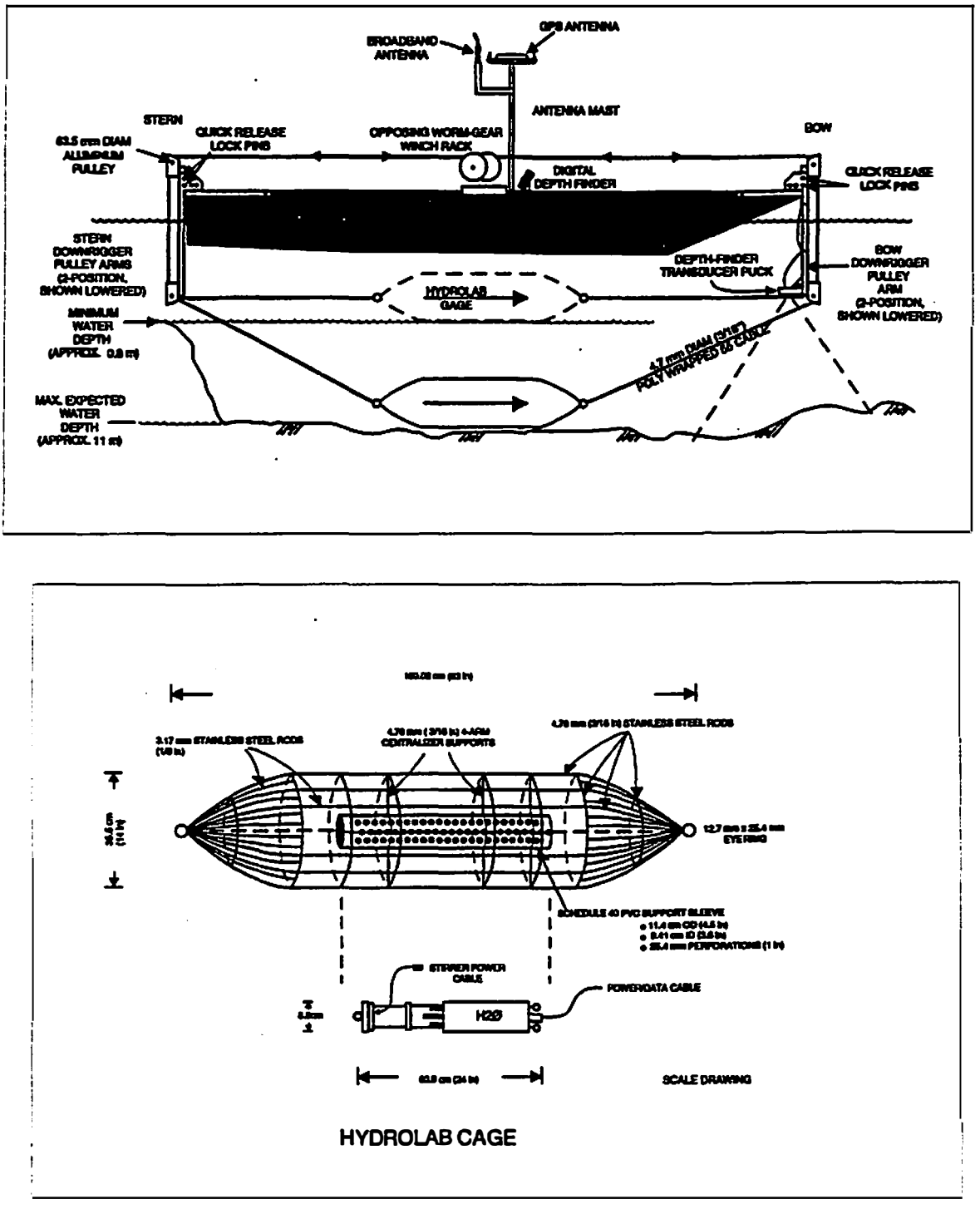


Figure 3.1. Schematic diagram of field data acquisition system. Upper figure shows the overall configuration. Lower figure shows Hydrolab cage details.

GPS receiver antenna was mounted in middle of the boat, directly above the Hydrolab cage and consequently, the position of the Hydrolab was also known. Real time differential corrections were simultaneously applied to the GPS data stream from the on-board GPS receiver.

The corrected position information was ported (serially) to two on-board portable computers (PCs), one of which was dedicated to data acquisition and the other used for navigational purposes. The serial data stream from the Hydrolab was synchronously merged with corrected GPS data using commercially available software (GeoLink, developed by GeoResearch, Inc.) and recorded on the data acquisition PC. The merged Hydrolab-GPS records were manually annotated with water depths read from the digital depth finder. Five deep-cycle marine DC batteries supplied power to the electronic components as well as an electronic trolling motor used to position the boat. Boat position was continuously charted over composite images of the site (high resolution orthophotos, thermal IR, geology, and bathymetry) on the navigational PC. Figure 3.2 schematically depicts the electronic components in this system.

With differentially corrected GPS (DGPS), location information is recorded by an onboard GPS receiver, in this case, Ashtech Ranger ME-XII units were used. In typical applications, data is simultaneously recorded at a base station of known location. The difference between the known location and the GPS determined location obtained for that base station are then used in a post-processing step to correct remote GPS receiver data. With real-time corrected (RTCM) DGPS, the locations obtained in the field are simultaneously corrected.

In this case, two modes of integrating real time corrections were employed. In the first case, a temporary GPS base station was established within the study area at a known location and UHF radios were used to transmit the corrections serially from this field base station to the remote, on-board GPS receiver. This was the method utilized during the 1995 field testing period. For the second method, correction data were transmitted to a

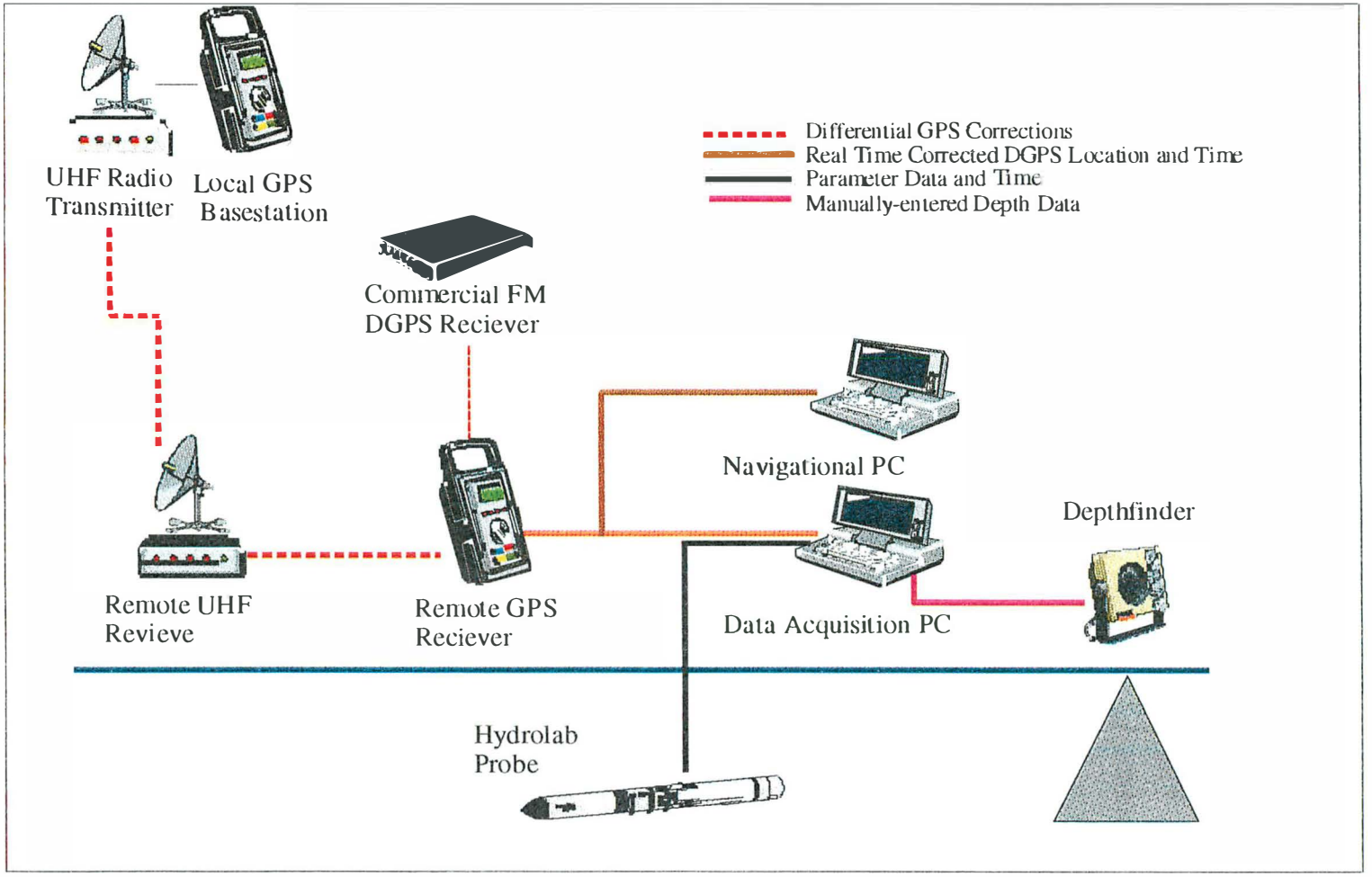


Figure 3.2. Schematic diagram of the principal electronic data acquisition components.

remote receiver via broadband FM radio broadcast from a commercial subscription service. Both methods are shown schematically on Figure 3.2. Based upon field experience with both methods, the former, though slightly more complicated and equipment intensive, proved more reliable. The lack of reliability for the FM broadband corrections may in part be attributed to the subscription service provider but also reflects limitations on FM signal reception in certain areas of the site. For example, the TVA high-tension power lines that transect the "M" bend on Poplar Creek as well topographic interferences within the Blackoak Ridge water gap and other deeply incised areas of Poplar Creek resulted in a loss of DGPS capability using the commercial correction service.

In order to optimize the probability of identifying subaqueous groundwater discharge, the field data acquisition was conducted during the period of the year when the greatest temperature differential between groundwater and surface water was expected to occur. As shown on Figure 2.6, which shows long term average monthly temperatures for both, this occurs during February and March, which also corresponds to the period of highest groundwater recharge. Comparing Clinch River surface water temperatures for the 1996 field period (6-6.5 °C)to the long term average groundwater temperature (~14.5 °C), yields a potential difference of 8 °C. Additionally, Figure 2.6 shows that this is also the period of the year when the river is maintained at low pool stage. Consequently, this reduces the surface area required for study considerably.

Specific conductance values for groundwater at the site (based upon site well data) range from 60 to 1200 uS/cm, with most values in the 200-300 uS/cm range. The highest SC values appear to be related to observed groundwater contamination. From data collected in the 1995 field testing period, the specific conductance of the Clinch River and Poplar Creek were observed to range from 228 to 252 uS/cm. The expected range of surface water conductivity falls within the range the range measured in groundwater Consequently, SC anomalies were expected to be minor, unless they

represented discharge of contaminated groundwater.

Stage data from nine continuously recording stage gages (shown on Figure 2.1) installed along the Clinch River and Poplar Creek provided necessary stage data for subsequent data reduction. Hourly precipitation data from an onsite rain gage operated by the Department of Energy were also used. Hourly discharge data for Melton Hill and Watts Bar dam during the study period were provided by TVA (1996).

4. RESULTS

Overview of Results

Field work was conducted over a period of 18 days in late-January to mid-March 1996. Additionally, several reaches of Poplar Creek and the Clinch River were revisited in December 1997 in order to attempt confirmation of key anomalies. However, the 1997 effort involved much less sophisticated methods: shallow anomalies were probed with a weighted digital thermistor dragged along the bottom from a canoe.

A total of 152 survey runs were performed in the Clinch River and Poplar Creek, yielding a total of 157,112 records. The field data were merged with continuous stage, calculated surface water flow, and dam discharge data. Although no distinct thermal stratification was observed in the river, a trend of gradually increasing temperatures with decreasing depth in the water column was noted during the field effort. Consequently, to insure that data are representative of bottom conditions, an initial step in evaluating the raw field data involved deleting records for locations where the suspended probe was greater than 1 m above the river/creek bottom. Note that 1 m represents the combined range of error for the digital depth finder and the Hydrolab transducer. After removing these records as well as duplicates, the final data set was reduced to 95,507 measurements of water and probe depth, bottom water temperature, specific conductance, precipitation, stage, and river flow rate. The results are summarized in Table 4.1. The overall survey coverage is depicted graphically in Figure 4.1. The field data are presented in tabular summary and graphic on a daily basis in Appendix A.

Additionally, the water depth measurements for the 1995 and 1996 field efforts were merged (total of 34,225 records) and contoured to produce a separate bathymetric map product. The bathymetry was used to determine the cross-sectional area and wetted perimeter profiles (shown in Appendix B) used to calculate flow rates in the Clinch River and Poplar Creek.

Table 4.1. Summary of field data.

DATE	RECORDS	WATER BODY	RUNS	TEMPERATURE (°C)			SPECIFIC CONDUCTANCE (uS/cm)			DEPTH (m)
				MIN	MAX	MEAN	MIN	MAX	MEAN	
1/23/96	2212	Clinch R	10	7.61	7.91	7.79	259	261	260	2.1-7.0
1/25/96	2118	Clinch R	4	7.33	7.37	7.35	219	234	228	3.7-10.4
1/29/96	781	Clinch R	4	5.94	6.01	5.97	236	240	238	1.2-8.8
2/14/96	6658	Poplar Ck	6	6.82	7.05	6.93	172	179	176	1.2-5.5
2/15/96	3737	Poplar Ck	5	7.33	8.09	7.74	184	189	186	0.9-6.4
2/19/96	5804	Poplar Ck	12	5.75	5.93	5.83	208	213	211	0.9-4.9
2/20/96	4978	Poplar Ck	10	**7.71**	**9.06**	8.17	**168**	**233**	178	1.0-3.7
2/21/96	6367	Poplar Ck	9	8.73	9.30	9.03	190	193	191	0.9-6.1
2/22/96	10319	Poplar Ck	14	9.81	9.97	9.88	188	194	191	0.9-6.4
2/23/96	3127	Poplar Ck	3	10.06	10.25	10.11	190	194	191	1.2-6.4
2/26/96	7737	Poplar Ck	12	11.02	12.19	11.53	203	209	205	0.9-4.6
2/27/96	3732	Poplar Ck	7	11.88	12.93	12.32	204	214	207	0.9-7.0
2/29/96	4064	Poplar Ck	5	11.80	12.40	12.07	205	212	207	0.9-6.1
	4070	Clinch R	6	8.91	9.42	8.98	258	274	260	1.2-10.4
3/4/96	3917	Clinch R	6	7.97	8.66	8.38	236	250	248	3.1-10.1
	2493	Poplar Ck	5	7.63	8.29	7.79	224	244	233	1.2-3.4
3/11/96	4273	Clinch R	6	7.07	8.22	7.66	206	243	227	0.9-7.9
3/12/96	6391	Clinch R	8	7.50	8.56	7.78	227	234	231	0.9-10.4
3/13/96	3695	Clinch R	8	8.15	9.24	8.32	223	236	230	1.2-9.1
3/14/96	9034	Clinch R	12	7.89	9.07	8.26	207	224	218	0.9-8.5

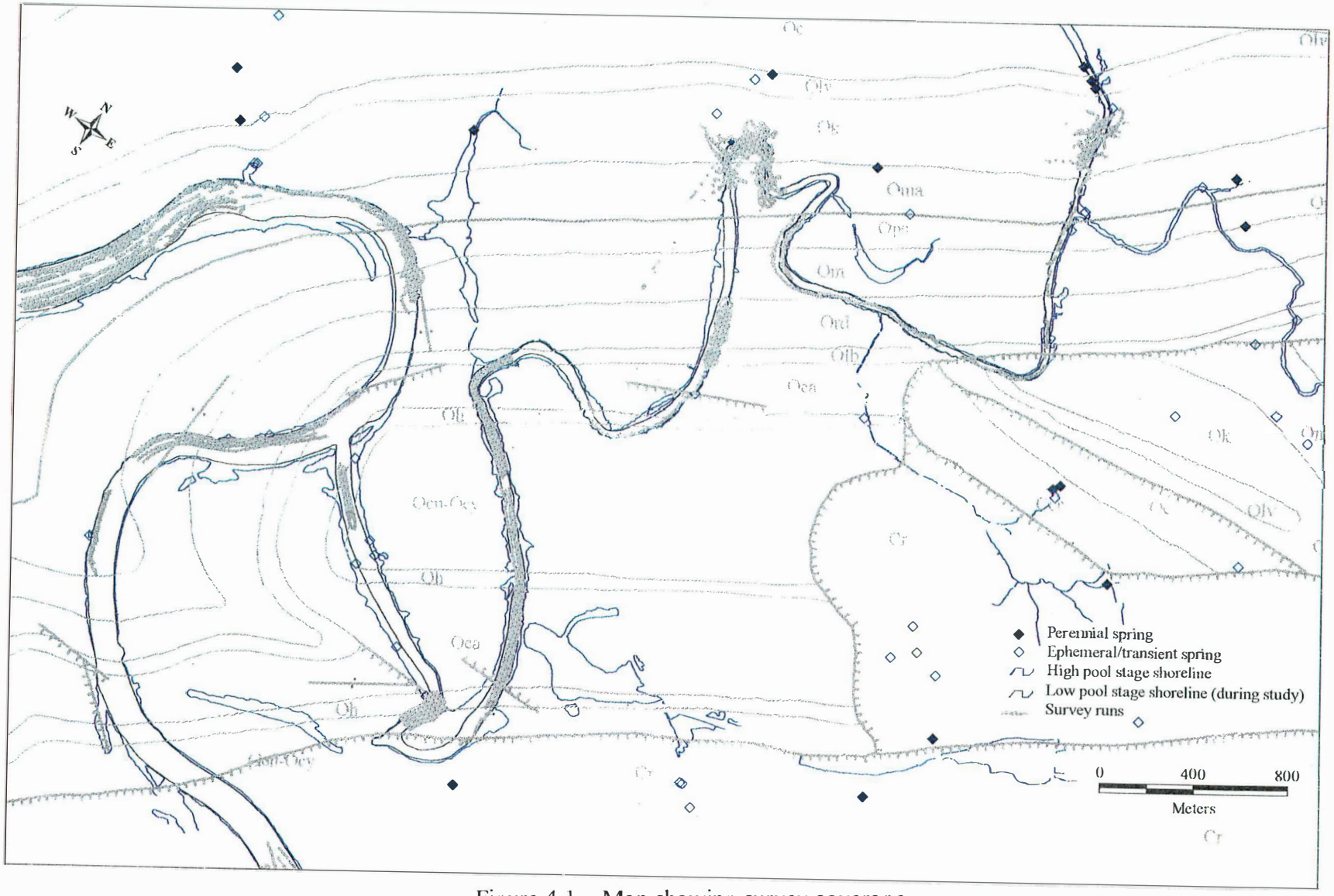


Figure 4.1. Map showing survey coverage.

Figure 4.1 also shows that some reaches of the Clinch River or Poplar Creek were not addressed at all in this effort. Weather conditions, equipment problems, and funding constraints prevented coverage of the entire study area. Specifically, little data was acquired in the Clinch River upstream of the confluence with Poplar Creek. However, working within those constraints, field data acquisition was focused on target reaches identified in Figure 2.11 as locations where subaqueous groundwater discharge might be expected.

Given the difference between surface water and groundwater temperatures (as much as 8.5 °C), it was expected that groundwater discharge would have been readily identifiable by anomalies on the order of several degrees at a minimum. However, from Table 4.1 it is clear that anomalies of that magnitude were not detected. In fact, for the most part, only temperature changes (dT) on the order of < 1.5 °C were observed over the course of a field day. Specific conductance (SC) variations were also relatively minor, but ranged up to 65 uS/cm in a given day. Further, not all temperature changes are accompanied by changes in SC.

Table 4.1 also shows that water temperatures varied greatly from day to day in both water bodies. Over the 18 days of fieldwork, ambient water temperatures in the Clinch River and Poplar Creek ranged from 5.94 to 9.42 and 5.75 to 12.93 °C, respectively.

Examining the data on a daily basis reveals that ambient surface water temperatures fluctuate over the course of a field day as well. For example, on February 20, 1996, temperature was observed to cover a 1.35 °C range, while specific conductance showed a 65 uS/cm range. Table 4.2 provides a more detailed look at the data for that day, breaking it down on a run-by-run basis. The run-by-run breakdown of data for February 20th illustrates that water temperature changes within runs 1-6 were minor while the bulk of the temperature and specific conductance variation implied in the daily range occurs primarily in run 7. Other potential anomalies are similarly implied in runs 8 and

Table 4.2. Summary of field data for February 20, 1996. Highlighted data suggests anomalies within those runs.

				TEMPERATURE (°C)				SPECIFIC CONDUCTANCE (uS/cm)				
RUN	SURVEY DIRECTION	TIME	RECORDS	MIN	MAX	MEAN	dT	MIN	MAX	MEAN	dSC	DEPTH (m)
1	Downstream	12:40-13:02	874	7.71	7.84	7.74	0.13	168	169	168.8	1	0.91-3.05
2	Downstream	13:17-13:32	493	7.81	7.83	7.81	0.02	168	171	169.0	3	0.91-2.74
3	Downstream	13:43-13:54	549	7.88	7.89	7.88	0.07	168	171	169.4	3	1.22-2.74
4	Downstream	14:04-14:15	456	7.92	7.94	7.94	0.02	168	171	169.1	3	1.22-2.13
5	Downstream	14:22-14:36	578	7.99	8.02	8.01	0.03	169	172	169.8	3	0.91-1.52
6	Downstream	14:42-14:51	230	8.04	8.06	8.05	0.02	169	171	169.9	2	1.22-1.83
7	Downstream	15:01-15:32	297	**8.04**	**9.06**	8.46	**1.02**	**169**	**233**	192.0	**64**	1.22-3.35
8	Downstream	15:47-16:03	417	**8.32**	**8.63**	8.50	**0.31**	**179**	**196**	188.0	**17**	0.91-2.13
9	Downstream	16:38-17:01	262	8.78	8.84	8.81	0.06	197	203	199.8	6	1.83-3.66
10	Downstream	17:06-17:25	822	**8.81**	**9.04**	8.86	**0.23**	**196**	**207**	199.0	**11**	1.22-3.66

10. In run 7, temperature was observed to increase 1.02 °C while specific conductance increased 64 uS/cm. Examining run 7 even closer (Figure 4.2), the bulk of the difference is associated with a single discrete anomaly (220R07-1) where the temperature increased sharply from 8.64 to 9.06 °C (dT = 0.64) and specific conductance increased from 188 to 226 uS/cm (dSC = 38) over a distance of ~ 10 m. The anomaly in this case spanned a distance of approximately 50 m along the survey run. For clarification, the anomaly numbers discussed in this document represent the date, run number, and anomaly identified along that run (e.g., 220R07-1 represents the first anomaly along run 7 on February 20th). Apart from true anomalies such as 220R07-1, the bulk of the temperature and specific conductance changes observed correlate with changing water depth. This observation holds true for all daily data sets, indicating a need to scrutinize the data in order to discern true anomalies from those associated with rapid changes in depth or probe position in the water column above bottom.

Originally, it was expected that data obtained from the surveys could be lumped together, at least on a daily basis, and temperature and specific conductance anomalies identified using standard contouring techniques. However, since the surface water conditions are highly transient and vary both daily and between runs, it was necessary to evaluate the data on a run-by-run basis. Initially, basic statistical summaries similar to that shown in Table 4.2 were used to rapidly screen the data to identify those runs where the range of temperature and/or specific conductance might indicate the presence of anomalies. Run-by-run statistical summaries for each day of fieldwork are presented in Appendix A.

Since the data in Tables 4.1, 4.2 and those in Appendix A do not indicate anomalies of the magnitude originally expected, a key question in initial data evaluation focuses on the expected magnitude of anomalies. A simple two-component mixing model, shown in Figure 4.3 (upper), which assumes conservation of mass and energy can be used to estimate the mixed temperatures. Parker and Krenkel (1970) use this

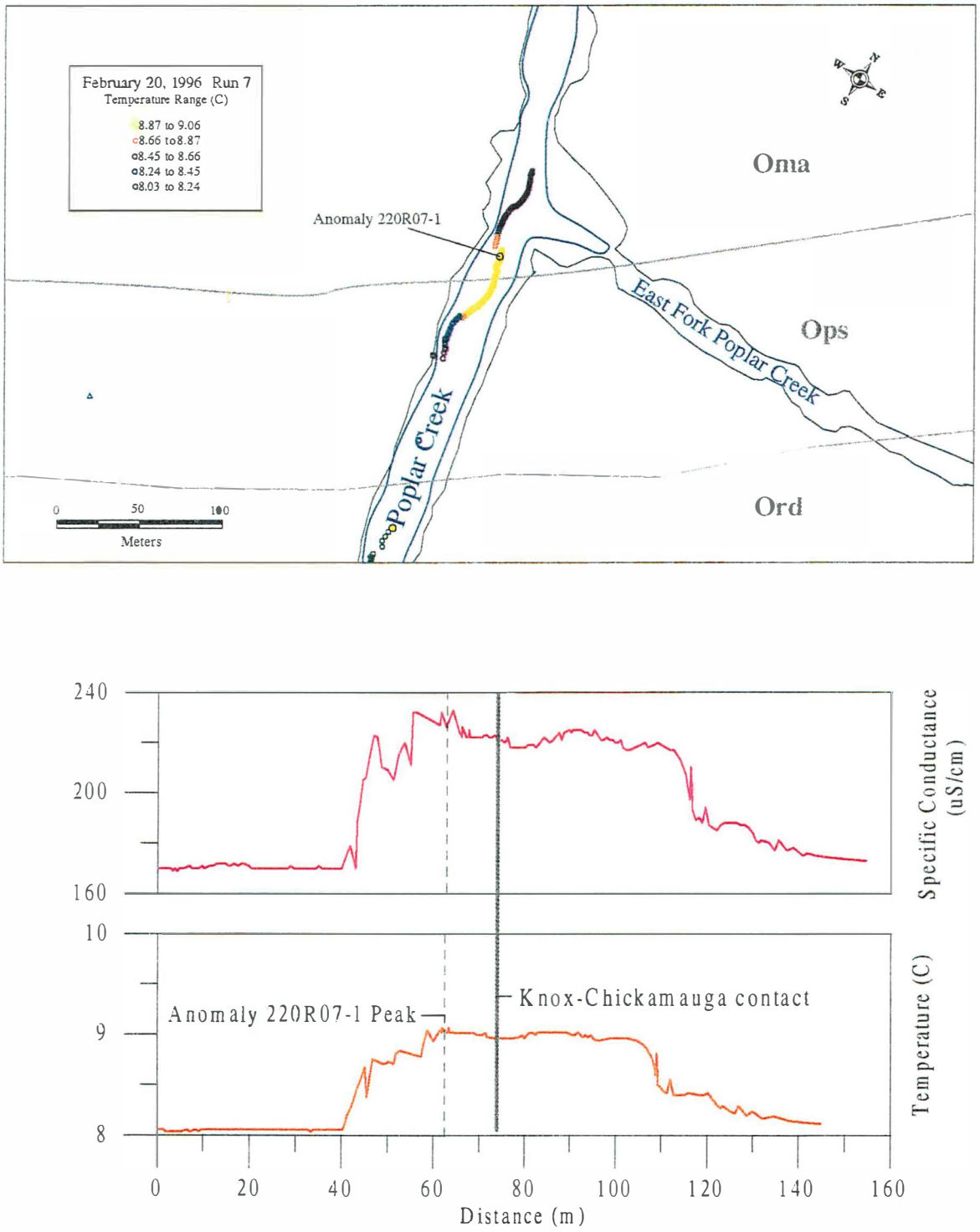
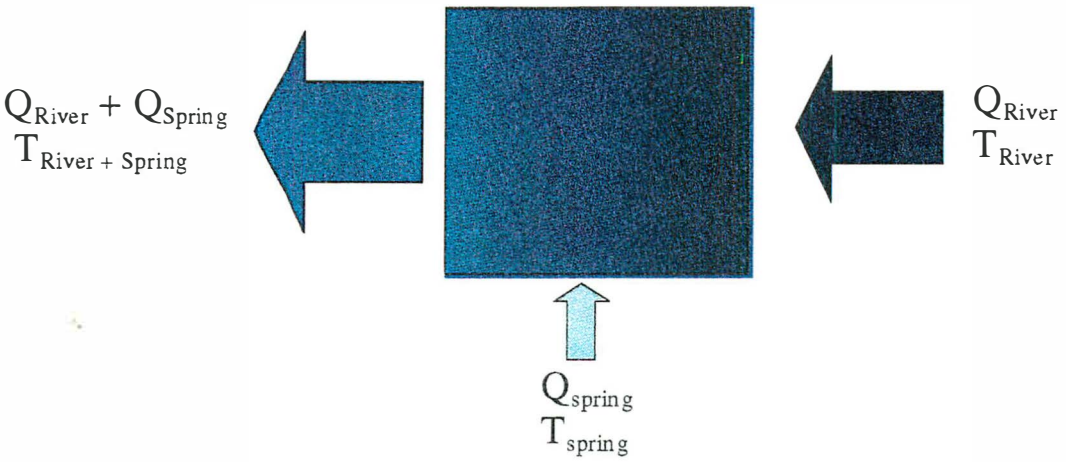


Figure 4.2. Survey results for February 20, 1996, Run 7 (Anomaly 220R07-1). The upper figure shows the temperature anomaly along the survey run, where brighter colors indicate warmer temperatures. The lower figures show plots of temperature and specific conductance versus distance along the run.

Simple Heat Transfer/Mixing Model
(Bouyant Jet in an Ambient Crossflow)



$$T_{R+S} = T_R(Q_R/(Q_R + Q_S)) + T_S(Q_S/(Q_R + Q_S))$$

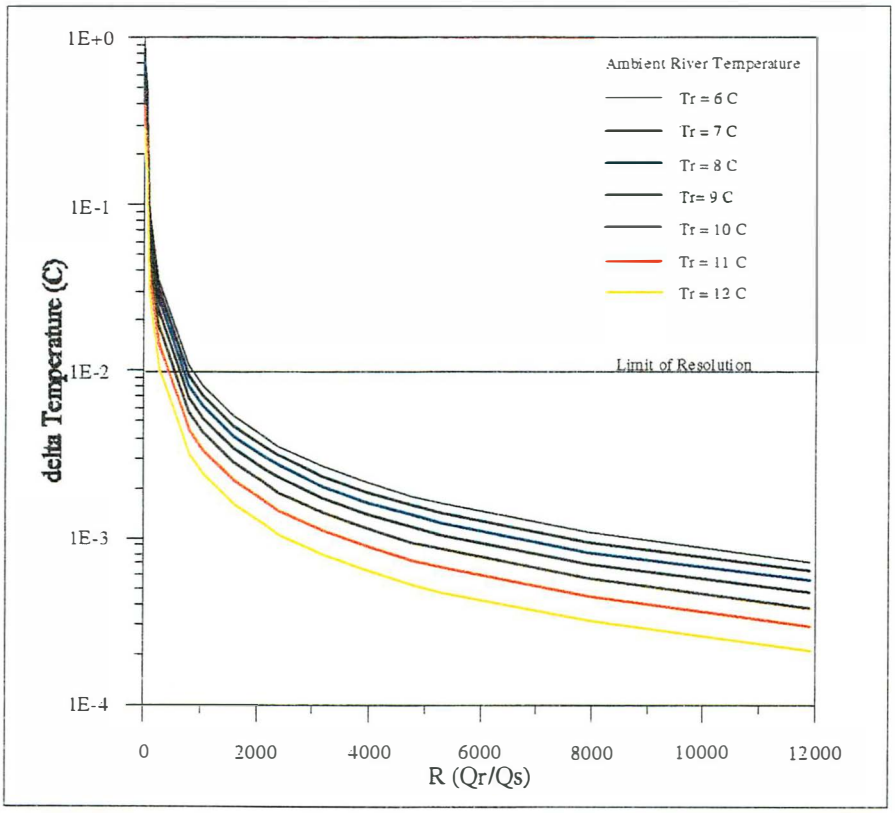


Figure 4.3. Simple two-component mixing model (upper); flow and ambient river temperature impacts on mixed temperatures (lower).

relationship to describe the final mixed temperature at the end of the mixing zone. Since this equation is neither time nor spatially dependent, it represents a conservative estimate of the potential mixed temperature, and can be applied to describe either instantaneous mixing at the spring outlet or the final mixed temperature at the end of a thermal plume. In this application, this represents the highest possible mixed temperature determined by the flow proportional difference in initial temperatures of groundwater and ambient surface water, as described by:

$$T_{R+S} = ((Q_R * T_R)/(Q_R+Q_S)) + ((Q_S * T_S)/(Q_R+Q_S)) \qquad (1)$$

where:

T_R = ambient river temperature (measured)

T_S = ambient spring (groundwater) temperature

T_{R+S} = resultant temperature resulting from mixing (measured)

Q_R = ambient river/creek discharge rate

Q_S = spring discharge rate

From equation (1) the potential anomaly, dT, is then equivalent to the difference between the observed mixed temperature and the ambient temperature measured along that survey run:

$$dT = T_{R+S} - T_R \qquad (2)$$

Assuming the more conservative case of instantaneous mixing model, (which is likely due to the high ambient flow rates of the Clinch River), it is expected that thermal anomalies would be very small. For example, considering a mean ambient river flow rate of 200 m^3/sec, a potential spring discharge rate of 0.28 m^3/sec (~ 10 cfs), and a temperature differential, T_S-T_R, of 8.5 °C (where T_S = 14.5 °C and T_R = 6 °C), Eq. (1) would yield a mixed temperature of 6.01 °C at the spring outlet. This would be represented by an anomaly of only 0.01 °C, which is the limit of resolution of the Hydrolab equipment used in this research (Hydrolab Corp., 1992).

Therefore, in order to identify anomalies of that magnitude within runs, a moving

average filter was first applied to both temperature and SC time series data within each run suspected of containing anomalies based upon the observed range of results obtained. The data were also screened manually to identify other anomalies not detected in the moving average method (such as end of run anomalies not subject to the filter). Data for each run were also analyzed graphically using a combination of GIS and standard plotting techniques in order to weed out thermal anomalies related to sudden decreases in depth.

Using the above screening techniques, a total of 198 temperature anomalies were identified in the data. Temperature anomalies ranged from 0.02 to 0.77 °C. Given the manufacturer's stated accuracy or +/- 0.15 °C and resolution of 0.01 °C , only anomalies with a dT greater than the stated accuracy may be considered "valid". A total of 52 anomalies were observed where dT exceeded 0.15 °C. With the exception of the larger temperature anomalies, many of the anomalies displayed little or no specific conductance change.

Figure 4.3 (lower) shows that the magnitude of an anomaly is directly related to R, which is the ratio of the ambient river flow to the spring discharge rate, as well as the temperature differential between groundwater and surface water. This demonstrates that the probability of detecting anomalies within the range of resolution (i.e., > 0.01 °C) decreases at elevated ambient river flow rates or very low spring discharge rates, and, with increasing ambient river temperatures. Given this, it is possible that many anomalies indicative of groundwater discharge are beyond the range of detection within the Clinch River. Further, minor anomalies detected under high flow, stage, or ambient temperature conditions may be just as significant as major anomalies.

Given the number of anomalies identified, some means of assessing the potential significance of each anomaly was needed. Although it is clear that ambient river flow and temperature affect the magnitude of the anomaly detected, there are also other factors which impact the occurrence of anomalies as will be discussed in Section 5. Consequently, a primary classification system based upon the magnitude of the anomalies

was used to "rank" anomalies. The classification system criteria are shown on Table 4.3.

In general, the anomalies are classified based on the magnitude of the temperature and/or specific conductance anomaly with respect to the Hydrolab limits of accuracy and resolution. For instance, a Class I anomaly reflects a temperature change of at least 3 times the instrument accuracy while a Class V anomaly, although clearly showing an increase in temperature in the time series data, hovers around the limit of resolution of the instrument. The classification also addresses relative changes in specific conductance with temperature anomalies. In this way, an anomaly displaying both temperature and specific conductance changes may be considered more reliable. Of course, while it is expected that the temperature differential between groundwater and surface water is ubiquitous, this is not the case with specific conductance. Consequently, valid subaqueous spring discharge anomalies do not require an associated specific conductance anomaly.

Figure 4.1 shows the areas surveyed in this research. Anomalies identified within the areas investigated are shown on Figure 4.4 as well as on detailed maps for each day of

Table 4.3. Anomaly classification system.

CLASS	TEMPERATURE ANOMALY (°C)	SPECIFIC CONDUCTANCE ANOMALY (uS/cm)
IA	$dT \geq 0.45$	$dSC \geq 10$
IB	$dT \geq 0.45$	$dSC \leq 10$
IIA	$0.15 \leq dT < 0.45$	$dSC \geq 10$
IIB	$0.15 \leq dT < 0.45$	$3 \leq dSC < 10$
IIIA	$0.10 \leq dT < 0.15$	$0 < dSC < 3$
IIIB	$0.10 \leq dT < 0.15$	0
IVA	$0.05 \leq dT < 0.10$	$0 < dSC < 3$
IVB	$0.05 \leq dT < 0.10$	0
V	$dT < 0.05$	--

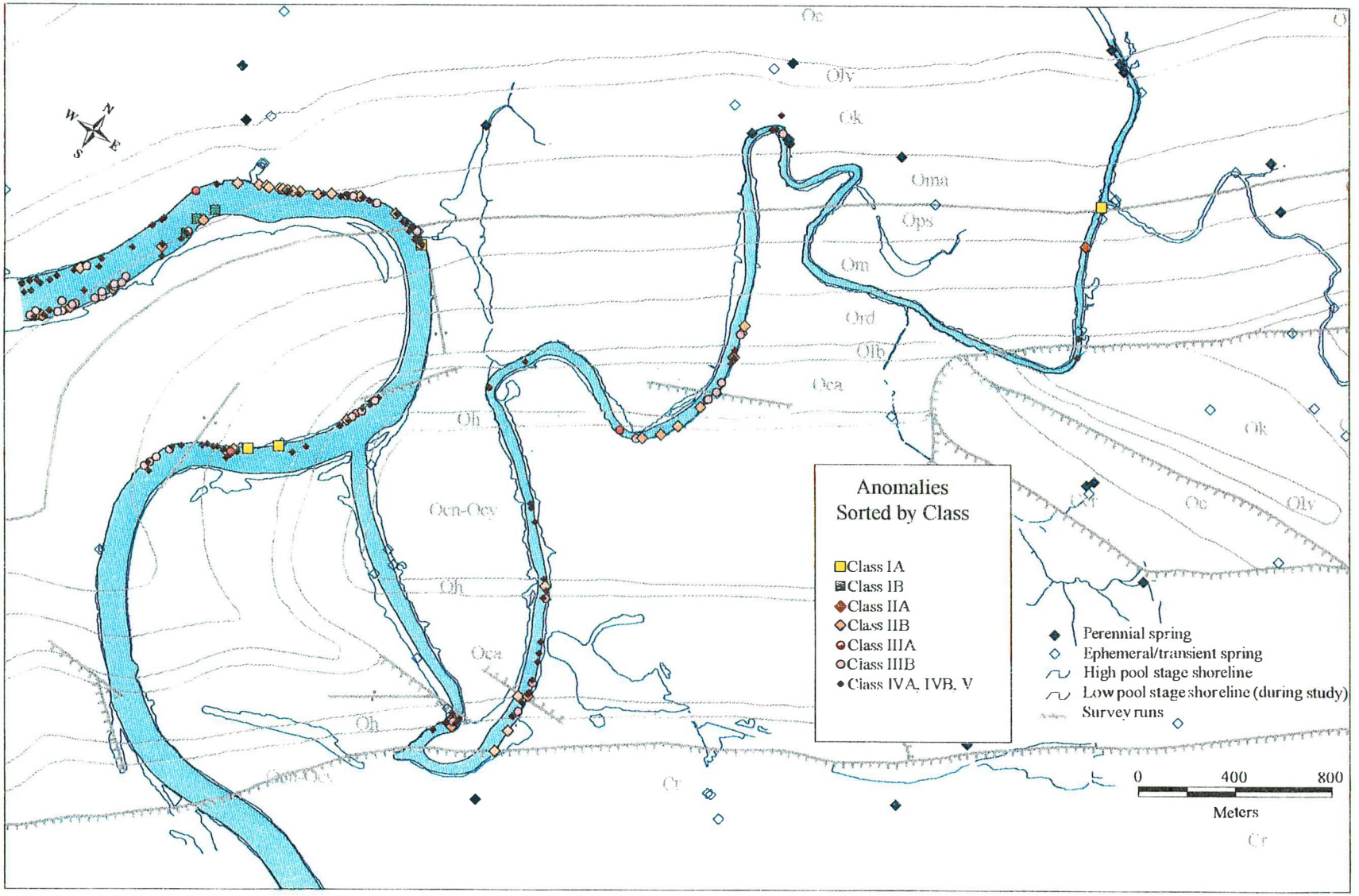


Figure 4.4. Anomaly location map.

field work presented in Appendix A. Potential anomalies implied in the data acquired in 1995 are also included in the Appendix A anomaly maps for reference and comparison. Data for each anomaly are summarized with the appropriate classifications in tabular form in Tables A.19.1 and A.19.2. Table 4.4 summarizes the distribution of anomalies by class and depth of occurrence and reveals that the majority of anomalies (66%) were detected in relatively shallow water less than 3 m deep. Only 14% of the anomalies identified occurred in water depths greater than 5 m; nine of these still showed anomalies in excess of 0.10 °C (Class III). Only 33% (67) temperature anomalies were accompanied by specific conductance changes.

Only a few of the anomalies encountered were represented by sharp changes in either temperature or specific conductance. Typically, temperature and specific conductance showed a Gaussian distribution across an anomaly, which may have spanned a distance of between 2-5 m along a run. The anomaly locations shown in Figure 4.4 represent the location of the peak temperature and/or specific conductance within each anomaly. Consequently, while the GPS equipment used in this research is capable of providing sub-meter accuracy for anomaly locations, actual subaqueous spring discharge may be less well controlled given the anomaly spread.

The locations of survey runs, for the most part, were considered reliable. A comparison of real-time corrected DGPS locations obtained in the field versus post-processed locations showed excellent agreement. However, as shown on Figure 4.1, and as discussed in Section 3, there were several areas where the survey runs show considerable drift, often deviating outside the limits of the mapped shoreline. Fortunately, with the exception of the three minor anomalies implied in the data for February 14, 1996 in the "M"-bend area of Poplar Creek, there were no anomalies identified in these data sets.

Representative Examples

While all anomalies are described in both descriptive, tabular, and graphic form in

Table 4.4. Distribution of Anomalies Classes (principal anomalies labeled)

DEPTH (m)	ANOMALY CLASS									n	% of Total
	IA	IB	IIA	IIB	IIIA	IIIB	IVA	IVB	V		
< 1	1 312R02-10	2 314R12-1 313R08-2		12	2	6		2		25	12.3
1-2	2 229R07-1 311R02-1	1 313R08-1	1 220R08-1	19	1	13	2	25	7	71	35
2-3	1 220R07-1		2 311R02-5 311R02-7	5	1	6	2	18	4	39	19
3-4				2		9	1	11	2	25	12.3
4-5				1		2	3	4	4	14	7
5-6				1		3		3	1	8	4
6-7			1	1		2	1	1	4	10	5
7-8						1	2	3	2	8	4
8-9								1		1	0.5
> 9								1		1	0.5
n	4	3	4	41	4	42	11	69	24		
% of total	2	1.5	2	20.5	2	21	5.5	34	12		

Appendix A, a few examples of representative anomalies are provided here to highlight key observations.

Figure 4.5 shows the location of one of the more significant Class IA anomalies identified in the field effort, anomaly 229R07-1 encountered on February 29, 1996 during run 7. Also shown are the three other lesser anomalies identified on overlapping runs performed either on that day or subsequently on March 12, 1996. Time series plots of data for these two dates showing ambient flow and stage conditions are shown in Figures A.13.1 and A.15.1 in Appendix A. These anomalies are noteworthy from a hydrogeologic perspective and are discussed further in Chapter 5. These anomalies were detected within a meter or so of each other on different runs and different dates and are illustrative of the effects of differing ambient conditions on observed anomalies. A comparison of the anomalies and prevailing field conditions for all four anomalies are shown in Table 4.5. As can be seen, the principal anomaly, 229R07-1 displayed a dT of 0.43 °C (temperature increasing from 8.99 to 9.42 across the anomaly) with a specific conductance anomaly of 15 uS/cm in water 1.43 m deep. Conversely, the other three anomalies represent Class IIIB or IVB anomalies encountered in close proximity but in deeper water and thus greater opposing hydrostatic heads. Anomaly 229R07-1 (run 7) and Class IIIB anomaly 229R06-1 (run 6) on February 29^{h} were detected under very low ambient flow (14-15 m^3/sec) but warmer ambient water temperature (~ 8.9 °C) and higher stage (~224.3) conditions. Conversely, the March 12th Class IVB anomalies 312R01-1 and 312R03-5 were encountered when the Clinch River was flowing at 140 to 170 m^3/sec, river stage was higher (~225 m) but ambient water temperatures were lower (~7.4-7.5). Perhaps more important, the March 12th anomalies were preceded by 193 mm of antecedent rainfall within the prior 7 day period while there was no rainfall for some time prior to the February 29th anomalies. The implication is that anomaly 229R07-1 was encountered under optimum conditions of lower stage (and thus opposing head), and ambient flow. With increasing water depth, such as for anomaly 229R06-1, the anomaly

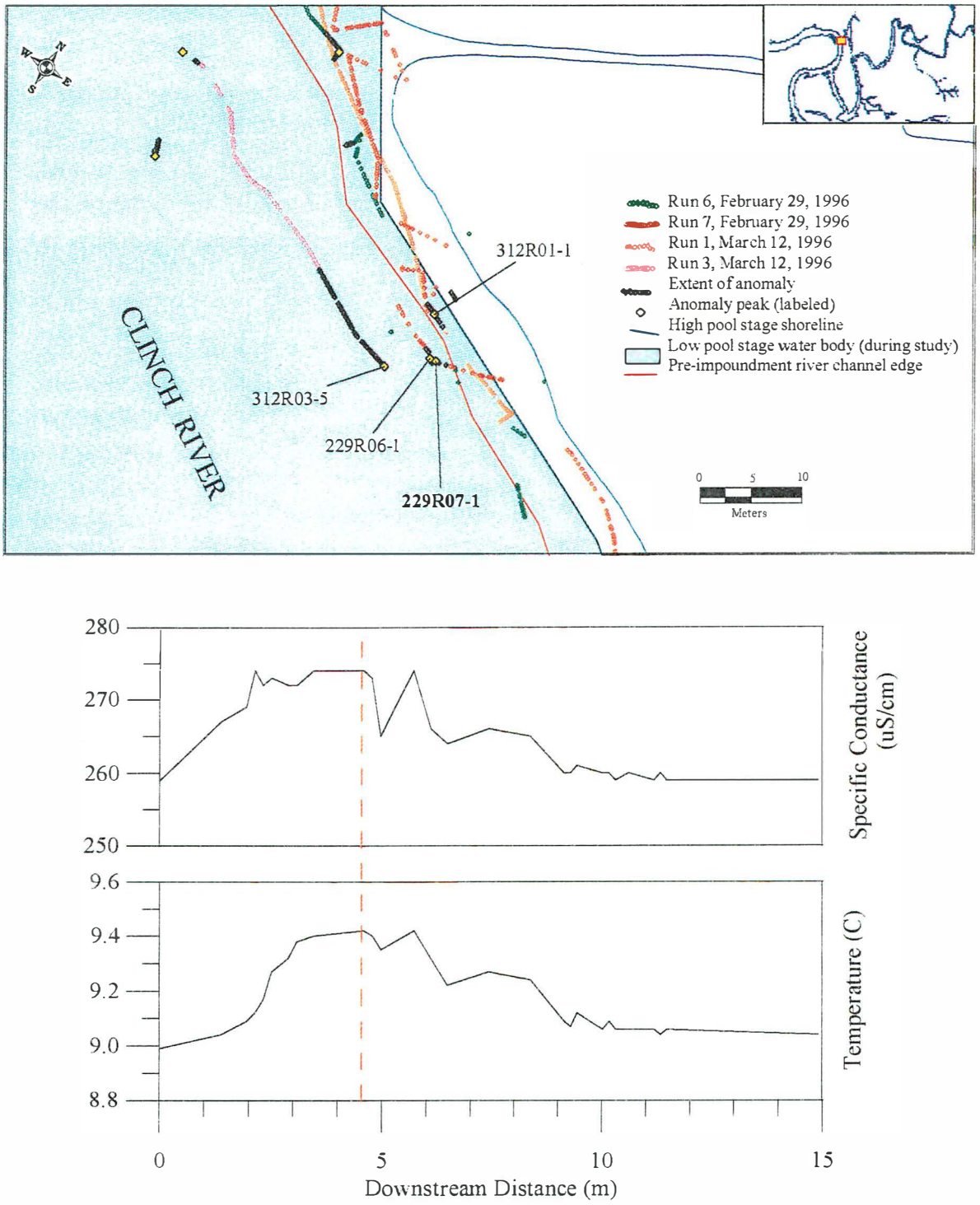


Figure 4.5. Comparison of anomalies in areas of overlapping surveys for February 29, 1996 and March 12, 1996. Upper figure shows the locations of the overlapping survey survey coverage with anomalies identified. Lower figure illustrates the abrupt increase in temperature and specific conductance associated with Anomaly 229R07-1.

Table 4.5. Overlapping anomaly comparison, February 29, 1996 and March 12, 1996.

Anomaly[1]	Class	Anomaly Range[2]		Water Depth (m)	Melton Hill Dam Discharge (m^3/sec)	River Flow (m^3/sec)	Stage Elevation (m)	Ambient T_R (°C)	Antecedent Rainfall[3] (mm)
		Temperature (°C)	SC (uS/cm)						
229R06-1	IIIB	8.99-9.06	260-264	2.47	0	15	224.34	8.91	0
229R07-1	IA	8.99-9.42	259-274	1.43	0	14	224.32	9.97	0
312R01-1	IVB	7.60-7.68	227-229	2.74	0	148	224.95	7.53	193
312R03-5	IVB	7.83-7.96	231-232	7.38	0	170	225.04	7.38	193

1 - Anomaly nomenclature denotes survey date, run, and anomaly within that run (e.g., 229R06-1 denotes anomaly 1 on Run 6 on February 29th)

2 - Denotes the range of temperature and SC from ambient to peak

3 - Represents the total rainfall occurring within the 10 day period preceding the survey.

providing a greater temperature differential). Finally, the other two Class IVB anomalies, occurred at greater depth, higher stage, and high ambient flow rates. However, they were also represented by lower ambient river temperature (which increase the temperature differential and thus the ability to detect these anomalies) and may represent more active groundwater discharge associated with recession after a recharge event (suggested by the antecedent rainfall).

The fact that the four anomalies were detected in approximately the same place at different times and under differing hydrologic conditions adds confirmation to the anomalies detected. Clearly this represents a discrete subaqueous spring or spring zone. This also suggests that although there was sufficient overlap in the two coverages (as existed in other reaches studied), groundwater discharge is dependent on hydraulic gradients in the adjacent aquifer, timing of recharge, and opposing hydrostatic head (reflected by stage changes and water depth where occurring). Further, elevated river flow rates and differences in ambient water temperatures control the magnitude of the anomaly detected. Consequently, this indicates that the magnitude of anomalies identified on a single survey run may not be a reliable indicator of the relative hydrologic significance of the springs of the springs causing the anomalies. Lesser anomalies may be equally significant as higher magnitude ones depending on the prevailing hydrologic conditions at the time of the surveys. This also points out that one cannot expect to duplicate an anomaly unless all hydrologic conditions are the same on different days.

As another example, anomalies 227R01-1 (IIB), 227R07-5 (IIB) and 229R01-1 (IVB) were detected within several meters of each other in Poplar Creek on February 27th and 29th, respectively. The anomalies are shown on Figure 4.6 and as time series plots in Figures A.12.1 and A.13.1 in Appendix A. As shown in Table 4.6, all three anomalies, though detected on different dates or different runs on the same day, represent essentially the same hydrogeologic conditions: creek flow was low (~12 to 14 m^3/sec) there was no antecedent rainfall in the 10 day period prior to the surveys and stage was consistent,

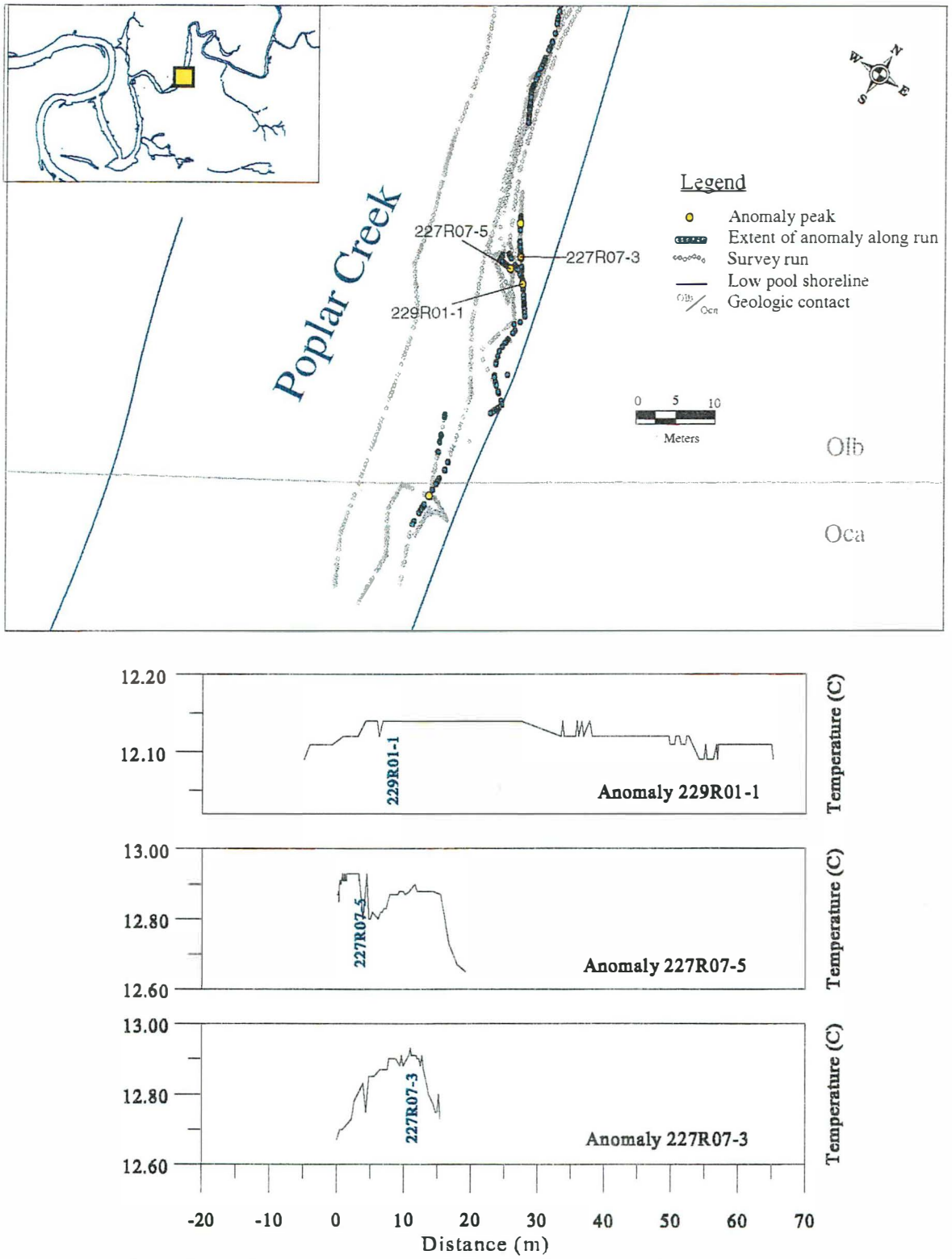


Figure 4.6. Map showing the location of anomalies identified on overlapping survey runs on February 27th and February 29th, 1996 (upper); lower figures show plots of temperature increases versus distance along each overlapping run.

Table 4.6. Overlapping anomaly comparison, February 27, 1996 and February 29, 1996.

Anomaly[1]	Class	Anomaly Range[2]		Water Depth (m)	Melton Hill Dam Discharge (m^3/sec)	River Flow (m^3/sec)	Stage Elevation (m)	Ambient T_R (°C)	Antecedent Rainfall[3] (mm)
		Temperature (°C)	SC (uS/cm)						
227R07-3	IIB	12.67-12.93	210-211	1.37	271	12	224.61	12.49	0
227R07-5	IIB	12.65-12.93	212	1.34	271	12	224.61	12.49	0
229R01-1	IVB	12.09-12.14	209-211	0.85	265	15	224.57	12.03	0

1 - Anomaly nomenclature denotes survey date, run, and anomaly within that run (e.g., 227R07-3 denotes anomaly 3 on Run 7 on February 27th)

2 - Denotes the range of temperature and SC from ambient to peak

3 - Represents the total rainfall occurring within the 10 day period preceding the survey.

~ 224.6 m. The ambient river temperature at the time of the surveys ranged from 12 to 12.49 °C. Consequently, although conditions were favorable to detect anomalies on both days from an ambient flow perspective, considering Figure 4.3 (lower) and Eq. (1), the high ambient temperatures makes detection of larger magnitude anomalies unlikely even under relatively low flow rates. At higher ambient temperatures, slight differences in ambient flow (3 m^3/sec) and/or temperature (0.46 °C) may be sufficient to yield markedly different anomalies. Subtle differences in hydrologic conditions may be expected to yield widely differing anomalies at the same location. Taken individually and based on the magnitude of the anomaly alone, these anomalies might be readily dismissed as insignificant, but together, they strongly suggest the location of a zone of groundwater discharge. The hydrogeologic significance of these anomalies will be discussed in Chapter 5.

As described previously, reservoir operations at the two dams cause flow reversals up into Poplar Creek. This creates mixing of the two water bodies which are often distinctly different in temperature, specific conductance and turbidity. Figure 4.7 depicts the results of surveys conducted in Poplar Creek near the mouth on March 4, 1996. A line of anomalies were identified at the end of each run which coincide with a mapped formation contact in the Chickamauga at the axis of the mapped scale synclinal structure. A run-by-run analysis and use of time-series filtering techniques a distinct change in temperature (dT = 0.18-0.64 °C) and specific conductance (up to 17 uS/cm) was readily apparent occurring at the downstream ends of runs 1-6, roughly 120 m above the confluence with the Clinch River. In this case, the temperature at the lower end of these runs ranged from 8.04 to 8.29 °C, while specific conductance ranges from 239 to 244 uS/cm. Poplar Creek temperature and specific conductance at the upstream end of the runs was ~7.63 °C and 224 uS/cm, respectively. In the Clinch River, the temperatures were much warmer, around 8.2 °C with specific conductance also higher at 247-250 uS/cm. Flow in the river at the mouth was quite high at 300 m^3/sec while flow in lower

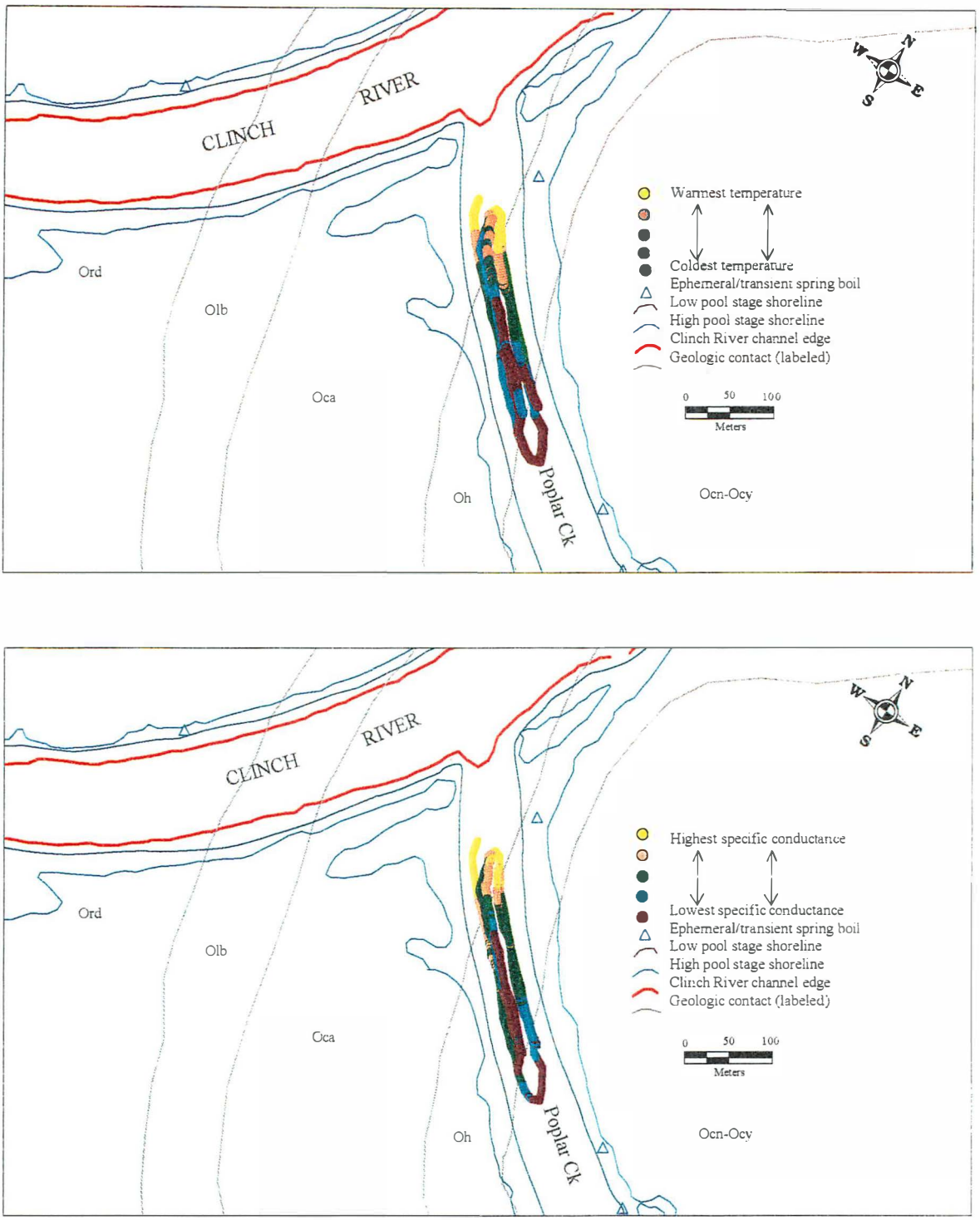


Figure 4.7. Mixing of Poplar Creek and Clinch River waters near the mouth of Poplar Creek, March 4, 1996. Upper figure shows temperature range; lower figure shows the range of specific conductance observed along parallel runs. Upstream backflow prevailed in Poplar Creek during survey runs.

Poplar Creek was ~ 15 m^3/sec. Backflow into Poplar Creek was observed in the field at the time of the surveys

With the ambient Poplar Creek and Clinch River temperatures and specific conductance values at the time of the surveys, Eq. (1) was used to estimate the temperatures and specific conductance that would be expected to result from mixing the waters. This analysis yielded a mixed temperature of 8.17 °C and a mixed specific conductance of 244 uS/cm. This calculated mixed temperature correlated well with the range of observed survey data. From this analysis, it is clear that a tongue of warmer river water is projecting up into Poplar Creek and that the anomalies observed are related to mixing at the mouth Poplar Creek rather than representing geologically controlled groundwater discharge. The bulk mixing of the two waters is supported by thermal IR imagery.

In the case described above, the river water was entering the creek, but on other occasions related to the rebound discussed previously, Poplar Creek discharge can project well out into the Clinch River beyond the mouth of the creek. It is believed that this is the mechanism that produced the 0.64 °C anomaly detected in the Clinch River across from the mouth of Poplar Creek in the 1995 field effort (Zondlo, 1995b). That anomaly was not repeated in 1996 although survey coverage for March 4th and March 11th 1996 overlapped the 1996 anomaly location. Consequently, this highlights the need to scrutinize anomalies identified in areas where mixing may occur, such as the mouth of Poplar Creek, or the junction of Poplar Creek and either Mitchell Branch or East Fork Poplar Creek within the study area.

Recognizing that the subaqueous groundwater discharge and the ability to detect anomalies caused by that discharge are impacted by ambient and antecedent conditions as discussed above, several key anomalies and reaches were revisited on December 12, 1997 in order to attempt confirmation. At that time, optimum conditions prevailed. Melton Hill generators had been off for nearly two days such that the river was not flowing and the

stage was relatively low (~224.4). Further, there had been two rain events yielding a total of 220 mm of rain within the 8 day period preceding the field survey.

Many of the anomalies indicated on Figure 4.4 in Poplar Creek and the Clinch River were replicated and in fact yielded higher temperature anomalies. For example, anomaly 229R07-1 described above (original dT = 0.43 °C) was revisited and found to display a 1.1 °C anomaly (increasing from 8.6 to 9.7 °C) in water ~ 2 m deep. However, no evidence of groundwater discharge was observed at the surface even though river flow was insignificant at the time of the resurvey.

Continuous water level and specific conductance data for key (active cavity flowpath) wells and river stage data were collected as part of another project at the same time as the December 1997 revisit. This data provides documentation of groundwater-surface water relationships not available during the 1996 field surveys. Figure 4.8 is a compound hydrograph relating rainfall, river stage, water levels and specific conductance for well BRW-6 and by simple calculation, hydraulic gradient from this well to the river over a seven day period including December 12th. As mentioned earlier, BRW-6 is a bedrock well where the screened interval monitors a large solution cavity that lies at an elevation approximately coincident with the base of the Clinch River. Additionally, this is one of the dye injection wells in the aforementioned 1996 dye tracer study (DOE, 1997a), and represents a fully saturated conduit flowpath.

Comparison of temporal trends in specific conductance, head, gradient, stage and precipitation show that groundwater-surface water interactions are complex. The hydrograph shows the lag between onset of precipitation and peak response in the well, as well as specific conductance changes on the order of 10-15 uS/cm which are interpreted to reflect actual groundwater flux in that well. The data also show that the head difference between the conduit and the river is ~9 m but the hydraulic gradient between the two fluctuates, indicating an ebb and flow condition attributed to the short term stage fluctuations. Other wells closer to the river (not shown) respond to every stage fluctuation

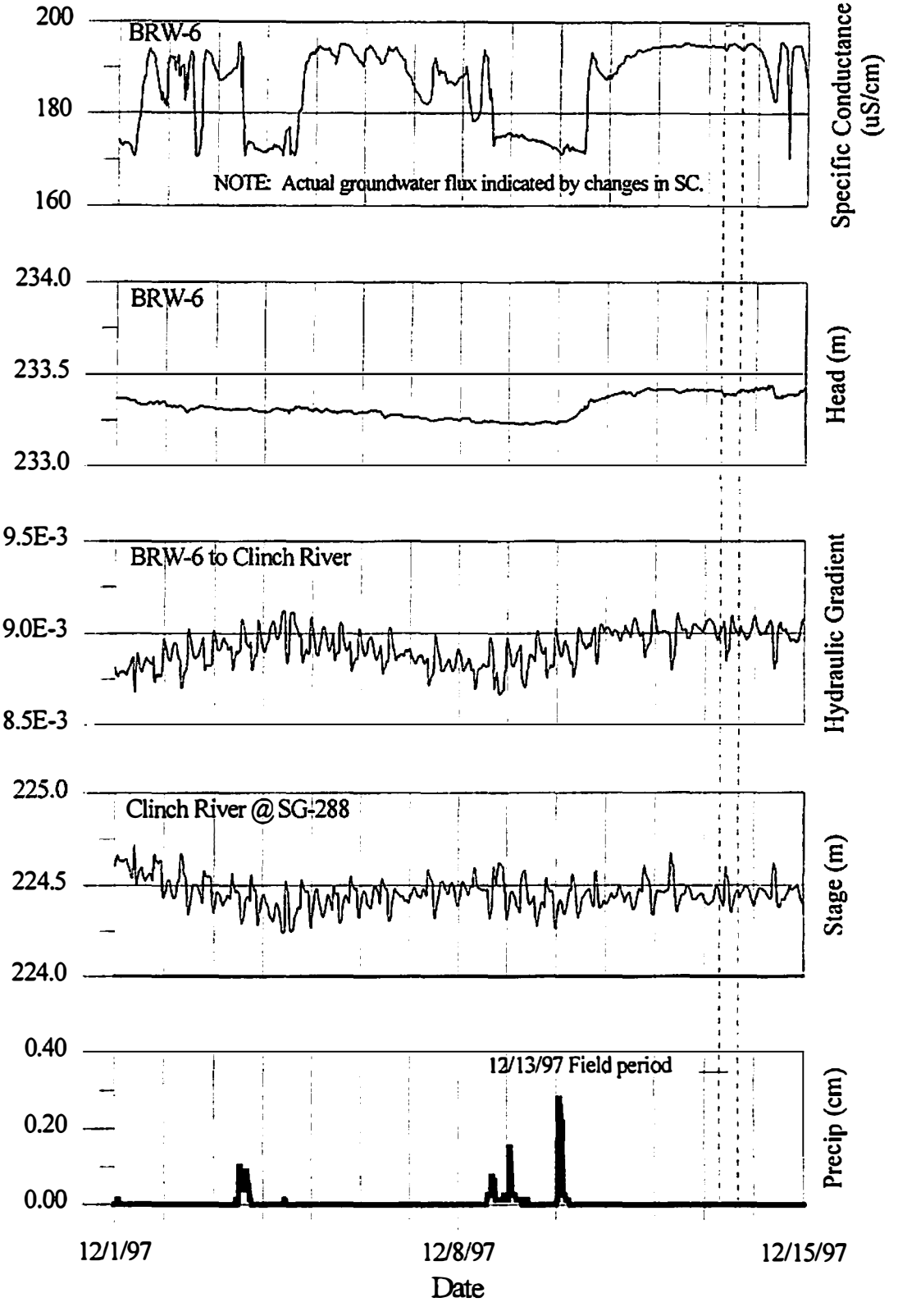


Figure 4.8. Composite hydrograph showing the complex relationships between river stage changes, rainfall, hydraulic gradient, changing aquifer water water levels and flux.

with little lag, suggesting that groundwater discharge is closely tied, temporally, to stage decreases. It is expected that there is some lag time between stage decrease and the actual initiation of groundwater discharge, but the timing is not known and likely varies depending on local hydrogeology. This also highlights that continuous well data collected concurrently with the survey data would greatly improve the ability to evaluate anomalies. If for example, continuous water levels and specific conductance were recorded at select wells within the study area at the time of the surveys, it would have been possible to evaluate the role of changes in hydraulic gradient and actual groundwater flux relative to recharge, stage, and magnitude of anomalies. At present, it is recognized that antecedent rainfall and stage are two factors which impact the magnitude of the anomalies observed, but without information on the conditions in the aquifer adjacent to the river, uncertainties surrounding anomalies cannot be unraveled.

5. DISCUSSION AND IMPLICATIONS

This study was intended to address two primary objectives: a) identification of anomalies indicative of groundwater discharge to determine whether groundwater continues to discharge to surface water as subaqueous springs following reservoir impoundment and: if so, b) to assess the role of key structural and/or karst features in focusing groundwater discharge, represented by the anomalies identified. Temperature and specific conductance anomalies observed along the river/creek bottom are expected to represent positive indications of groundwater discharge. Considering the number of anomalies detected within the areas surveyed, it is assumed that groundwater discharge is in fact occurring at discrete locations. However, the transient nature of the surface water boundary conditions and the variability in observed anomalies in areas where survey coverage overlapped, suggests such discharge is also transient, possibly occurring via a complex distributary network.

Investigations to provide direct evidence for actual groundwater discharge (such as diving or installation of lake bottom seepage meters) were not carried out for any of the anomalies identified in this study. Hence it cannot be conclusively demonstrated that discharge from subaqueous springs were the cause of the anomalies, but it is possible to assess the likelihood that anomalies represent springs. The following discussion deals with: a) an evaluation of the ability of the system used to detect anomalies, b) an evaluation of factors that impact detection or the magnitude of the anomalies themselves, and finally, c) the potential significance of the anomalies as points of focused groundwater discharge and indications of the role of key hydrogeologic features in groundwater flow.

Heat Transfer Hydrodynamic Implications

Because groundwater specific conductance at this site , although variable, falls within the range of surface water specific conductance, it is expected that temperature anomalies representing the difference between groundwater and surface water will be the

most reliable indicator of subaqueous groundwater discharge. The ability to detect groundwater discharges as temperature anomalies is limited by the range of the temperature probe being used. The Hydrolab used in this case represents current state-of-the-art with respect to field equipment with a resolution of 0.01 °C and an accuracy of +/- 0.15 °C. The system utilized in this research proved capable of detecting temperature anomalies ranging from 0.02 to 0.77 °C. However, there may be many more instances of groundwater discharge where, due to factors which will be discussed below, anomalies are below the limit of resolution of the tool and thus below detection.

Anomalies identified in this study included both sharp temperature changes occurring over a distance of several meters (such as anomaly 229R07-1 shown in Figure 4.5) and anomalies where temperature and specific conductance increased gradually over a distance of 10-30 m along a run. Survey runs were performed at slow boat speeds such that at the 1-sec sampling rate, data points are often only 0.03 to 0.05 m apart. Consequently, the method used is capable of detecting even small springs along survey runs. However, considering the large surface area to survey within the study area, and a run spacing of <1 to 10 m, it is quite possible that some major springs were missed altogether. The results and conclusions reached in this research are therefore only representative of the area covered, specifically along the path of each run. Where no anomalies were encountered along a given survey run, the negative evidence is also important as it indicates there is a lower probability of a major spring existing in this area. However, it is not definitive because at a different time, there may be significant groundwater discharge is association with different boundary conditions.

A lower magnitude anomaly encountered along a run could represent either a minor spring encountered along the survey run or the edge of a thermal plume from a larger spring located between runs. To address this uncertainty, one must be able to predict the potential geometry of thermal plumes under the prevailing hydrologic conditions encountered within the study area.

Tokar (1971), Madding *et al.* (1975), and Frigo and Frye (1972) showed that

thermal plumes resulting from heated cooling water discharged horizontally into Lake Michigan could be detected at distance up 1 km from the outfall. In these studies, the temperature differential between ambient surface water and the effluent stream was on the same order of magnitude as in this research, ~ 6 to 8 °C, but the flow conditions were quite different. In the Lake Michigan studies, the effluent discharge velocities were very high (25 to 55 m^3/sec), commonly many times greater than those in the receiving water body, if any. This sharply contrasts with the flow conditions within the ETTP study area where a mean Clinch River discharge rate of 200 m^3/sec was observed and where spring flow, based upon comparison with nearby subaerial springs would be expected to be < 2 m^3/sec. Hence, it is expected that thermal plumes would be less persistent. The Lake Michigan studies therefore represent an end-member case where thermal plumes are quite extensive in the absence of ambient flows.

The closest analogy to subaqueous groundwater springs in a flowing system are single- or multi-port diffuser jets used to dissipate excess heat from utility plant cooling water discharges to flowing water bodies. Such structures are typically placed along the river bottom oriented perpendicular to the ambient flow direction. There is abundant literature that addresses design considerations for diffuser jets, much of which is applicable to this evaluation. Most solutions to describe the fate of buoyant thermal effluent discharges in a cross-flow attempt to simultaneously solve the integral equations for conservation of mass, energy, and momentum. The principal parameters that influence thermal plumes are: the initial conditions at the jet/spring outlet (discharge velocity, outlet diameter, and outlet orientation relative to the cross-flow direction), water depth or hydrostatic head, the buoyancy force, the ambient water velocity and temperature, temperature stratification, and turbulence, both related to the jet discharge and to ambient conditions attributed to bottom and shoreline geometries (Shirazi, 1972; Parker and Krenkel, 1970, Hirst, 1971a).

There are three principal zones of influence for heated discharges which are typically of interest from a design perspective: the zone of flow establishment (i.e., at the

discharge orifice), the zone of established flow extending from it and finally, the far field zone, at the end of which thermal differences are fully mixed. In the design mode, all the input parameters affecting the resulting plume geometry and mixing are known or assumed such that idealized, often complex integral solutions involving turbulent equations of state, such as presented by Hirst (1971a), can be applied in plume prediction for one or more of the three zones. Since the precise effects of all these factors are not well defined in a natural setting the idealized solutions cannot be applied to the inverse problem at hand. However, the principals that apply in prediction can be used to bracket the range of possibility related to subaqueous groundwater discharges in cross-flowing ambients.

Shirazi (1972) have collected the primary variables impacting flow into four dimensionless parameters, the densiometric Froude number, the velocity ratio, the channel aspect ratio, and a stratification number. The aspect ratio, A, reflects the ratio of spring orifice diameter to water depth. Discharge characteristics (velocity, temperature or density differences) are described by the Froude number, F_o, which represents the ratio of the inertial forces due to the spring/jet discharge velocity to the buoyant forces attributed to the density differences with respect to ambient. This is expressed as

$$F_o = Q_s / (\Delta\rho_o g D/\rho_o)^{0.5} \qquad (3)$$

where:

Q_s = the spring flow rate

D = the diameter of the spring outlet

g = gravitational constant

$\Delta\rho_o$ = the density difference between groundwater and surface water

ρ_o = the ambient surface water density at the spring discharge depth

The velocity ratio, R, is simply the ratio of the ambient river discharge to the spring discharge, Q_R/Q_S. In design work, the jet discharge rate is known or assumed, but in this study, it is unknown. However, rearranging Eq. (1) allows for prediction of an estimate for the discharge rate of a subaqueous spring if the other parameters are either known or

assumed. The calculated spring discharge rate, Q_s, reflects the discharge rate required to produce a dT anomaly of the magnitude observed and is given by

$$Q_S = [((T_{R+S}-T_R)/(T_S-T_R)*Q_R] \quad (4)$$

where:

$(T_{R+S}-T_R)$ = dT, the observed temperature anomaly

(T_S-T_R) = ambient surface water-groundwater difference during a run $(14.5-T_R)$

The spring discharge rate was calculated for all anomalies identified in this study by applying Eq. (4) and using the observed dT, ambient river temperature (the minimum temperature during that run), calculated river discharge, and an assumed mean groundwater temperature of 14.5 °C. The resulting calculated spring discharge rates are tabulated in Table A.19.2. Calculated spring discharge rates were found to range from 0.01 up to 16.28 m^3/sec (0.35 to 574 cfs). In general, the Clinch River anomalies required much higher calculated spring discharge rates to justify the anomalies observed owing to the elevated flow rates relative to Poplar Creek.

Since groundwater is warmer than the ambient surface water it is discharged into, there is a density difference (as much as 0.468 kg/m^3 when surface water temperatures are at the minimum 6 °C) between them that adds a buoyant force to the discharge. Temperature and thus water density stratification within the surface water column further inhibit buoyant plume rise and depending on the spring/jet discharge rate, force the plume to spread laterally rather than vertically. Effectively, with increasing height in the water column, the buoyancy forces become less significant as the density differences between ambient and spring plume waters diminishes. Stratification is described in terms of a dimensionless stratification number, S_t, expressed numerically as:

$$S_t = (\Delta\rho_o/D)/(\Delta\rho_a/\Delta z) = (\Delta T_o/D)/(\Delta T_a/\Delta z) \quad (5)$$

where:

$\Delta\rho_a/\Delta z$ = the ambient density gradient within the water column

ΔT_o = the excess temperature difference at the spring discharge point

$T_a/\Delta z$ = the ambient surface water temperature gradient

Shirazi (1972) used these dimensionless parameters to develop a complete set of compound nomograms that allow for determining the dimensions of a thermal plume in the vertical or horizontal direction in proportion to jet orifice diameter under varying conditions. However, these were strictly intended for true "jet' discharges and only address applications where the jet discharge exceeds the ambient flow rates ($R < 1$). Consequently, in these nomograms the Froude numbers are also in the 20 to 50 range, indicating inertial forces related to the jet momentum are more dominant. For comparison, values for F_o for conditions in the study area are expected to range from 0.1 to 6.3.

For comparison purposes, Shirazi's nomographs for discharge of a buoyant jet into a flowing, stratified ambient where $R = 0.5$ (i.e., Q_S is twice Q_R) showed the position where the jet centerline excess temperature was fully mixed to be at a distance of 8.5 times the jet orifice diameter, while the maximum horizontal, downstream spreading distance was shown to be 11.5 times the diameter. Substituting in a diameter of 0.3 m for a hypothetical spring with a round orifice, would yield a maximum plume height of 2.55 m and a plume length of 9.6 m.

Parker and Krenkel (1970), and Hirst (1971a, 1971b) document that ambient current velocities significantly impact the configuration of a thermal plume, dramatically reducing the zone of flow establishment (the initial mixing zone at the orifice) and accelerating the rate of heat dissipation. Therefore, for conditions within the study area where $R >> 1$, it can be expected that the plume geometry described above using Shirazi's nomographs where $R < 1$ is even further reduced, possibly with complete mixing occurring within a distance of < 1 m of the orifice and little lateral plume development. The net effect is that it is unlikely that minor anomalies identified in this study represent the edges of larger thermal plumes, but rather the result of near instantaneous mixing due to the high ambient flow conditions.

As further evidence of the impacts of elevated ambient flows in effecting rapid mixing, in February 1997 a groundwater spring was observed flowing at a rate of ~0.0009 m^3/sec (15 gpm) from a solutionally enlarged fracture in a bedrock outcrop which formed

the bank in the "M-bend" on Poplar Creek (spring PCTZ-1 on Figure 2.8). The creek water was very turbid and flowing at a rate of approximately 15 m^3/sec in response to a rain event, and a plume of clear water was observed extending nearly 2 m out from the bank spring. Temperatures and specific conductance were measured at the spring orifice, and at several distances out from the spring. While a 3 °C and 14 uS/cm difference existed between the spring water and the creek, the temperature had decreased 1 °C and 4 uS/cm at 0.15 m and was completely mixed at 1.2 m from the outfall, though the clear water extended out beyond this point. This example further illustrates how rapidly a thermal plume is dissipated in a flowing ambient.

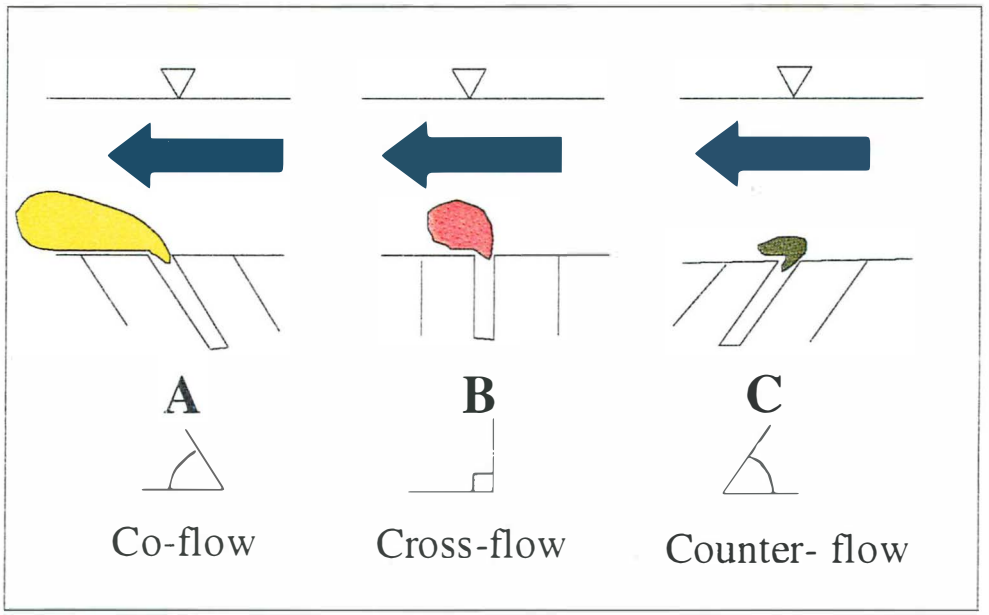
Spring orifice geometry (shape, dimension) plays a major role in the rate of mixing of thermal effluents and thus impacts the potential to detect a subaqueous spring. For instance, Hirst (1971b) and Wang and Papell (1983) have shown that multiport diffusers, effectively a linear bank of single port diffusers, are more efficient in dissipating heat than a single round jet. Therefore, groundwater discharging from a discrete orifice rather than along a bedding plane fracture or cavity, may be more easily detected.

One final point regarding the hydrodynamics of thermal plumes involves the angle of incidence of a subsurface discharge with a cross-flow current. The angle with which a spring is discharged along the river bottom relative to the ambient flow direction significantly impacts the rate of entrainment and thus heat dissipation. The lowest rate of entrainment is associated with a co-flowing discharge, oriented in the same direction as the ambient cross-flow. Conversely, heat associated with thermal discharges is most rapidly accomplished where discharged vertically at angles between 30 and 90° to the cross-flow current direction. Plume modeling by Hirst (1971a) showed that the smallest mixing zones are associated with jets discharged at oblique angles of 30-45° to the cross-flow current (i.e., in an up-current direction). On the other hand, the largest mixing zones are obtained with horizontally discharged jets representing co-flowing discharge (essentially at angles from 0-30° in a downstream direction). The three cases of co-flowing, cross-flowing and counter-flowing discharge and resulting mixing zone geometries are shown

conceptually in Figure 5.1.

Since the dip of bedding exposed along the river bottom and thus the orientation of discharge relative to the flow direction is ~40-45° in the study area, it can be expected that heat dissipation is rapid (especially due to high R). This implies that for this study where groundwater discharge is occurring along bedding plane parallel solution or fracture zones, if the angle of dip is oriented in an upstream, up-current direction, the angle of discharge may be assumed to be co-flowing with the ambient flow direction. This is equivalent to case "A" shown on Figure 5.1. In this case, a thermal "plume" related to spring discharge may be expected to be represented by a higher magnitude anomaly of greater longitudinal extent. Consequently the probability of detection may be increased. If bedrock dip is oriented opposing the ambient river current direction (case "C" in Figure 5.1), mixing can be expected to be immediate, with little lateral development of the zone of established flow. Such a situation would occur on the north limb of the map-scale anticlinal structure or on the south limb of the synclinal structure as indicated in Figure 5.1. Along axis of the map-scale syncline or anticline, groundwater discharge is likely vertical associated with bedding-perpendicular features. This is depicted as case "B" in Figure 5.1. Consequently, in addition to transient boundary conditions (stage, flow rates, ambient temperature), where subaqueous springs are associated with bedrock features, the orientation of bedrock relative to the flow direction at the time of the survey may limit the detection of anomalies in some cases, and accentuate them in another.

Where the flow direction is parallel to bedding strike, bedding dip orientation relative to river flow direction would be expected to have no impact on spring detection. Finally, since the direction of flow in the river reverses in response to reservoir operations, assuming all other parameters (Q_R, T_R, antecedent rainfall and stage) remain the same, a spring may be co-flowing during normal flow conditions and counter-flowing during backflow conditions. Consequently, a spring may be more readily detectable on one occasion and non-detectable on another depending on the ambient flow rates and direction relative to the geometry and orientation of the spring orifice.



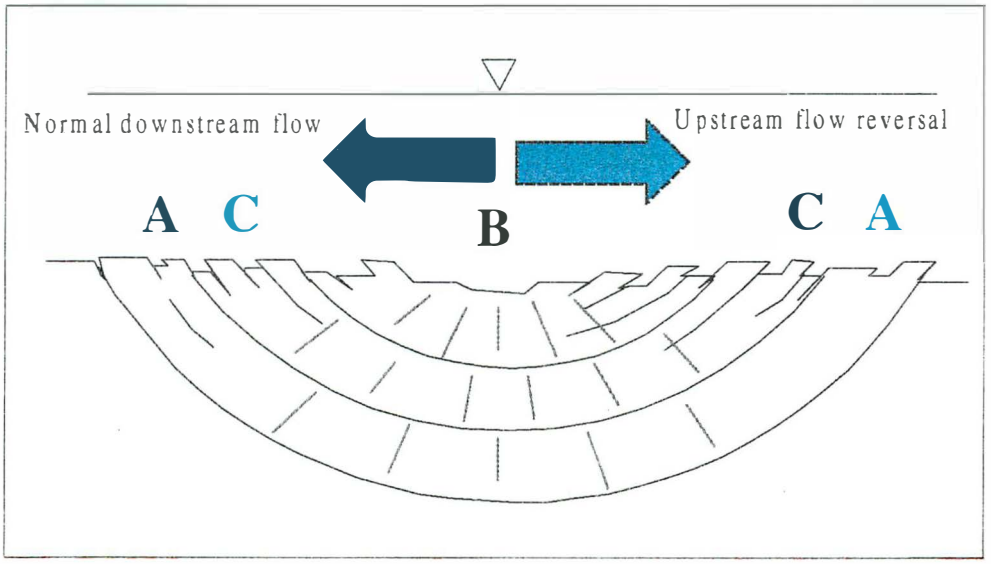


Figure 5.1. Conceptual diagram showing the significance of geologic structure and the angle of incidence of a river bottom spring relative to ambient river flow directions on heat dissipation and thermal plume geometry (upper). Lower figure shows the impacts of changing river flow direction and geologic structure on the potential for thermal anomaly detection.

In contrast, where fine grained sediments mantling bedrock form the river bottom, subaqueous springs may be expected to be represented by boils, similar to those observed along the river banks. In these springs, groundwater discharge is effectively vertical, oriented perpendicular to the ambient cross-flow direction, and the degree of mixing would be large with little lateral development of a thermal plume. This is especially true under low spring discharge rates. However, the "potholes" that develop around these springs may limit mixing in the immediate zone around the orifice (i.e., within the zone of flow establishment). Additionally, such features may be evident as bathymetric anomalies.

It should be noted that since the ambient river discharge rates within the study area are typically elevated, even minor temperature anomalies yield calculated groundwater discharge rates that may be considered unreasonable from a hydrologic perspective. As mentioned previously, the range of calculated spring discharge using Eq. (4) is 0.01 to 2.31 m^3/sec for anomalies in Poplar Creek and 0.06 to 16.24 m^3/sec (up to 257,000 gpm) for anomalies in the Clinch River. In comparison to the range of flow rates presented in Chapter 2 for large springs in the Valley and Ridge, these flow rates may be possible, but are not likely.

Further, a water balance was completed by the author (reported in DOE, 1996) to evaluate groundwater discharge from the ETTP Main Plant area to Poplar Creek. From this evaluation, it was determined that during low pool stage, winter conditions the total groundwater discharge along the 7030 m length of Poplar Creek seepage face evaluated was minimal, ranging from 0.021 to 0.033 m^3/sec, or, ~ $3.9E^{-6}$ to $4.7E^{-6}$ m^3/sec per linear meter of shoreline (~ 0.05 to 0.08 gpm/m). In general, higher discharge rates were obtained for nodes where bedrock was exposed along the shore, owing to somewhat higher hydraulic conductivities for several Chickamauga bedrock formations. Given these low discharge rates, underflow of Poplar Creek was deemed unlikely and it was suggested that groundwater discharge as a continuous seepage face was not unreasonable. Considering the lack of bank springs along the shoreline, it may be assumed that this minimal flow can be focused along discrete subaqueous springs, but the total flow rate cannot approach

some of the calculated spring discharge rates inferred from Eq. (4). Seepage flow rates were not determined for the groundwater discharge to the Clinch River, but can be expected to be similar for reaches such as along Duct Island where the area available for groundwater recharge is limited.

The Poplar Creek water balance calculations show that every 0.5 m increase in creek stage, (assuming heads in the aquifer remain the same or lag behind stage increases), results in a $8.5E^{-7}$ m^3/sec decrease in discharge. While this is a small value, this is equivalent to an approximate 20% reduction in flux per 0.5 m increase in stage. This again demonstrates that river stage impacts groundwater discharge which in turn increases the flow ratio R and yields lower magnitude anomalies. Given such low flow rates, unless the ambient flow was effectively zero, temperature anomalies should have been beyond detection.

The anomalously high calculated spring discharge rates may be explained somewhat by considering that the calculated river flow rates used in Eq (1) are not consistent across the entire cross-sectional area or entire reach of river for which flow was determined. Ambient flow rates vary substantially along the river bottom and thus affect mixing and the potential magnitude of anomalies detected. As a result, anomalies may be more readily detected in reaches of the study area where flow is minimal due to channel geometry in spite of the high ambient flow rates.

This is illustrated in Figure 5.2, which graphically depicts the calculated discharge rates, $Q_{s,}$, for each anomaly. From this plot it can be seen that many of the anomalies occur in areas of the Clinch River where the ambient flow is reduced due to channel geometry. For example, there were a number of anomalies identified on the March 14, 1996 surveys even though the river flow was as high as 176 m^3/sec. However, the anomalies were largely identified along the south shore of the Clinch River below Campbell's Bend, which represents the downstream side of an inside meander bend. The decreased river flow rates in these backwater portions of the river could enhance the ability to detect anomalies. However, the calculated spring discharge rates associated with the

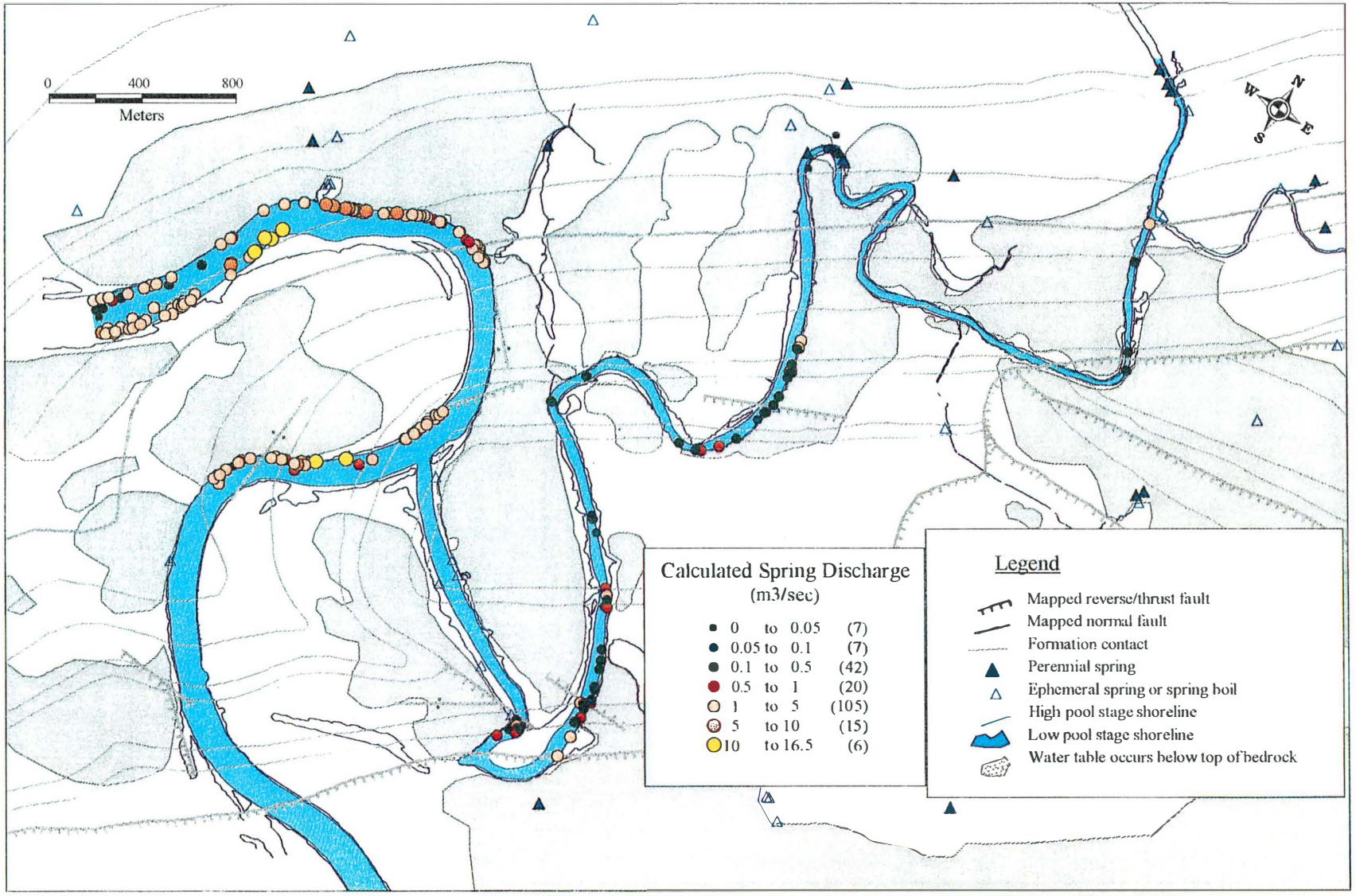


Figure 5.2. Spatial patterns of calculated subaqueous spring discharge.

observed temperature anomalies in these areas would be erroneously high when the ambient flow rates representing main channel flow are used in Eq (4). The key point is that the surface water flow field is not uniform across an entire river channel or reach of river. Minor eddies caused by bottom features or other obstructions to flow may reduce the ambient flow rate locally and thus decrease the mixing, making some anomalies stand out even under reportedly high flow conditions. Consequently, one cannot discard an anomaly on the basis of the magnitude of *calculated* spring discharge rates using Eq. (4). In contrast, the fact that the majority of the anomalies identified in the Clinch River occurred in areas where the actual flow rate is less than the overall flow rate in that reach suggests that one cannot conclusively state that a lack of anomalies in areas where the calculated flow rate is representative of actual flow conditions indicates a lack of groundwater discharge in that reach. Rather, it may be that mixing is just more significant such that anomalies are beyond resolution.

Given the above discussion, the classification system used in this study thus far appears most appropriately used as a means of describing anomalies, but other factors such as the ambient to spring discharge ratio, R, ambient river temperature, T_R, stage height (opposing head) or water depth also control the resulting anomalies. Crossplots of anomaly dT as a function of each of these parameters are shown in Figures 5.3 through 5.8. From these figures, the following observations can be made:

- the majority of the anomalies as well as the largest magnitude anomalies occur where opposing hydrostatic heads (i.e., water depth) are lower.
- based upon this it would be expected that a linear trend of dT versus stage elevation would emerge, yet this is not the case.
- the higher magnitude temperature and specific conductance anomalies occur in association with the lowest ambient temperatures.
- few anomalies were encountered at ambient flow rates in excess of the mean for each water body; most anomalies occur at lower ambient flow rates but lower flow rates do not directly correlate with higher magnitude anomalies.

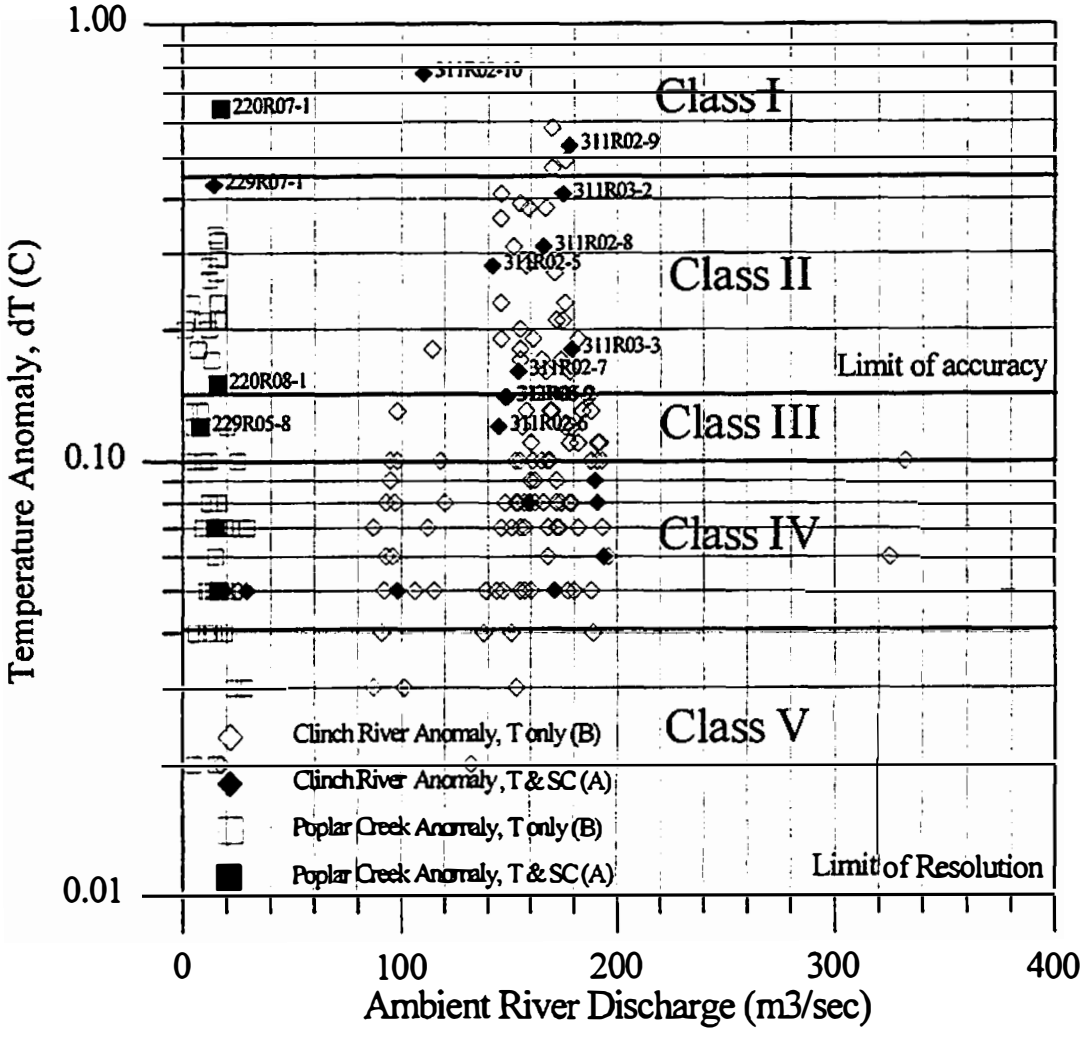


Figure 5.3. Plot of identified temperature anomalies as a function of ambient river discharge. Clinch River versus Poplar Creek anomalies are distinguished; Class I and II anomalies are labeled.

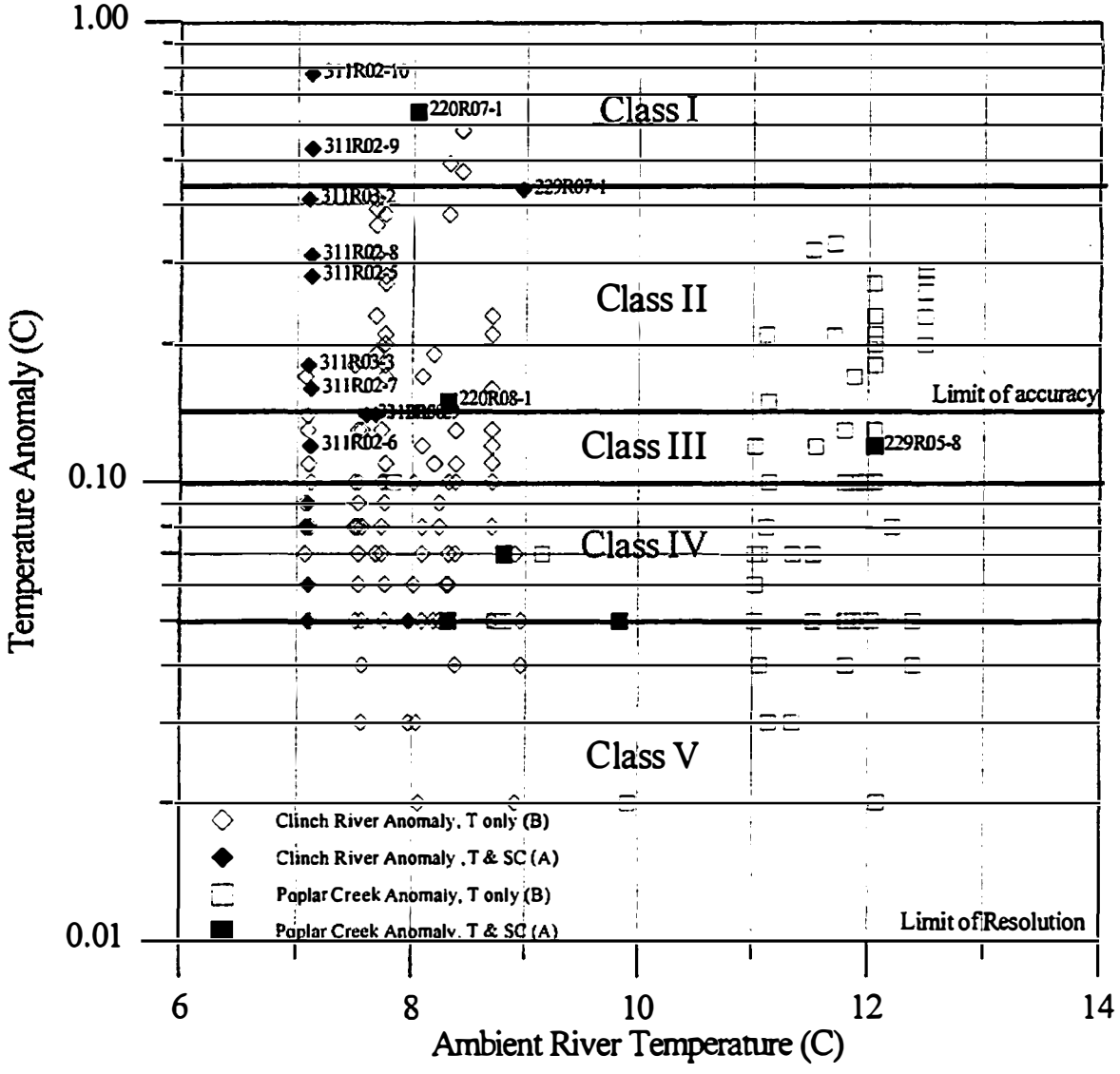


Figure 5.4. Plot of temperature anomalies as a function of the ambient river temperature at the time of detection. Anomalies are differentiated by the water body in whcih they occur.

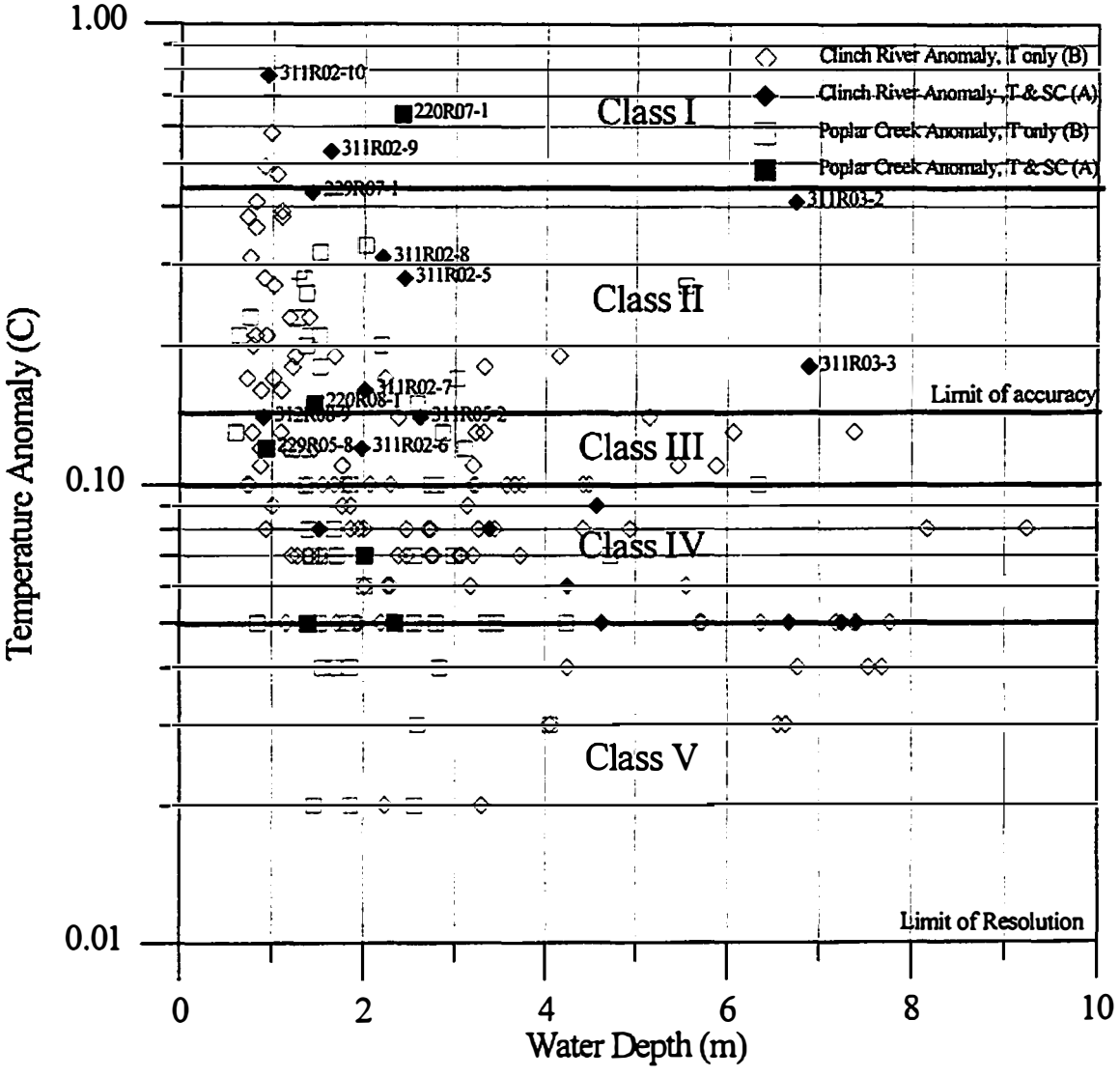


Figure 5.5. Plot of identified temperature anomalies as a function of the water depth in which they occur (opposing hydrostatic head).

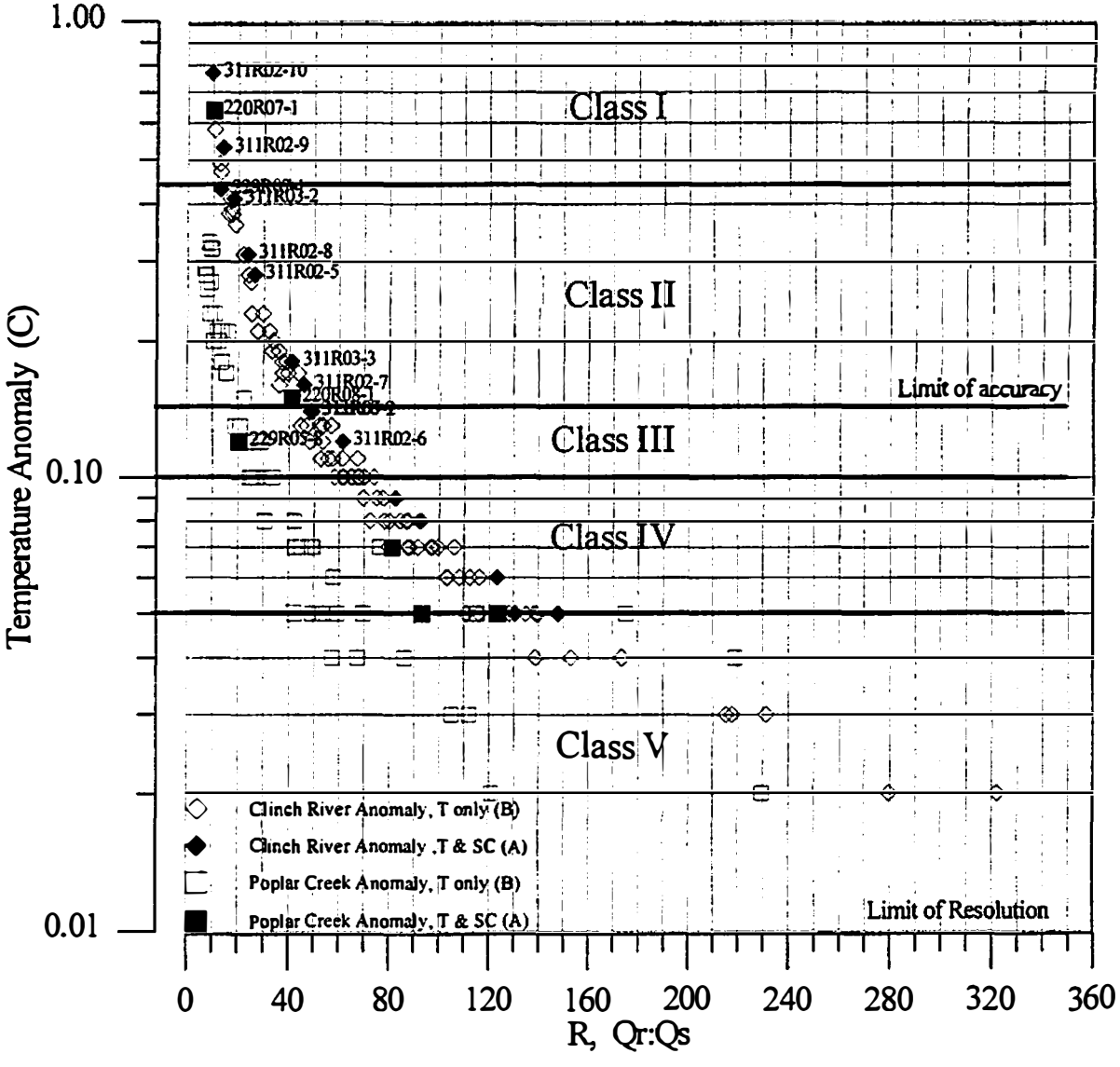


Figure 5.6. Plot of identified temperature anomalies as a function of R, the ratio of ambient river discharge to calculated spring discharge. Anomalies are differentiated by water body.

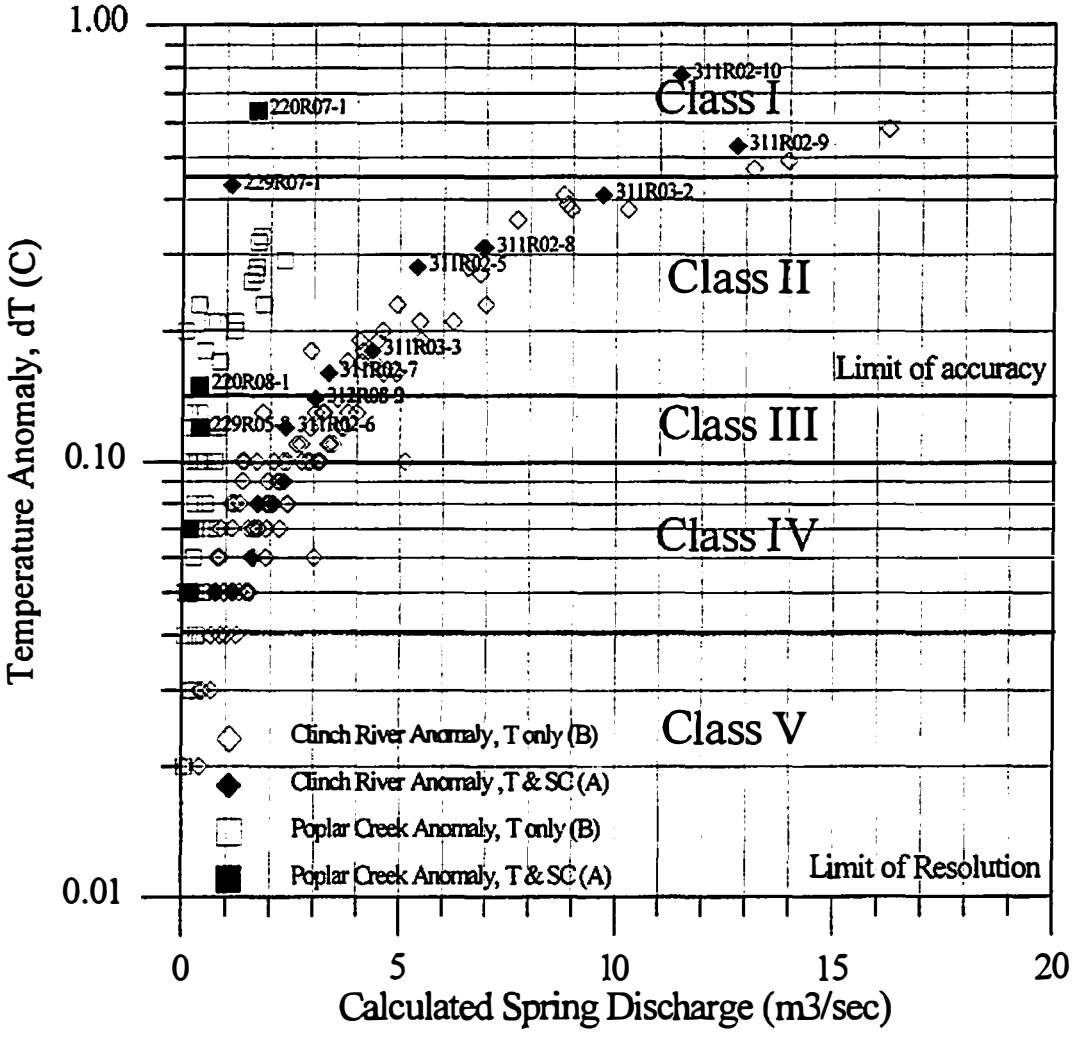


Figure 5.7. Plot of identified temperature anomalies as a function of the calculated spring discharge rate. Anomalies are differentiated by water body in which they occur.

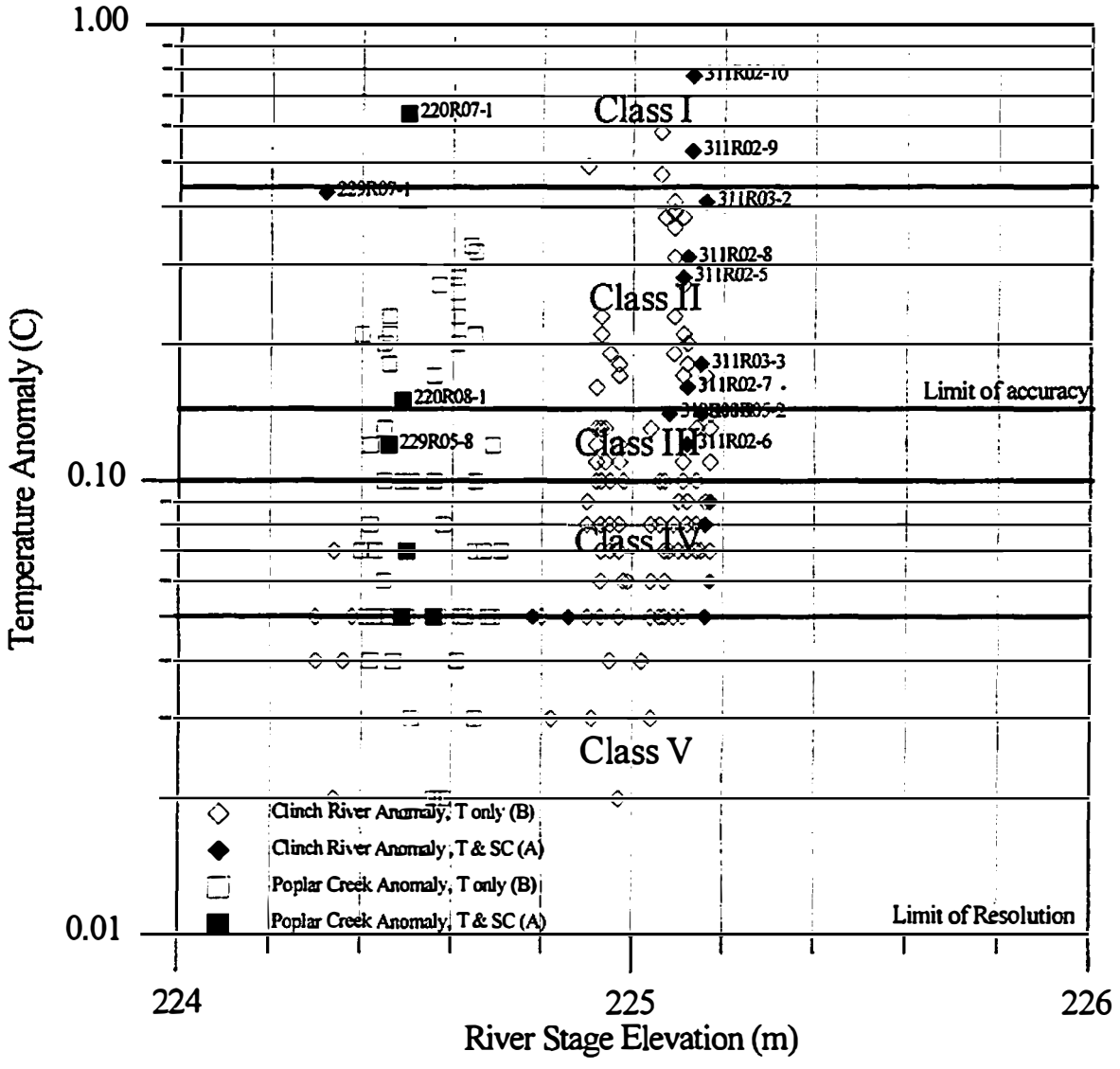


Figure 5.8. Plot of identified temperature anomalies as a function of river stage.

Based upon these observations, it is clear that all of these represent independent variables that play a role in groundwater discharge or in otherwise impacting the ability to detect this discharge. However, since the plots indicate that none of these factors are linearly related to the magnitude of a detected anomaly, these parameters cannot be directly applied in refining the anomaly magnitude classifications. Further, another factor which impacts groundwater discharge is the hydraulic gradient in the adjacent aquifer, and in particular, temporal relationships between recharge, hydraulic gradients to the river, and shorter term transient stage conditions. The data necessary to evaluate the conditions in the adjacent aquifer at the time of the surveys was not available.

From the preceding discussion, the transient nature of the surface water boundary conditions results in complex groundwater-surface water interactions, which complicate the interpretation of the significance of anomalies identified in this study. No simple decision rules emerge to further allow for discrimination among the 198 anomalies detected.

Hydrogeologic Significance

Considering the sparsity of subaerial springs in the study area, subaqueous groundwater discharge to surface water is likely. This is supported by the number of anomalies detected in this study. The locations of anomalies offers some insight into the nature of that discharge, whether occurring as discrete subaqueous springs, spring zones, or diffuse seepage. Further, anomaly locations may be indicative of the role key hydrogeologic features or trends play in localizing groundwater discharge. This section provides a comparison of anomalies identified in this study to expected locations of subaqueous groundwater discharge based upon current understanding of the hydrogeology of the study area. Considering the uncertainties imposed by the transient boundary conditions in the study and their impact on the magnitude of anomalies identified, the locations of those anomalies relative to expected areas of focused groundwater discharge may be used to further validate the anomalies.

Based upon the results of the surveys conducted and for those areas covered,

subaqueous groundwater discharge does appear to occur in the Clinch River and Poplar Creek. Figure 5.9 shows the locations of identified anomalies relative to expected locations of groundwater discharge. Table 5.1, 5.2, and 5.3 summarize those features for which anomalies can be correlated in the areas covered in this work. Comparing the areas where the water table occurs below the top of bedrock (shown on Figure 2.8) to the locations of identified anomalies (Figure 4.4), groundwater discharge appears to be focused as discrete subaqueous springs or spring zones in those reaches where bedrock is exposed along the bank (i.e., there is no saturated unconsolidated zone). In those areas, key bedding, karst dissolution, or structural features (such as faults, folds) appear to localize groundwater discharge. In other areas where discrete springs were not identified within the area covered by the surveys, groundwater can be assumed to discharge as a continuous seepage face.

A large number of anomalies were encountered in the lower Chickamauga and upper Knox Group outcrop belt in shallow water roughly coincident with the pre-impoundment channel edge. These may represent subaqueous springs or spring zones that were inundated following impoundment of the river but still function under certain hydrologic boundary conditions. This is exemplified by anomalies such as 229R07-1 shown in Figure 4.5, which occurs along the edge of the former, pre-impoundment channel along the trend of karst features in the lower Pond Springs Formation. As described in Chapter 4, this anomaly was confirmed based upon detection on four separate occasions. From examination of bedrock outcrops along the bank, this anomaly appears to coincide with a highly solutioned cleaner, fossiliferous limestone unit of the lower Pond Springs Fm near the contact with the underlying Knox Group. This anomaly also correlates with a deep, bedding plane "hole" observed along the river bottom in the river channel and a dye resurgence point from a dye tracer study performed in November 1997 while still under high pool stage conditions. While it was expected that similar anomalies related to this trend would have been encountered at other points of intersection with Poplar Creek, no other anomalies were detected. However, the only other intersection surveyed was near

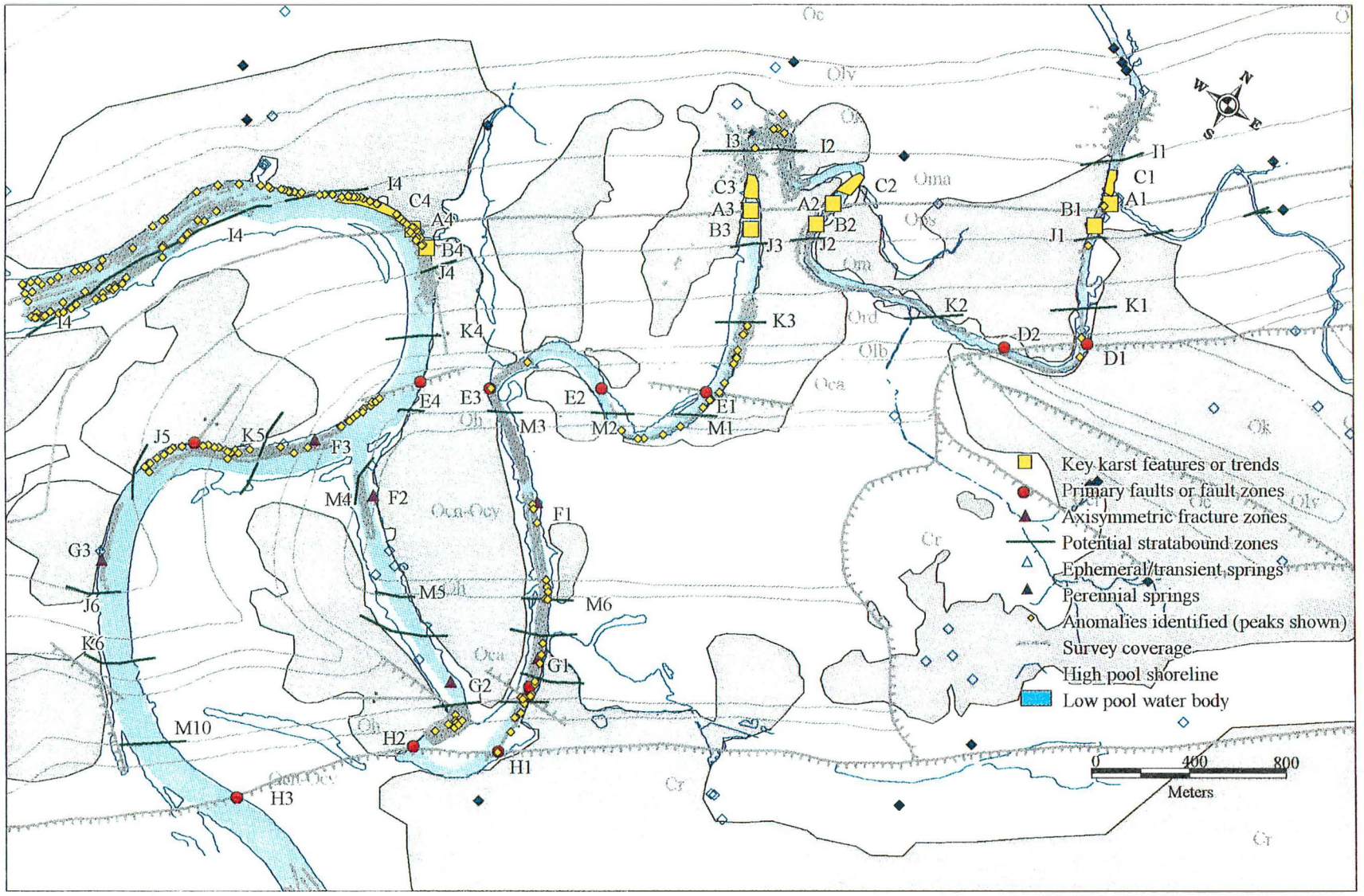


Figure 5.9. Locations of identified anomalies with respect to expected areas of groundwater discharge.

Table 5.1. Summary of anomalies potentially related to expected areas of groundwater discharge associated with karst features or trends. Not all expected target locations were surveyed; only results for those expected locations that were actually surveyed are presented here.

Type	Hydrogeologic Feature or Trend	Map Occurrence[1]		Related Anomalies[2]	Comments
		Poplar Creek	Clinch River		
Karst Features or Trends	Knox-Chickamauga contact (paleokarst)	A1		**220R07-1,**	On strike with spring 16-007
			A4	312R02-2, 312R03-3	
	Trend of karst features (sinkholes) in the lower Pond Springs Fm	B1		None	
		B2		None	
			B4	**229R07-1**, 229R06-1, 312R01-1, 312R03-5	Point of dye emergence in 1997 dye test
	Upper Mascot Fm trend of microgravity anomalies, cavities, and subaerial springs	C1		None	
		C3		None	
			C4	312R03-1, 312R03-2	

1 Map occurrences refer to locations labeled on Figures 2.11 and 5.2.

2 Those anomalies observed within close proximity of the feature of interest. Highlighted (bold) anomalies identify Class I or II anomalies

Table 5.2. Summary of anomalies potentially related to expected areas of groundwater discharge associated with key structural features. Not all expected target locations were surveyed; only results for those expected locations that were actually surveyed are presented here.

Type	Hydrogeologic Feature or Trend	Map Occurrence[1]		Related Anomalies[2]	Comments
		Poplar Creek	Clinch River		
Structural Features	K-25 Fault	D1		None	Minor anomalies encoutered in adjacent Fms
		D2		None	
	Structural features within the deformation zone	E1		229R04-2, 229R05-1, 229R05-2, 229R05-3	
		E3		221R01-1, 221R02-1	
			E4	**311R06-5**, 311R04-4, 311R06-6	
	Map scale syncline (axisymmetric fractures)	F1		222R13-1, 222R13-2, 222R14-1	May be related to outfall discharge
		F2		None	In mixing zone of Clinch and Poplar Creek waters
			(F3)	**311R02-9, 311R02-10**, 304R11-1, 304R10-1	Several transient spring-boils along shore; discharge from west side of river.
	Map scale anticline (axisymmetric fractures, faults, folds)	G1		226R09-1, 226R10-1, 226R11-1	Many anomalies associated with fault
			G3	None	Surveyed west bank, proximal spring
	White Oak Mountain fault	H1		226R12-2	

1 Map occurrences refer to locations labeled on Figures 2.11 and 5.2.

2 Those anomalies observed within close proximity of the feature of interest. Highlighted (bold) anomalies identify Class I or II anomalies

Table 5.3. Summary of anomalies related to potential stratabound flow zones.

Type	Hydrogeologic Feature or Trend	Map Occurrence[1]		Related Anomalies[2]	Comments
		Poplar Creek	Clinch River		
Potential Stratabound Flow Zones	Along the Mascot-Kingsport contact	I1		None	
		I2		None	
		I3		None	
			I4	312R07- 3313R07-3, 313R08-1	
	Pond Springs-Murfreesboro contact	J1		220R08-1	
		J2		None	
			J4	None	
			J5	None	
	Along the middle Ridley Ls calcareous shale	K2		None	
		K3		227R07-1	
			K5	311R02-9, 311R02-10	(?)
	Along the basal Hermitage calcareous shale unit	M1		None	
		M2		None	
		M3		None	
		M5		??	Coincides with PC-CR mixing zone
		M7		226R01-2, 226R02-1	
		M8		226R04-2, 226R10-1	

the "M"-bend on Poplar Creek.

As indicated in Table 5.1, a number of anomalies were identified along karst features in the Knox Group carbonates. Among them, anomaly 220R07-1, shown in Figure 4.2 and 5.9, is the most significant in that it appears to coincide with the Knox-Chickamauga contact along which the majority of the large springs in East Fork valley occur. This anomaly occurs at the most upstream point on Poplar Creek where this trend is intersected (a knick point) and was the highest magnitude anomaly (both temperature and specific conductance) encountered in this study. Further, this anomaly lies approximately 30 m away from a thermal infrared "hotspot" identified along strike in shallow water within the mouth of East Fork Poplar Creek on the 1994 imagery. Several minor anomalies were identified where the unconformity intersects the Clinch River as well. However, it cannot be established whether these occurrences are hydrologically significant or coincidental.

A number of anomalies were identified in connection with mapped structural features in the Chickamauga Group carbonates along Poplar Creek. As shown on Figure 5.9, there are a number of anomalies that were identified within the Carters Limestone along the mapped "deformation zone". Perhaps most significant are Class IIIB anomalies 229R05-1 and 229R05-2 (see Figure A.13.5 in Appendix A), which occur at the upgradient-most intersection of Poplar Creek and the deformation zone. Both of these anomalies appear to correlate with the projection of a mapped reverse fault (oriented 49/39SE) observed in outcrop along the east side of the creek at this point. A small hanging wall anticline is associated with the fault, plunging to the southeast. A small flowing spring was observed along the bank at the base of the outcrop along the trace of the fault. Small kink folds and solutionally enlarged bedding plane perpendicular fractures observed in outcrops along the shoreline may also focus flow in this area. Lemiszki (1995) noted that the faulted and folded beds in this area are sheared, pulled-apart and may be brecciated with a cataclastic (fault rock) fabric.

In December 1998, this area was revisited and several 0.4 °C anomalies detected

along the fractured outcrop. These latter anomalies are four times greater than previously identified during the 1996 field surveys. This may be attributed to the fact that the 1997 surveys were conducted under ambient river flow conditions that were more favorable to identifying springs (i.e., no flow). Other anomalies were detected in the deformation zone further downstream in Poplar Creek. Typically, the anomalies coincided with areas where bedrock was exposed along the shore. The implication is that small scale structural features within the deformation zone may in fact be focusing groundwater discharge and that active groundwater discharge may be limited to areas of the creek where bedrock is exposed.

Another key example of the potential significance of structural controls on groundwater flow is suggested by anomalies identified within the Carters Ls along the axis of the map-scale anticline along Poplar Creek (map location G1 on Figure 5.9). Bedding in this area defines a large anticline-syncline pair that is offset by a northwest-dipping fault that offsets bedding on the southeast limb of the fold (Lemiszki, 1995). Deformation is concentrated in beds on the hanging wall of the fault. Anomalies 226R09-1, 226R10-1, and 226R11-1 are all Class IIIB or lesser anomalies that appear to confirm a zone of groundwater discharge that coincides with the projection of the fault (trending 71/49NW) exposed in outcrop along the east shore of Poplar Creek. Probing along the base of the bluff in December 1997, a 0.3 °C change in temperature was observed along the projection of the fault plane. It is possible that this fault and the deformation zone associated with it plays an important role in focusing groundwater flow. Further, this site marks the upgradient-most intersection of the map-scale anticline and bounding surface water, suggesting a high potential for localized groundwater discharge at this location.

With few exceptions, most of the Poplar Creek anomalies suggest calculated groundwater discharge rates that, as discussed previously, are well in excess of the possible range of discharge determined in the water balance which focused on groundwater discharge in this reach of Poplar Creek. It may be that the thick alluvial sediment which forms the bottom of Poplar Creek limits overall groundwater discharge

and focuses it at key points, related to underlying structural features which lie beneath the alluvium. Cherkauer and Nader (1989) reported anomalously high offshore seepages in Green Bay correlated with local thinning of the relatively low hydraulic conductivity glacial sediments which overlie the bedrock aquifer along the bottom of the bay. Similarly, within Poplar Creek in the study area where the creek bottom is comprised of thick accumulations of relatively low permeability alluvial sediments, it is expected that groundwater discharge is restricted such that anomalies of greater magnitude are uncommon. Additionally, groundwater discharge may be more likely occurring as a larger zone of diffuse seepage rather than as discrete springs. This is supported by the width of the anomalies identified along runs. Since it is unlikely that plumes of any significance persist when the river/creek are flowing, the Gaussian distribution of temperature or specific conductance over anomalies 5-10 m in length suggest diffuse seepage zones. Conversely, sharp anomalies with little lateral dimension may imply discrete locations of more concentrated groundwater discharge.

Although it was expected that marked changes in lithology in the Chickamauga Group carbonates might create a potential for stratabound flow, in many cases along Poplar Creek, these are either not exposed at the surface or not obvious. Consequently, it is not possible at this time to fully evaluate the potential impacts of such stratigraphic zones in controlling groundwater flow. Only limited correlations (listed in Table 5.3) are suggested between detected anomalies and potential stratabound zones.

Not all anomalies identified represent groundwater discharge. For example, in Poplar Creek, the ETTP site sanitary sewer treatment plant discharges water that is 14.4 °C directly to Poplar Creek at a rate of approximately 0.02 m^3/sec, well in excess of the calculated groundwater seepage rate. Temperature probing in the creek in the vicinity of the outfall in December 1997 suggests the discharge stream projects outward into the creek about 3-4 m before being swept downstream. Minor anomalies 222R13-1, 222R13-2, and 222R14-1 appear to occur in the path of the effluent plume and may likely reflect the treatment plant effluent.

Within the more cavernous Knox Group bedrock, it's quite likely that groundwater discharge is through a network of interconnected distributary flowpaths rather than one or two major integrated springs. From field examination, there are a phenomenal number of solutionally enlarged fractures and bedding planes exposed in outcrop along the Clinch River and parts of Poplar Creek, all of which may function as points of groundwater discharge to varying degrees under the certain boundary conditions. Conversely, within the Chickamauga, the hydraulic gradients to the creek are low and given the low permeability (silty clay) alluvium that forms most of the creek bed, groundwater may be discharging as a continuous seepage face, especially where the overburden above bedrock is saturated. Again, this suggests that the most concentrated groundwater discharge, manifested by detectable discrete springs or spring zones, may be restricted to areas where the bedrock is exposed in and along the surface water body. The locations of transient spring boils observed along the banks of Poplar Creek and the Clinch River may represent areas of thinner alluvium overlying primary bedrock flowpaths. Such boils likely represent overflow springs related to direct groundwater discharge to the creek/river.

6. SUMMARY AND CONCLUSIONS

The data acquisition system developed and applied in this research provides a viable means of identifying subaqueous groundwater discharge to large scale surface water bodies in karst settings or other applications where remote methods are not effective. The system was proven capable of detecting temperature and specific conductance anomalies as low as 0.02 ° C and 2 uS/cm, respectively, in water depths up to 16 m. Based upon the results obtained in this study, temperature anomalies reflecting the difference between groundwater and surface water appear to reflect subaqueous groundwater discharge. Specific conductance anomalies were observed to provide confirmation of temperature anomalies in some cases, but because ambient surface water conductivities fall within the range expected for groundwater, cannot be used exclusively to identify groundwater discharge, at least in this study area.

A total of 198 anomalies were identified within the area surveyed; it's possible that other anomalies indicative of groundwater discharge exist but were not surveyed. Overall, the anomalies identified were of low magnitude especially considering the expected differences in temperature and potentially specific conductance between ambient groundwater and surface water. Since the range of specific conductance for surface and groundwater overlap in this system, groundwater discharge is best represented by thermal anomalies. However, dissipation of heat from thermal plumes discharged to surface water is controlled by ambient river flow, ambient river water temperature, and the geometry and orientation of the discharge structure with respect to ambient cross-flow currents. All of these factors impact the potential for detection of anomalies under highly varying and transient conditions. For example, although a number of larger magnitude anomalies were detected, even minor anomalies identified under high flow, stage, or elevated ambient river temperatures may be equally significant. In light of the complexity of surface water hydrodynamics and groundwater-surface water interactions in this study

area, it is not possible to conclusively determine the validity or significance of the anomalies identified without further investigations. Minimally, each anomaly must be carefully scrutinized within the context of site hydrogeologic knowledge to insure they are valid reflections of actual groundwater discharge. In the current application, this method has proven useful as a preliminary survey to identify suspected areas of subaqueous groundwater discharge where other methods, such as infrared thermography, were simply not applicable.

Due to the transient nature of the hydrologic system in this study area, there are inherent uncertainties that cannot be addressed using this method alone. Since subaqueous groundwater discharge is a function of antecedent recharge, hydraulic gradients in the aquifer adjacent to the river, and river stage height, in applications where stage heights are known to fluctuate over short periods of time, it may be useful to include continuous monitoring of both stage and key groundwater wells adjacent to the surface water body. This could allow for improved evaluations of anomalies in light of changing hydraulic gradients and groundwater flux. While this method has proven to be a useful survey tool for identification of subaqueous discharge in complex, transient hydrologic conditions such as prevailed in the study area, it is expected that this method would be best applied in hydrologic settings where conditions are less transient. In particular, this method would be best suited to settings where surface water flow rates are negligible to non-existent, and where surface water temperatures remain fairly constant, at least over the time required to complete a survey.

The nature and locations of anomalies identified in this study provide insights about the complexity of groundwater-surface interactions in the study area, the nature of groundwater discharge, and the role key hydrogeologic features and trends play in controlling groundwater flow and thus discharge to surface water. In this study and for the areas investigated, it appears that where thick alluvium blankets the river/creek bottom few anomalies were detected. These areas were typically characterized by lower magnitude, broader anomalies. Similar results were encountered along reaches where the

unconsolidated zone above bedrock was saturated and unconsolidated zone flowpaths were intersected by surface water bodies. In both of these settings, groundwater discharge likely occurs as a continuous seepage face or zone of diffuse seepage along the creek bottom.

Conversely, it appears that larger magnitude, more discrete anomalies were more commonly detected in areas where either the unconsolidated zone above bedrock was unsaturated (i.e., the water table occurs below the top of bedrock and bedrock flowpaths prevail) or where bedrock was exposed along the river/creek bottom. In these areas, groundwater flow is likely occurring along primary flowpaths in the bedrock, including faults, fractures, solutionally enlarged fractures and karst conduits. In many cases, the locations of anomalies were well correlated to mapped or suspected hydrogeologic features or trends. However, it appears that groundwater discharge is closely regulated by transient boundary conditions in the receiving surface water body such that groundwater discharge from these features is variable. Rather than serving as discrete integrators of groundwater discharge, it is more likely that each of these flowpaths function as part of a larger, interconnected, distributary network that functions differently in response to changing boundary conditions, recharge, and hydraulic gradients in the aquifer.

Finally, the results of this study indicate the highly complex nature of groundwater-surface water interactions in settings where groundwater systems are bounded by TVA run-of-the-river impoundments. The locations of anomalies in the Clinch River appear to occur along the pre-impoundment river channel which suggests that these locations may represent pre-impoundment springs that are now inundated.

REFERENCES

REFERENCES

Alfaro, C. and M. Wallace. 1994. Origin and classification of springs and historical review with current applications. Environmental Geology. **24**: 112-124.

Banks, W.S.L., R.L. Paylor, and W.B. Hughes. 1996. Using thermal-infrared imagery to delineate ground-water discharge. Groundwater. 34 (3):434-443.

Bogle, F.R. and K. Loy. 1995. The application of thermal infrared thermography in the identification of submerged springs in Chickamauga Reservoir, Hamilton County, Tennessee. Karst GeoHazards, B. Beck editor. Balkema Press. Rotterdam. pp. 415-424.

Bonacci, O. 1987. Karst Hydrology. Springer-Verlag. Heidelberg. 183 pp.

Bowman, N. 1996. Personal communication (data) from Norman Bowman of the K-25 Plant Utilities Group to T.F. Zondlo.

Cherkauer, D.S. and D.C. Nader. 1989. Distribution of groundwater seepage to large surface-water bodies: the effect of hydraulic heterogeneities. Journal of Hydrology. **109** (1989): 151-165.

Cherkauer, D.S. and P.M. McKereghan. 1991. Ground-water discharge to lakes: focusing on embayments. Ground Water. 29 (1): 72-80.

DeBuchananne, G.D. and R.M. Richardson. 1956. Groundwater resources of East Tennessee, Parts 1 & 2. Tennessee Division of Geology Bulletin 58. Nashville, TN.

DOE. 1996. Groundwater Remedial Site Evaluation Report (RSER) for the Oak Ridge K-25 Site. DOE/OR/01-1468V1&D1. May 1996. Oak Ridge, Tennessee.

DOE. 1997a. Remedial Investigation for the K-1070-A burial ground at the Oak Ridge K-25 Site, Oak Ridge, Tennessee. Vol.1. DOE/OR/01-1519&D0.

DOE. 1997b. Design Data Acquisition Report for the Mitchell Branch, K-1070C/D Classified Burial Ground, and K-27/29 Plumes Project, East Tennessee Technology Park, Oak Ridge, Tennessee. K/ER-324.

Drogue, C. and M. Razack. 1984. Survey of a coastal karstic aquifer by analysis of the effects of sea-tide: example of the Kras of Slovenia, Yugoslavia. Environmental Geology and Water Science. **6** (2): 103-109.

Energy Systems. 1995. Summary report of continuous water level monitoring at ten groundwater monitoring wells as the Oak Ridge K-25 Site, Oak Ridge, Tennessee. K/ER-247. Martin-Marietta Energy Systems, Inc. Environmental Restoration Division. Oak Ridge, Tennessee.

Ford, D. and P. Williams. 1989. Karst geomorphology and hydrology. Chapman and Hall, 601 pp.

Frigo, A.A. and D.E. Frye. 1972. Physical measurements of thermal discharge into Lake Michigan: 1971. Argonne National Laboratory Report ANL/ES-16. 168 p.

Garrett, A.J., and T. Evers. 1997. Aqueous mixing and potential contaminant transport at the Poplar Creek/Clinch River confluence. Final Report. July 1997. Oak Ridge National Laboratory. Oak Ridge, Tennessee.

Hatcher, R.D., P.J. Lemiszki, R.B. Dreier, R.H. Ketelle, R.R. Lee, D.A. Leitzke, W.M. McMaster, J.L. Foreman, and S.Y. Lee. 1992. Status report on the geology of the Oak Ridge Reservation. ORNL/TM-12074. Martin-Marietta Energy Systems, Inc. Oak Ridge, Tennessee.

Hess, J.W., S.G. Wells and T.A Brucker. 1974. A survey of springs along the Green and Barren Rivers, Central Kentucky Karst. National Speleological Society Bulletin. 36 (3): 1-7.

Hirst, E.A.. 1971a. Analysis of round, turbulent, buoyant jets discharged to flowing stratified ambients. ORNL-4685. Union Carbide Corporation. Oak Ridge national Laboratory. Oak Ridge, Tennessee. 37 pp.

Hirst, E.A.. 1971b. Analysis of buoyant jets within the zone of flow establishment. ORNL/TM-3470. Union Carbide Corporation. Oak Ridge national Laboratory. Oak Ridge, Tennessee. 42 pp.

Hollyday, E.C. and M.A. Smith. 1990. Large springs in the Valley and Ridge Province in Tennessee. U.S. Geological Survey Water Resources Investigation Report 89-4295. 9 p.

Hydrolab Corporation. 1992. Performance manual for field water quality instrumentation. Publication No. 3039-687. Austin, Texas. 28 pp.

Ketelle, R.H. and R.R. Lee. 1992. Migration of a groundwater contaminant plume by stratabound flow in Waste Area Grouping 1 at Oak Ridge National Laboratory, Oak Ridge, Tennessee. ORNL/ER-126. Martin Marietta Energy Systems, Inc. Oak Ridge National Laboratory. Oak Ridge, Tennessee.

Lee, D. R. and R. Dal Bianco. 1994. Methodology for locating and quantifying acid mine drainage in ground waters entering surface waters. *In* Proceedings, Third International Conference on the Abatement of Acidic Drainage. Pittsburgh, Pennsylvania. pp. 327-335.

Lemiszki, P. 1994. Geological mapping of the Oak Ridge K-25 Site, Oak Ridge, Tennessee. K/ER-111. Martin-Marietta Energy Systems Inc. Oak Ridge, Tennessee.

Lemiszki, P. 1995. Mesoscopic structural analysis of bedrock exposures at the Oak Ridge K-25 Site, Oak Ridge, Tennessee. K/ER-259. Lockheed-Martin Energy Systems, Inc. Environmental Restoration Division. Oak Ridge, Tennessee.

Linsley, R.K., M.A. Koehler, and J.L. Paulhus. 1958. Hydrology for engineers. McGraw-Hill. New York. 340 pp.

Madding, R.P., J.V. Tokar, and G.J. Marmer. 1975. A comparison of aerial infra-red and in-situ thermal plume measurement techniques. *In* Proc. Environmental Effects of Cooling Systems at Nuclear power Plants. International Atomic Energy Agency. Vienna. pp. 163-186.

McMaster, W.M.. 1962. Geologic map of the Oak Ridge Reservation, Tennessee. Scale 1:31680. ORNL/TM-713. Oak Ridge National Laboratory, Oak Ridge, Tennessee.

Milanovic, P.T. 1981. Karst Hydrogeology. Water Resources Publications. Littleton, Colorado. 434 pp.

Milanovic, P. 1986. Influence of the karst spring submergence on the karst aquifer regime. J. Hydrology; 84: 141-156.

Montanez, I.P. and J.F. Read. 1992. Fluid-rock interaction history during stabilization of early dolomites, Upper Knox Group (Lower Ordovician), U.S. Appalachians. Journal of Sedimentary Petrology. **62** (5):753-778.

Mussman, W.J., I.P. Montanez, and J.F. Read. 1988. Ordovician Knox paleokarst unconformity, Appalachians. In *Paleokarst*, edited by N.P. James and P.W. Choquette. Springer-Verlag. pp. 211-229.

Palmer, M.V. and A.N. Palmer. 1989. Paleokarst in the United States. In *Paleokarst: a systematic review*. Edited by P. Bosak, D.C. Ford, J. Glazek, and I. Horacek. Elsevier. pp. 337-367.

Parker, F.L. and P.A. Krenkel. 1970. Physical and engineering aspects of thermal pollution. CRC Press. Cleveland, Ohio. 100 pp.

Rodgers, J. 1953. Geologic map of east Tennessee with explanatory text. Scale 1:125,000. Tennessee Division of Geology Bulletin 58.

Shirazi, M.A. 1972. Workbook on thermal plume predictions: Volume 1, Submerged discharge. U.S.E.P.A. National Environmental Research Center report EPA-R2-72-005A. Corvallis, Oregon. 229 pp.

Swain, L.A., E.F. Hollyday, C.C. Daniel, and O.S. Zapecza. 1991. Plan of study for the regional aquifer-system analysis of the Appalachian Valley and Ridge, Piedmont, and Blue Ridge physiographic provinces of the eastern and southeastern United States, with a description of study-area geology and hydrogeology. U.S. Geological Survey Water Resources Investigation Report 91-4066. 44 p.

Tennessee Synfuels Associates. 1981. Coal-to-gasoline facility, Oak Ridge, Tennessee: environmental impact report, Vols. I through IX. December 1981.

Tokar, J.V.. 1971. Thermal plumes in lakes: compilations of field experience. Argonne National Laboratory Report ANL/ES-3. 169 p.

TVA. 1996. Digital daily stage and dam discharge data for Watts Bar and Melton Hill Dams provided to T.F. Zondlo by J. Pinkston. TVA Reservoir Operations. Planning and Development Group. Knoxville, Tennessee.

Vroblesky, D.A., M.M. Lorah, and S.P. Trimble. 1991. Mapping zones of contaminated groundwater discharge using creek-bottom-sediment vapor samplers, Aberdeen Proving Ground, Maryland. Ground Water. **29** (1): 7-12.

Wang, Chi-Rong and S.S. Papell. 1983. Three-dimensional turbulent mixing-length modeling for discrete-hole coolant injection into a crossflow. NASA Technical paper 2200. NASA Lewis Research Center. Cleveland, Ohio. 13 pp.

Zektser, I.S. and A.V. Meskheteli. Methods for studying subsurface discharge of karst water. *In*: IAH 21st Congress on Karst Hydrogeology and Karst Environment Protection. October 10-15 1988, Guilin, China. pp. 677-681.

Zondlo, T.F. 1995a. Methodology for identification of subaqueous groundwater discharge to large scale surface water bodies at the DOE K-25 site, Oak Ridge, Tennessee. (Abstr) presented at the Southeast Regional Meeting of the Geological Society of America. Knoxville, Tennessee. April 1995.

Zondlo, T.F. 1995b. Identification of subaqueous groundwater discharge in the Clinch River: Summary report of fieldwork completed in 1995. Prepared as a directed study for a course entitled Karst Spring Studies. Department of Geological Sciences. University of Tennessee. Knoxville, Tennessee.

Zondlo, T.F. 1996. Technical action plan: subaqueous seep and spring survey of Poplar Creek and the Clinch River. K/ER-219. Rev.1. Lockheed-Martin Energy Systems, Inc. Oak Ridge, Tennessee.

Zondlo, T.F. 1997. Unpublished data from continuous monitoring of wells, springs, stage, and cave streams at the ETTP site. Lockheed-Martin Energy Research. Oak Ridge National Laboratory. Oak Ridge, Tennessee.

APPENDICES

APPENDIX A

FIELD DATA SUMMARIES AND RESULTS

APPENDIX A CONTENTS

Appendix	Title	Page
A.1	January 23, 1996	124
A.2	January 25, 1996	128
A.3	January 29, 1996	133
A.4	February 14, 1996	137
A.5	February 15, 1996	141
A.6	February 19, 1996	146
A.7	February 20, 1996	151
A.8	February 21, 1996	159
A.9	February 22, 1996	164
A.10	February 23, 1996	169
A.11	February 26, 1996	173
A.12	February 27, 1996	179
A.13	February 29, 1996	187
A.14	March 4, 1996	197
A.15	March 11, 1996	203
A.16	March 12, 1996	209
A.17	March 13, 1996	215
A.18	March 14, 1996	221
A.19	Anomaly Summary Tables	227

APPENDIX A LIST OF FIGURES

Figure	Title	Page
A.1.1	Survey data and ambient hydrologic conditions, January 23, 1996	126
A.1.2	Survey location map, January 23, 1996.	127
A.2.1	Survey data and ambient hydrologic conditions, January 25, 1996.	131
A.2.2	Survey location map, January 25, 1996.	132
A.3.1	Survey data and ambient hydrologic conditions, January 29, 1996	135
A.3.2	Survey location map, January 29, 1996	136
A.4.1	Survey data and ambient hydrologic conditions, February 14, 1996.	139
A.4.2	Survey location map, February 14, 1996.	140
A.5.1	Survey data and ambient hydrologic conditions, February 15, 1996.	143
A.5.2	Survey location map, February 15, 1996.	144
A.5.3	Anomaly location map, February 15, 1996.	145
A.6.1	Survey data and ambient hydrologic conditions, February 19, 1996.	148
A.6.2	Survey location map, February 19, 1996.	149
A.6.3	Anomaly location map, February 19, 1996.	150
A.7.1	Survey data and ambient hydrologic conditions, February 20, 1996.	154
A.7.2	Survey location map, runs 1-8, February 20, 1996.	155
A.7.3	Survey location map, runs 7-10, February 20, 1996.	156
A.7.4	Anomaly location map, runs 1-8, February 20, 1996.	157
A.7.5	Anomaly location map, runs 7-10, February 20, 1996.	158
A.8.1	Survey data and ambient hydrologic conditions, February 21, 1996	161
A.8.2	Survey location map, February 21, 1996.	162
A.8.3	Anomaly location map, February 21, 1996	163
A.9.1	Survey data and ambient hydrologic conditions, February 22, 1996	166
A.9.2	Survey location map, February 22, 1996.	167
A.9.3	Anomaly location map, February 22, 1996.	168
A.10.1	Survey data and ambient hydrologic conditions, February 23, 1996.	171
A.10.2	Survey location map, February 23, 1996	172
A.11.1	Survey data and ambient hydrologic conditions, February 26, 1996.	176
A.11.2	Survey location map, February 26, 1996	177
A.11.3	Anomaly location map, February 26, 1996.	178
A.12.1	Survey data and ambient hydrologic conditions, February 27, 1996.	182
A.12.2	Survey location map, lower Poplar Creek area, February 27, 1996..	183
A.12.3	Survey location map, upper Poplar Creek area, February 27, 1996.	184
A.12.4	Anomaly location map, lower Poplar Creek area, February 27, 1996..	185

APPENDIX A LIST OF FIGURES (Continued)

Figure	Title	Page
A.12.5	Anomaly location map, upper Poplar Creek area, February 27, 1996..	186
A.13.1	Survey data and ambient hydrologic conditions during Runs 1-5, February 29, 1996.	191
A.13.2	Survey data and ambient hydrologic conditions during Runs 6-11, February 29, 1996.	192
A.13.3	Survey location map, runs 1-5 on Poplar Creek, February 29, 1996.	193
A.13.4	Survey location map, runs 6-11 on the Clinch River, February 29, 1996.	194
A.13.5	Anomaly location map, runs 1-5 on Poplar Creek, February 29, 1996.	195
A.13.6	Anomaly location map, runs 6-11 on the Clinch River, February 29, 1996.	196
A.14.1	Survey data and ambient hydrologic conditions, March 4, 1996.	200
A.14.2	Survey location map, March 4, 1996.	201
A.14.3	Anomaly location map, March 4, 1996.	202
A.15.1	Survey data and ambient hydrologic conditions, March 11, 1996.	206
A.15.2	Survey location map, March 11, 1996.	207
A.15.3	Anomaly location map, March 11, 1996	208
A.16.1	Survey data and ambient hydrologic conditions, March 12, 1996.	212
A.16.2	Survey location map, March 12, 1996	213
A.16.3	Anomaly location map, March 12, 1996	214
A.17.1	Survey data and ambient hydrologic conditions, March 13, 1996.	218
A.17.2	Survey location map, March 13, 1996	219
A.17.3	Anomaly location map for March 13, 1996.	220
A.18.1	Survey data and ambient hydrologic conditions, March 14, 1996.	224
A.18.2	Survey location map, March 14, 1996.	225
A.18.3	Anomaly location map, March 14, 1996.	226

APPENDIX A LIST OF TABLES

Figure	Title	Page
A.1.1	Summary of field data for January 23, 1996	125
A.2.1	Summary of field data for January 25, 1996.	130
A.3.1	Summary of field data for January 29, 1996.	134
A.4.1	Summary of field data for February 14, 1996.	138
A.5.1	Summary of field data for February 15, 1996.	142
A.6.1	Summary of field data for February 19, 1996.	147
A.7.1	Summary of field data for February 20, 1996.	153
A.8.1	Summary of field data for February 21, 1996.	160
A.9.1	Summary of field data for February 22, 1996	165
A.10.1	Summary of field data for February 23, 1996	170
A.11.1	Summary of field data for February 26 1996.	175
A.12.1	Summary of field data for February 27 1996.	181
A.13.1	Summary of field data for February 29 1996.	190
A.14.1	Summary of field data for March 4, 1996.	199
A.15.1	Summary of field data for March 11, 1996.	205
A.16.1	Summary of field data for March 12, 1996.	211
A.17.1	Summary of field data for March 13, 1996.	217
A.18.1	Summary of field data for March 14, 1996.	223
A.19.1	Anomaly summary information, sorted by class	228
A.19.2	Summary of hydrogeologic information for anomalies	235

APPENDIX A.1

DATE: **January 23, 1996**

SURVEY AREA: Clinch River just upstream of the Gallaher (Highway 58) Bridge in the water gap in Pine Ridge. Survey covers Cambrian Rome Formation bedrock exposed in the river bottom.

DESCRIPTION: A total of 10 relatively short runs were performed in this area, in water depths ranging from 2 -7 m.

HYDROLOGIC CONDITIONS: Hydrologic conditions prevailing during the field data acquisition period are summarized graphically on Figure A.1.1. Discharge from Melton Hill continued throughout the field period (though decreasing in later runs) such that flow rates in the Clinch River were consistently above 250 m^3/sec. With the decline in Melton Hill discharge, stage dropped approximately 0.25 m from early runs (1-4) to later runs (6-10).

There was no rainfall during the field day. Antecedent rainfall conditions were as follows:

within last 24 hours:	0 mm
within past 4 days:	0 mm
within past 7 days:	95.50 mm

DATA: Data are summarized graphically on Figure A.1.1. Summary statistics on a run-by run basis are provided in Table A.1.1. Runs are shown on Figure A.1.2. Temperature and SC maps are not provided since there the results indicated little or no variation along runs.

ANOMALIES: No anomalies indicative of springs were noted in the field. Review of the data confirms this with water temperatures varying only 0.02 °C within runs and 0.3 °C over the course of the day. Overall, there was a very slight warming trend over the course of the field period and with decreasing water depth. Specific conductance varied only 2 uS/cm over all runs.

Table A.1.1. Summary of field data for January 23, 1996.

				TEMPERATURE (°C)			SC (uS/cm)				ANOMALIES			
RUN	DIRXN	TIME	RECORDS	MIN	MAX	MEAN	MIN	MAX	MEAN	DEPTH (m)	Class I	Class II	Class III	Class IV
1	DS	11:38-11:42	188	7.61	7.63	7.62	259	260	259.1	3.96-5.18				
2	DS	11:55-11:59	145	7.61	7.62	7.61	260	260	260	4.57-5.49				
3	DS	12:51-12:56	170	7.69	7.72	7.70	259	261	260	3.05-4.88				
4	DS	13:04-13:11	231	7.72	7.78	7.74	260	261	260	2.13-3.96				
5	DS	13:22-13:28	229	7.75	7.76	7.75	260	260	260	4.57-5.49				
6	DS	14:16-14:21	244	7.83	7.84	7.84	260	260	260	4.27-5.49				
7	DS	14:29-14:35	299	7.84	7.85	7.84	260	260	260	4.57-5.49				
8	DS	14:43-14:51	272	7.85	7.89	7.85	260	261	260	3.66-6.40				
9	DS	14:58-15:03	233	7.87	7.91	7.88	260	261	260	5.49-7.01				
10	DS	15:10-15:18	201	7.89	7.91	7.90	260	260	260	4.27-6.40				

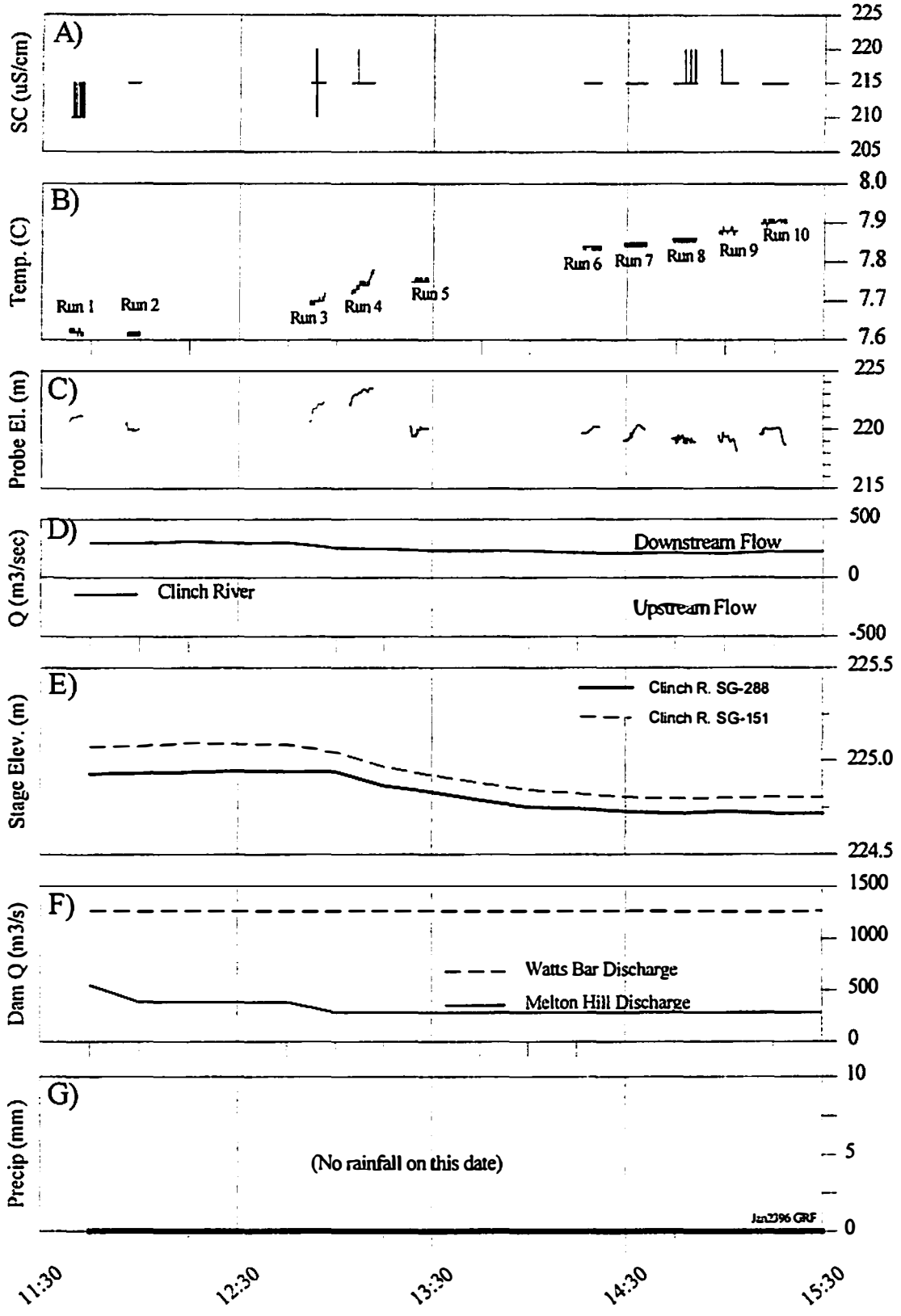


Figure A.1.1. Survey data and ambient hydrologic conditions, January 23, 1996.

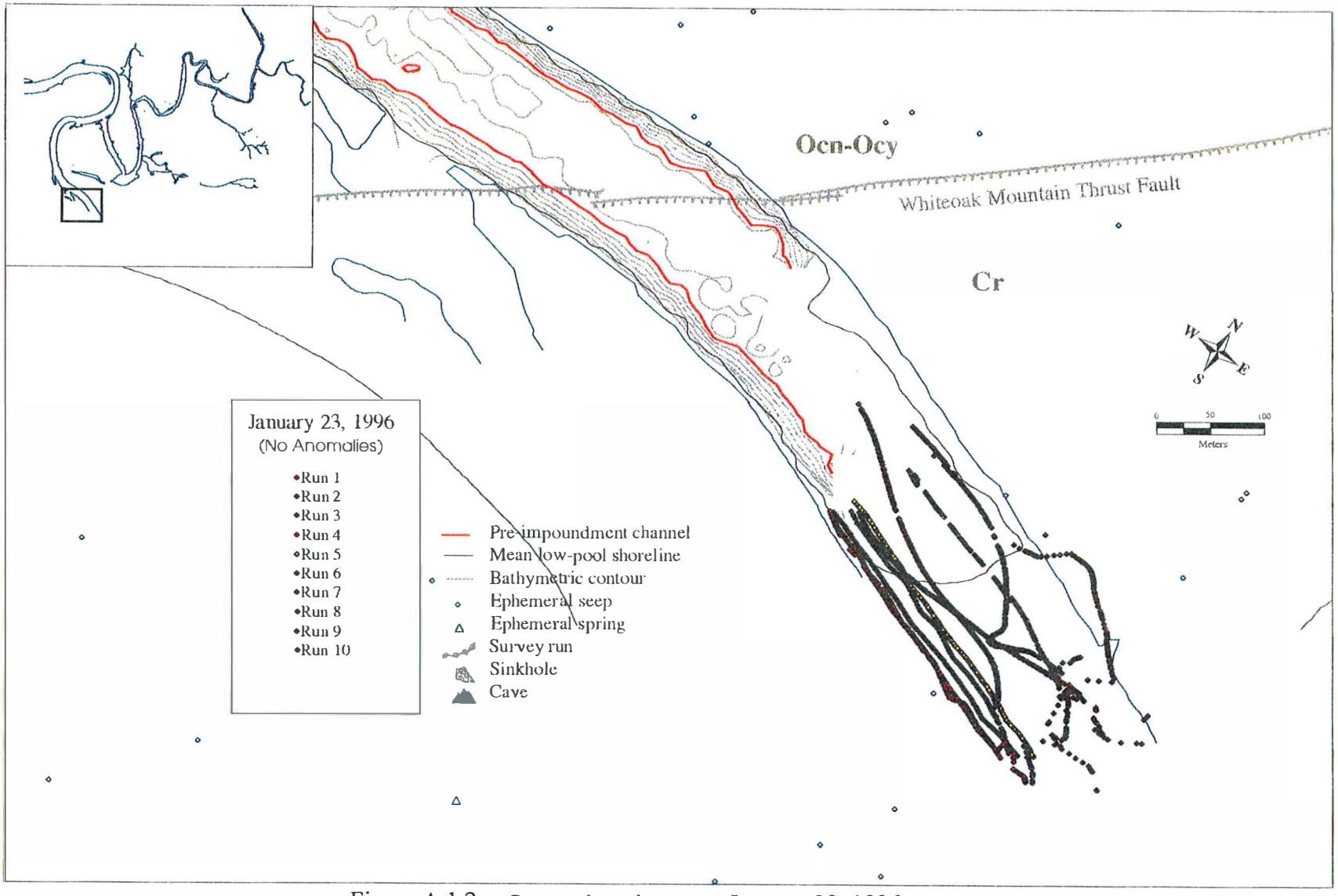


Figure A.1.2 Survey location map, January 23, 1996.

APPENDIX A.2

DATE: **January 25, 1996**

SURVEY AREA: Clinch River downstream of the confluence with Poplar Creek in the vicinity of stage gage SG-288. Survey covers lower Chickamauga (Pond Springs, Murfreesboro Ls) and upper Knox (Mascot Dolomite) bedrock exposed along bank and in river bed.

DESCRIPTION: A total of 6 runs were performed in this area, in water depths ranging from 6.7 to 10.4 m. Differential GPS locations were apparently not recorded for runs 5 and 6, such that no data is usable for these runs. Differential corrections (Acc-Q-Point) were sporadic during runs 1-4. No base station data was available to later post-process these records. Attempts at utilizing an additional source of base station data proved unsuccessful. Consequently, data is only available for Runs 1-4 and locations are considered suspect (especially since the traverse course for on run appears to be on-shore at one point). Survey runs overlap with coverage from 2/29/96 and 3/12/96, conducted under differing hydrologic conditions. Also, survey runs overlap with coverage from March of 1995.

HYDROLOGIC CONDITIONS: Hydrologic conditions prevailing during the field data acquisition period are summarized graphically on Figure A.2.1. Melton Hill dam was generating during the field surveys resulting in strong downstream Clinch River flow rates. Discharge at Melton Hill and Watts Bar were constant during the 2 hrs of fieldwork at approximately 260 and 1250 m^3/sec, respectively. Consequently, Clinch River flow rates in the study area were consistent at ~ 200 m^3/sec.

There was no rainfall during the field day. Antecedent rainfall conditions were as follows:

within last 24 hours:	0 mm
within past 4 days:	49.78 mm
within past 7 days:	138.17 mm

DATA: Data are summarized graphically on Figure A.2.1. Summary statistics on a run-by run basis are provided in Table A.2.1. Runs are shown on Figure A.2.2. Temperature and SC anomalies are shown on Figure A13.2 (February 29, 1996).

ANOMALIES: No anomalies indicative of springs were noted in the field. Review of the data confirms this with water temperatures varying only 0.02 to 0.04 °C within runs and 0.04 °C over the course of the day. Specific conductance varied 15 uS/cm over all runs, but given the lack of temperature anomalies, are not believed to indicate groundwater discharge alone. Given the high flow rates, it is not surprising that anomalies were not detected.

Table A.2.1. Summary of field data for January 25, 1996.

				TEMPERATURE (°C)			SC (uS/cm)				ANOMALIES			
RUN	DIRXN	TIME	RECORDS	MIN	MAX	MEAN	MIN	MAX	MEAN	DEPTH (m)	Class I	Class II	Class III	Class IV
1	DS	14:05-14:12	351	7.33	7.35	7.34	225	230	226.6	NA				
2	DS	14:20-14:34	428	7.33	7.37	7.35	219	227	223.4	3.66-7.32				
3	DS	14:43-15:01	664	7.35	7.37	7.35	225	234	229.2	6.10-10.36				
4	DS	15:10-15:29	674	7.35	7.37	7.36	229	234	230.8	5.79-10.36				
5	DS	-	-	-	-	-	-	-	-	-				
6	DS	-	-	-	-	-	-	-	-	-				

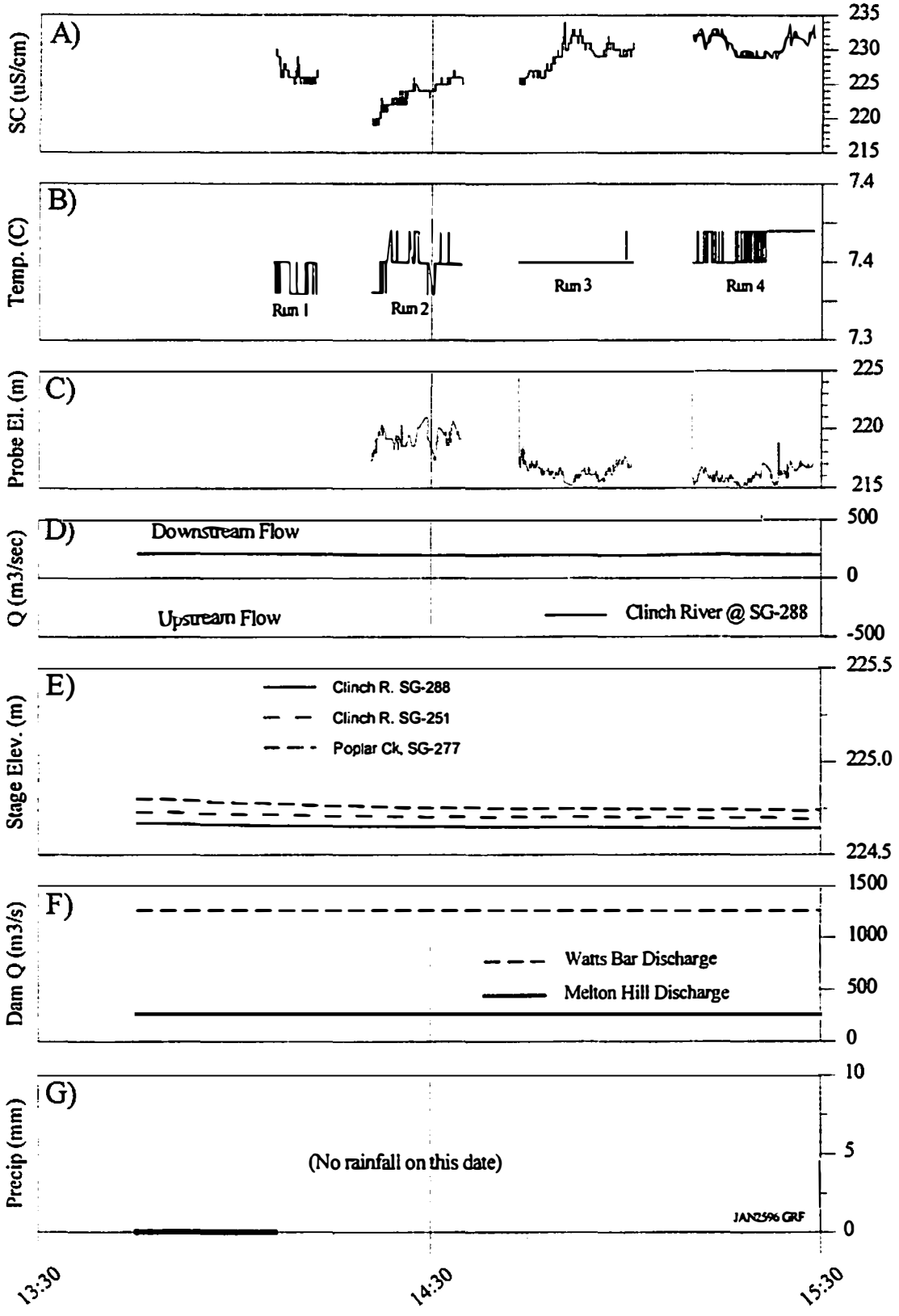


Figure A.2.1. Survey data and ambient hydrologic conditions, January 25, 1996.

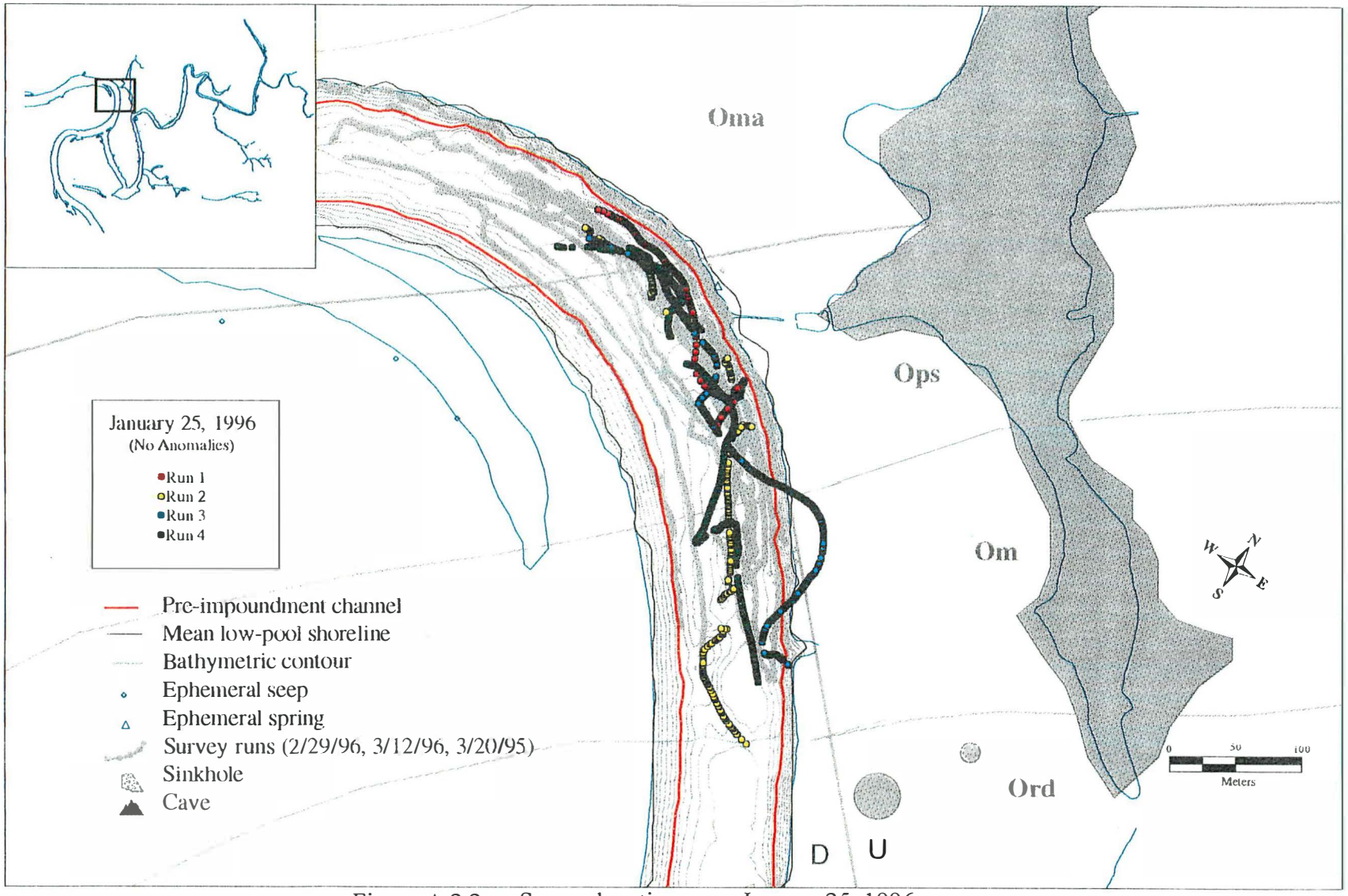


Figure A.2.2. Survey location map, January 25, 1996.

APPENDIX A.3

DATE: **January 29, 1996**

SURVEY AREA: Clinch River upstream of the confluence with Poplar Creek in the vicinity of the Powerhouse area Survey covers lower Chickamauga (Pond Springs Fm) bedrock exposed along bank and in river bed roughly coincident with the axis of the map-scale anticlinal structure.

DESCRIPTION: A total of 4 relatively short runs were performed in this area, in water depths ranging from 1.2 to 8.8 m. Considerable rainfall in the week prior to 1/29/96 created favorable groundwater recharge conditions but also elevated stage heights and high flow rates in the Clinch River, limiting the ability to detect anomalies indicative of groundwater discharge.

HYDROLOGIC CONDITIONS: Hydrologic conditions prevailing during the field data acquisition period are summarized graphically on Figure A.3.1. Melton Hill dam was generating at near full capacity during the field surveys resulting in strong downstream Clinch River flow rates.

Though not raining during the field surveys, antecedent rainfall conditions were as follows:

within last 24 hours:	1.02 mm
within past 4 days:	152.39 mm
within past 7 days:	202.18 mm

DATA: Data are summarized graphically on Figure A.3.1. Summary statistics on a run-by run basis are provided in Table A.3.1. Runs are shown on Figure A.3.2. Maps depicting temperature and SC results are not provided since the data on Table A.3.1 indicate no anomalies and the ambient river flow rates prohibit application of this method under these conditions.

ANOMALIES: No anomalies indicative of springs were noted in the field. Review of the data confirms this with water temperatures varying only 0.01 to 0.05 °C within runs and 0.07 °C over the course of the day. Specific conductance varied only 5 uS/cm over all runs. Although the surface water temperature was very cold (~ 5.94 °C) and presents optimum temperature contrast conditions, given the high flow rates, it is not expected anomalies could have been detected.

Table A.3.1. Summary of field data for January 29, 1996.

				TEMPERATURE (°C)			SC (uS/cm)				ANOMALIES			
RUN	DIRXN	TIME	RECORDS	MIN	MAX	MEAN	MIN	MAX	MEAN	DEPTH (m)	Class I	Class II	Class III	Class IV
1	DS	12:39-12:45	169	5.96	6.01	5.98	238	240	238.9	1.22-3.35				
2	DS	12:55-13:00	141	5.96	5.98	5.96	238	239	238.7	2.74-8.23				
3	DS	13:06-13:15	252	5.96	5.97	5.97	238	239	238.5	5.49-8.84				
4	DS	14:37-14:45	218	5.94	5.99	5.96	236	239	238.4	7.01-8.23				

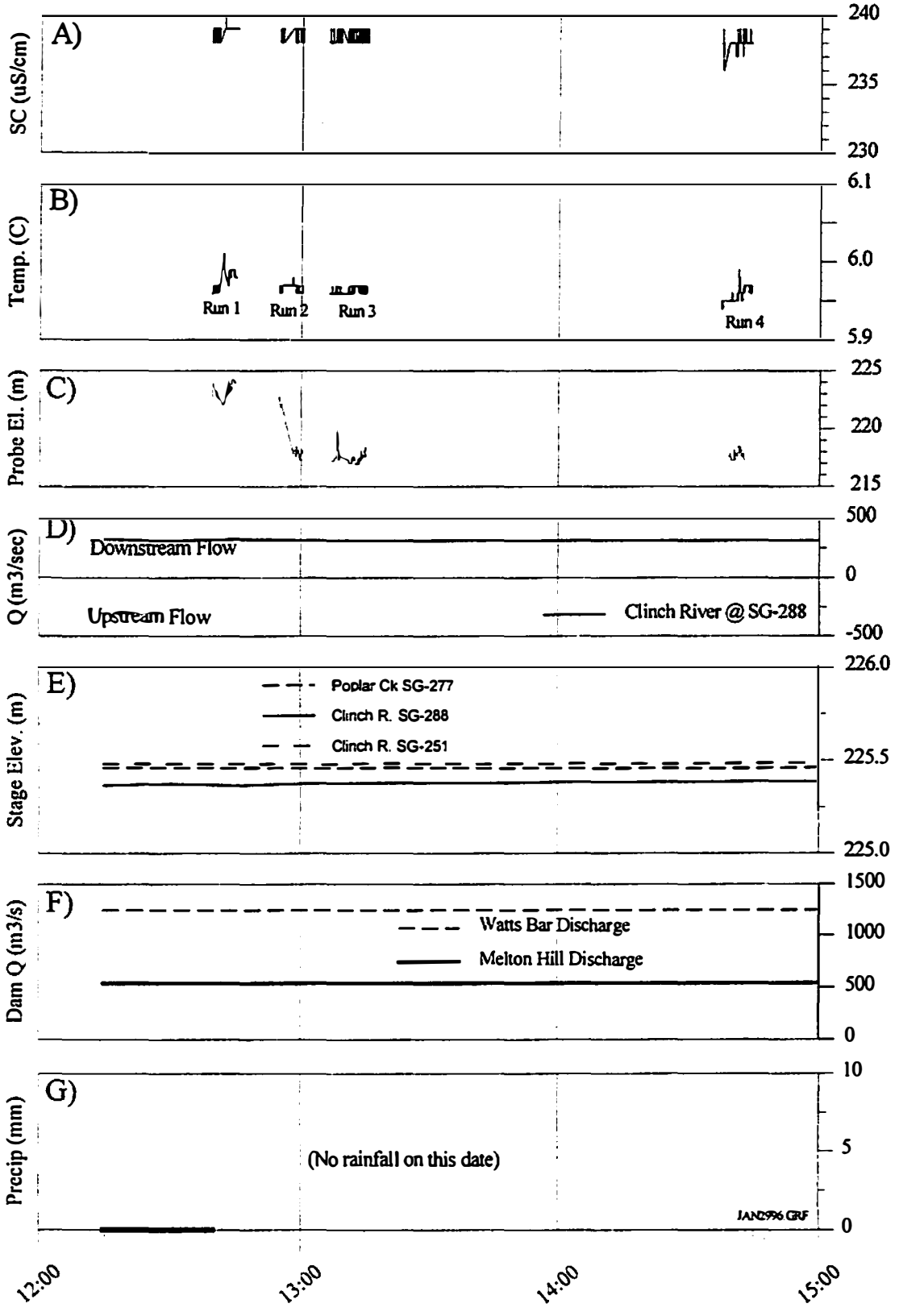


Figure A.3.1. Survey data and ambient hydrologic conditions, January 29, 1996.

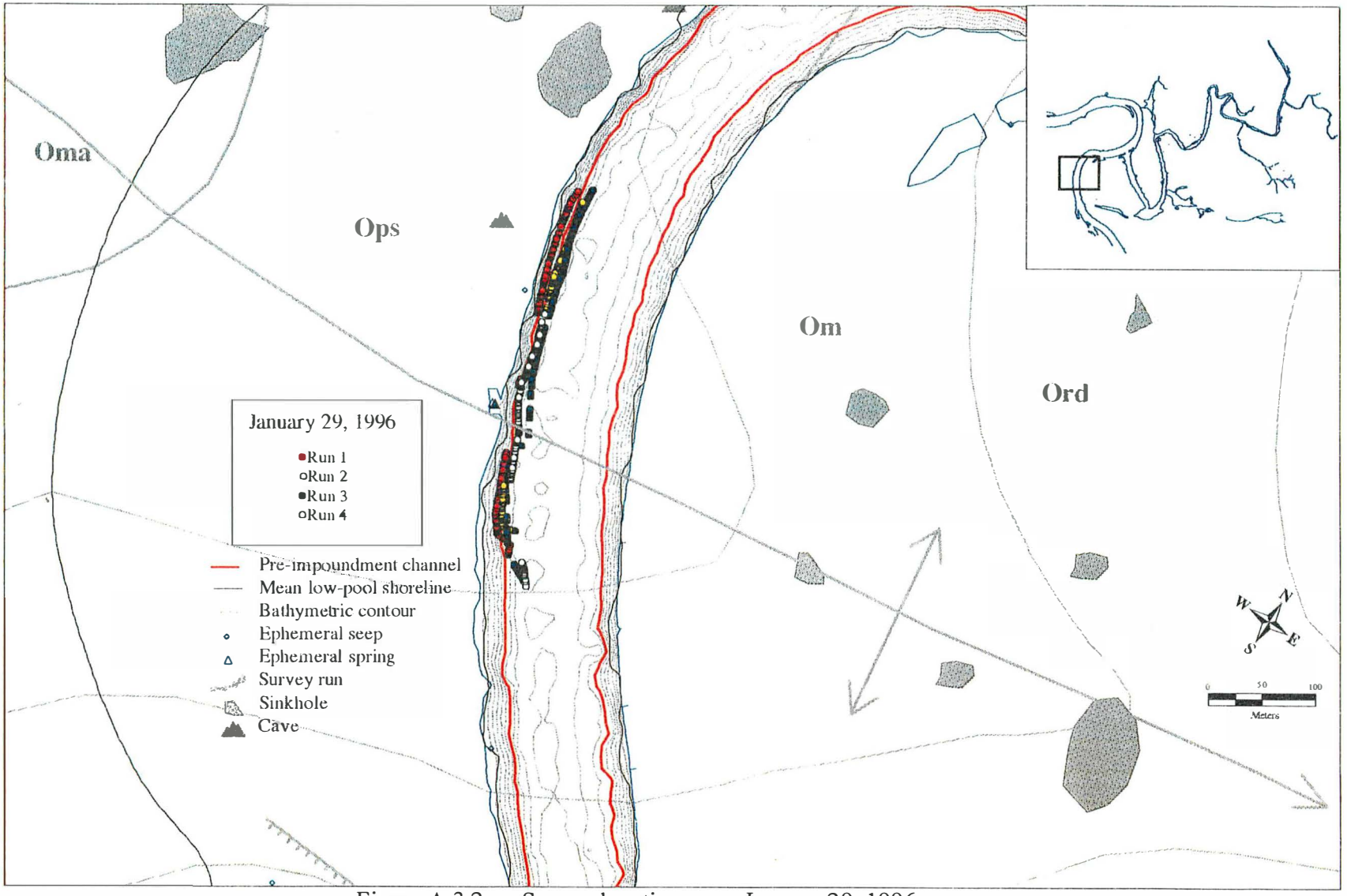


Figure A.3.2. Survey location map, January 29, 1996.

APPENDIX A.4

DATE: **February 14, 1996**

SURVEY AREA: Poplar Creek from above confluence with Mitchell Branch (at stage gage SG-279) to the "M"-shaped bend near stage gage SG-282. Survey covers the lower Chickamauga section extending from the contact of the Ridley and Lebanon Limestones to the Pond Springs-Mascot Dolomite contact.

DESCRIPTION: A total of 6 runs were performed in this area, in water depths ranging from 1.2 to 5.5 m. Although real-time differential corrections were applied, data, especially for run 3, shows survey locations drifting on-shore. Post processing could not correct for the drift recorded on the remote GPS receiver. It is believed the overhead power lines may have prevented maintaining adequate satellite lock, and thus the remote receiver did not record accurate position data. Other runs are unaffected.

HYDROLOGIC CONDITIONS: Hydrologic conditions prevailing during the field data acquisition period are summarized graphically on Figure A.4.1. Flow rates in Poplar Creek were on the order of 10-21 m^3/sec, being the lowest during runs 4 and 5 when Melton Hill discharge was zero and there was a slight backflow condition prevailing in the lower reaches of Poplar Creek. As Melton Hill discharge began during Run 6, flow rates increased accordingly in Poplar Creek.

There was no rainfall during the survey period. Antecedent rainfall conditions were as follows:

within last 24 hours:	0 mm
within past 4 days:	16.3 mm
within past 7 days:	164.6 mm

DATA: Data are summarized graphically on Figure A.4.1. Summary statistics on a run-by run basis are provided in Table A.4.1. Runs are shown on Figure A.4.2.

ANOMALIES: No anomalies indicative of springs were noted in the field. Although water temperatures were very low (< 7°C) such that optimal temperature differentials should exist, review of the data confirms this with water temperatures varying only 0.03 to 0.09 °C within runs and 0.23 °C over the course of the day. Specific conductance varied by only 7 uS/cm over all runs. Consequently, no springs were identified in this area from the available data.

Table A.4.1. Summary of field data for February 14, 1996.

				TEMPERATURE (°C)			SC (uS/cm)				ANOMALIES			
RUN	DIRXN	TIME	RECORDS	MIN	MAX	MEAN	MIN	MAX	MEAN	DEPTH (m)	Class I	Class II	Class III	Class IV
1	DS	12:46-13:07	672	6.84	6.89	6.85	172	175	173.3	1.2-4.9				
2	DS	13:19-13:30	339	6.82	6.91	6.87	174	177	175.4	1.8-4.9				
3	DS	13:39-14:50	3005	6.86	6.94	6.89	173	178	175.3	1.5-5.2				
4	DS	15:04-15:33	1131	6.94	6.97	6.95	176	177	176.4	3.4-5.5				
5	US	15:41-16:04	892	6.99	7.02	7.00	177	178	177.6	1.2-5.5				
6	DS	16:16-16:31	619	7.02	7.05	7.04	177	179	177.5	2.4-4.8				

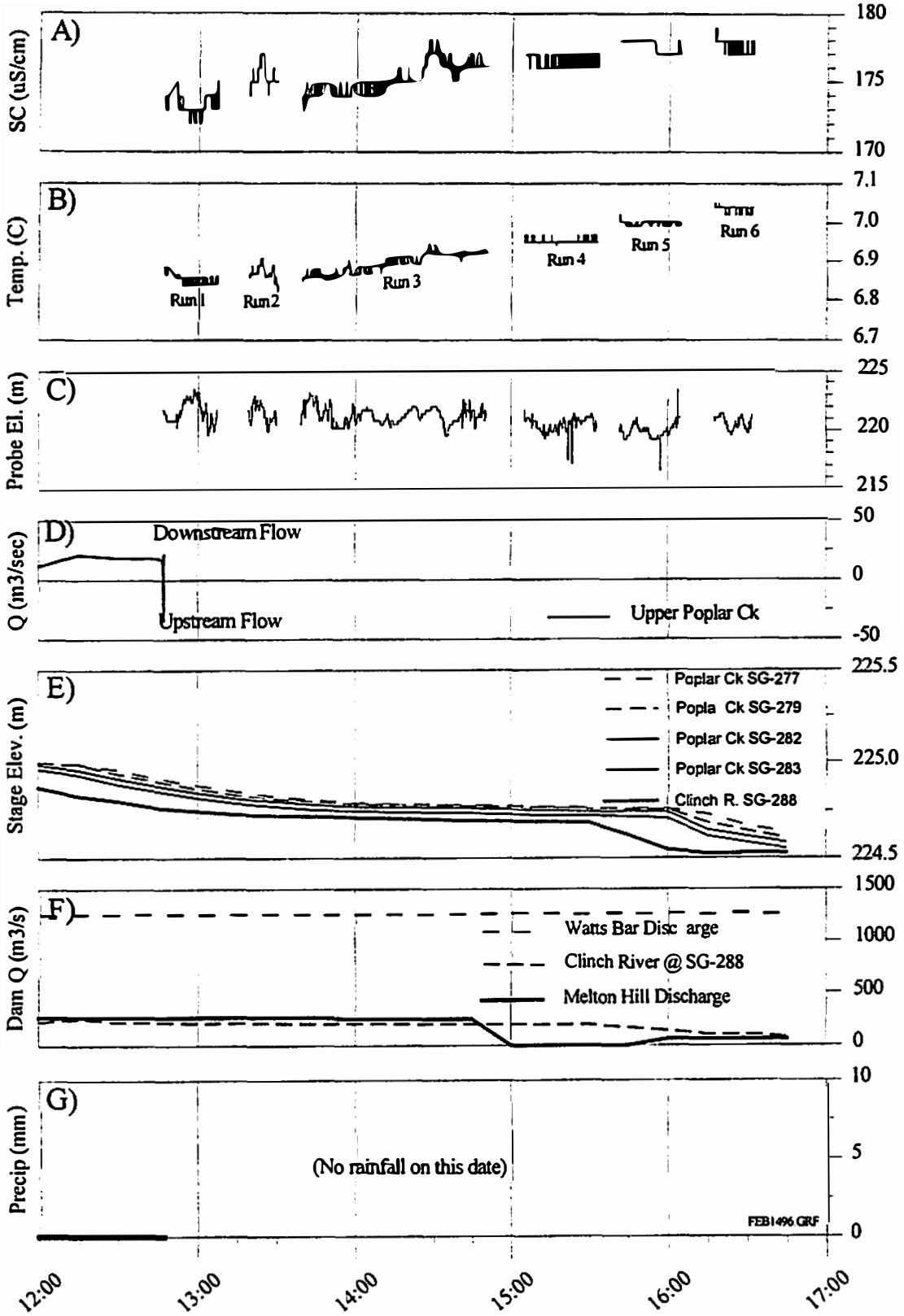


Figure A.4.1. Survey data and ambient hydrologic conditions, February 14, 1996.

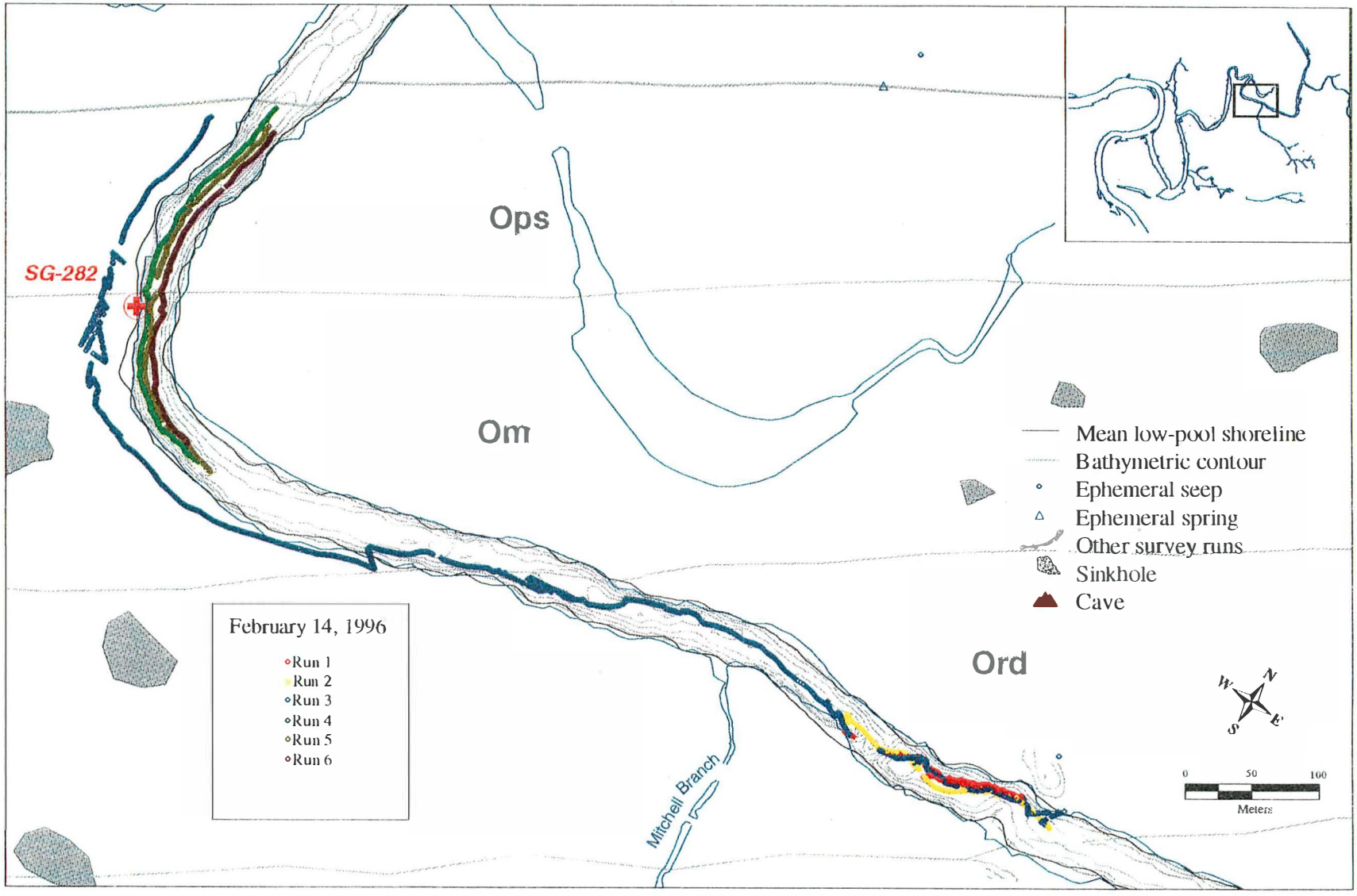


Figure A.4.2. Survey location map, February 14, 1996.

APPENDIX A.5

DATE: **February 15, 1996**

SURVEY AREA: Poplar Creek from SG-282 to the "M"-shaped bend. Study area covers Knox group (Mascot Dolomite and upper Kingsport Dolomite) bedrock exposed in the creek bank and along the bottom.

DESCRIPTION: A total of 5 runs were performed in this area, in water depths ranging from 0.9 to 6.4 m. This survey area is located in an incised ravine with bluffs and trees along the shore. Further, TVA power lines run right across the study reach. Consequently, real-time differential GPS was unavailable in this study area, probably due to a combination of less-than-reliable commercial RTCM service, overhead power wires, and working in a deep ravine. Partial base station data allowed for correction of some of the data (through Run 2) but even post-processing failed to improve the data where possible.

HYDROLOGIC CONDITIONS: Hydrologic conditions prevailing during the field data acquisition period are summarized graphically on Figure A5.1. Flow rates in Poplar Creek were on the order of 10-12 m^3/sec, all downstream.

There was no rainfall during the field surveys. Antecedent rainfall conditions were as follows:

within last 24 hours:	0 mm
within past 4 days:	0 mm
within past 7 days:	64.5 mm

DATA: Data are summarized graphically on Figure A.5.1. Summary statistics on a run-by run basis are provided in Table A.5.1. Runs are shown on Figure A.5.2.

ANOMALIES: No anomalies indicative of springs were noted in the field. Review of the data confirms this with water temperatures varying only 0.06 to 0.26 °C within runs and 0.66 °C over the course of the day. Specific conductance varied by only 5 uS/cm over all runs. A number of small bank seeps and one larger spring were noted along the north bank of Poplar Creek in this reach in 1996 and 1997. The only anomaly noted in the survey data was located in the vicinity of the bank springs, though the location may be considered tenuous given the GPS problems described above. This anomaly is shown on Figure A.5.3.

Table A.5.1. Summary of field data for February 15, 1996.

				TEMPERATURE (°C)			SC (uS/cm)				ANOMALIES			
RUN	DIRXN	TIME	RECORDS	MIN	MAX	MEAN	MIN	MAX	MEAN	DEPTH (m)	Class I	Class II	Class III	Class IV
1	DS	12:03-13:11	942	7.33	7.50	7.44	184	186	185.6	0.91-6.10				
2	DS	13:59-14:30	885	7.71	7.78	7.75	186	188	186.5	2.74-6.40				
3	DS	14:37-14:56	744	7.79	7.86	7.83	185	187	186	2.74-6.40				
4	US	14:58-15:05	319	7.83	8.09	7.92	185	189	186.5	1.31-1.40			1	
5	DS	15:05-15:24	847	7.88	7.94	7.90	185	187	186	1.22-6.40				

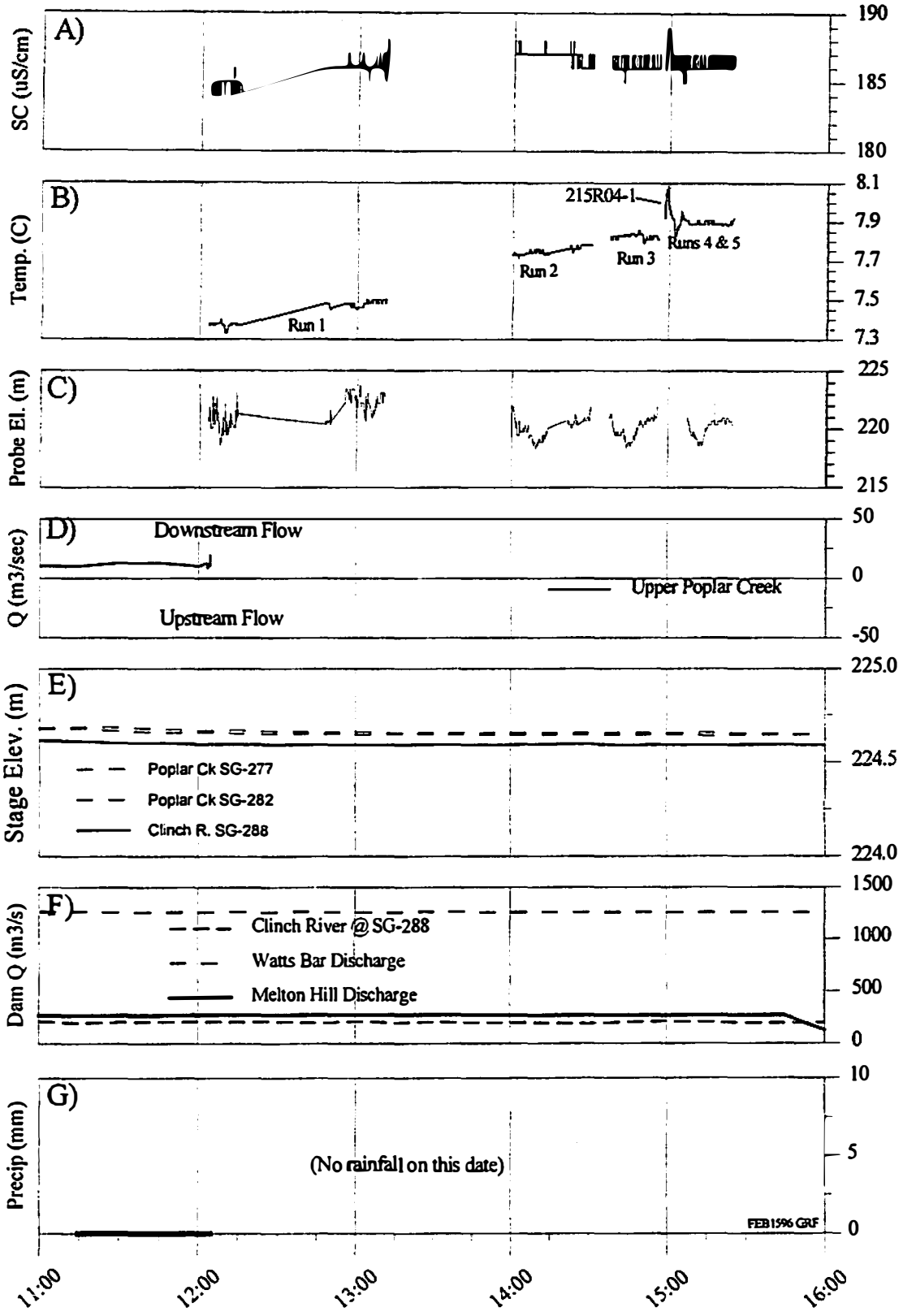


Figure A.5.1. Survey data and ambient hydrologic conditions, February 15, 1996.

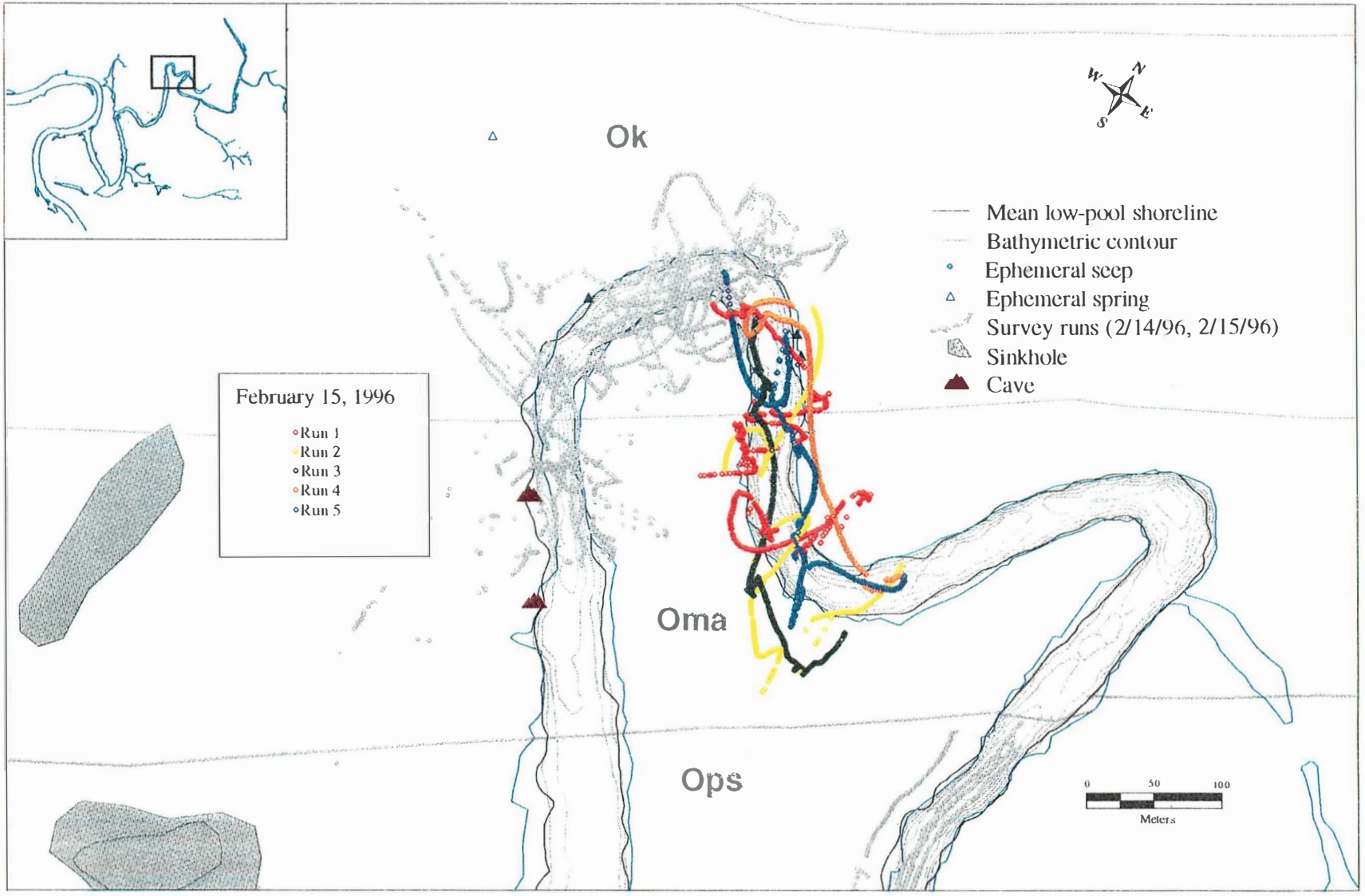


Figure A.5.2. Survey location map, February 15, 1996.

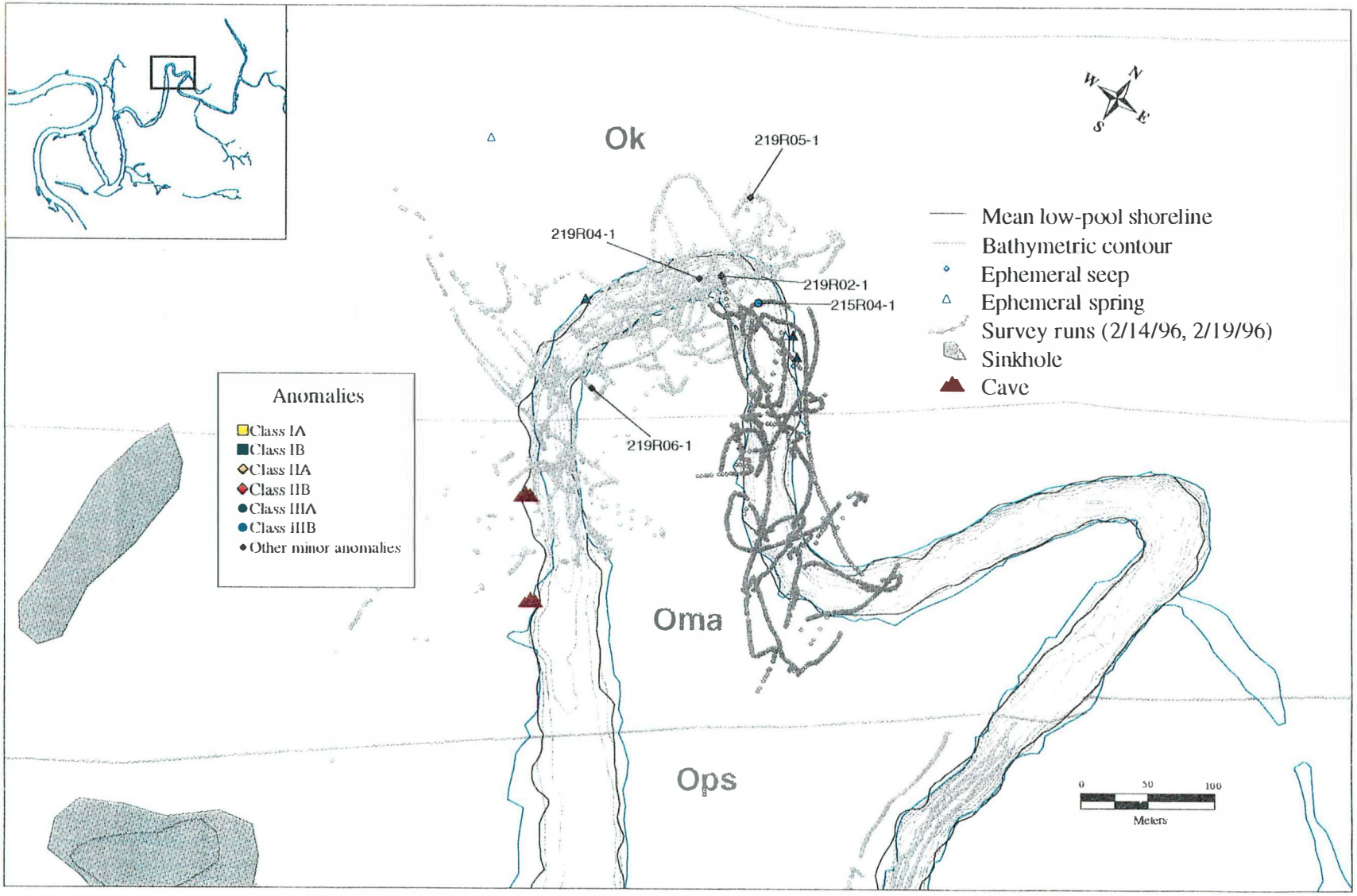


Figure A.5.3. Anomaly location map, February 15, 1996.

APPENDIX A.6

DATE: **February 19, 1996**

SURVEY AREA: Poplar Creek from the "M"-shaped bend to stage gage SG-283. Study area covers Knox group (Kingsport Dolomite and Mascot Dolomite) bedrock exposed in the creek bank and along the bottom. The downstream components of runs in this reach are adjacent to caves developed in the Mascot in the bluffs along the creek. A number of perennial springs have been monitored along the bank in the Kingsport. The surveys were conducted in a deeply incised portion of Poplar Creek with steep bluffs on one side and TVA power lines crossing directly overhead.

DESCRIPTION: A total of 12 runs were performed in this area, in water depths ranging from 0.9 to 4.9 m. Note that there was a total loss of differential correction signal in the field due to the topographic relief and overhead power lines. Consequently, runs appear to wander all over, often exceeding the bank. Additionally, loss of base station data needed to perform post-processing prevented retrieving the actual survey run locations. The result is that data cannot be used to determine spring locations.

HYDROLOGIC CONDITIONS: Hydrologic conditions prevailing during the field data acquisition period are summarized graphically on Figure A.6.1. Flow rates in Poplar Creek were on the order of 5-16 m^3/sec, with decreased flow rates (5-9 m^3/sec) during runs 6-12. Stage also declined ~ 0.15 m from early runs (1-2) .There was no rainfall during the field period, nor any rainfall within the prior 7 days.

DATA: Data are summarized graphically on Figure A.6.1. Summary statistics on a run-by run basis are provided in Table A.6.1. Runs are shown on Figure A.6.2.

ANOMALIES: No anomalies indicative of springs were noted in the field. Review of data shows small temperature and SC anomalies (on the order of 0.03 - 0.04 °C, with very slight SC changes) in runs 2, 4, 5 and 6. Anomalies are summarized in Table A.19.1. Calculated spring discharges are provided in Table A.19.2.

Table A.6.1. Summary of field data for February 19, 1996.

				TEMPERATURE (°C)			SC (uS/cm)				ANOMALIES			
RUN	DIRXN	TIME	RECORDS	MIN	MAX	MEAN	MIN	MAX	MEAN	DEPTH (m)	Class I	Class II	Class III	Class IV
1	DS	12:56-13:10	607	5.80	5.92	5.85	208	210	209.3	0.91-3.96				
2	DS	13:18-13:30	444	5.75	5.83	5.77	210	212	211.1	2.44-4.57				
3	DS	13:37-13:48	473	5.75	5.78	5.77	210	213	211.9	3.66-4.57				
4	DS	13:55-14:07	457	5.75	5.83	5.78	210	212	211.3	3.35-4.88				1
5	DS	14:12-14:37	1108	5.77	5.83	5.79	209	213	210.9	2.13-4.88				
6	DS	14:43-15:11	901	5.80	5.87	5.83	210	213	211.2	1.52-4.57				
7	US	15:13-15:15	100	5.85	5.85	5.85	210	212	211.0	2.13-3.35				
8	DS	15:18-15:27	220	5.85	5.87	5.85	210	212	211.21	1.83-4.57				
9	DS	15:35-15:47	402	5.87	5.90	5.88	209	213	211.36	2.44-4.88				
10	DS	15:53-16:02	413	5.87	5.90	5.89	211	212	211.83	3.66-4.57				
11	DS	16:09-16:18	344	5.90	5.93	5.91	210	212	211.93	2.74-4.57				
12	DS	16:26-16:34	335	5.90	5.93	5.92	212	213	212.42	3.35-4.27				

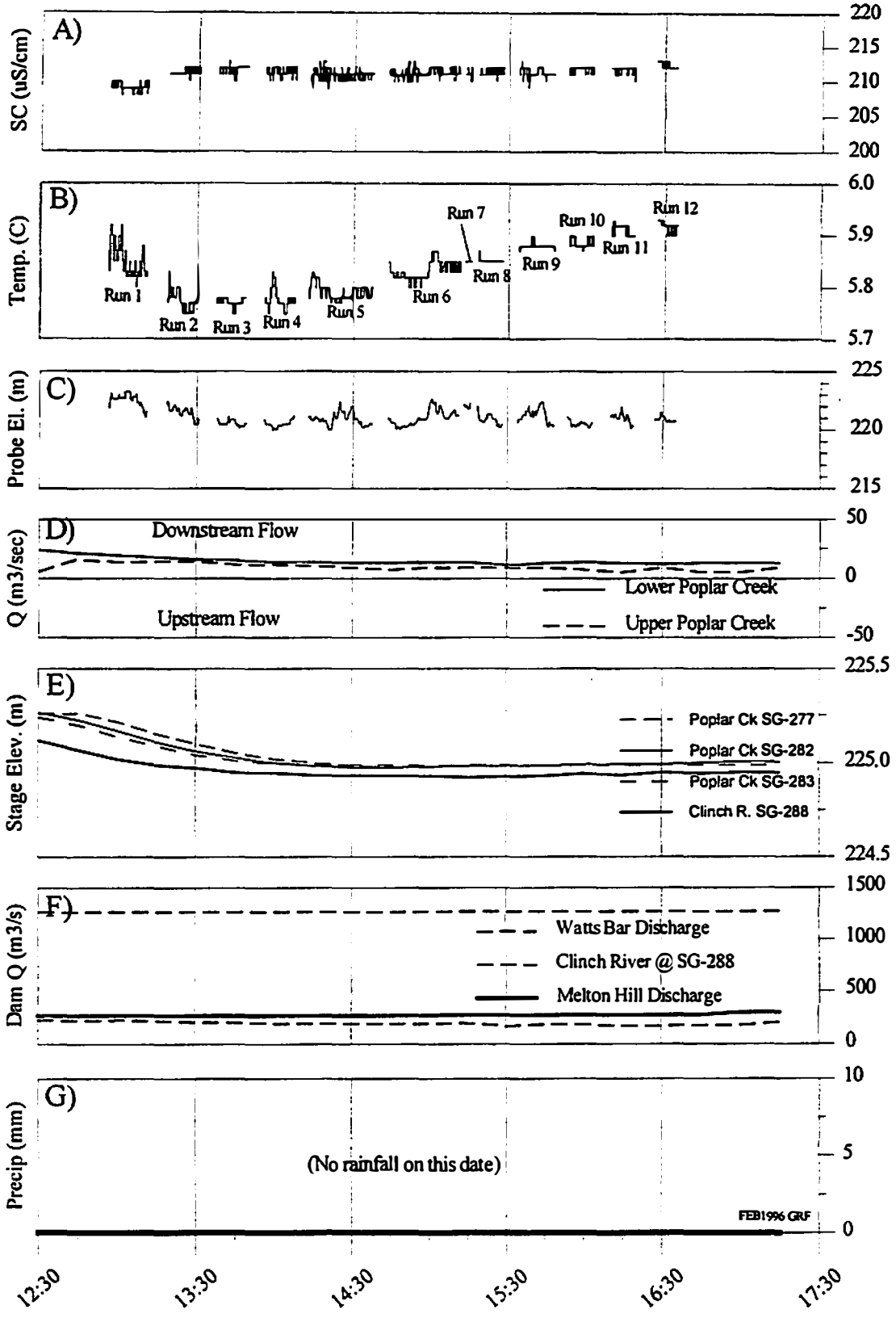


Figure A.6.1. Survey data and ambient hydrologic conditions, February 19, 1996.

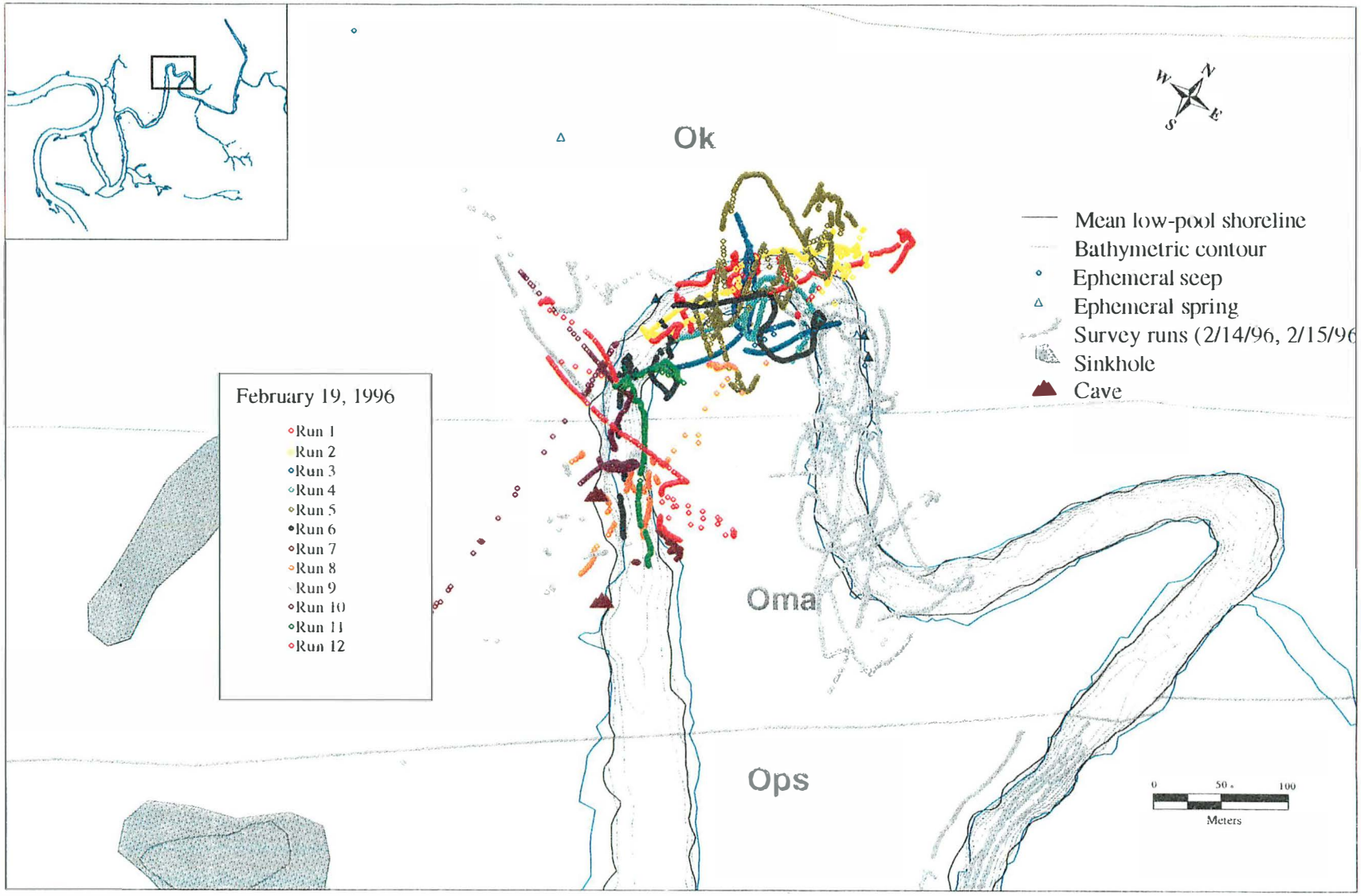


Figure A.6.2. Survey location map, February 19, 1996.

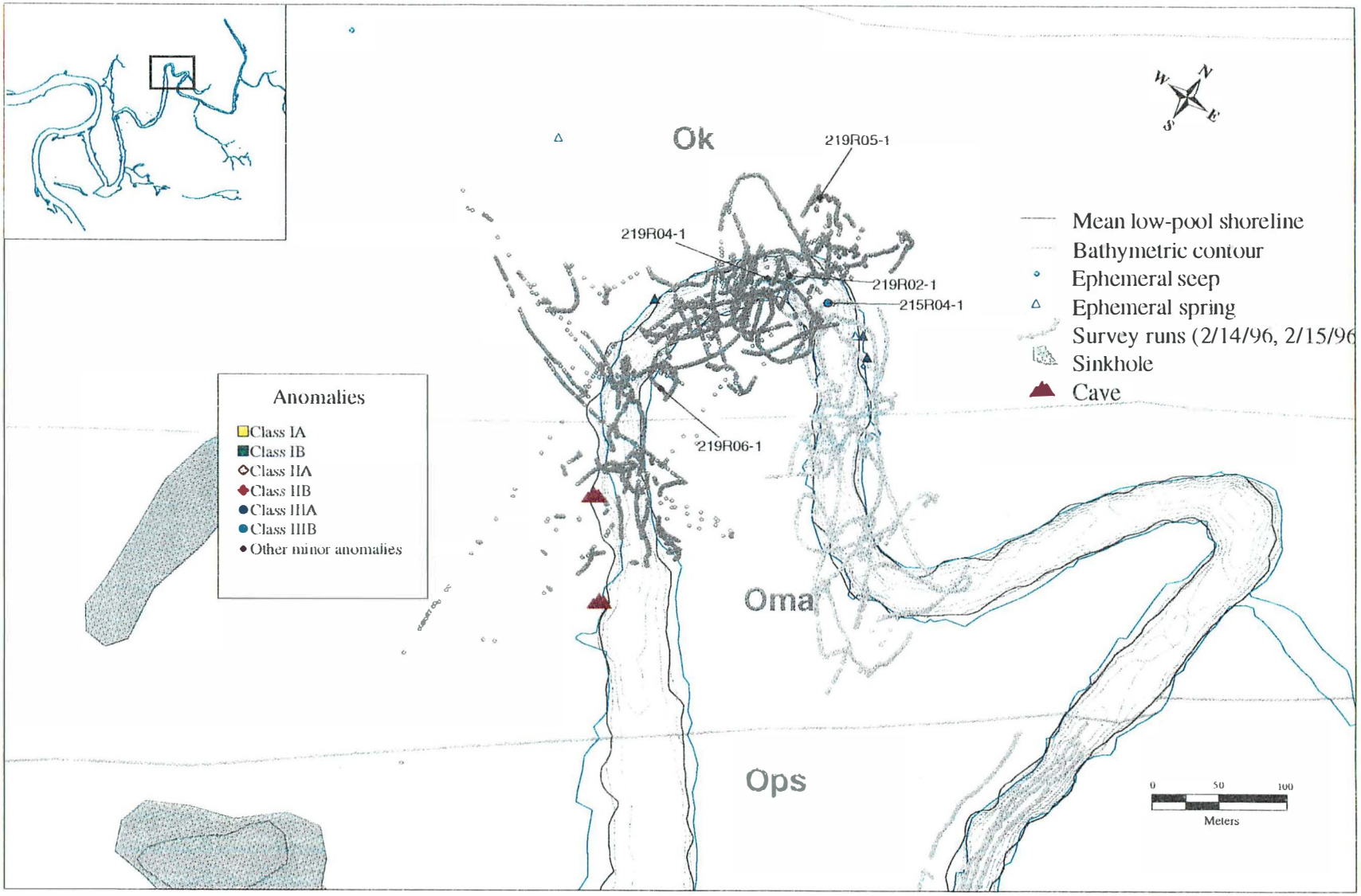


Figure A.6.3. Anomaly location map, February 19, 1996.

APPENDIX A.7

DATE: **February 20, 1996**

SURVEY AREA: Poplar Creek from above the Blair Road railroad bridge upstream to the Poplar Creek water gap above confluence with East Fork Poplar Creek. Study area covers lower Chickamauga Group bedrock (Lebanon Ls, Ridley Ls, Murfreesboro Ls, Pond Springs Fm) and upper Knox group (Mascot Dolomite, Kingsport Dolomite, Longview Dolomite) bedrock exposed in the creek bank and along the bottom. Additionally, run 10 addresses the mapped K-25 Fault where Knox Group bedrock is thrust up over the Chickamauga Lebanon Ls.

DESCRIPTION: A total of 10 runs were performed in this area, in water depths ranging from 0.9 to 3.6 m. Runs 1-6 were performed in the Blackoak Ridge water gap; the topographic relief associated with the gap apparently prevented acquisition of GPS location data during those runs. Once out of the gap, GPS data became reliable again. Runs 1-6 were performed upstream of the confluence with East Fork Poplar Creek (EFPC) and focused on a reach where bank springs in the Kingsport were observed (also on strike with spring 21-002). Runs 7-10 address Poplar Creek below the confluence with EFPC.

HYDROLOGIC CONDITIONS: Hydrologic conditions prevailing during the field data acquisition period are summarized graphically on Figure A.7.1. Flow rates in Poplar Creek were on the order of 14-20 m^3/sec, with decreased flow rates (14-16 m^3/sec) during runs 7-10. A total of 40.64 mm of rainfall occurred within the 24 hour period prior to the field survey, providing a potential driving head in the groundwater. No other rainfall occurred within the preceding 7 days.

DATA: Data are summarized graphically on Figure A.7.1. Summary statistics on a run-by run basis are provided in Table A.7.1. Runs are shown on Figure A.7.2 (Runs 1-7) and A.7.3 (runs 8-10).

ANOMALIES: No anomalies indicative of springs were noted in the field. Review of data shows a total of 5 anomalies in the reach studied, encountered on runs 7, 8, and 10 only. The largest observed temperature and SC anomalies (on the order of 1 °C, and a 63 uS/cm SC change) in the entire study area was seen in run 7. Anomalies are shown on Figures A.7.4 and A.7.5, and tabulated in Tables A.19.1 and A.19.2..

Anomaly 220R07-1 was located immediately downstream of the confluence with EFPC, where a spring is implied near the mouth on thermal IR data. However, the flow from EFPC (as evidenced by turbidity plumes during high EFPC discharge periods) tends to hug the east shore of Poplar Creek in this reach such that this anomaly, located in the middle of the channel and Poplar Creek flow, is likely real. Based upon the ambient flow rate and observed temperature differential, a spring discharge rate, (Qs_{calc}) of ~2.48 m^3/sec (87 cfs) is suggested.

Table A.7.1. Summary of field data for February 20, 1996.

				TEMPERATURE (°C)			SC (uS/cm)				ANOMALIES			
RUN	DIRXN	TIME	RECORDS	MIN	MAX	MEAN	MIN	MAX	MEAN	DEPTH (m)	Class I	Class II	Class III	Class IV
1	DS	12:40-13:02	874	7.71	7.84	7.74	168	169	168.8	0.91-3.05				
2	DS	13:17-13:32	493	7.81	7.83	7.81	168	171	169.0	0.91-2.74				
3	DS	13:43-13:54	549	7.88	7.89	7.88	168	171	169.4	1.22-2.74				
4	DS	14:04-14:15	456	7.92	7.94	7.94	168	171	169.1	1.22-2.13				
5	DS	14:22-14:36	578	7.99	8.02	8.01	169	172	169.8	0.91-1.52				
6	DS	14:42-14:51	230	8.04	8.06	8.05	169	171	169.9	1.22-1.83				
7	DS	15:01-15:32	297	8.04	9.06	8.46	169	233	192.0	1.22-3.35	1			
8	DS	15:47-16:03	417	8.32	8.63	8.50	179	196	188.0	0.91-2.13		1		1
9	DS	16:38-17:01	262	8.78	8.84	8.81	197	203	199.8	1.83-3.66				
10	DS	17:06-17:25	822	8.81	9.04	8.86	196	207	199.0	1.22-3.66				2

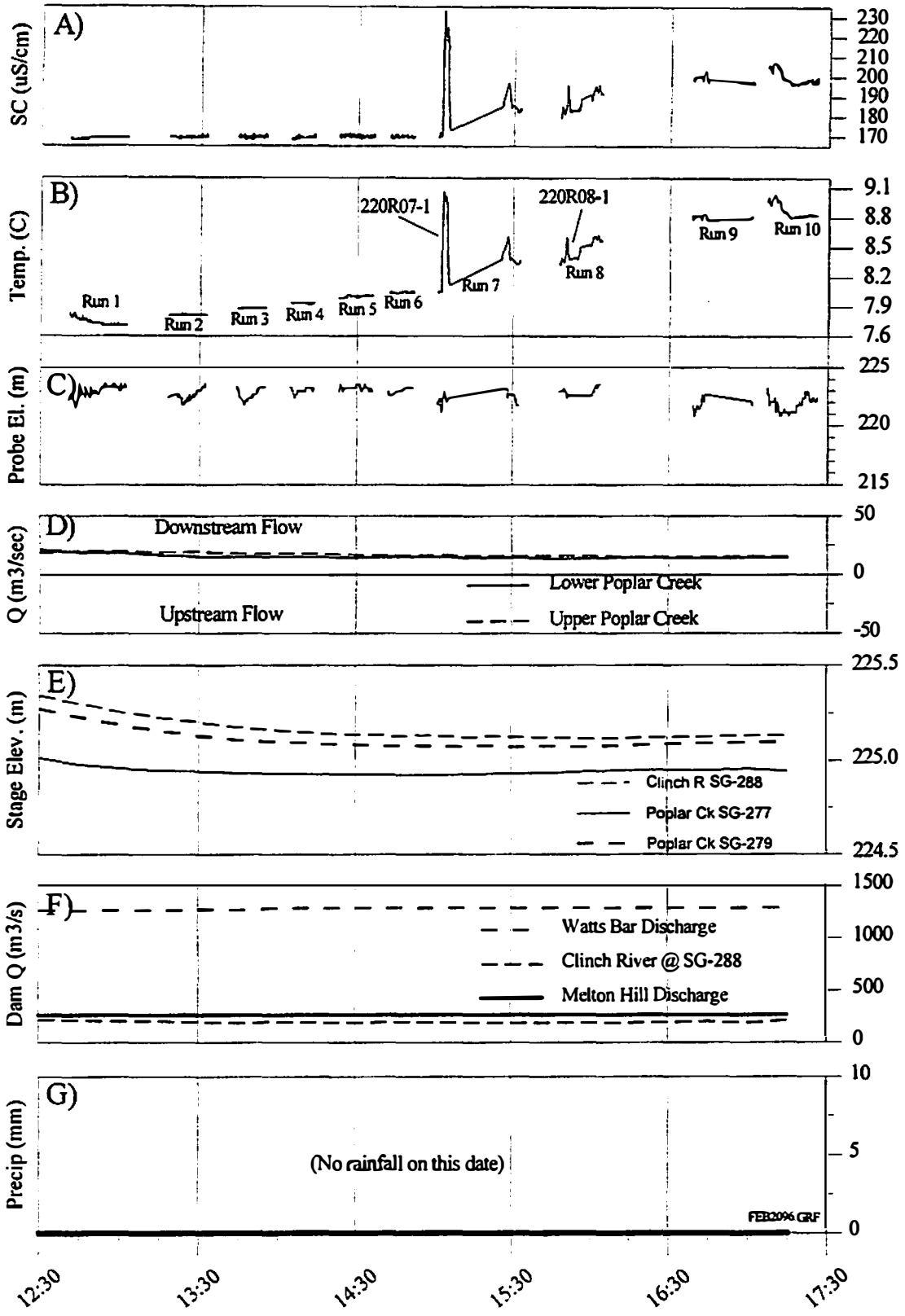


Figure A.7.1. Survey data and ambient hydrologic conditions, February 20, 1996.

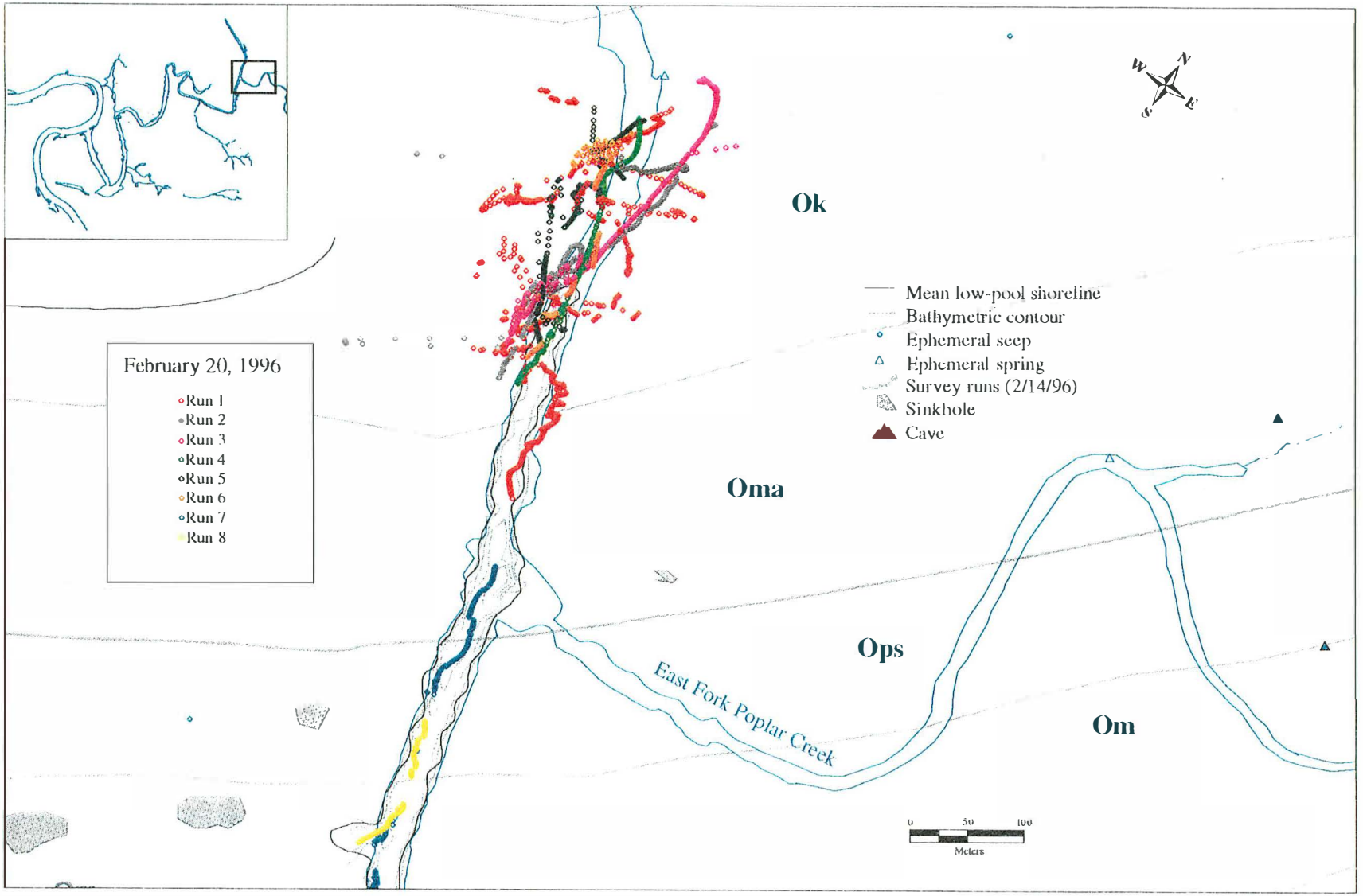


Figure A.7.2. Survey location map, runs 1-8, February 20, 1996.

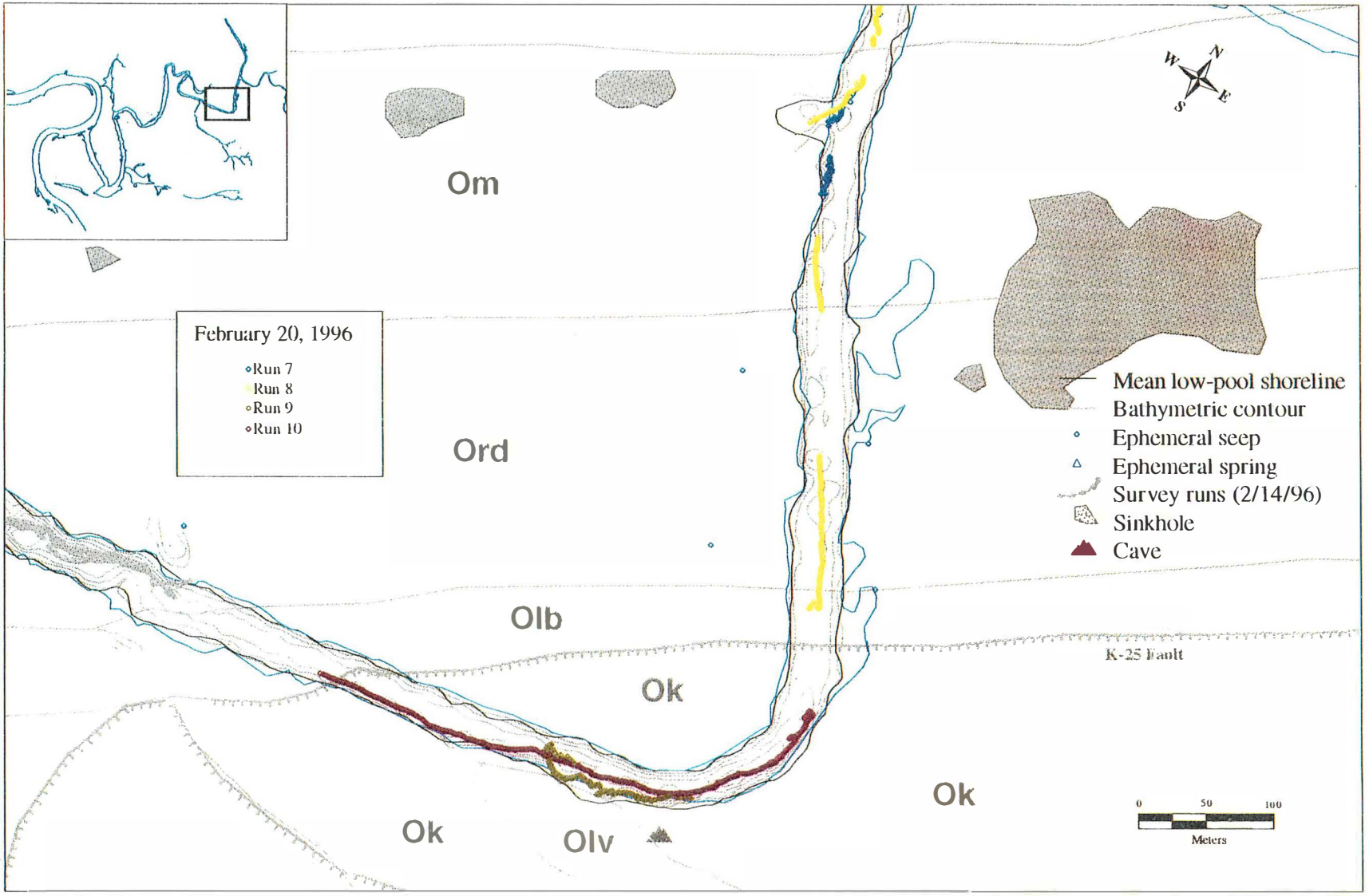


Figure A.7.3. Survey location map, runs 7-10, February 20, 1996.

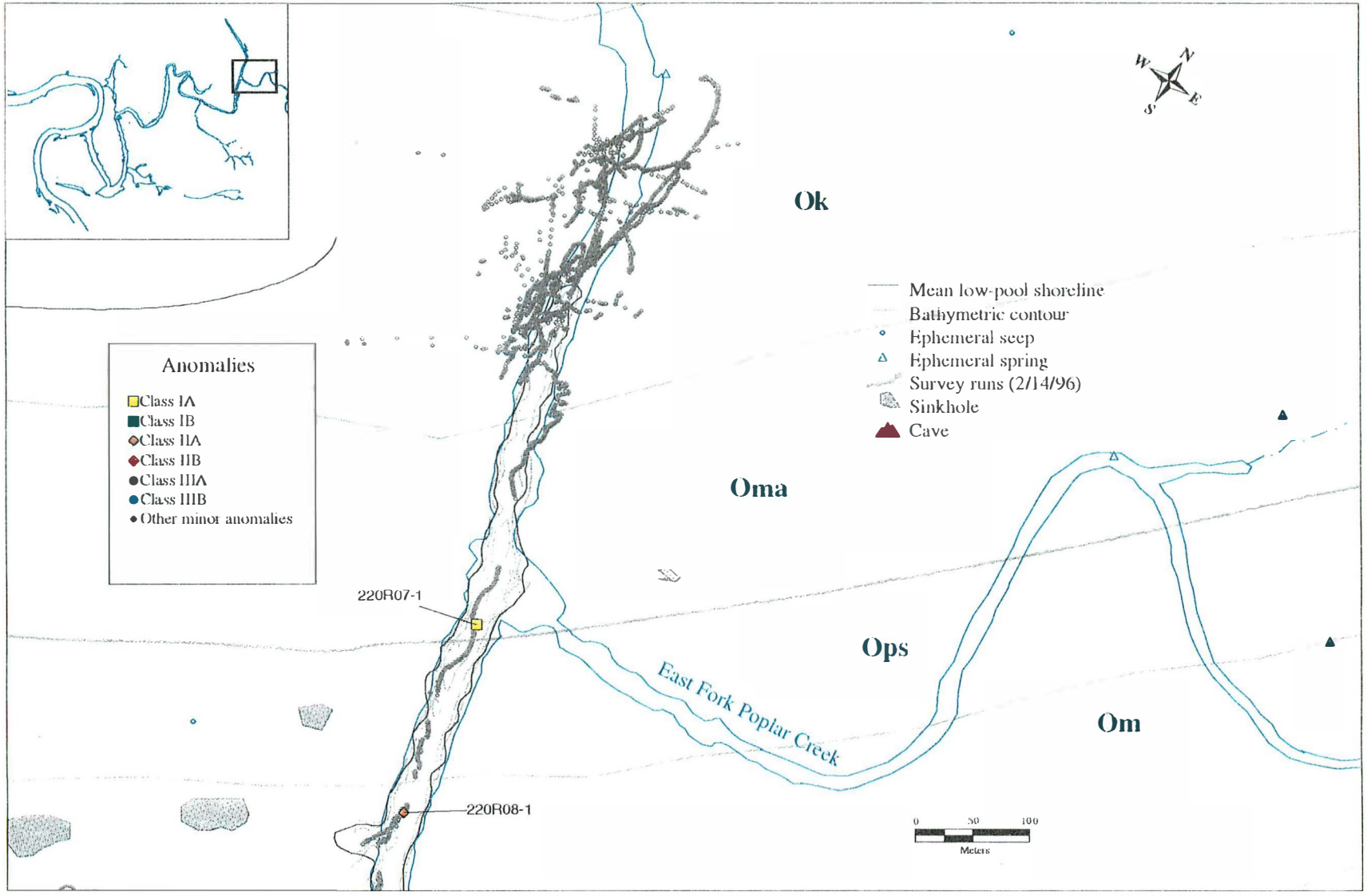


Figure A.7.4. Anomaly location map, runs 1-8, February 20, 1996.

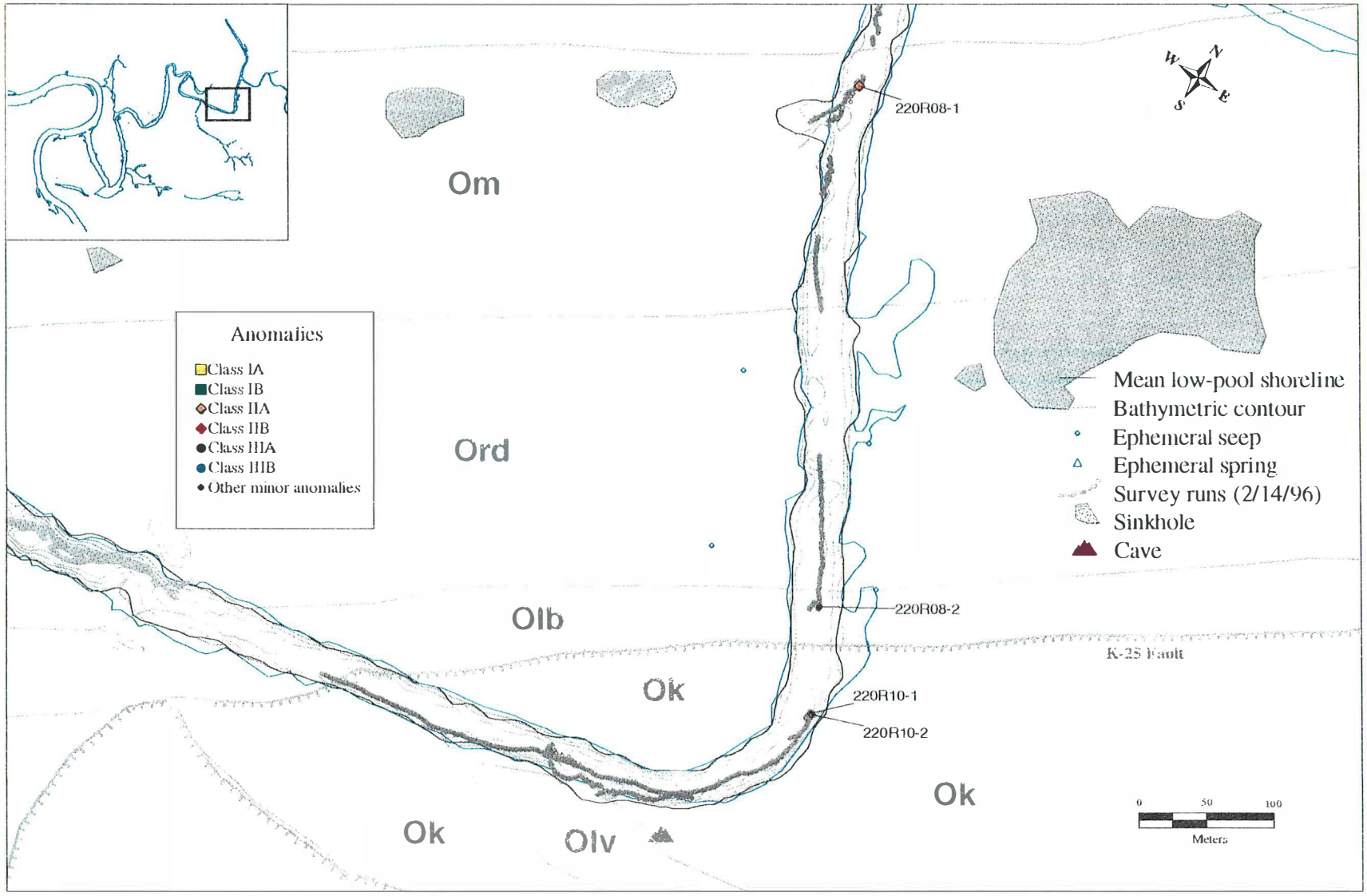


Figure A.7.5. Anomaly location map, runs 7-10, February 20, 1996.

APPENDIX A.8

DATE:	**February 21, 1996**
SURVEY AREA:	Poplar Creek in the vicinity of the Perimeter Road Bridge. Survey covers outcrop belt of the Chickamauga Group Lebanon Ls and the Carters formation. Further, the survey area straddles the deformation zone mapped by Lemiszki (1996), which is interpreted to potentially represent a strike-parallel thrust fault dipping to the southeast.
DESCRIPTION:	A total of 9 runs were performed in this area, in water depths ranging from 0.9 to 6.1 m. The downstream ends of most runs overlaps with survey runs from February 22, 1996.
HYDROLOGIC CONDITIONS:	Hydrologic conditions prevailing during the field data acquisition period are summarized graphically on Figure A.8.1. Flow rates in Poplar Creek were on the order of 13-25 m^3/sec, with decreased flow rates (14-15 m^3/sec) during runs 6-9. A total of 40.64 mm of rainfall fell within the 24 hour period prior to the field surveys, providing the opportunity to detect groundwater discharge associated with this recharge event. There was no rainfall in the previous 7 days.
DATA:	Data are summarized graphically on Figure A.8.1. Summary statistics on a run-by run basis are provided in Table A.8.1. Runs are shown on Figure A.8.2. Figure A8.3 is a map showing anomalies observed within the study reach.
ANOMALIES:	No anomalies indicative of springs were noted in the field. Subsequent review of data identified a total of 3 minor (Class IV) anomalies associated with runs 1, 2, and 7. Anomalies are described in Table A.19.1. Potential spring discharge rates are listed in Table A.19.2. Anomalies 221R01-1 and 221R02-1 corroborate a potential location of groundwater discharge identified on separate runs (i.e., anomaly locations coincide) within the middle Carters Ls. Other minor anomalies were noted but correlate with a decrease in water depth thus suggesting they are not valid.

Table A.8.1. Summary of field data for February 21, 1996.

				TEMPERATURE (°C)			SC (uS/cm)				ANOMALIES			
RUN	DIRXN	TIME	RECORDS	MIN	MAX	MEAN	MIN	MAX	MEAN	DEPTH (m)	Class I	Class II	Class III	Class IV
1	DS	10:29-10:57	958	8.73	8.81	8.77	191	193	192	0.91-4.57				1
2	DS	11:02-11:26	850	8.76	8.86	8.81	190	192	191.8	0.91-4.88				1
3	DS	11:48-12:09	484	8.88	8.93	8.88	190	191	190.9	3.66-5.49				
4	DS	12:12-12:23	420	8.91	8.94	8.92	190	191	190.1	1.52-5.49				
5	DS	13:00-13:21	761	9.06	9.11	9.07	190	190	190	3.05-5.49				
6	DS	13:35-13:53	716	9.11	9.17	9.14	190	191	190.1	3.35-5.49				
7	DS	14:10-14:36	1079	9.15	9.27	9.21	190	191	190.9	3.05-5.49				1
8	DS	14:54-15:13	841	9.25	9.30	9.28	190	191	191	2.44-6.10				
9	DS	15:26-15:31	258	9.27	9.29	9.28	191	191	191	4.88-5.49				

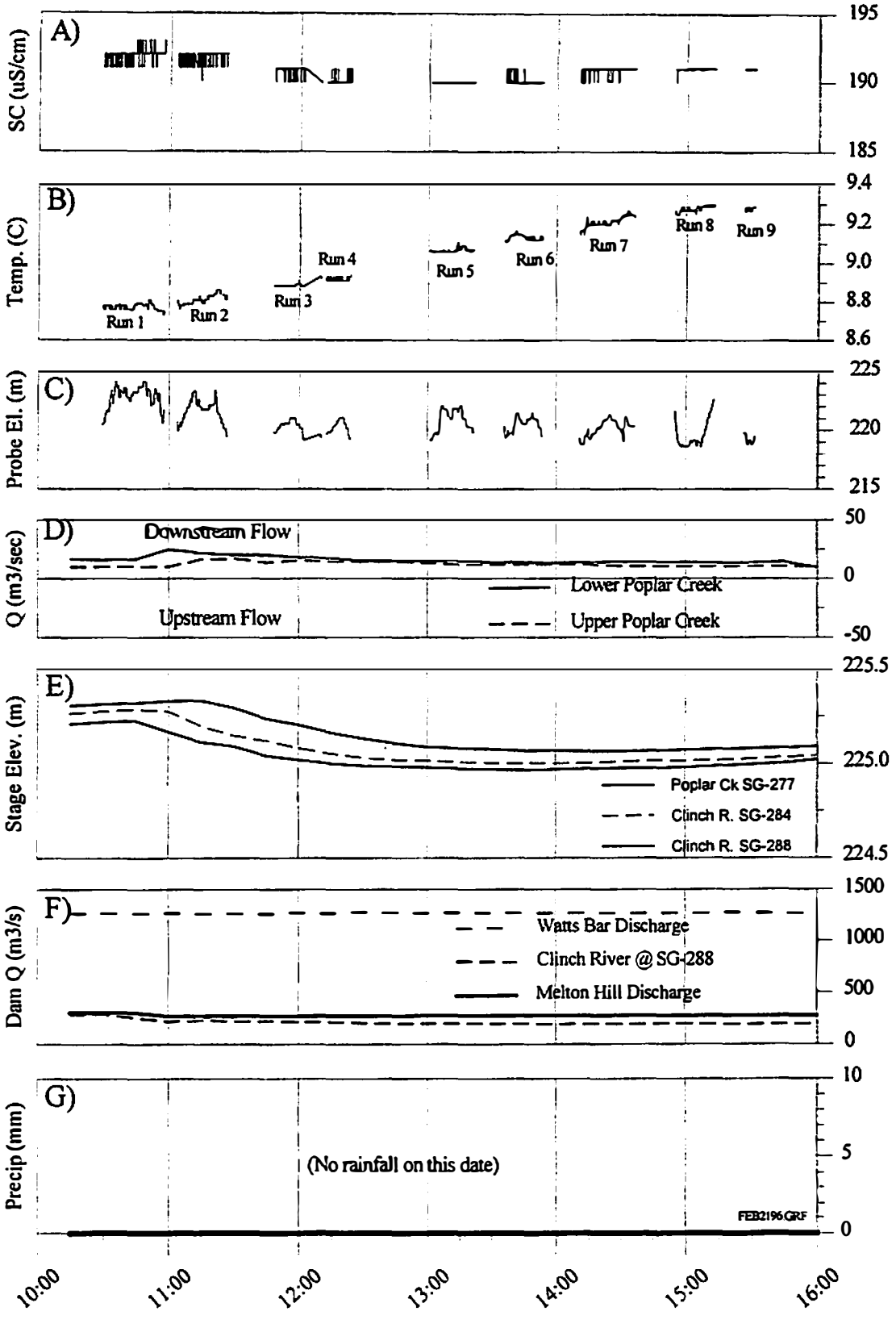


Figure A.8.1. Survey data and ambient hydrologic conditions, February 21, 1996.

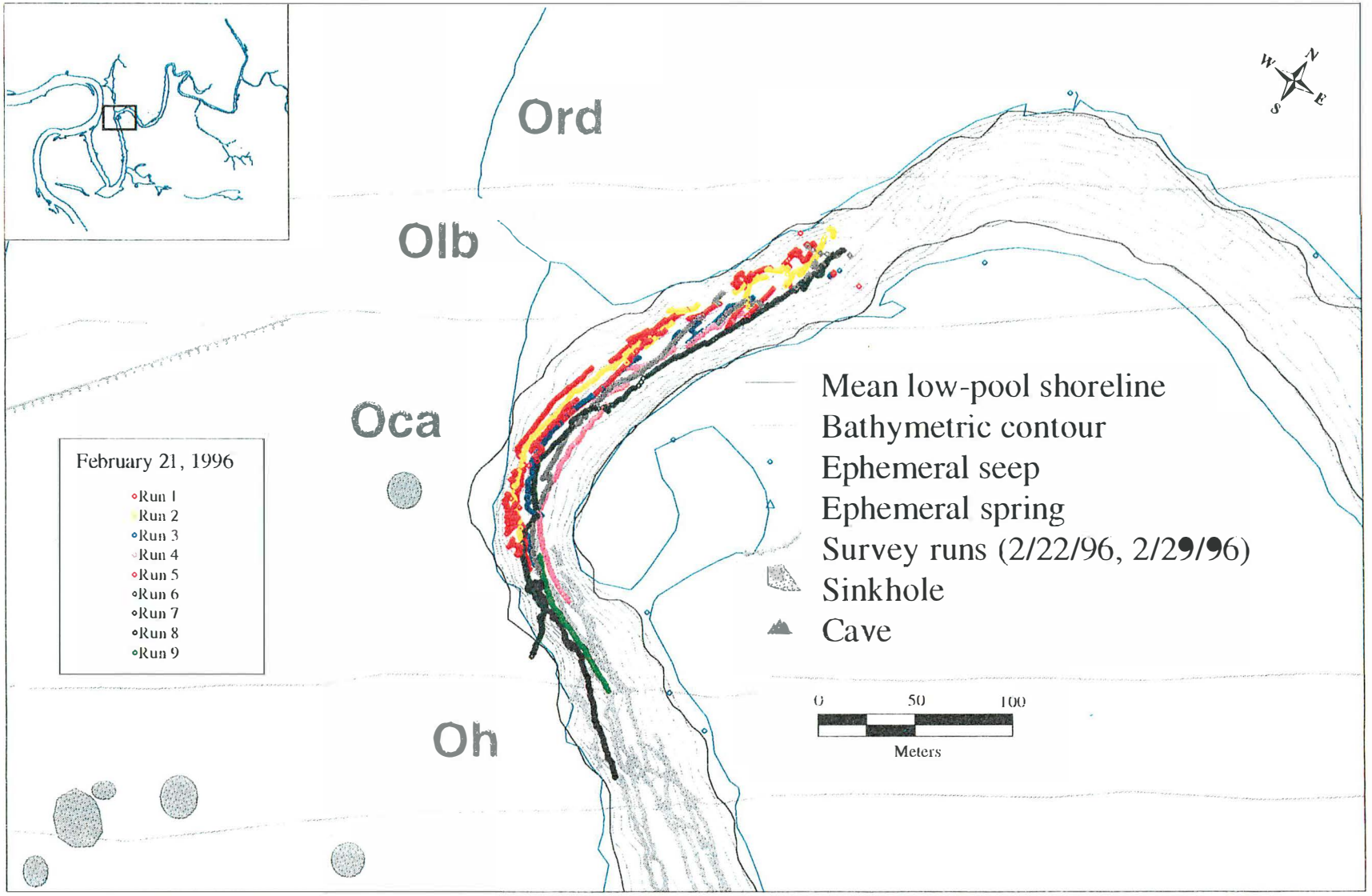


Figure A.8.2. Survey location map, February 21, 1996.

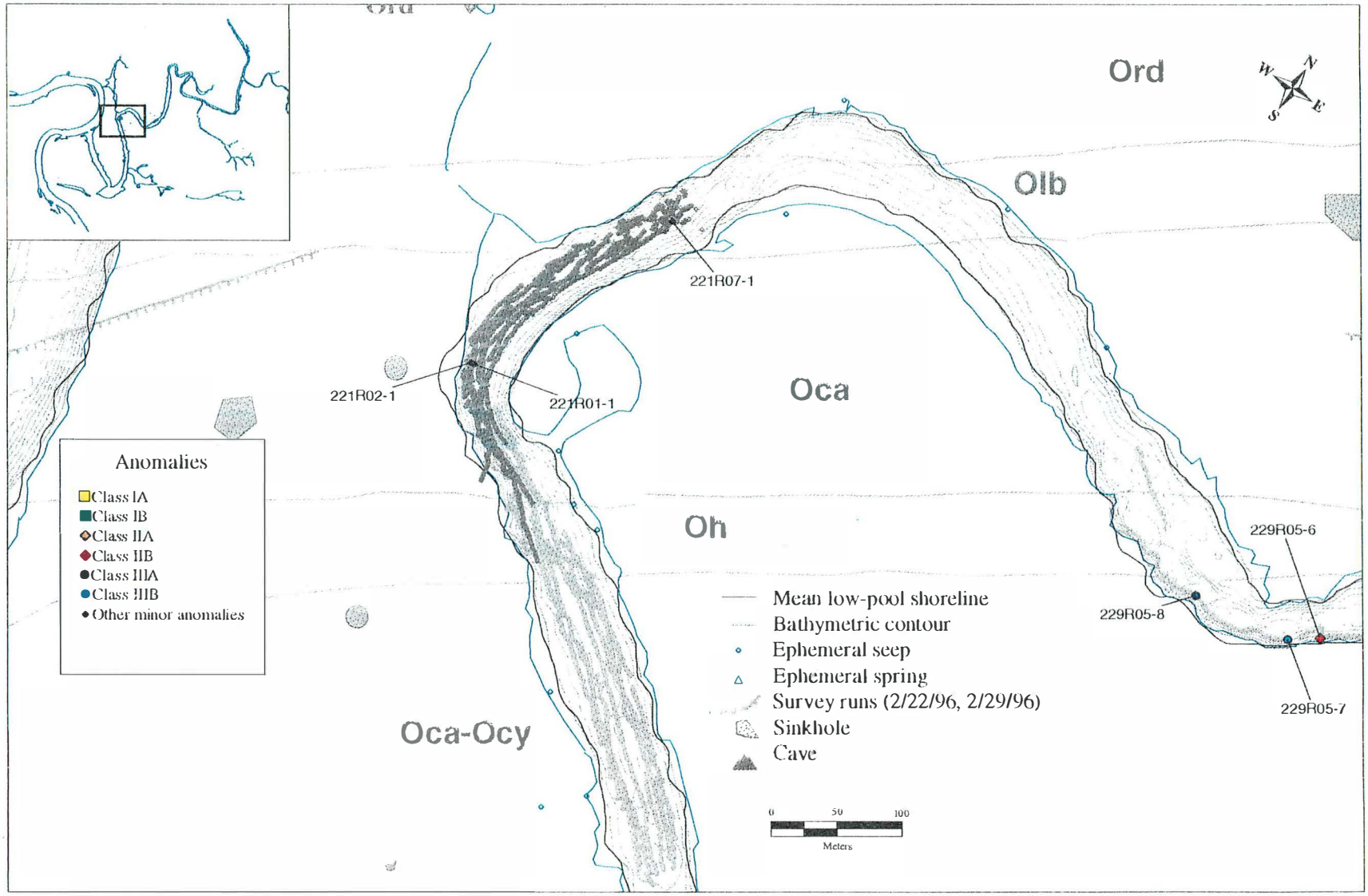


Figure A.8.3. Anomaly location map, February 21, 1996.

APPENDIX A.9

DATE: **February 22, 1996**

SURVEY AREA: Poplar Creek between the Perimeter Road Bridge and the K-1007 Pond. Survey covers outcrop belt of the Chickamauga Group Cannon-Catheys formation along the axis of the map-scale synclinal structure.

DESCRIPTION: A total of 14 runs were performed in this area, in water depths ranging from 0.9 to 6.4 m. Survey runs overlap with coverage from 2/21/96 on the upstream end and with survey runs from 2/23/96 and 2/26/96 on the downstream end.

HYDROLOGIC CONDITIONS: Hydrologic conditions prevailing during the field data acquisition period are summarized graphically on Figure A.9.1. Flow rates in Poplar Creek were on the order of 9 m^3/sec upstream (runs 1 and 2) to 25 m^3/sec downstream during runs 4 and 5, with decreased flow rates (14-16 m^3/sec) during runs 12-14.

There was no rainfall during the field period. Antecedent rainfall conditions were as follows:

within last 24 hours:	0 mm
within past 4 days:	40.64 mm
within past 7 days:	40.64 mm (2/20/96)

DATA: Data are summarized graphically on Figure A.9.1. Summary statistics on a run-by run basis are provided in Table A.9.1. Runs are shown on Figure A.9.2. Figure A.9.3 is a map showing locations of anomalies identified.

ANOMALIES: No anomalies indicative of springs were noted in the field. Subsequent review of data in Table A.9.1 shows that temperature varied 0.16 °C over the course of the day while SC displayed only a 6 uS/cm change. A total of 3 minor (Class IV or V) anomalies were noted in the data in runs 13 and 14 in shallow water between 1.5-2.4 m deep. These anomalies are shown on Figure A.9.3 and described in Table A.19.1. Other minor temperature fluctuations (< 0.05 °C) occur apparently in response to decreasing water depth along runs.

Table A.9.1. Summary of field data for February 22, 1996.

RUN	DIRXN	TIME	RECORDS	TEMPERATURE (°C)			SC (uS/cm)			DEPTH (m)	ANOMALIES			
				MIN	MAX	MEAN	MIN	MAX	MEAN		Class I	Class II	Class III	Class IV
1	DS	9:20-9:30	418	9.88	9.97	9.92	190	192	190.9	1.52-6.40				
2	DS	9:34-9:48	560	9.86	9.89	9.87	190	192	191.1	3.96-5.79				
3	DS	9:53-10:07	480	9.84	9.88	9.86	190	192	191.1	2.74-5.49				
4	DS	10:14-10:54	1650	9.84	9.91	9.87	190	193	190.8	0.91-6.10				
5	DS	11:05-11:12	316	9.86	9.89	9.88	190	192	190.8	1.52-2.74				
6	DS	11:22-11:35	552	9.86	9.89	9.88	190	192	191	1.52-3.35				
7	DS	11:50-12:02	536	9.86	9.88	9.87	191	194	192	1.83-3.96				
8	DS	12:07-12:26	869	9.84	9.88	9.86	190	194	191.5	2.13-3.96				
9	DS	13:04-13:20	654	9.81	9.88	9.84	188	192	190.2	1.22-2.44				
10	DS	13:36-13:53	577	9.81	9.84	9.83	189	192	190	1.22-3.35				
11	DS	13:59-14:13	535	9.81	9.86	9.83	189	191	190	1.22-3.35				
12	DS	14:22-14:48	1140	9.86	9.97	9.89	189	193	190.8	1.83-3.66				
13	DS	14:58-15:24	1052	9.91	9.96	9.94	191	194	192.6	0.91-3.05				
14	DS	15:31-15:55	980	9.84	9.94	9.89	189	193	190.4	2.44-4.57				1

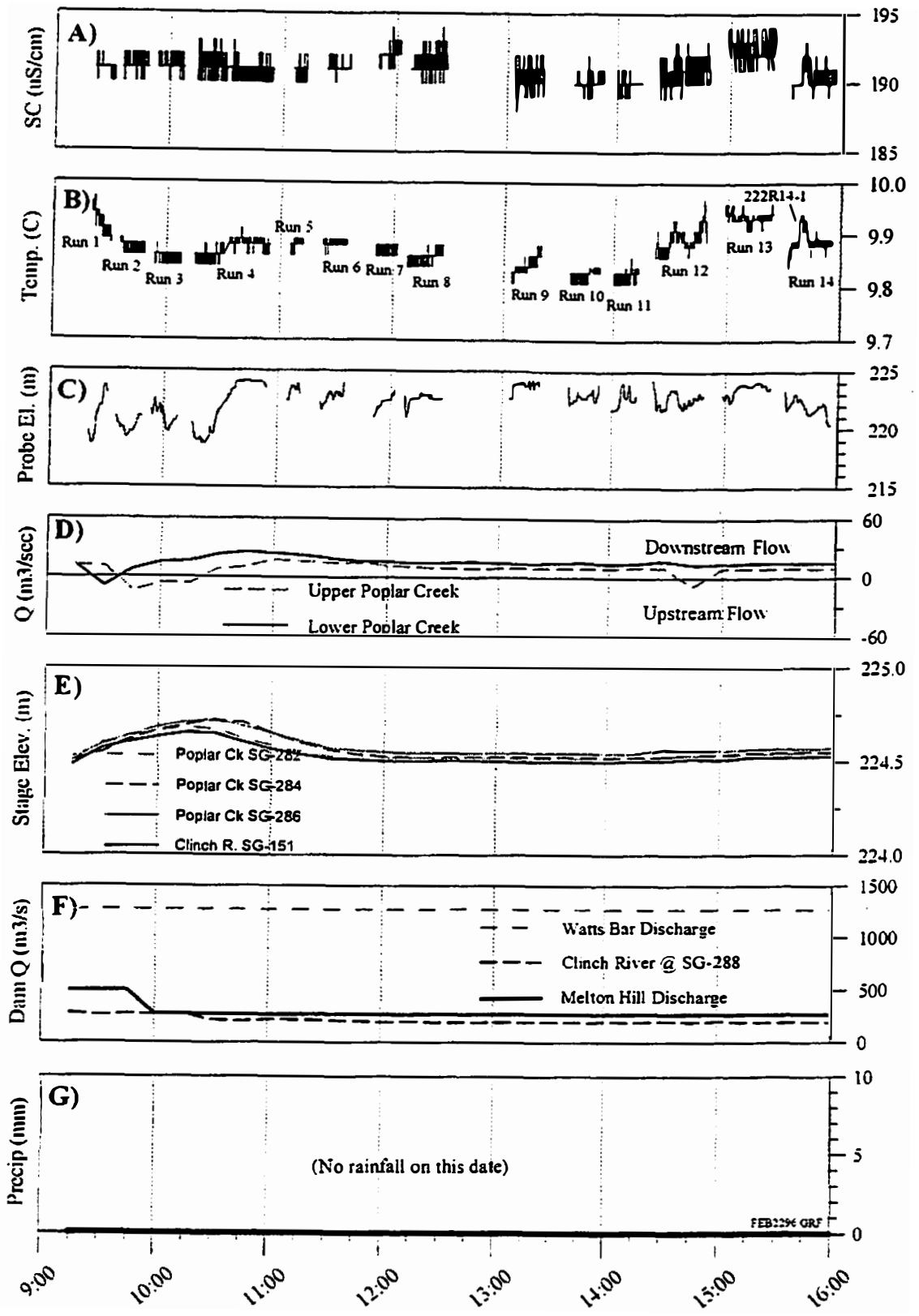


Figure A.9.1 Survey data and ambient hydrologic conditions, February 22, 1996.

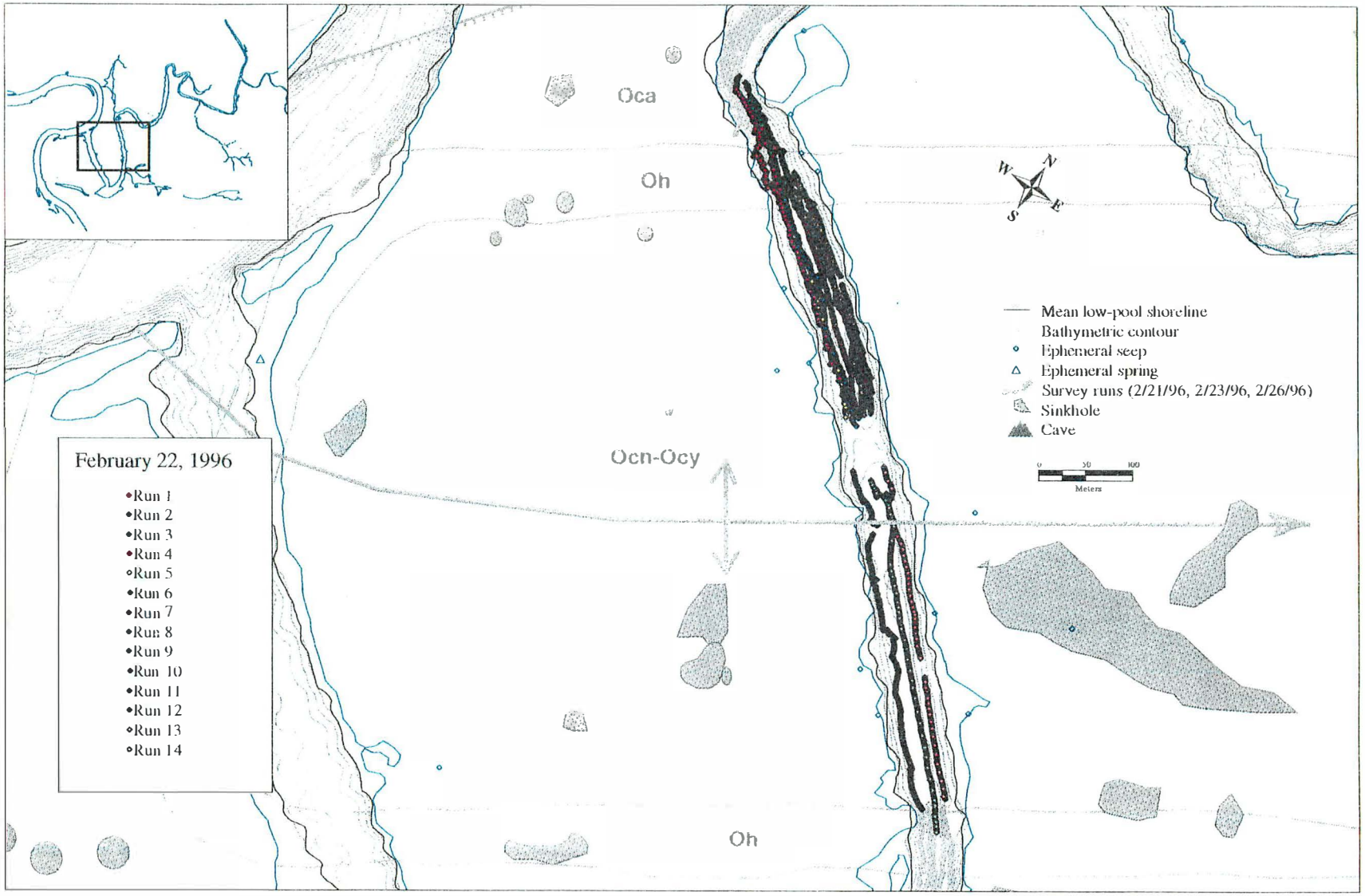


Figure A.9.2. Survey location map, February 22, 1996.

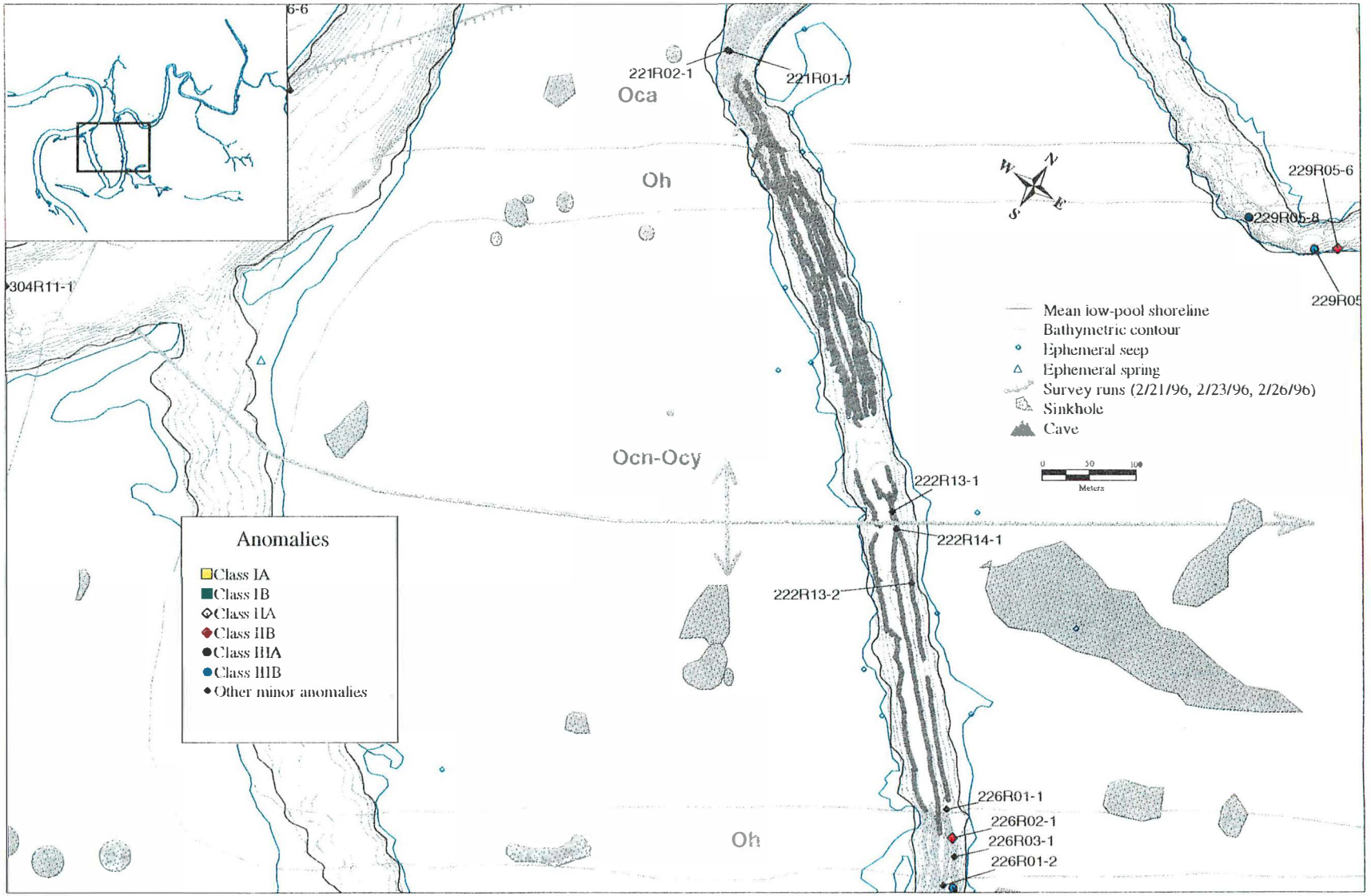


Figure A.9.3. Anomaly location map, February 22, 1996.

APPENDIX A.10

DATE: **February 23, 1996**

SURVEY AREA: Poplar Creek between the Perimeter Road Bridge and the K-1007 Pond. Survey covers outcrop belt of the northwest- dipping Chickamauga Group Hermitage and Carters Limestones along the south flank of the map-scale synclinal structure.

DESCRIPTION: A total of 3 fairly long runs were performed in this area, in water depths ranging from 1.2 to 6.4 m. Runs overlap with survey coverage from 2/22/96 (at the upstream end only) and 2/26/96.

HYDROLOGIC CONDITIONS: Hydrologic conditions prevailing during the field data acquisition period are summarized graphically on Figure A.10.1. Flow rates in Poplar Creek ranged from 21 to 23 m^3/sec.

There was no rainfall during the field period. Antecedent rainfall conditions were as follows:

within last 24 hours:	0 mm
within past 4 days:	40.64 mm
within past 7 days:	40.64 mm (2/20/96)

DATA: Data are summarized graphically on Figure A.10.1. Summary statistics on a run-by run basis are provided in Table A.10.1. Runs are shown on Figure A.10.2.

ANOMALIES: No anomalies indicative of springs were noted in the field. Review of data in Table A.10.1 shows that temperature varied 0.19 °C over the course of the day while SC displayed only a 4 uS/cm change. Subsequent review of data confirms a lack of anomalies along the runs surveyed, under the given hydrologic conditions. Only minor temperature increases (<0.03 °C) were noted but in conjunction with decreasing water depth along runs. Anomalies on overlapping coverage are shown on Figure A.11.3 (2/26/96).

Table A.10.1. Summary of field data for February 23, 1996.

RUN	DIRXN	TIME .	RECORDS	TEMPERATURE (°C)			SC (uS/cm)			DEPTH (m)	ANOMALIES			
				MIN	MAX	MEAN	MIN	MAX	MEAN		Class I	Class II	Class III	Class IV
1	DS	9:35-10:02	1207	10.09	10.25	10.14	190	193	190.9	1.22-3.35				
2	DS	10:00-10:32	1017	10.06	10.12	10.09	190	194	191.7	1.83-6.10				
3	DS	10:38-10:59	903	10.06	10.12	10.10	190	193	191.1	3.05-6.40				

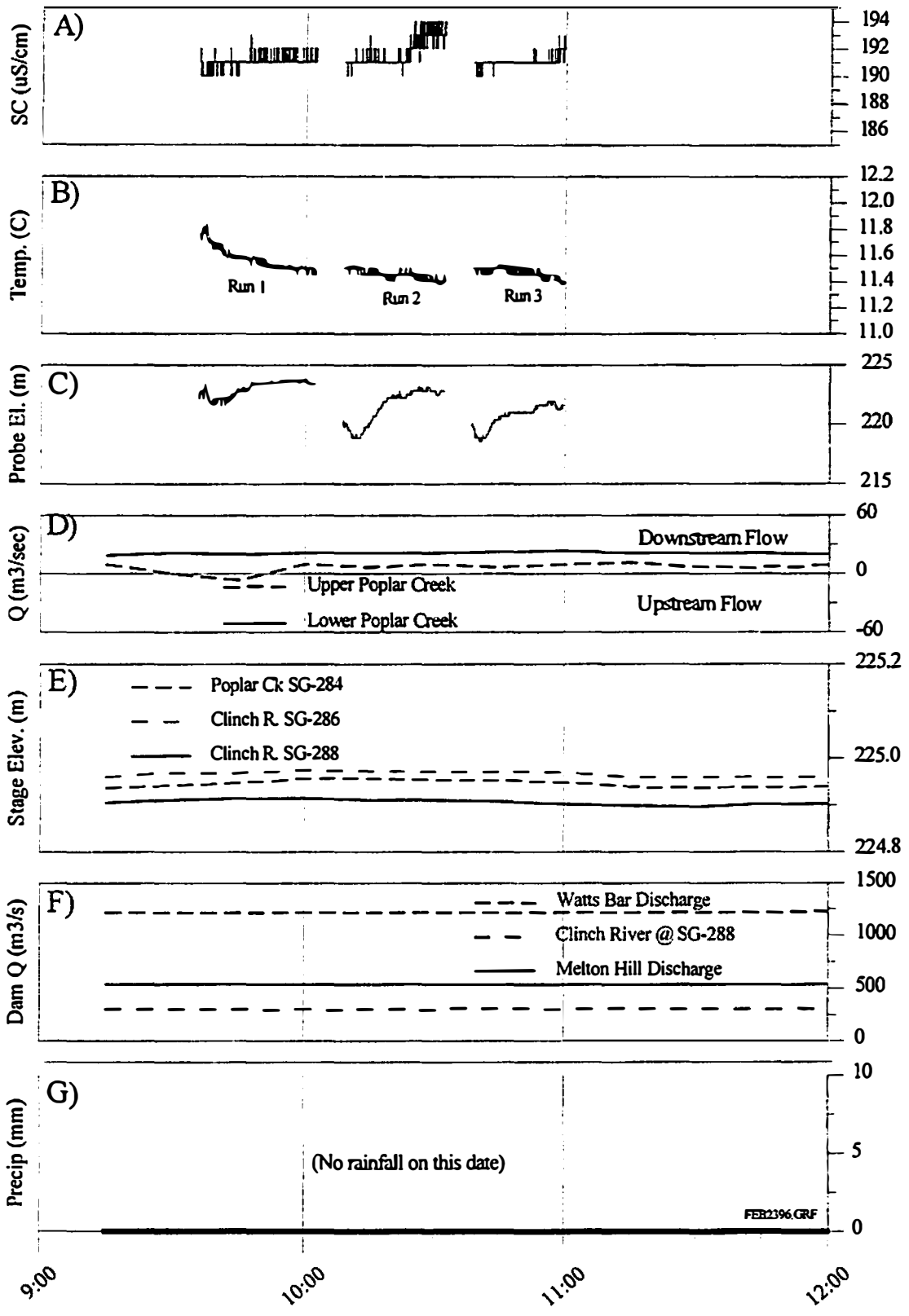


Figure A.10.1. Survey data and ambient hydrologic conditions, February 23, 1996.

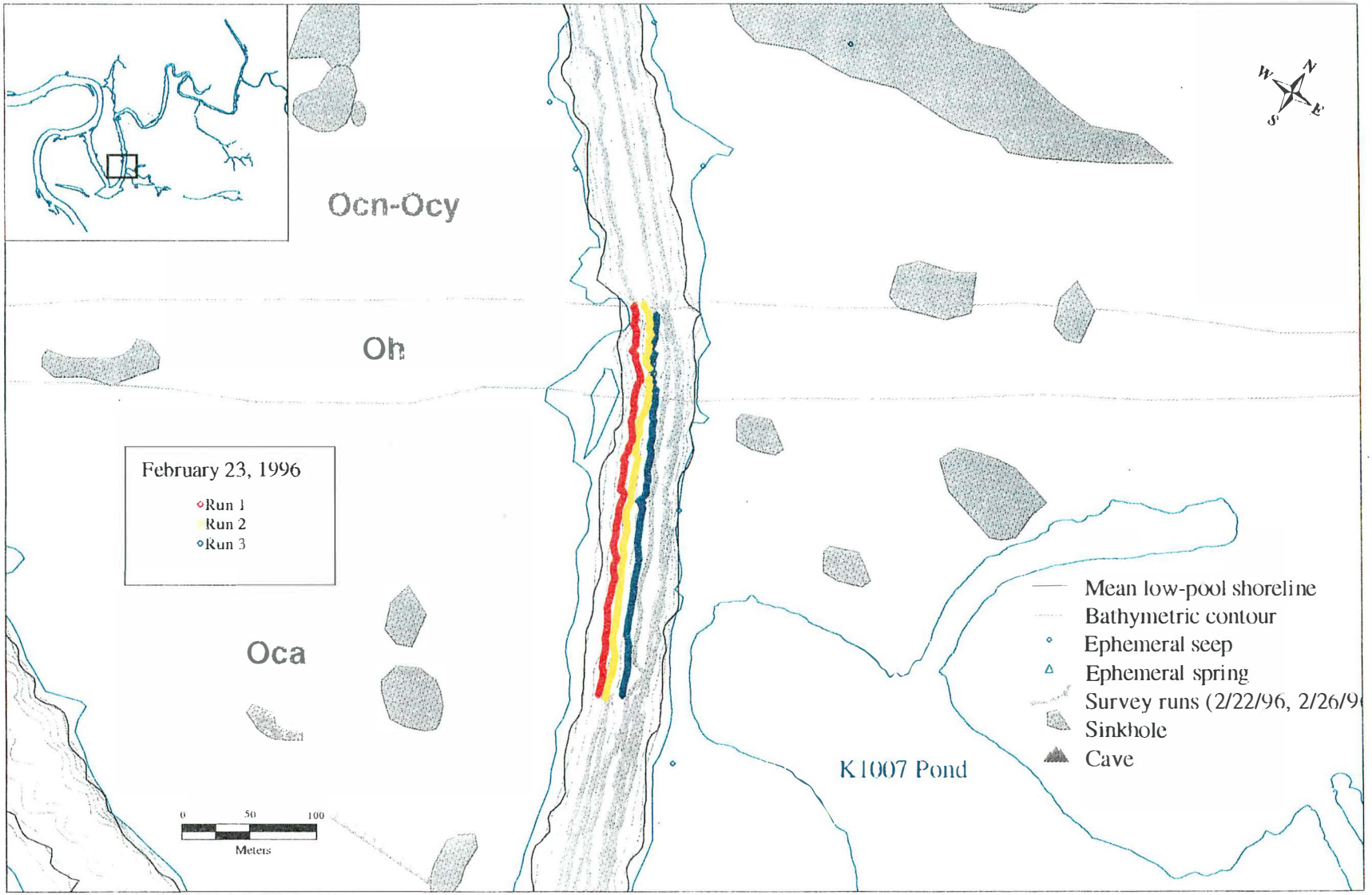


Figure A.10.2. Survey location map, February 23, 1996.

APPENDIX A.11

DATE: **February 26 1996**

SURVEY AREA: Poplar Creek in the vicinity of the K-1007 Pond. Runs cover the map-scale anticline in the Carters Ls and the faulted, structurally complex zone in the Hermitage Ls.

DESCRIPTION: A total of 12 runs were performed in this area, in water depths ranging from 0.9 to 4.6 m. Survey coverage overlaps with runs performed on 2/23/96.

HYDROLOGIC CONDITIONS: Hydrologic conditions prevailing during the field data acquisition period are summarized graphically on Figure A.11.1. Flow rates in Poplar Creek ranged from 13 to 29 m^3/sec with upstream flows of 37 m^3/sec downstream during run 5. Melton Hill dam discharge was zero during runs 1-2, but ranged from 168 up to 268 m^3/sec for the rest of the field day.

There was no rainfall during the field effort or within the 4 day period prior to the field surveys. Most recent rainfall within 7 days occurred on 2/20/96 (40.64 mm).

DATA: Data are summarized graphically on Figure A.11.1. Summary statistics on a run-by run basis are provided in Table A.11.1. Runs are shown on Figure A.11.2.

ANOMALIES: A 0.4 °C anomaly was noted in the field near the end of run 11. Otherwise, review of data in Table A.11.1 shows that temperature varied 1.17 °C over the course of the day while SC displayed only a 6 uS/cm change. Potential anomalies are indicated in most runs by a 0.15 or greater change in temperatures over the course of the run. A total of 22 anomalies were noted in the data, occurring along all 12 runs. Anomalies are shown on Figure A.11.3 and described in Table A.19.1 and A.19.2.

With the exception of 5 (Class IIB) anomalies, all others are less than the Hydrolab accuracy range of 0.15 °C. Anomalies 226R04-1 and 226R05-2, observed on separate runs, cluster around Class IIB anomaly 226R04-2. All of these occur effectively at the contact of the Carters and Hermitage Limestones and approximately coincidental with a mapped reverse fault. Similarly, minor anomalies 226R09-1 and 226R10-1 cluster around Class IIB

anomaly 226R11-1, again coincident with the formation contact and fault. These clustered anomalies suggest a potentially stratigraphically or structurally controlled zone of groundwater discharge. Anomalies 226R08-1 is an end (beginning) of run anomaly that corroborates nearby anomaly 226R09-2, though both are minor (Class IVB) anomalies with no SC change. Two of the strongest anomalies (226R12-1 and -2) encountered that day occurred in the Cannon-Catheys formation .

Table A.11.1 Summary of field data for February 26 1996.

				TEMPERATURE (°C)			SC (uS/cm)				ANOMALIES			
RUN	DIRXN	TIME	RECORDS	MIN	MAX	MEAN	MIN	MAX	MEAN	DEPTH (m)	Class I	Class II	Class III	Class IV
1	DS	10:14-10:27	576	11.35	11.52	11.41	204	205	204.1	2.74-4.57				1
2	DS	10:34-10:47	468	11.14	11.32	11.21	204	206	204.9	1.83-3.35		1	1	
3	DS	11:00-11:15	848	11.02	11.32	11.15	203	209	205.2	0.91-2.44			1	3
4	DS	11:15-11:36	497	11.12	11.38	11.24	205	208	205.7	0.91-3.05		1		1
5	DS	11:52-12:14	929	11.06	11.19	11.11	204	206	205.0	1.52-3.35				1
6	DS	12:56-13:12	804	11.55	12.01	11.80	204	208	206.0	1.83-3.66			1	
7	US	13:14-13:32	766	11.83	12.04	11.97	205	207	205.7	2.13-3.96				1
8	US	13:39-14:01	932	11.53	11.98	11.73	204	207	205.4	2.74-3.96				1
9	DS	14:03-14:14	431	11.53	11.75	11.64	204	206	205.0	2.13-3.35				2
10	DS	14:20-14:30	468	11.50	11.68	11.63	204	207	205.3	1.83-2.74				
11	DS	14:36-14:50	627	11.52	12.12	11.72	204	207	205.2	1.22-2.13		1		
12	DS	15:05-15:20	396	11.71	12.19	11.87	205	208	206.5	1.22-3.05		2		

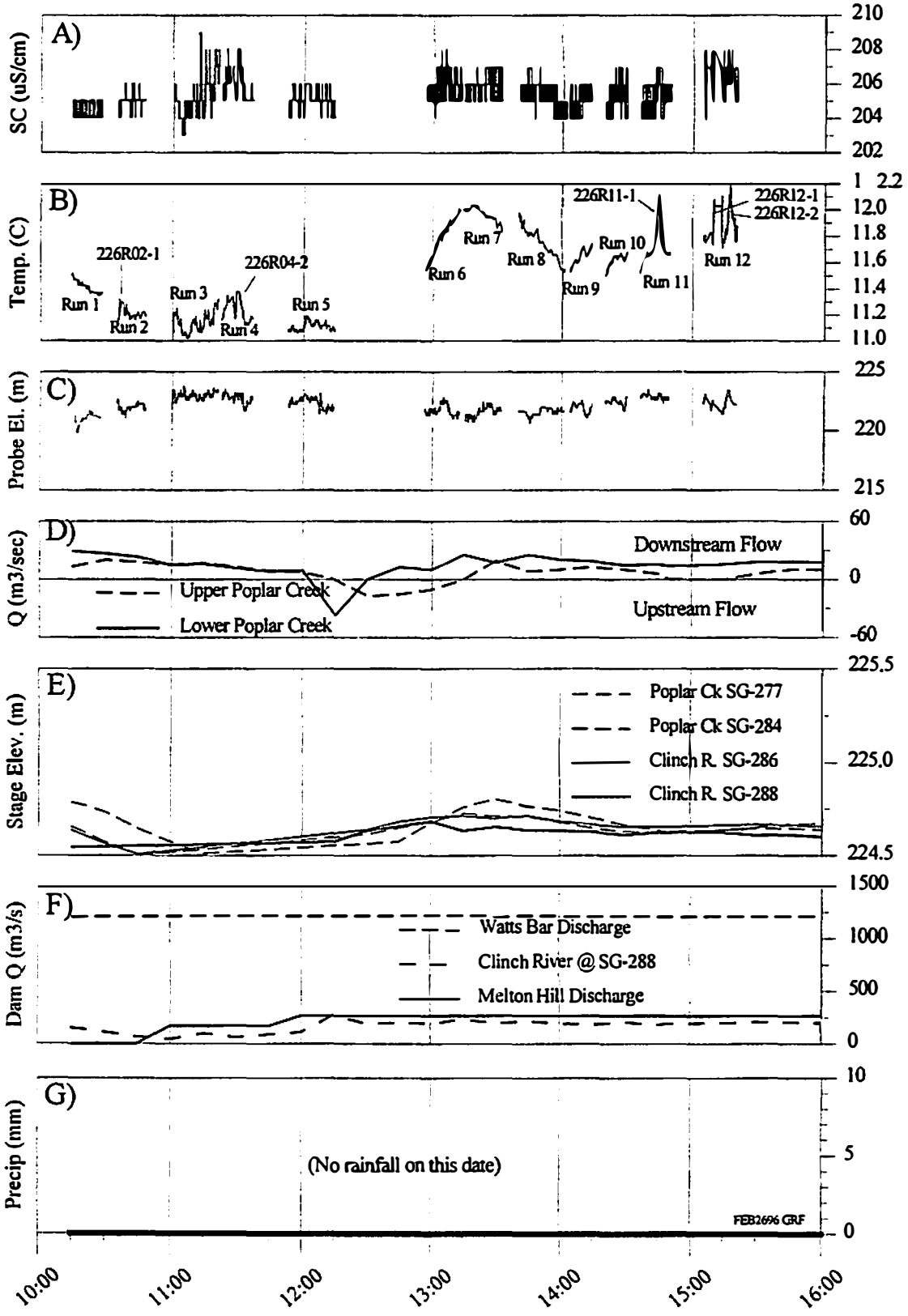


Figure A.11.1. Survey data and ambient hydrologic conditions, February 26, 1996.

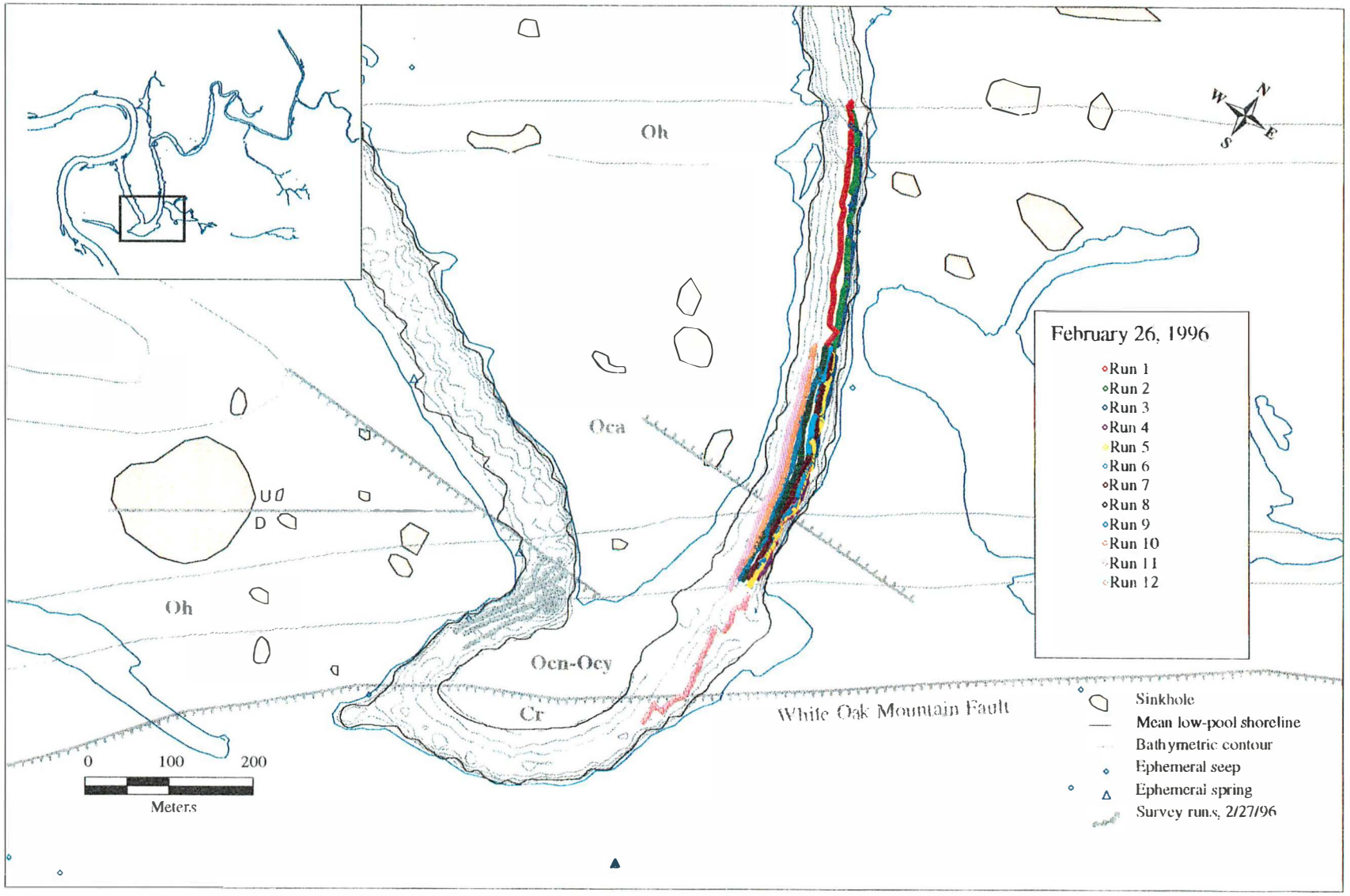


Figure A.11.2 Survey location map, February 26, 1996.

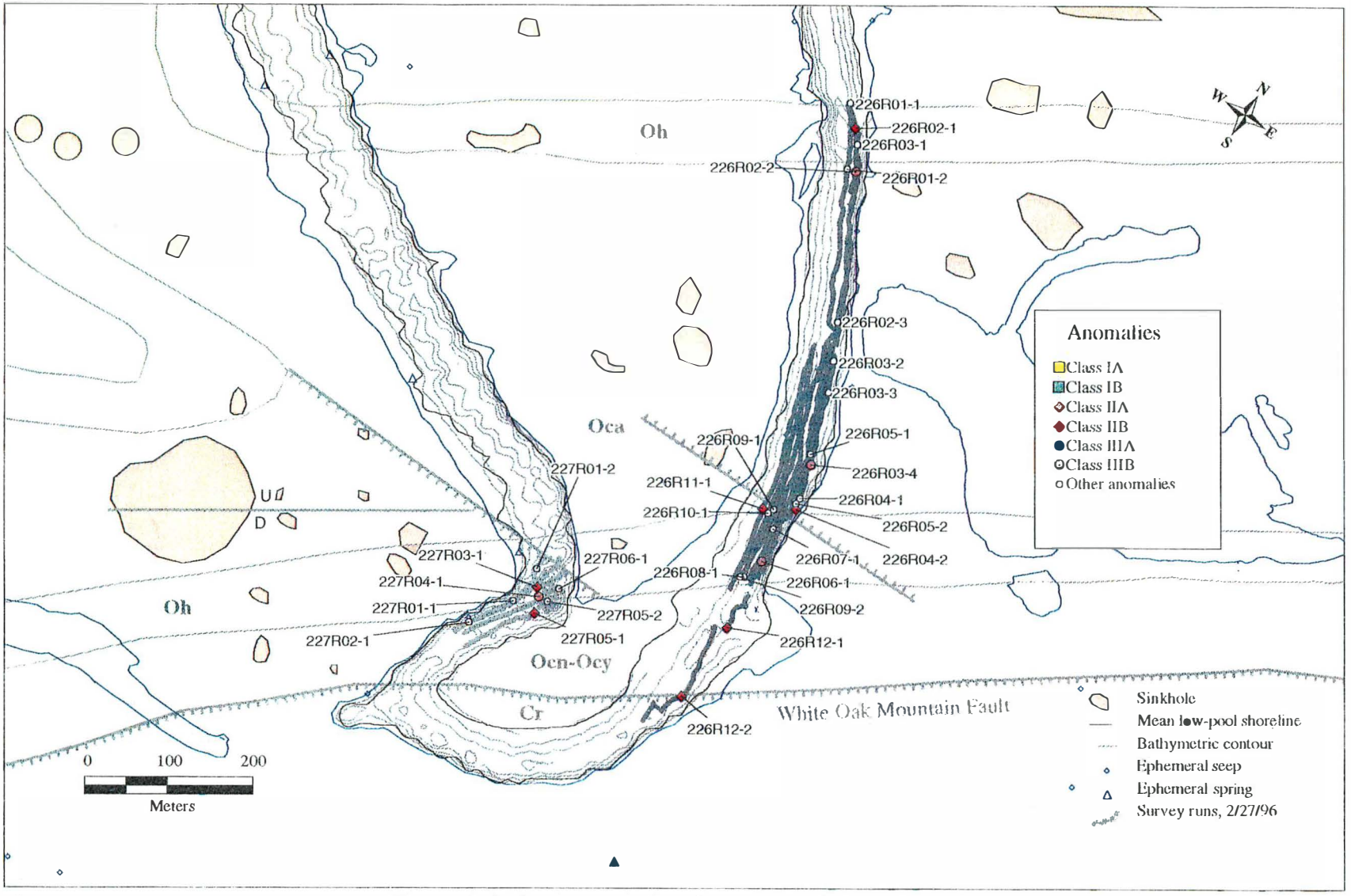


Figure A.11.3 Anomaly location map, February 26, 1996.

APPENDIX A.12

DATE: **February 27 1996**

SURVEY AREA: Surveys were conducted in two areas in Poplar Creek. Runs 1-6 were conducted in the area of the first bend in Poplar Creek, straddling the Hermitage and Catheys-Cannon Limestone contact in the vicinity of a mapped reverse fault. Note that this reach includes the deepest hole in Poplar Creek, with water depths observed to 7.01 m.

Run 7 was conducted along Poplar Creek above the Perimeter Road bridge in the Lebanon and Ridley Limestones.

DESCRIPTION: A total of 7 runs were performed in two areas, in water depths ranging from 0.9 to 7 m. Survey coverage for run 7 overlaps with runs performed on 2/29/96. There is no other coverage for the area covered by runs 1-6.

HYDROLOGIC CONDITIONS: Hydrologic conditions prevailing during the field data acquisition period are summarized graphically on Figure A.12.1. Flow rates in Poplar Creek ranged from 10 (run 4) to 20 m^3/sec (Run 1) with upstream flows of 5 m^3/sec during run 6. Run 7 is considerably upstream and flow rates, though downstream were slightly lower. Melton Hill dam discharge remained constant at 271 m^3/sec throughout the field day.

There was no rainfall during the field effort or within the 7 day period prior to the field surveys.

DATA: Data are summarized graphically on Figure A.12.1. Summary statistics on a run-by run basis are provided in Table A.12.1. Runs are shown on Figure A.12.2 (runs 1-6) and A.12.3 (run 7).

ANOMALIES: A 0.4 °C anomaly was noted in the field during run 7. Otherwise, review of data in Table A.12.1 shows that temperature varied only 0.24 °C over the course of the day while SC displayed a 10 uS/cm change. Subsequent review of the data revealed a total of 13 anomalies, occurring along all 7 runs. Anomalies are shown on Figure A.12.4 (runs 1-6) and A.12.5 (run 7) and described in Table A.19.1 and A.19.2.

A number of small anomalies were observed during runs 1-6,

apparently roughly coincident with the Hermitage and Catheys-Cannon formation contact. Two anomalies indicated 0.27 and 0.17 oC temperature changes though no SC changes (227R03-1 and 227R05-1, respectively). No anomalies were noted in association with the projection of the mapped reverse fault. Interestingly, a number of anomalies, though minor, cluster within the deepest hole observed on Poplar Creek; the significance of this coincidence is not known. The prominent temperature change on run 6 appears to correlate with a decrease in water depth.

A number of significant (Class IIB) anomalies with temperature increases of 0.2-0.29 °C were observed during run 7. In particular, anomalies 227R07-3 and -4 coincide with an anomaly noted on 2/29/96 (229R01-1), and anomaly 227R07-2 coincides with 2/29/96 anomaly 229R02-1. This suggests corroborated sites of groundwater discharge as indicated by anomalies identified on two separate dates.

Table A.12.1 Summary of field data for February 27 1996.

RUN	DIRXN	TIME	RECORDS	TEMPERATURE (°C)			SC (uS/cm)			DEPTH (m)	ANOMALIES			
				MIN	MAX	MEAN	MIN	MAX	MEAN		Class I	Class II	Class III	Class IV
1	DS	11:41-11:49	260	12.39	12.47	12.42	204	207	205	1.22-4.27				1
2	DS	11:53-12:05	365	12.21	12.42	12.28	205	207	206.3	1.52-5.18				1
3	DS	12:11-12:22	421	12.04	12.31	12.19	205	208	206.5	1.83-6.71		1		
4	DS	12:27-12:43	607	11.98	12.27	12.17	205	208	206	0.91-7.01			1	1
5	DS	12:49-13:00	425	11.88	12.31	12.08	205	208	207	1.52-4.27		1		1
6	DS	14:09-14:40	806	12.08	12.44	12.23	205	208	207	1.22-6.71				
7	DS	15:24-16:02	848	12.49	12.93	12.69	207	214	209	0.91-3.35		5		

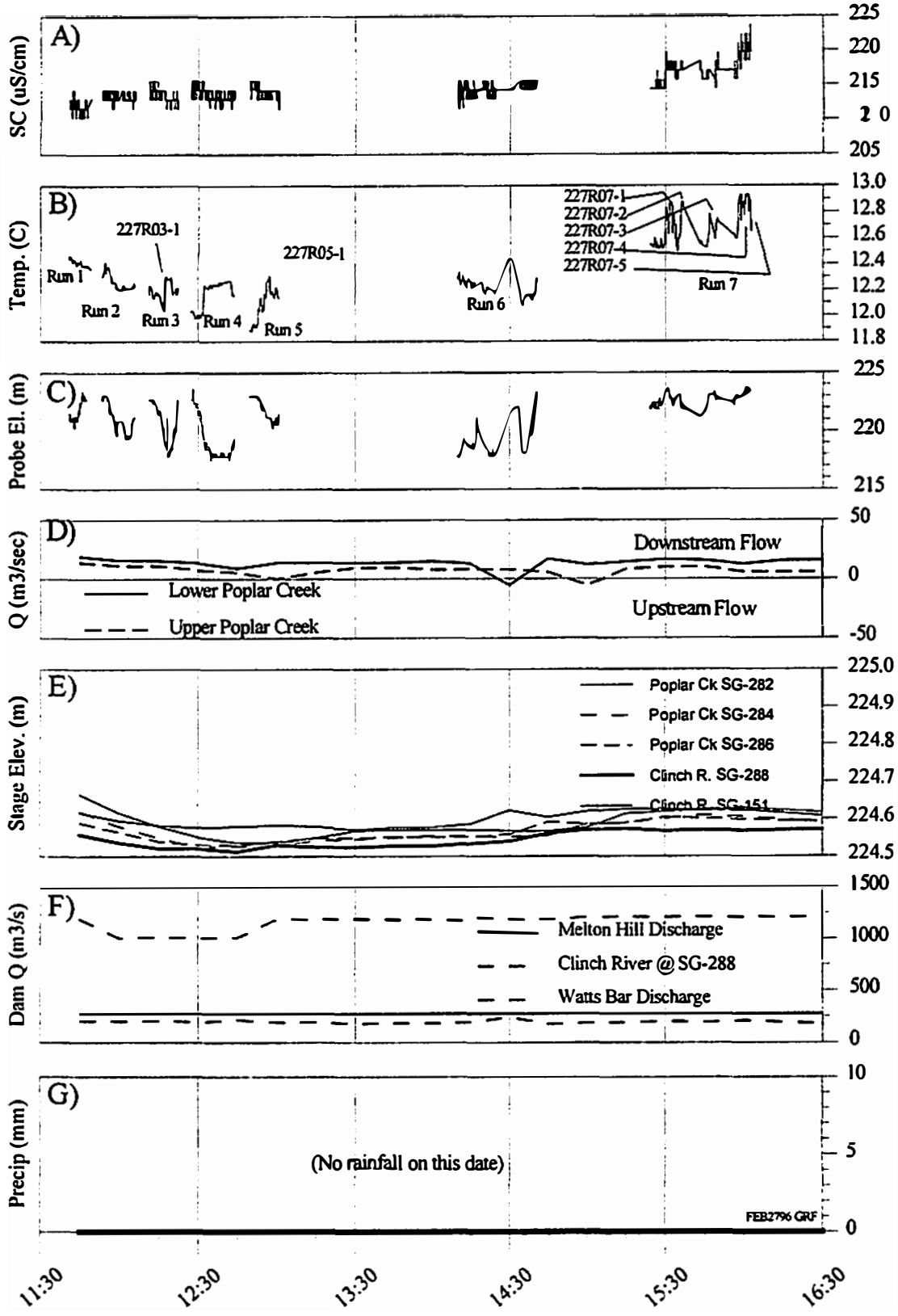


Figure A.12.1. Survey data and ambient hydrologic conditions, February 27, 1996.

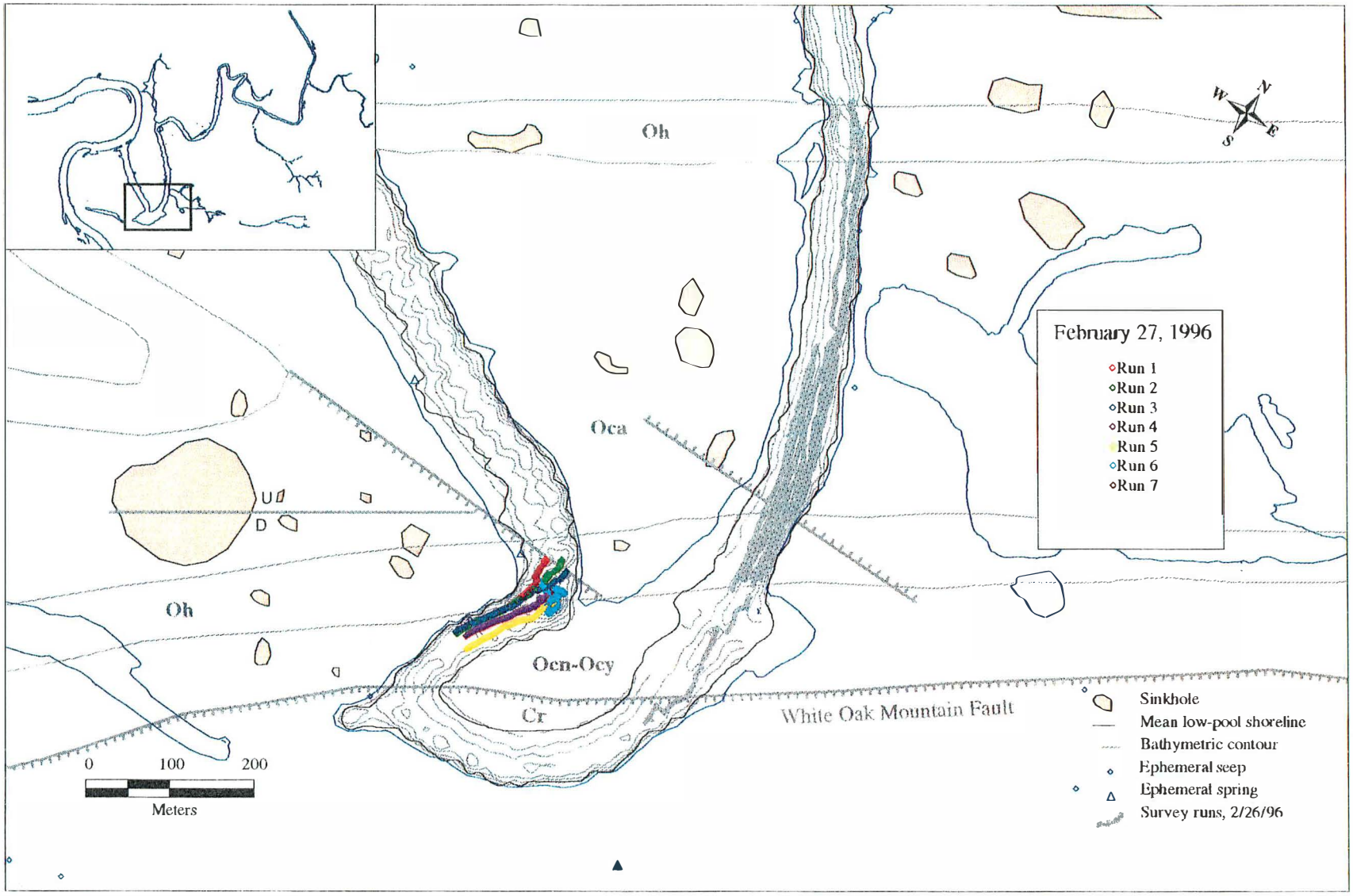


Figure A.12.2 Survey location map, lower Poplar Creek area, February 27, 1996.

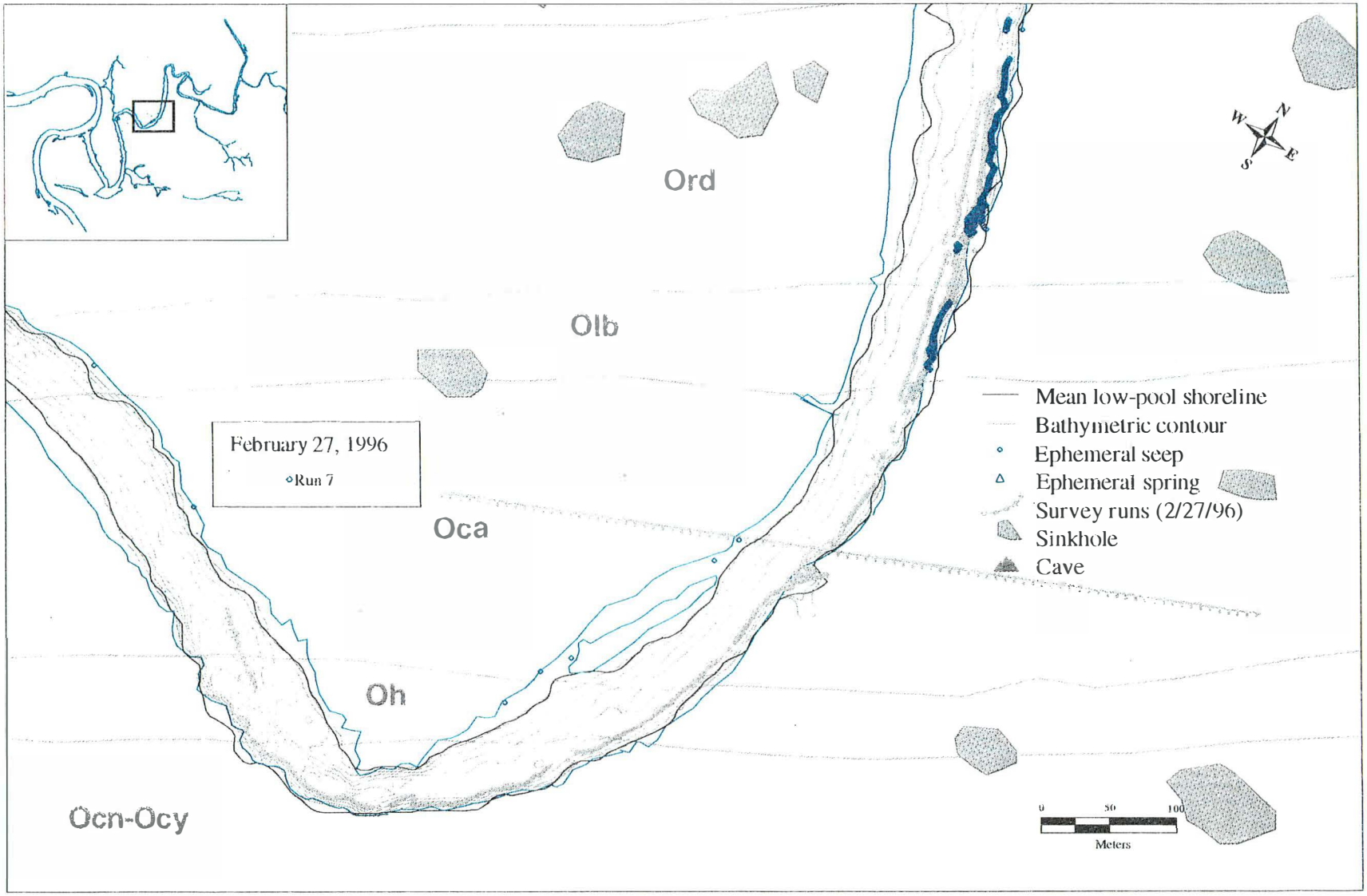


Figure A.12.3. Survey location map, upper Poplar Creek area, February 27, 1996.

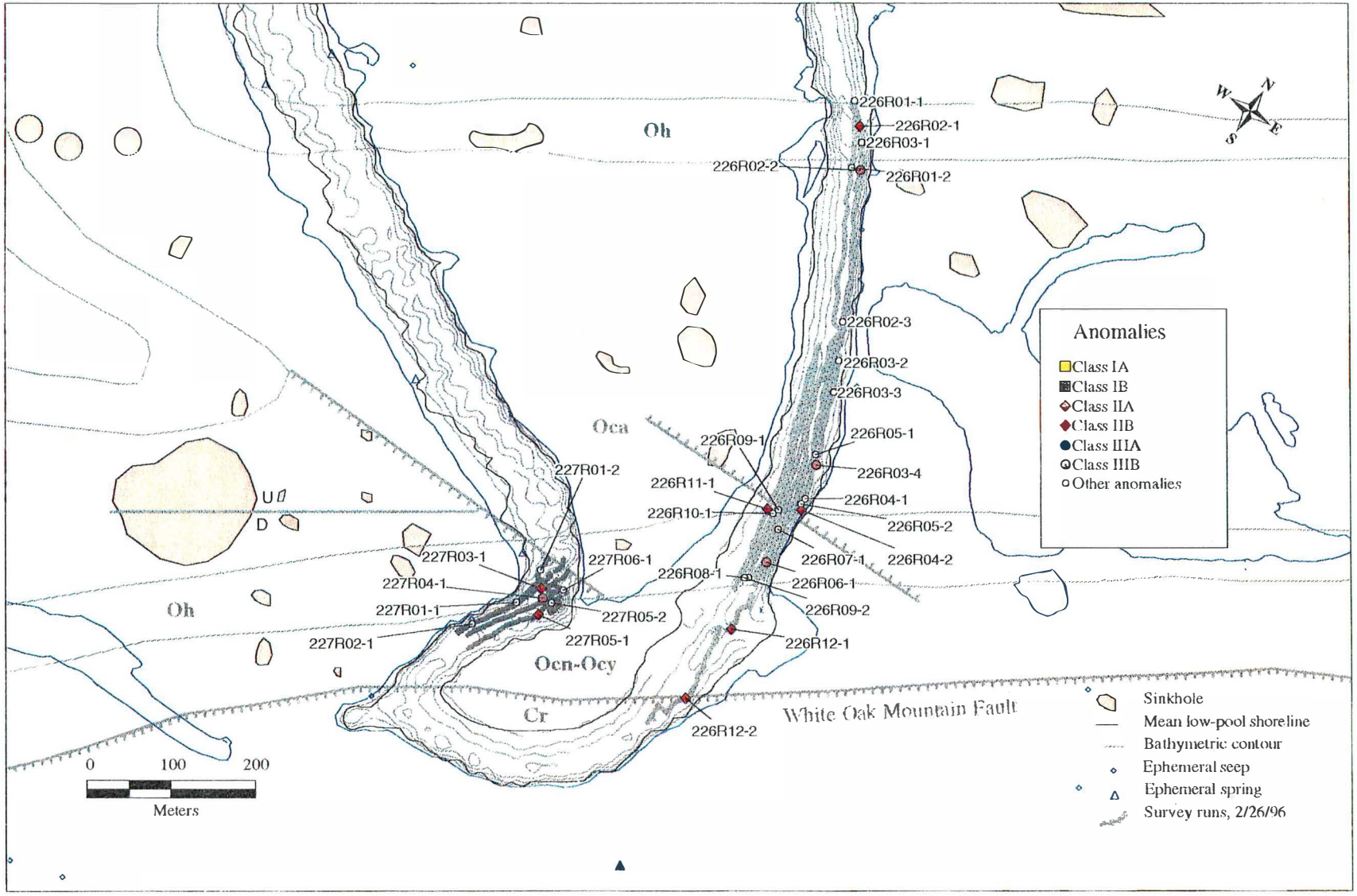


Figure A.12.4 Anomaly location map, lower Poplar Creek area, February 27, 1996.

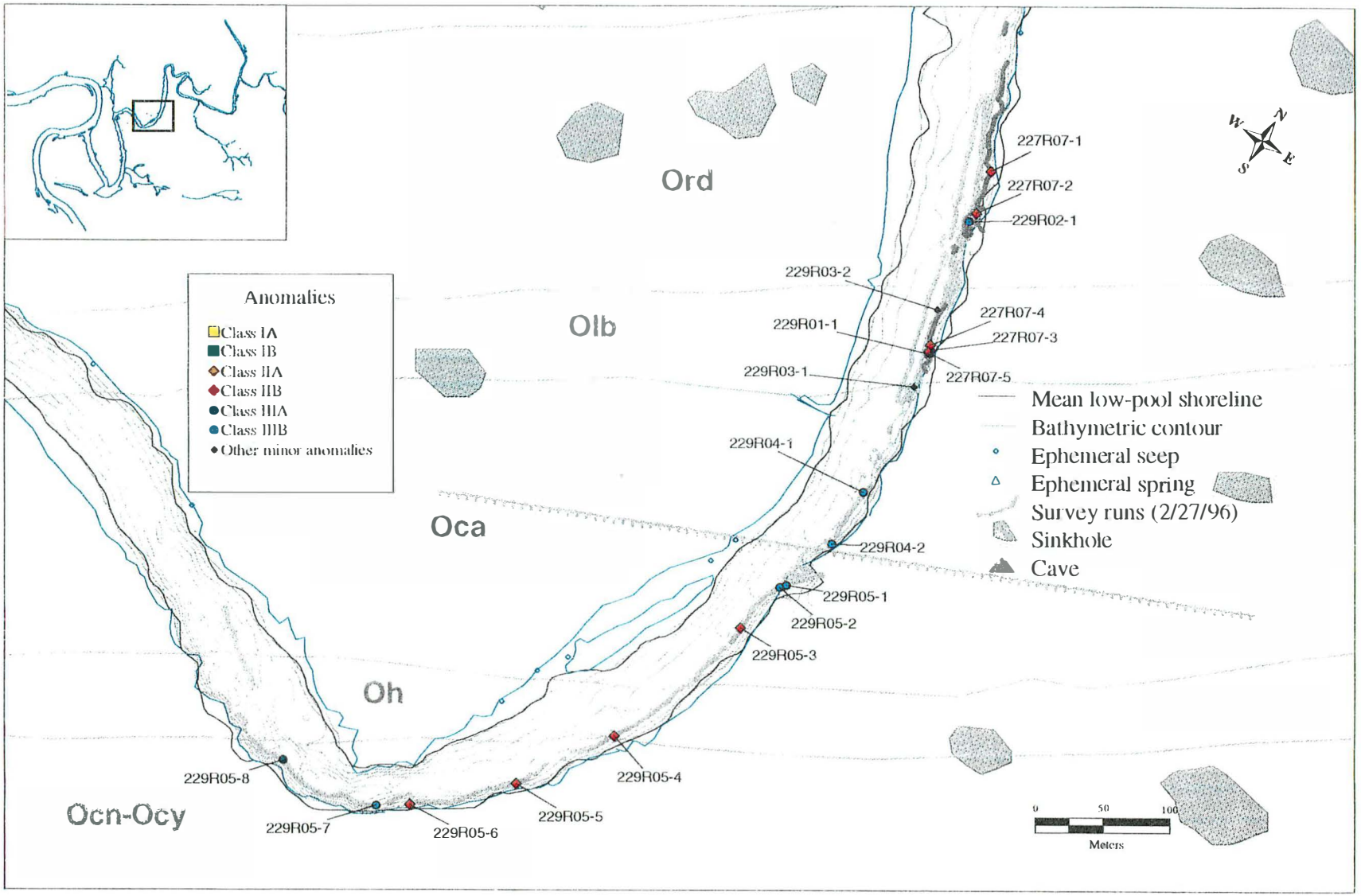


Figure A.12.5. Anomaly location map, upper Poplar Creek area, February 27, 1996.

APPENDIX A.13

DATE: **February 29 1996**

SURVEY AREA: Surveys were conducted in two areas, on the Clinch River and the other in Poplar Creek. Runs 1-5 were conducted in Poplar Creek, extending from the Ridley Ls up-section through the Lebanon, Carters, Hermitage and Catheys-Cannon Limestone formations of the Chickamauga Group on the north flank of the map scale syncline. Runs 4 and 5 cross a mapped reverse fault and traverse the "deformation zone" believed to represent a blind thrust fault that bounds the syncline.

Runs 6-11 are in the Ridley Ls and Pond Springs formation in the Clinch River adjacent to the K-901 Pond. All runs are on the northeast bank and extend from stage gage SG-288 downstream to the Mascot-Pond Springs contact.

DESCRIPTION: A total of 11 runs were performed covering 2 areas. Water depths in Poplar Creek ranged from 0.9 to 6.1 m while in the Clinch, depths ranged from 1.2 to 10.4 m. Survey runs 1-5 are overlapped by survey coverage from 2/27/96. Survey runs 6-11 are overlap coverage from 1/25/96 and 3/12/96 as well as survey runs performed in March 1995.

HYDROLOGIC CONDITIONS: Hydrologic conditions prevailing during the field data acquisition period are summarized graphically on Figures A.13.1 and A.13.2. Flow rates in Poplar Creek ranged from 1 (run 5) to 14 m^3/sec (run 1. Stage in Poplar Creek declined nearly 0.3 m from run 1 to run 4 and remained low through run 5. Flow rates in the Clinch River were extremely low during runs 6-7, ranging from 65 to 88 m^3/sec. A slight backflow was noted in the field during the early part of run 6. Melton Hill discharge was zero over the course of runs 6-10, but Watts Bar discharge increased considerably in two steps beginning in run 7. Due to the lag in local response, these operational changes drove a subsequent increase in Clinch River flow rates in runs 8-11 (to ~220 m^3/sec). Clinch River stage was lowest during run 7. There was no rainfall during the field effort or within the 7 day period prior to the field surveys.

DATA: Data are summarized graphically on Figure A.13.1 and A.13.2. Summary statistics on a run-by-run basis are provided in Table

A.13.1. Runs are shown on Figure A.13.3 (runs 1-5) and A.13.4 (run 6-11).

ANOMALIES: Review of Table A.13.1 shows an overall temperature change of 0.60 and 0.51 °C in the Poplar Creek and Clinch River surveys, respectively. SC varied 7 uS/cm in Poplar Creek runs but 16 uS/cm in Clinch River runs. Subsequent review of the data indicates a total of 17 anomalies, 14 of which were observed in Poplar Creek. Anomalies encountered in Poplar Creek are shown on Figure A.13.5 while those in the Clinch River are shown on A.13.6. All anomalies are described on Tables A.19.1 and A.19.2.

Poplar Creek: Anomalies 229R01-1 (a minor, Class IVB anomaly) coincides with anomalies 227R07-3 and -4. Similarly, anomaly 229R02-1 (IIIB) coincides with anomaly 227R07-2. Both instances of overlap corroborate potential groundwater discharge at these locations under differing hydrologic conditions.

Anomaly 229R04-2 occurs within the "deformation zone" in the middle Carters Ls, very near to the projected location of a map-scale reverse fault and possibly may indicate structural control on groundwater discharge associated with that structure. Other Class IIB and IIIB anomalies lie slightly downstream on the hanging wall of the fault, again in the deformation zone along the north flank of the map scale syncline.

Other anomalies (IIB and IIIB) occur in the Lebanon Ls along the outside meander loop. 226R05-4 appears to occur at the contact of the Cannon-Catheys and the underlying Hermitage Ls. It should be noted that from a regional sense, this point marks the most upvalley position where the Cannon-Catheys is breached by surface water.

Clinch River: The most significant anomaly encountered is a Class IA anomaly, 229R07-1, observed in the Pond Springs fm above the K-901 outfall where a temperature change of 0.43 °C was encountered accompanied by a 15 uS/cm SC anomaly. This anomaly was observed right at the edge of the former pre-impoundment channel in water 1.43 m deep. It was corroborated by anomaly 229R06-1 which although smaller, occurred in close proximity (within ~ 1 m) but in slightly deeper water (2.47 m). Further, anomalies encountered on 3/12/96 (312R01-1 and 312R03-5) occur in very close proximity. Anomalies encountered in March 1995 data occur within about 15 m along strike, but in

deep water. Given the low Clinch River flow rates and low stage, this represents optimal conditions for detecting such an anomaly, which under different hydrologic conditions as encountered in other survey runs, would be less noticeable. It should be noted that the outcrop along shore shows a deeply weathered bedding plane which correlates to a deep, bedding plane hole that extends out across the channel along these anomalies. Finally, the anomaly occurs along the axis of the trend of sinkholes that extend up and downvalley on both sides of the river, suggesting association with an underlying karst feature of considerable magnitude.

Table A.13.1 Summary of field data for February 29 1996.

				TEMPERATURE (°C)			SC (uS/cm)				ANOMALIES			
RUN	DIRXN	TIME	RECORDS	MIN	MAX	MEAN	MIN	MAX	MEAN	DEPTH (m)	Class I	Class II	Class III	Class IV
1	DS	11:45-11:58	473	12.03	12.14	12.09	207	211	209	0.91-3.35				1
2	DS	12:03-12:20	630	11.93	12.09	12.01	205	208	207	1.22-3.05			1	
3	DS	12:28-12:43	587	11.81	11.98	11.89	205	208	206.1	1.83-3.05				1
4	DS	12:50-13:10	699	11.80	12.14	11.91	205	207	206.7	0.91-2.44			2	
5	DS	13:14-14:04	1675	12.06	12.40	12.22	205	212	207.7	0.91-6.10		4	4	
6	DS	15:36-16:02	947	8.91	9.06	8.97	258	262	259.5	1.83-5.79				1
7	US	16:06-16:35	581	8.97	9.42	9.03	258	274	259.7	1.22-3.05	1			
8	DS	16:44-17:07	851	8.96	8.99	8.97	259	260	259.9	7.62-9.75				
9	US	17:11-17:23	488	8.97	9.01	8.99	259	260	259.9	4.88-9.14				
10	US	17:24-17:52	1108	8.96	8.99	8.97	258	260	258.9	7.01-10.36				
11	US	17:55-17:58	95	8.96	8.97	8.96	259	260	259.9	6.10-7.92				

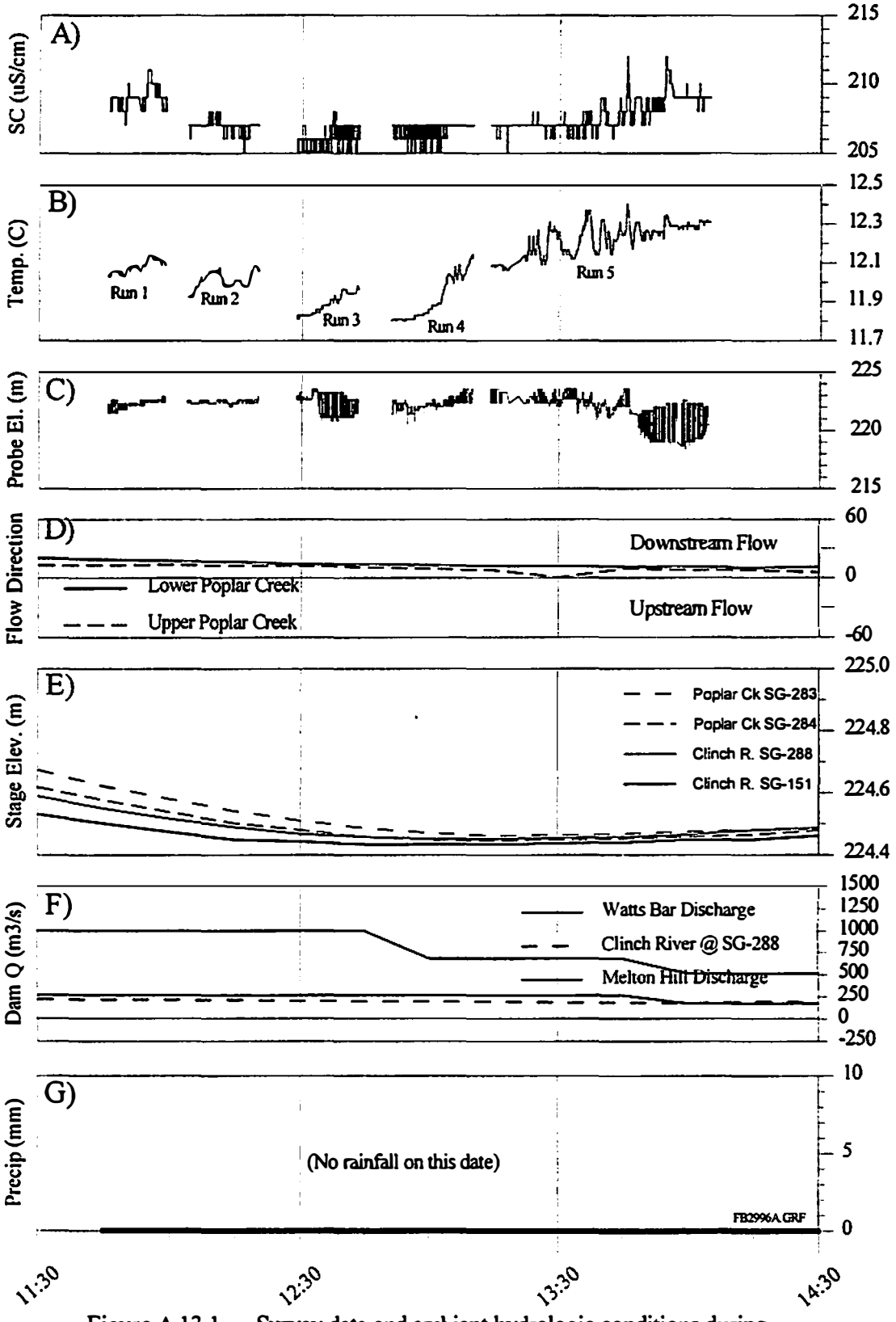


Figure A.13.1. Survey data and ambient hydrologic conditions during Runs 1-5, February 29, 1996.

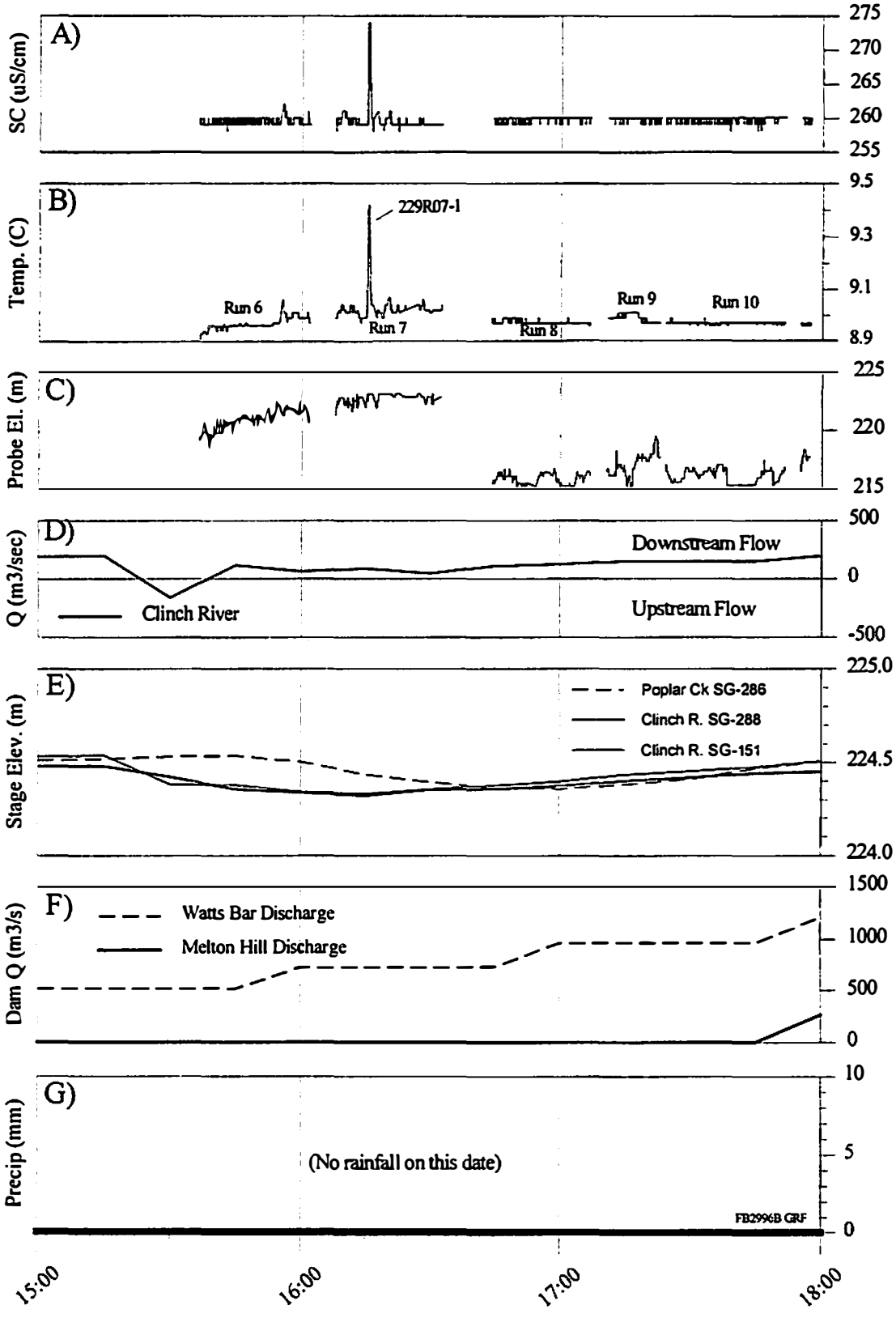


Figure A.13.2. Survey data and ambient hydrologic conditions during Runs 6-11, February 29, 1996.

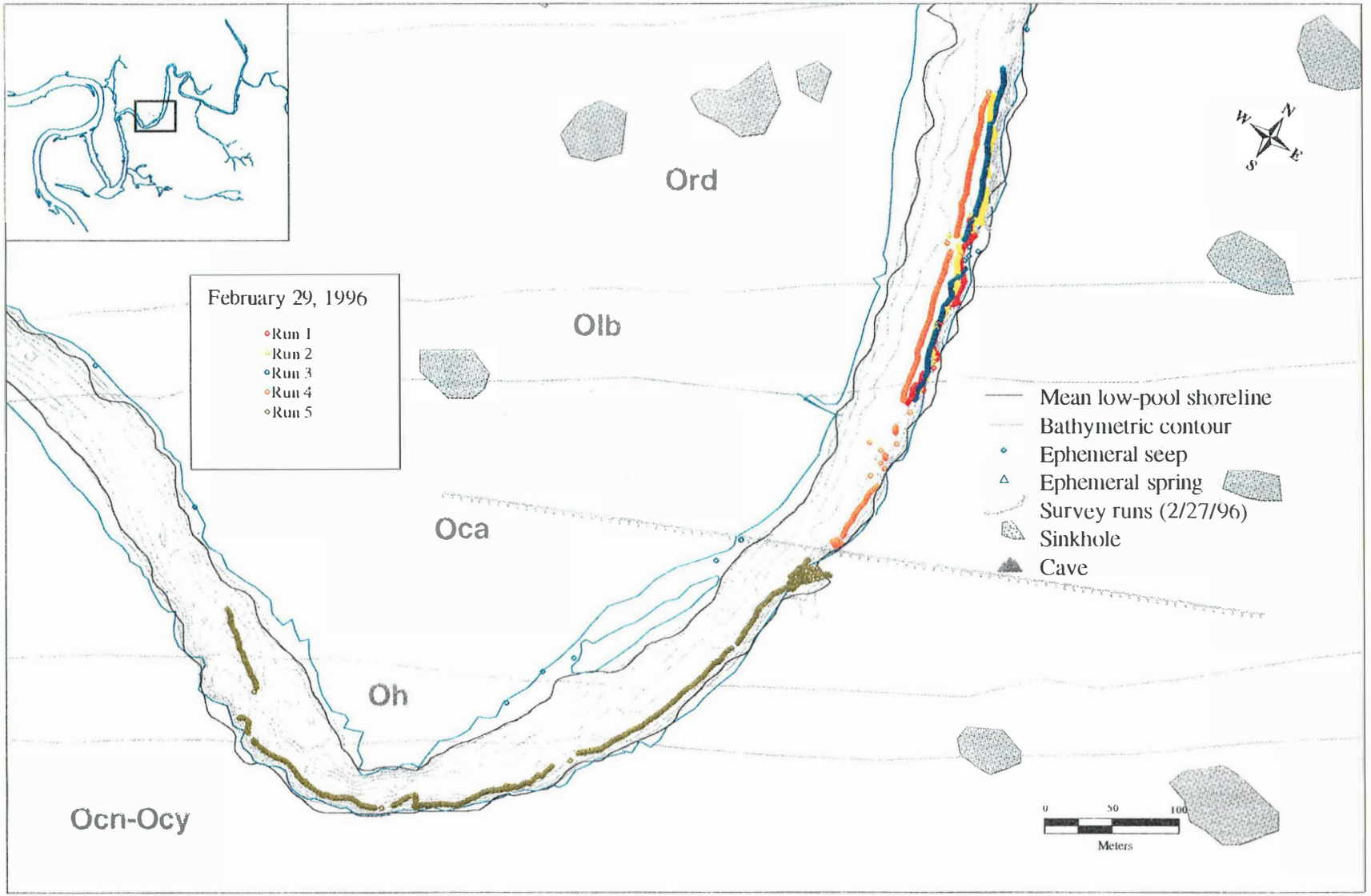


Figure A.13.3. Survey location map, runs 1-5 on Poplar Creek, February 29, 1996.

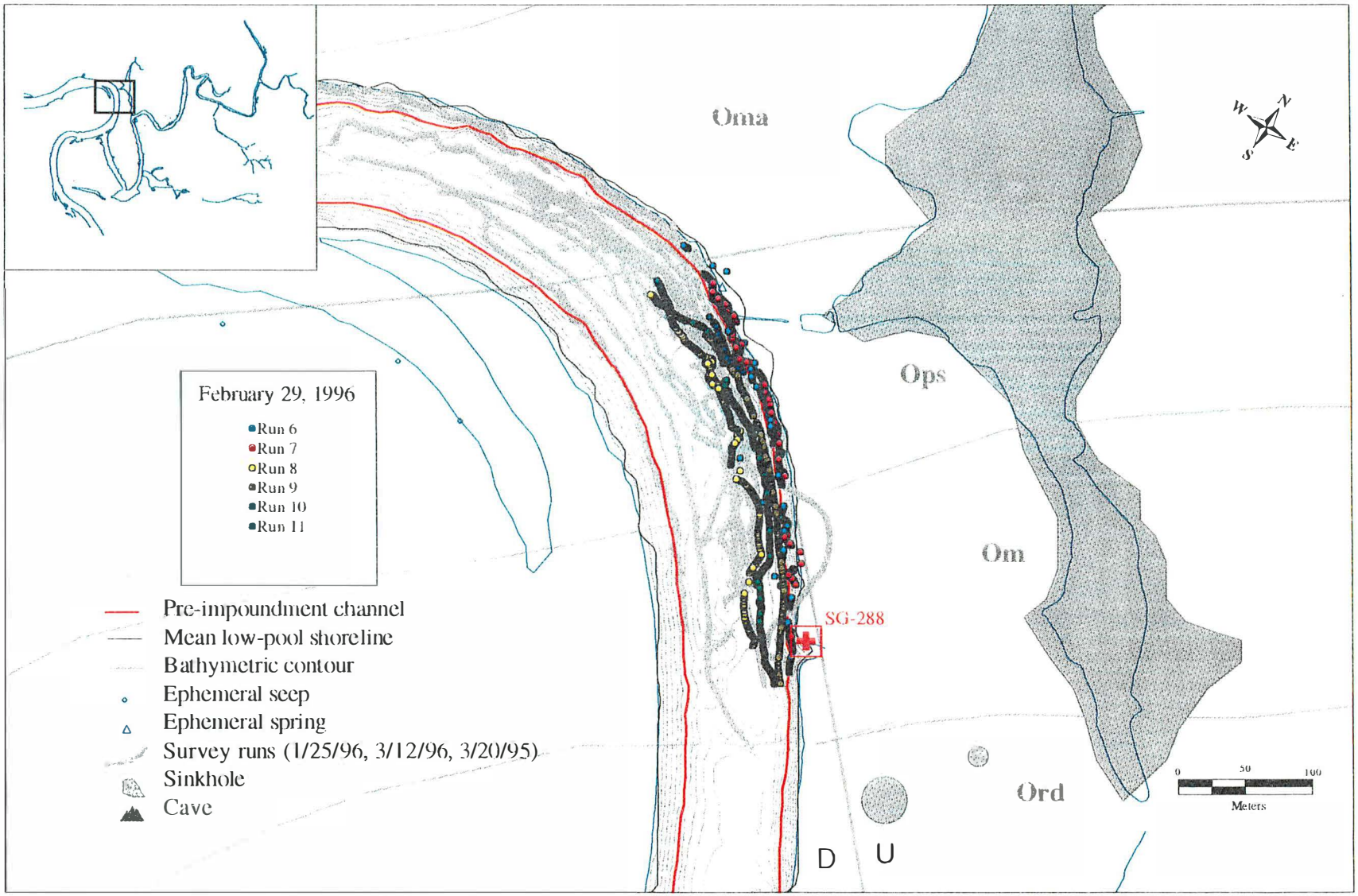


Figure A.13.4. Survey location map, runs 6-11 on the Clinch River, February 29, 1996.

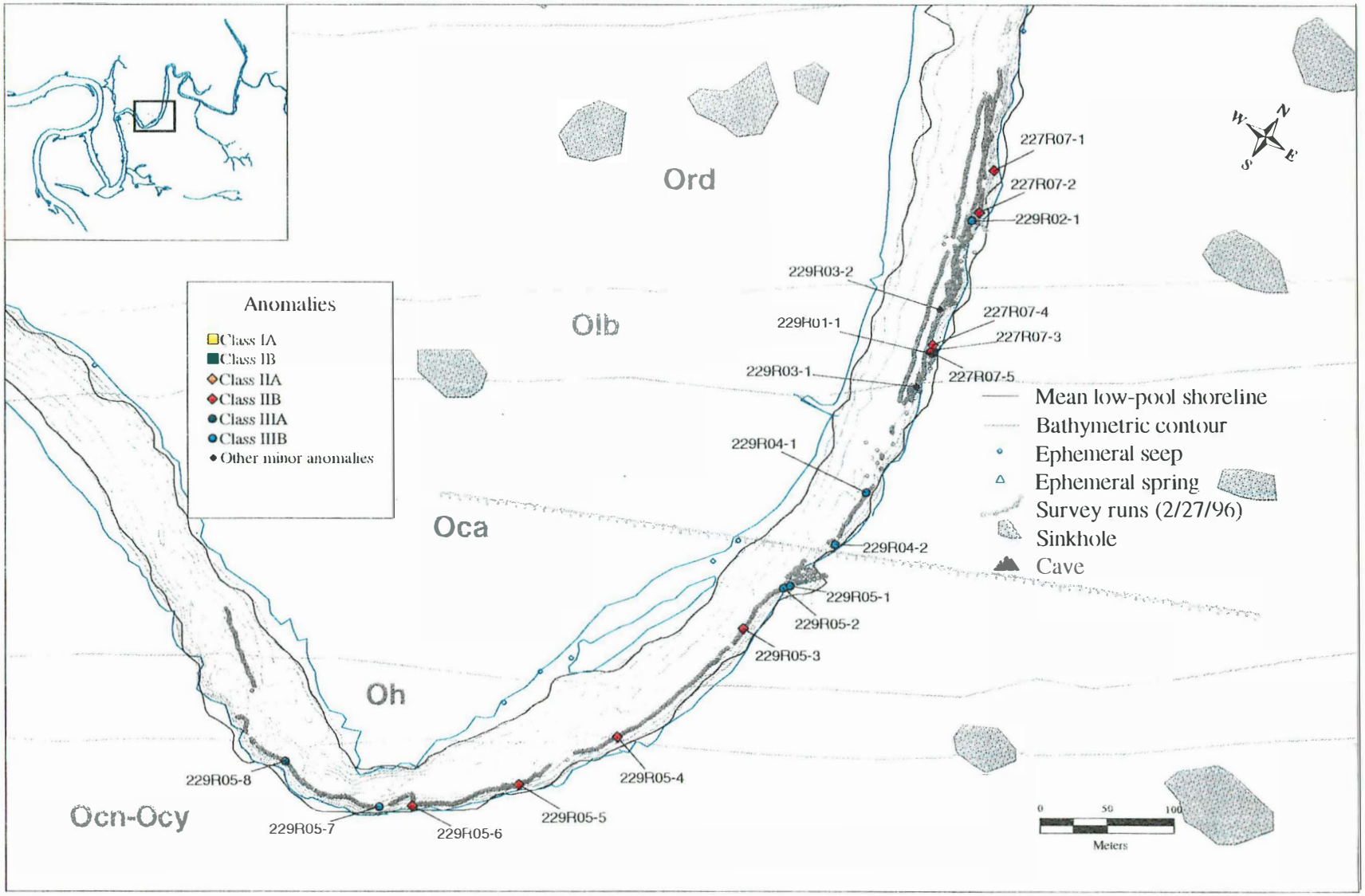


Figure A.13.5. Anomaly location map, runs 1-5 on Poplar Creek, February 29, 1996.

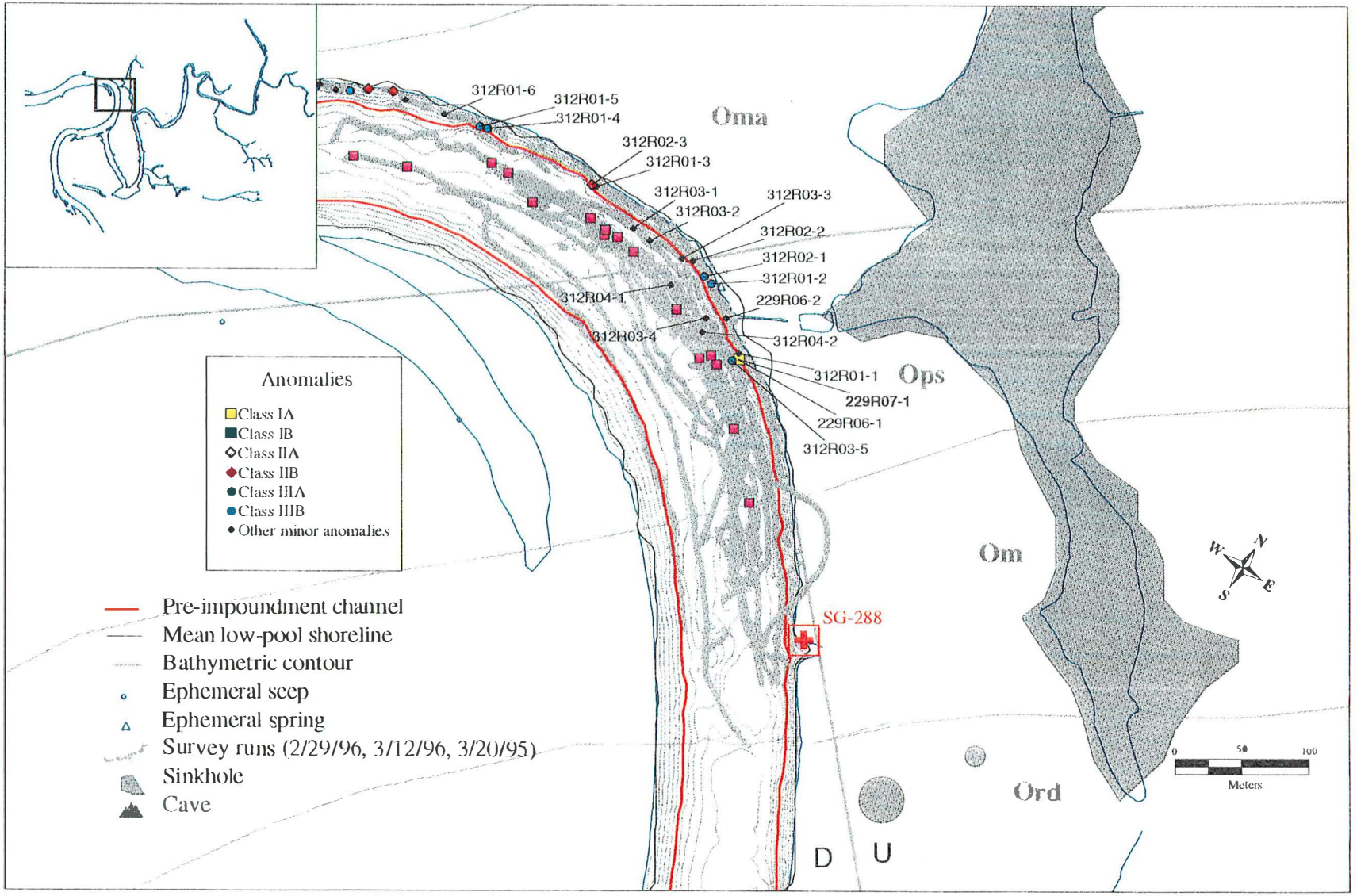


Figure A.13.6. Anomaly location map, runs 6-11 on the Clinch River, February 29, 1996.

APPENDIX A.14

DATE: **March 4, 1996**

SURVEY AREA: Surveys were performed at the lower end of Poplar Creek just upstream of the confluence with the Clinch River, spanning the Hermitage and upper Carters Ls along the deformation zone and axis of the map scale syncline. Also in the Clinch River just upstream of the mouth of Poplar Creek. Clinch River runs span the Carters through Murfreesboro formations of the Chickamauga Group. Upstream ends of runs cross a mapped normal fault in the Murfreesboro.

DESCRIPTION: A total of 11 runs were performed in the two areas. Initially work was started in the Clinch River but due to high flow conditions, moved to lower Poplar Creek. Later, surveying was resumed on the Clinch. Runs 1, 2, 8, 9, 10, and 11 were performed in the Clinch River while runs 3-7 were in Polar Creek. Runs overlap with survey coverage for March 11, 1996. Clinch River survey area also overlaps survey area from March 1995 surveys.

HYDROLOGIC CONDITIONS: Hydrologic conditions prevailing during the field data acquisition period are summarized graphically on Figure A.14.1. During runs 1 and 2 on the Clinch River, the river was flowing at extremely high rates (~ 300 m^3/sec) in response to Melton Hill discharges of 500 m^3/sec; this resulted in strong upstream backflow into the lower portion reaches of Poplar Creek. During runs 3 through 7 on lower Poplar Creek, downstream flow was increasing, causing mixing of cooler (~ 7.6 °C) Poplar Creek water with warmer Clinch River water (~ 8.2 °C) within lower Poplar Creek. This mixing was evident on the downstream ends of all 5 Poplar Creek runs (though diminishing in later runs). Melton Hill discharge was terminated at 12:00 with the Clinch flow rates in the study area dropping to as low as 40 m^3/sec during run 9 before picking back up to 160 m^3/sec by run 11 as the rebound flow from Poplar Creek kicked in. Melton Hill discharge remained at zero throughout the remainder of the day.

There was no rainfall during the field day. Antecedent rainfall conditions were as follows:

within last 24 hours:	0 mm
within past 4 days:	0 mm
within past 7 days:	37.59 mm

DATA: Data are summarized graphically on Figure A.14.1. Summary statistics on a run-by run basis are provided in Table A.14.1. Runs are shown on Figure A.14.2. Temperature and SC anomalies are shown on Figure A.14.3, along with runs and anomalies from other dates.

ANOMALIES: No distinct anomalies indicative of springs were noted in the field. Review of the data suggest minor temperature and SC anomalies associated with runs 3-7 in Poplar Creek. However, these are clearly related to mixing with a tongue of warmer Clinch River pushing up into poplar Creek. Despite low flow rates in the Clinch during runs 8-11, only several minor anomalies were noted. Anomalies are listed on Table A.19.1. No anomalies were noted in relation to the mapped normal fault. The anomalies noted in 1995 were not confirmed though only one was directly intersected and then, only at the end of run 11.

Table A.14.1. Summary of field data for March 4, 1996.

				TEMPERATURE (°C)			SC (uS/cm)				ANOMALIES			
RUN	DIRXN	TIME	RECORDS	MIN	MAX	MEAN	MIN	MAX	MEAN	DEPTH (M)	Class I	Class II	Class III	Class IV
1	US	10:17-10:30	543	7.97	8.06	8.01	247	250	248.2	3.05-4.57				
2	US	10:39-10:46	294	8.06	8.14	8.09	248	250	248.8	3.66-4.88				
3	US	11:41-11:50	445	7.73	8.04	7.87	229	239	234.5	2.13-3.35				
4	DS	11:50-12:14	395	7.69	8.22	7.87	229	244	233.6	1.22-3.05				
5	US	12:15-12:28	660	7.63	8.29	7.79	227	244	231.8	1.22-3.35				
6	DS	12:30-12:36	250	7.63	7.83	7.72	226	230	227.9	1.83-2.44				
7	US	12:37-12:47	493	7.66	7.84	7.74	224	230	226.5	1.83-3.05				
8	US	13:10-13:34	859	8.47	8.55	8.51	247	250	248	5.18-8.53				
9	US	13:47-14:05	283	8.53	8.60	8.56	247	250	248.7	3.35-9.45				
10	US	14:20-14:45	1053	8.52	8.61	8.55	247	250	248.8	6.71-9.75				1
11	US	15:06-15:27	885	8.53	8.66	8.59	236	250	246.5	7.01-10.06				1

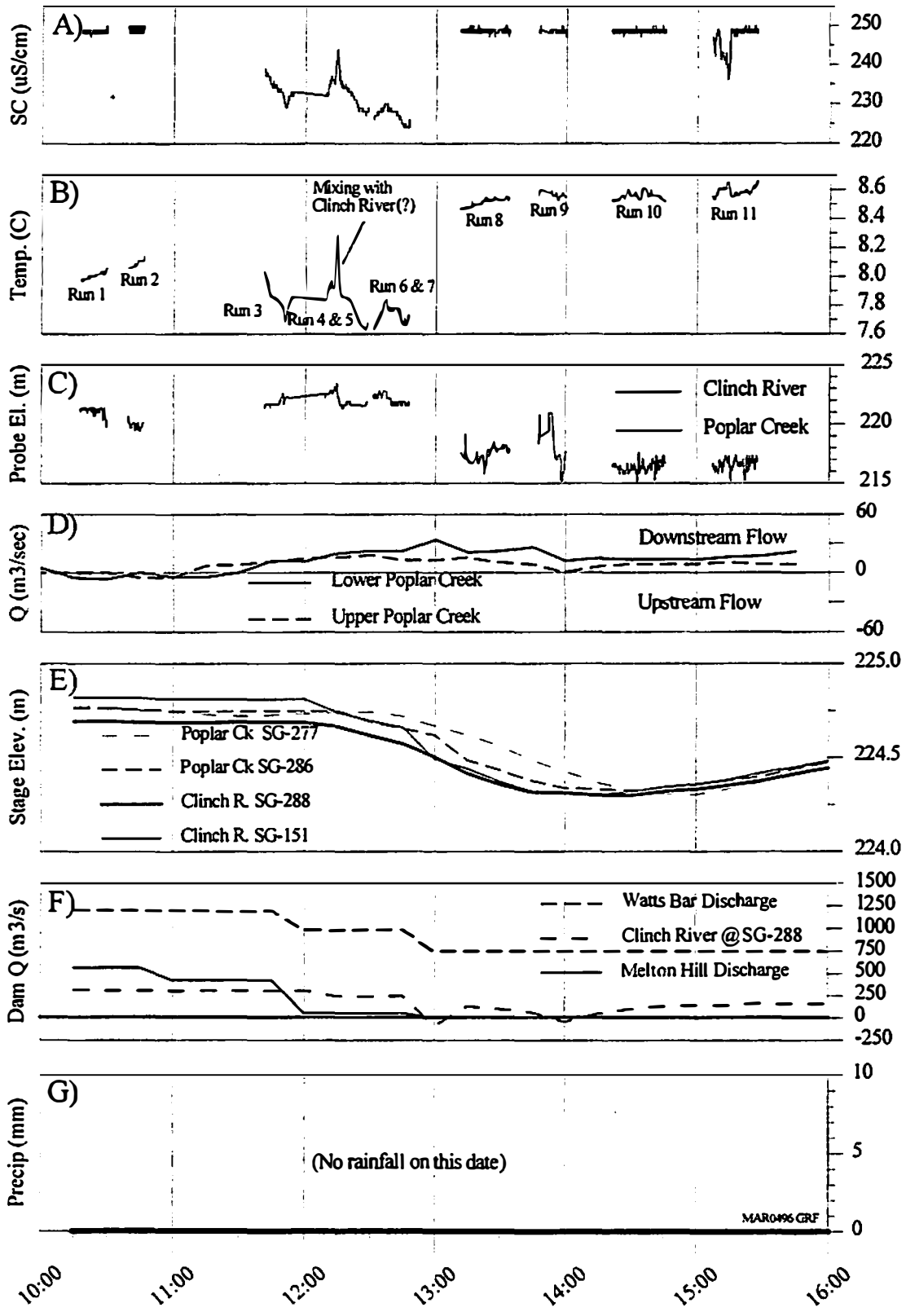


Figure A.14.1. Survey data and ambient hydrologic conditions, March 4, 1996.

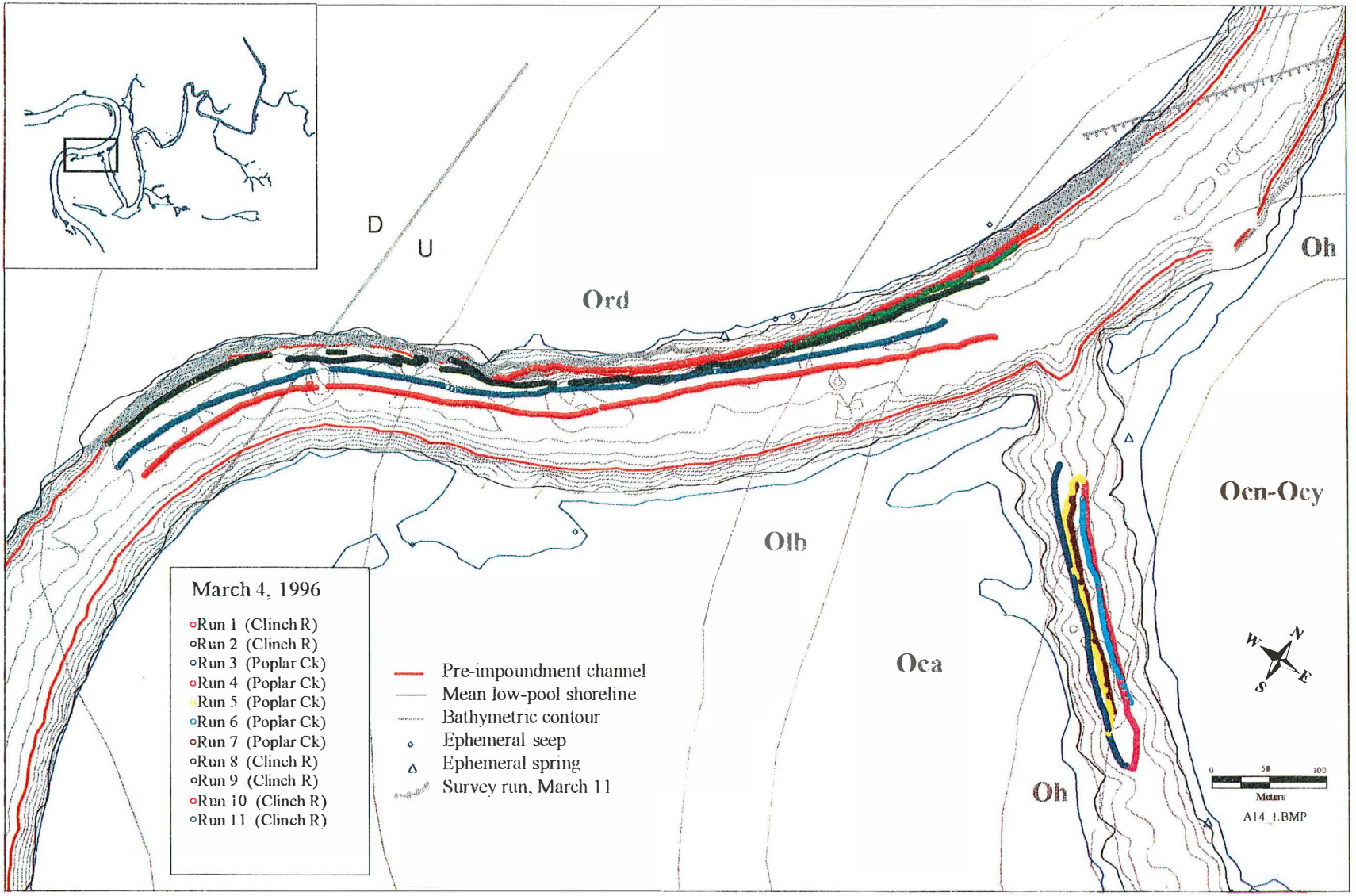


Figure A.14.2. Survey location map, March 4, 1996

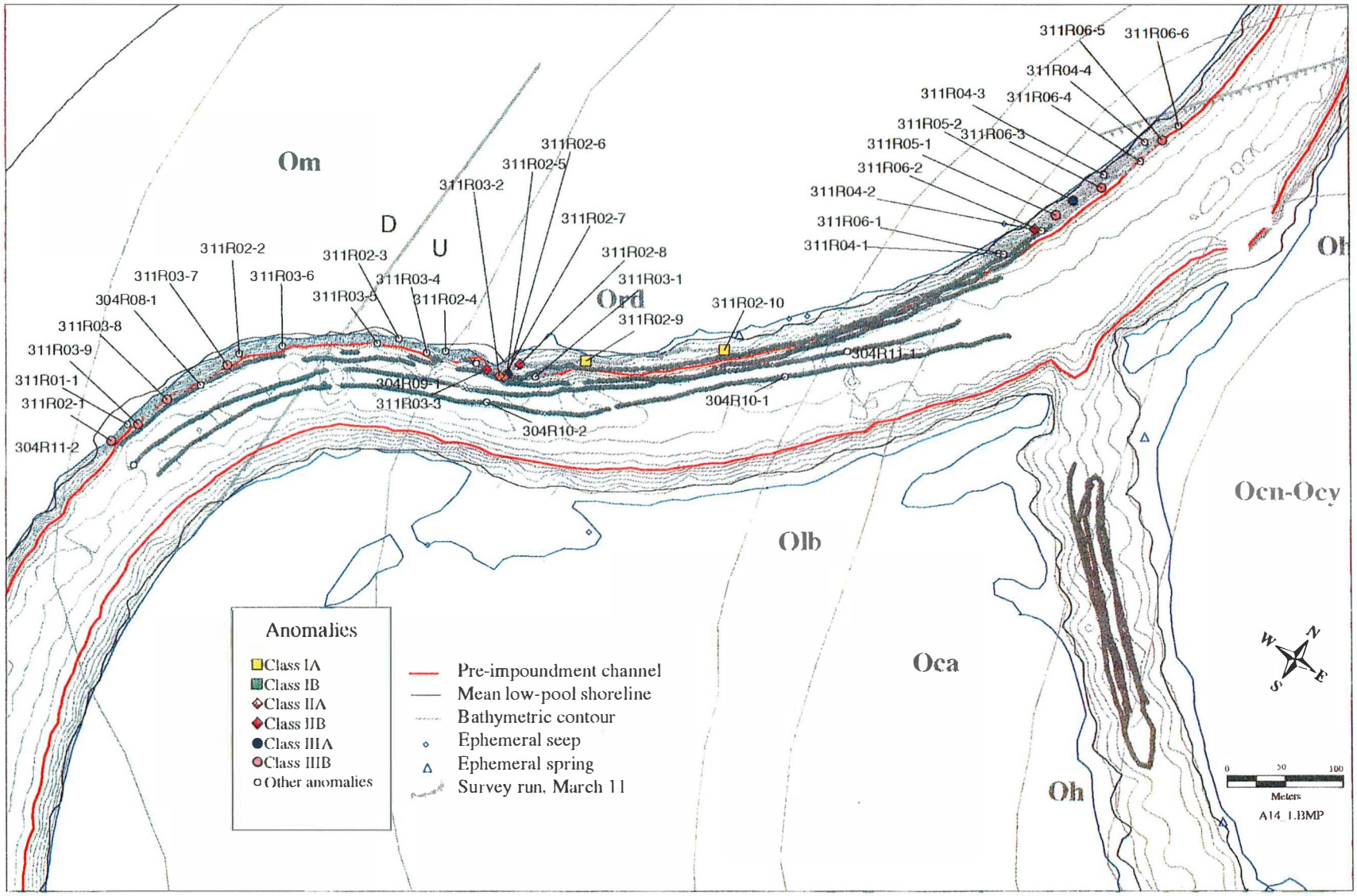


Figure A.14.3. Anomaly location map, March 4, 1996 .

APPENDIX A.15

DATE: **March 11, 1996**

SURVEY AREA: Clinch River near the mouth of Poplar Creek. Runs 1-3 were performed upstream of the confluence with Poplar Creek extending from the Pond Springs-Murfreesboro contact, crossing the mapped normal fault to terminate in the Ridley Ls. Runs 4-6 were performed on the point bar on the inside of the meander bend from the Carters-Lebanon contact into the middle Carters Ls. However, bedrock does not outcrop in this area. Both areas covered were in relatively shallow water above or along the pre-impoundment channel edge on the southwest (far) shore of the river. A number of [highly transient] ephemeral springs and seeps have been identified along the clayey river bank in this area.

DESCRIPTION: A total of 6 runs were performed in this area. Overlaps coverage of March 4, 1996. Additionally, overlaps with March 1995 survey coverage.

HYDROLOGIC CONDITIONS: Hydrologic conditions prevailing during the field data acquisition period are summarized graphically on Figure A.15.1. Throughout the survey period, Melton Hill discharge was zero. Flow rates in the Clinch River in the study area were consistently downstream but low, ranging from 110 to 190 m^3/sec. Stage height varied 0.1 m over the survey period, reaching a maximum during run 3.

There was no rainfall during the survey period. Antecedent rainfall conditions were as follows:

within last 24 hours:	0 mm
within past 4 days:	0 mm
within past 7 days:	220.46 mm

DATA: Data are summarized graphically on Figure A.15.1. Summary statistics on a run-by run basis are provided in Table A.15.1. Runs are shown on Figure A.15.2.

ANOMALIES: No distinct anomalies indicative of springs were noted in the field. Review of the data suggest 32 temperature and SC anomalies associated with runs 1 through 6. Anomalies are shown on Figure A.15.3, along with anomalies identified on other days with overlapping survey coverage. Anomalies are summarized in Table A.19.1 and A.19.2. Two of the largest (Class IA) anomalies

identified, 311R02-9 and 311R02-10, showed temperature changes of 0.53 and 0.77 °C with SC changes of 22 and 12 uS/cm, respectively. Both of these are discrete anomalies that occur in water depths of less than 2 m on the shallow shoulder near the pre-impoundment channel edge in the middle of the Ridley formation. Other key (Class IIA) anomalies include 311R02-5, 311R02-7, and 311R03-2, located on or near the mapped contact of the Ridley and Murfreesboro Limestones. Other lesser anomalies (including one from March 4, 1996) cluster on or around these, corroborating an overall groundwater discharge "zone. However, anomalies of this magnitude were not identified at these exact locations on overlapping survey runs from other days performed under different hydrologic conditions. Given ambient flow conditions, a calculated discharge rate of 3-5 m^3/sec is suggested. No anomalies were identified associated with the mapped normal fault in the Murfreesboro.

Table A.15.1. Summary of field data for March 11, 1996.

				TEMPERATURE (°C)			SC (uS/cm)				ANOMALIES			
RUN	DIRXN	TIME	RECORDS	MIN	MAX	MEAN	MIN	MAX	MEAN	DEPTH (M)	Class I	Class II	Class III	Class IV
1	DS	12:46-12:53	271	7.76	7.84	7.80	241	243	241.8	1.83-3.35				1
2	DS	13:44-14:36	1531	7.12	8.22	7.73	206	243	231.1	0.91-7.01	2	3	2	3
3	US	14:54-15:30	1181	7.10	7.81	7.42	208	238	233.1	2.13-7.92		2	3	4
4	DS	15:51-16:06	397	7.07	7.97	7.61	213	231	221.1	1.22-3.96		2		3
5	DS	16:13-16:23	445	7.60	7.88	7.76	222	225	222.6	1.83-3.35			2	
6	DS	16:27-16:41	448	7.73	8.09	7.91	219	226	223.2	3.05-6.10			2	4

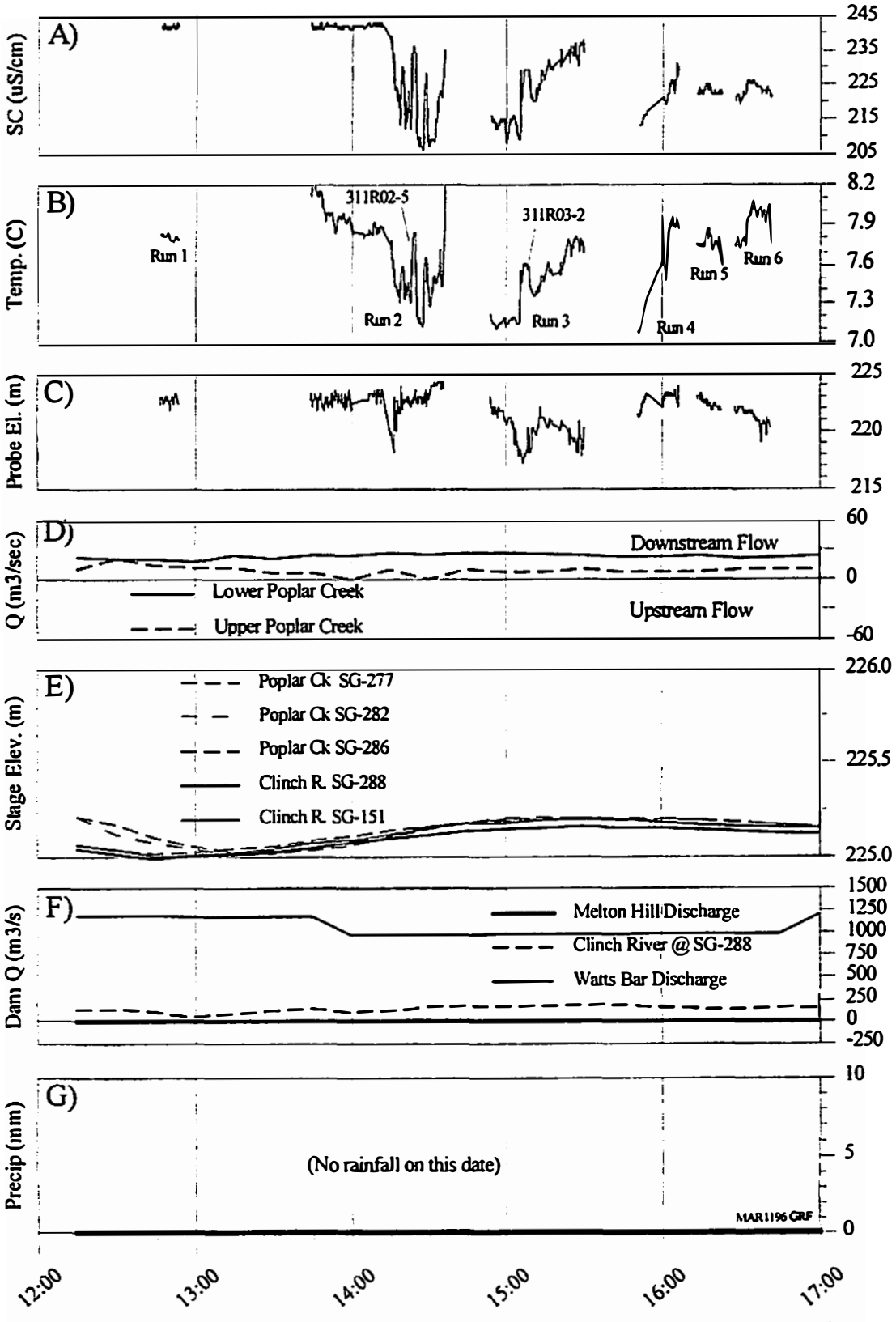


Figure A.15.1. Survey data and ambient hydrologic conditions, March 11, 1996.

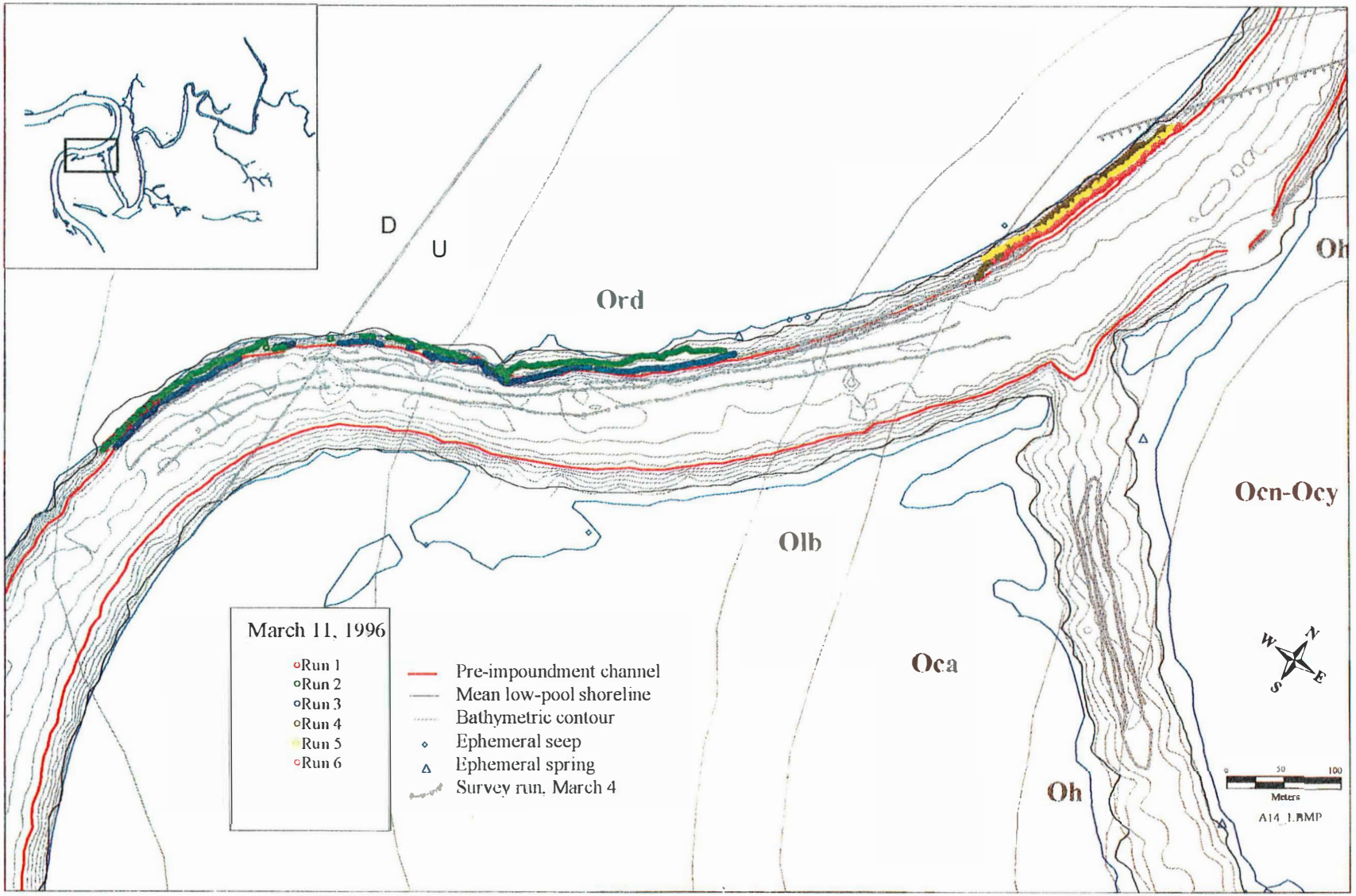


Figure A.15.2. Survey location map, March 11, 1996.

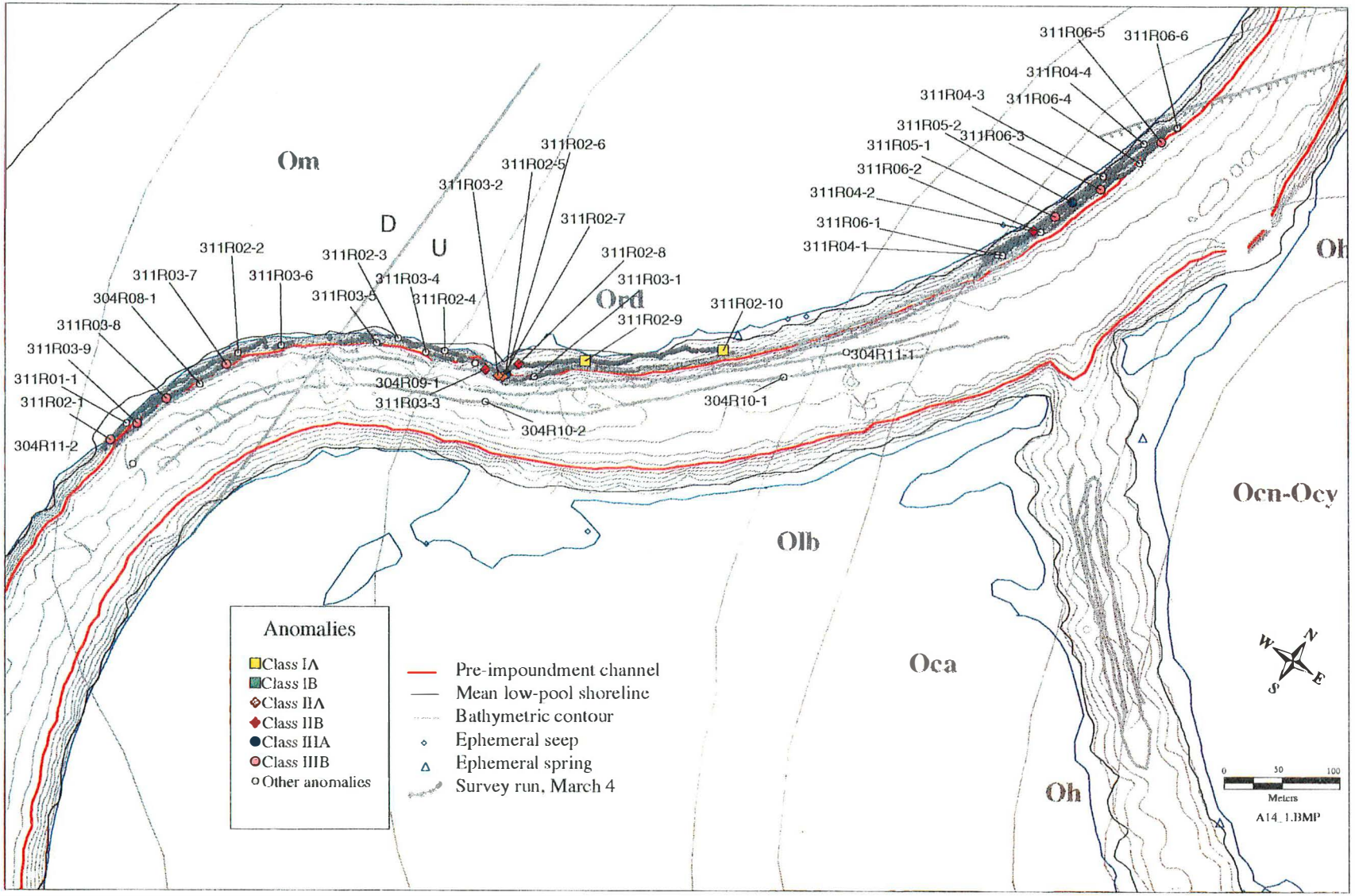


Figure A.15.3. Anomaly location map, March 11, 1996.

APPENDIX A.16

DATE: **March 12, 1996**

SURVEY AREA: Clinch River extending from the K-901 Pond outfall downstream approximately 1.1 km. Survey area covers the Chickamauga-Knox contact and extends across the Knox group Mascot and Kingsport Dolomites. Bedrock is exposed along the entire river bank and forms the bottom of the river in this area. Near the Kingsport-Mascot contact, the river turns to flow subparallel to geologic strike such that the bedrock dips towards the river; numerous solutionally enlarged bedding plane perpendicular fractures were observed along the entire outcrop.

DESCRIPTION: Performed 8 runs; upstream backflow conditions were noted during initial run while null flow noted during Run 8. All runs were performed in relatively shallow water along the pre-impoundment channel edge or on the shallow shoulder above it. Specific attention was paid to the lower Pond Springs and upper Mascot where other anomalies were noted on other overlapping surveys. March 12 survey runs overlap with survey runs conducted on 1/25/96 and 2/29/96 at the upstream end and with survey runs conducted on 3/13/96 on the downstream end. The survey area was also covered by surveys performed in March of 1995 as well.

HYDROLOGIC CONDITIONS: Hydrologic conditions prevailing during the field data acquisition period are summarized graphically on Figure A.16.1. Optimal survey conditions prevailed with no Melton Hill discharge throughout the field period and Clinch River flow rates in the survey area ranging from a low of 87 to 180 m^3/sec, though typically less than 150 m^3/sec. Flow rates were lowest during runs 1 and 2. Overall, the stage changed ~ 0.1 m over the field period, being highest during run 6 and lowest during runs 1 and 2.

No rainfall occurred during field survey period. Antecedent rainfall conditions were as follows:

within last 24 hours:	0 mm
within past 4 days:	0 mm
within past 7 days:	193.03 mm

DATA: Data are summarized graphically on Figure A.16.1. Summary statistics on a run-by run basis are provided in Table A.16.1. Runs are shown on Figure A.16.2. Temperature and SC anomalies are

shown on Figure A.16.3.

ANOMALIES: A trend of warmer water was noted along shore during run 7 in the field. Analysis of the data anomalies revealed a total of 42 anomalies; anomalies were encountered in all runs. Anomalies area summarized in Table A.19.1 and A.19.2. Although several temperature anomalies as high as 0.41 °C were identified, there was typically little or no associated SC change. However, in many cases, anomalies on one run occur in close associated with those on previous or subsequent runs, providing corroboration of a potential groundwater discharge site. The largest anomalies were encountered in shallow water above or along the pre-impoundment channel in water less than 2 m deep.

Table A.16.1. Summary of field data for March 12, 1996.

				TEMPERATURE (°C)			SC (uS/cm)				ANOMALIES			
RUN	DIRXN	TIME	RECORDS	MIN	MAX	MEAN	MIN	MAX	MEAN	DEPTH (m)	Class I	Class II	Class III	Class IV
1	DS	12:12-12:52	982	7.53	7.73	7.63	227	230	228.9	0.91-4.57			3	4
2	DS	13:03-13:32	858	7.50	7.83	7.59	229	234	230.0	2.44-5.79		1	1	1
3	US	13:52-14:08	599	7.56	7.96	7.72	230	232	230.6	5.49-9.14			1	2
4	US	14:16-14:29	436	7.51	7.91	7.69	231	233	231.2	7.01-10.36				2
5	DS	14:42-15:02	506	7.53	7.92	7.71	231	233	231.2	1.22-5.18				4
6	US	15:11-15:30	566	7.56	7.96	7.64	231	232	231.2	3.35-7.01				1
7	DS	15:47-16:28	1155	7.76	8.37	7.95	229	233	231.2	0.91-3.66		7	2	2
8	DS	16:37-17:24	1289	7.68	8.56	8.02	227	234	231.6	1.22-4.88		7	1	1

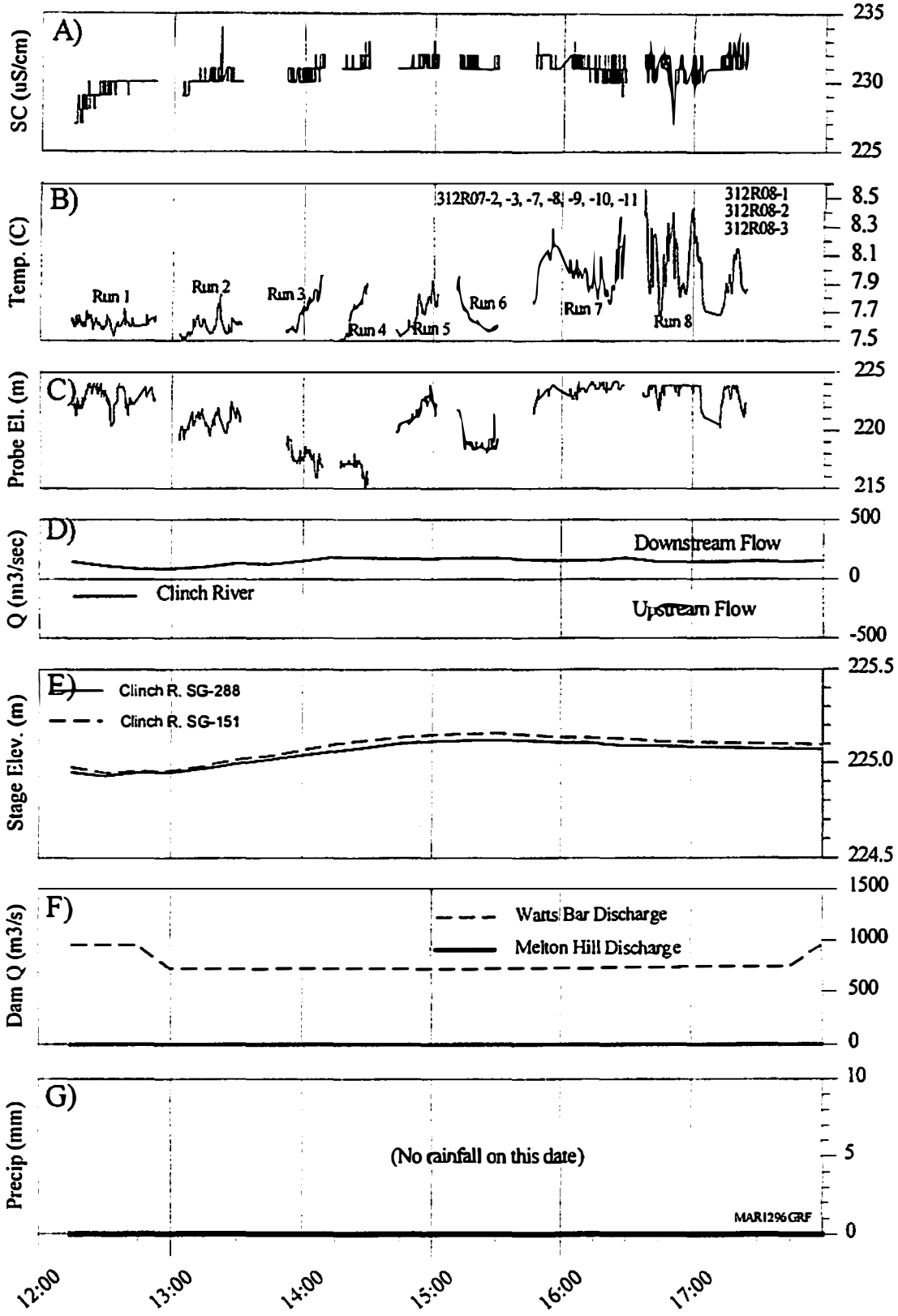


Figure A.16.1. Survey data and ambient hydrologic conditions, March 12, 1996.

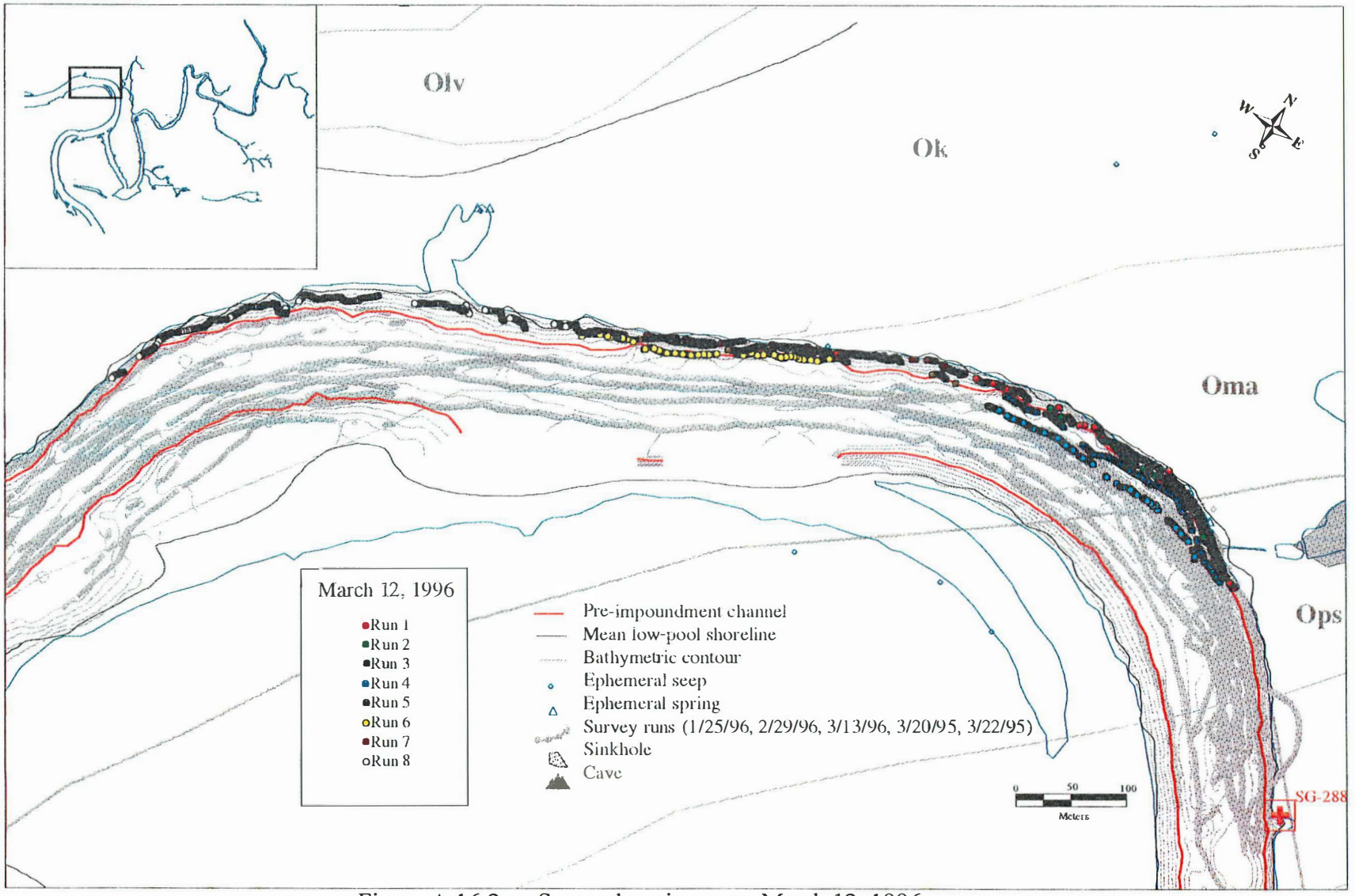


Figure A.16.2. Survey location map, March 12, 1996.

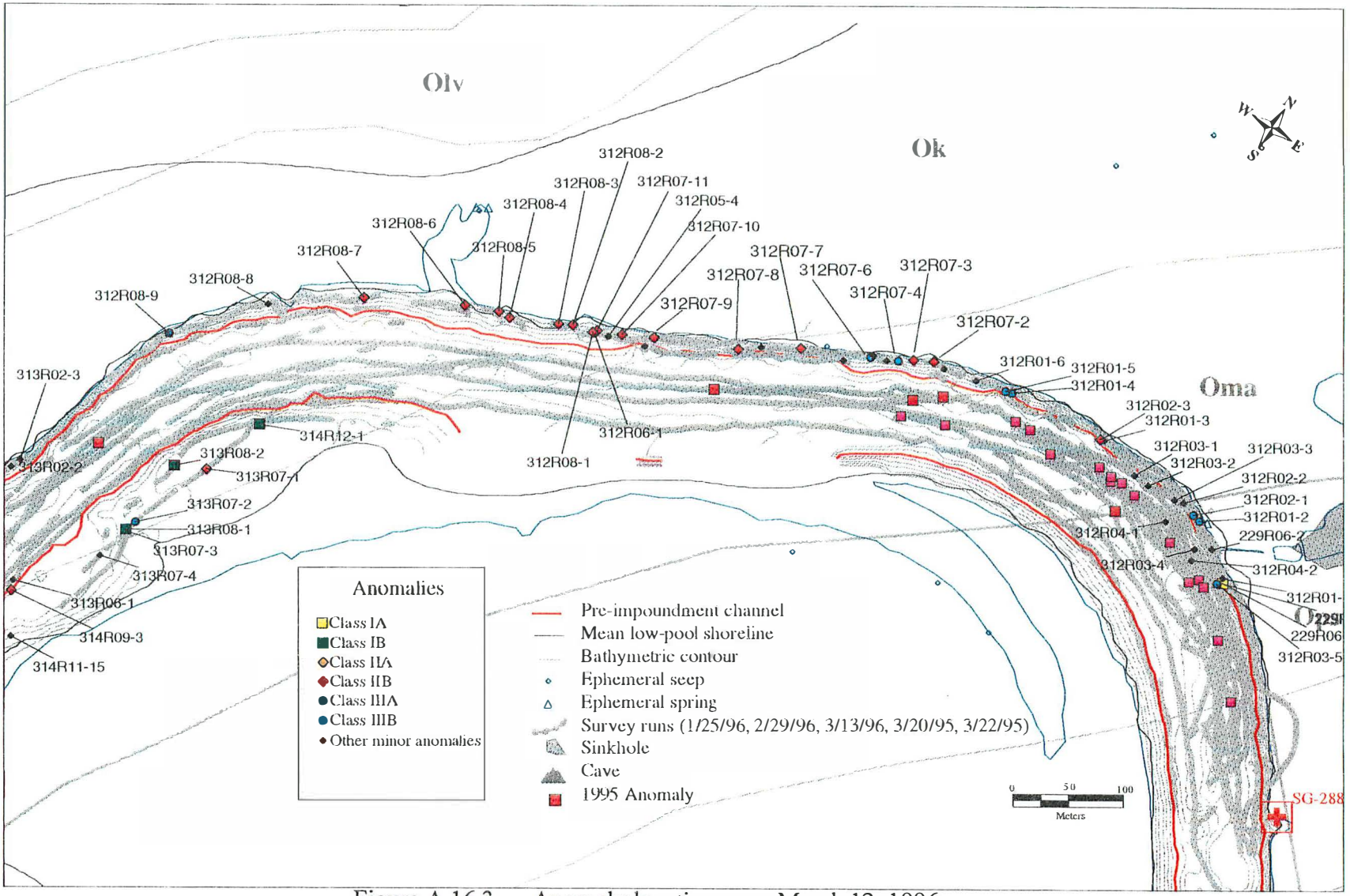


Figure A.16.3. Anomaly location map, March 12, 1996.

APPENDIX A.17

DATE: **March 13, 1996**

SURVEY AREA: Clinch River approximately 1 km below the K-901 Pond outfall adjacent to large sand bar. Surveys performed in reach where Knox Group (Kingsport Fm) bedrock exposed along banks and river bottom. River course and thus runs roughly parallel geologic strike, with bedrock dipping in towards the river. Solutionally enlarged bedding-plane perpendicular fractures observed all along bedrock outcrop on north shore.

DESCRIPTION: A total of 8 runs were performed in this area. Survey runs overlap with runs from 3/12/96 and 3/14/96, as well as survey runs conducted in March of 1995.

HYDROLOGIC CONDITIONS: Hydrologic conditions prevailing during the field data acquisition period are summarized graphically on Figure A.17.1. Favorable flow conditions prevailed during this survey period, with zero Melton Hill discharge and Clinch River flow rates typically below 170 m^3/sec. The lowest flow rates (< 100 m^3/sec) occurred during runs 1 and 2.

Antecedent rainfall conditions were as follows:

within last 24 hours:	0 mm
within past 4 days:	0 mm
within past 7 days:	105.66 mm

DATA: Data are summarized graphically on Figure A.17.1. Summary statistics on a run-by run basis are provided in Table A.17.1. Runs are shown on Figure A.17.2. Temperature and SC anomalies are shown on Figure A.17.3.

ANOMALIES: Anomalies indicative of springs were not noted in the field. Subsequent review of the data indicate a total of 10 anomalies, largely restricted to runs 2, 6, 7, and 8. Anomalies are summarized in Tables A.19.1 and A.19.2. The highest temperature anomalies were noted in runs 7 (313R07-1) and 8 (313R08-2 and -3) where observed temperature differentials were 0.38, 0.47 and 0.58 °C, respectively. There was virtually no SC change associated with these anomalies which were all observed in water depths < 1 m on the shallow shoulder above the channel edge along the southwest (far) shore. Anomalies 313R08-1 and 313R07-3 occur in virtually the exact location, thus corroborating potential groundwater

discharge at this site. 313R06-1 is a minor anomaly that roughly coincides with a larger Class IIB anomaly identified on March 14, 1996 (314R09-3).

Table A.17.1. Summary of field data for March 13, 1996.

				TEMPERATURE (°C)			SC (uS/cm)				ANOMALIES			
RUN	DIRXN	TIME	RECORDS	MIN	MAX	MEAN	MIN	MAX	MEAN	DEPTH (M)	Class I	Class II	Class III	Class IV
1	DS	12:35-12:52	708	8.15	8.19	8.16	226	233	229.7	4.57-6.71				
2	US	13:03-13:33	974	8.24	8.43	8.28	228	230	229.2	1.22-7.32				3
3	DS	13:42-13:58	547	8.19	8.22	8.19	223	236	229.7	6.71-7.62				
4	US	14:05-14:17	314	8.27	8.43	8.30	229	235	229.9	7.01-9.14				
5	US	14:26-14:27	15	8.25	8.27	8.27	230	230	230.0	6.71				
6	US	14:44-14:56	442	8.30	8.48	8.38	229	231	229.6	5.18-7.01				1
7	DS	15:31-15:43	348	8.32	8.93	8.55	229	232	230.3	1.22-5.79		1	1	2
8	US	15:53-16:04	347	8.43	9.24	8.72	230	232	230.9	1.22-4.57	2			

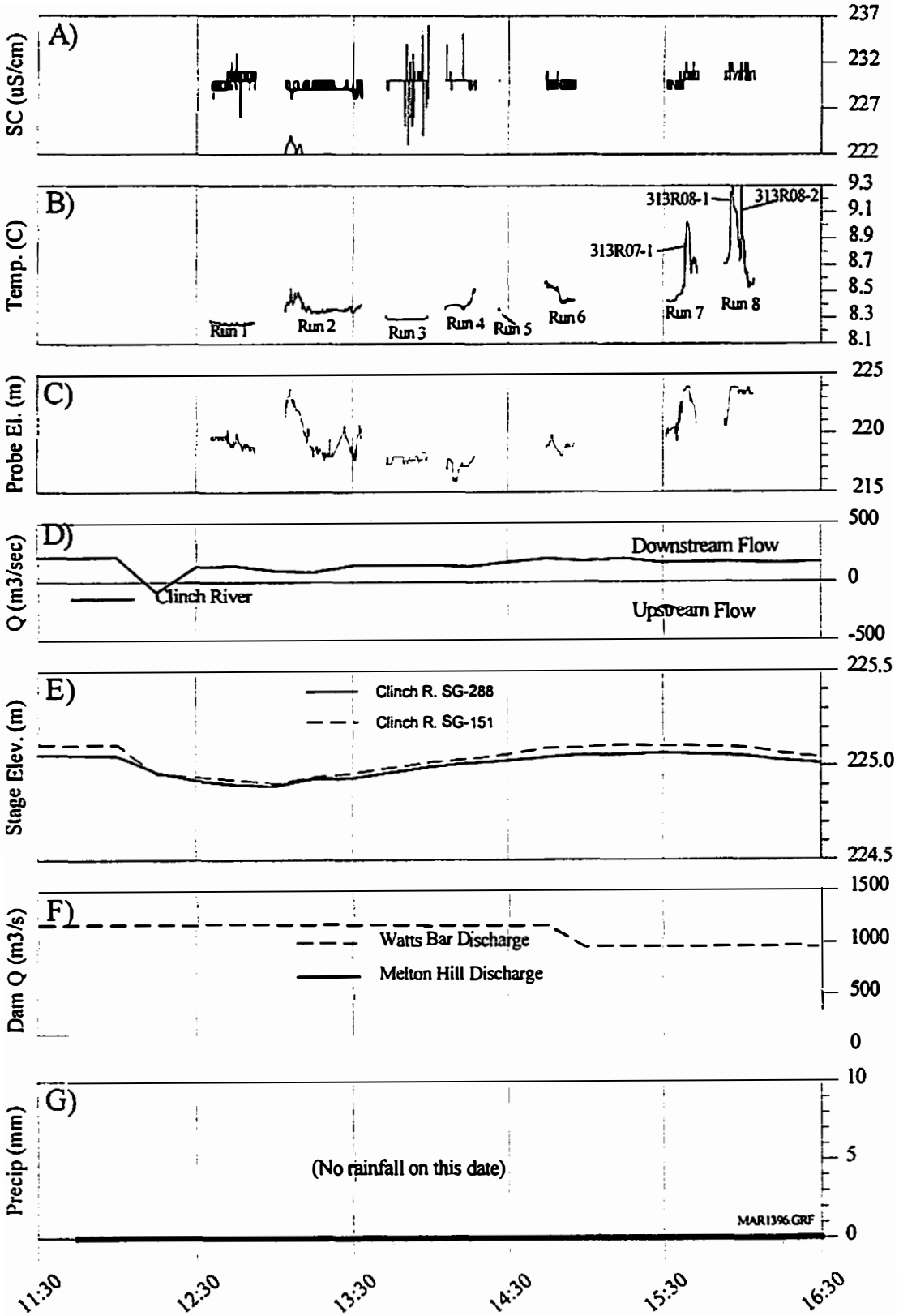


Figure A.17.1. Survey data and ambient hydrologic conditions, March 13, 1996.

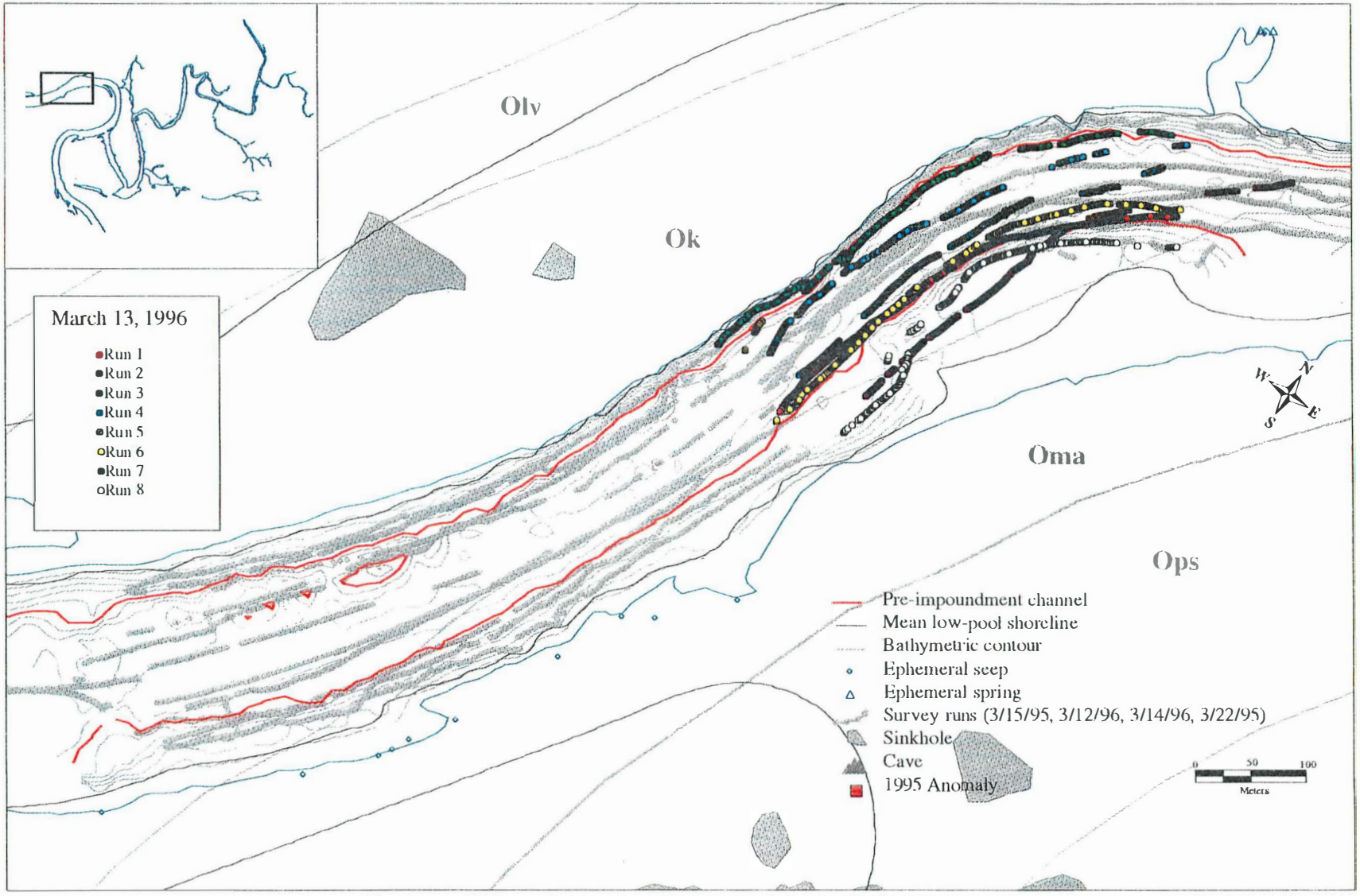


Figure A.17.2. Survey location map, March 13, 1996.

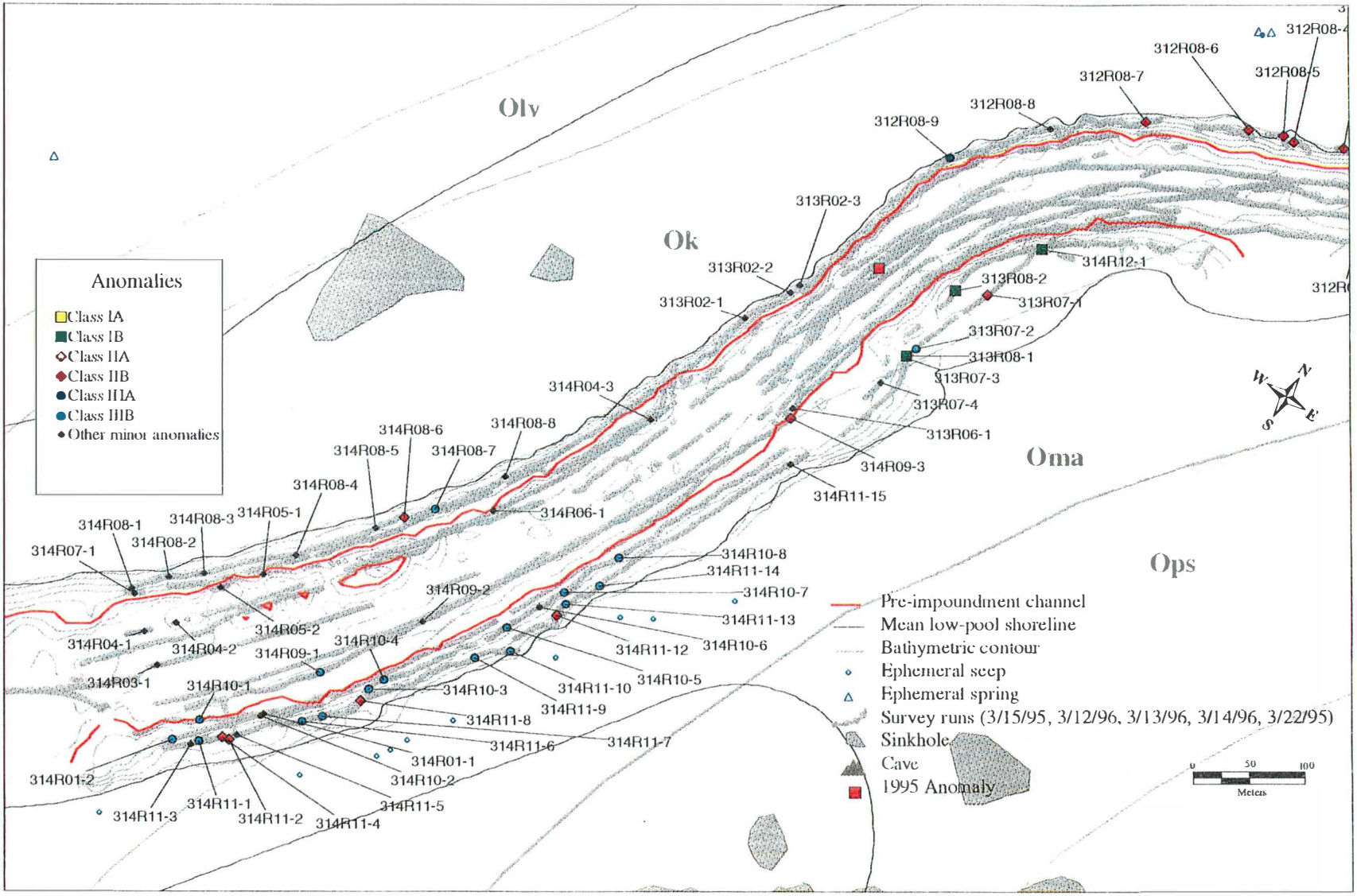


Figure A.17.3. Anomaly location map, March 13, 1996.

APPENDIX A.18

DATE: **March 14, 1996**

SURVEY AREA: Clinch River just upstream Brashears Creek at downstream-most reach of study area. Knox Group bedrock (Kingsport and Mascot Dolomite) exposed along the river bank and bottom. The contact between the two lies along or within the channel such that the Kingsport is exposed in outcrop along the north shore. The Mascot is masked with sediment along the south shore and is note exposed at the surface. Geologic strike is roughly coincident with the course of the river so that runs are subparallel to strike and dip is towards the river in this reach.

DESCRIPTION: A total of 12 runs were performed in this area, focusing on channel edge and shallower shoulder above the channel. The survey area overlaps with that of 3/12/96 and 3/13/96 at the upstream-most end. This reach was not addressed in the March 1995 surveys.

HYDROLOGIC CONDITIONS: Hydrologic conditions prevailing during the field data acquisition period are summarized graphically on Figure A.18.1. Melton Hill was in the process of shutting down generation discharge at the start of the field effort and remained at zero after run 1. However, given the lag between the dam discharge and the downstream river discharge response, the flow rates were extremely high (~335 m^3/sec) during run 1, dropping to 77 m^3/sec during run 3, and 19 m^3/sec during run 4. Upstream backflow conditions (-98 m^3/sec) prevailed during run 5 after which downstream flow rates increased to around 150-70 m^3/sec. Melton Hill began discharging again during run 10 and flows increased thereafter in response. Stage fluctuated nearly 0.25 m over the course of the field day, being lowest during runs 3 and 4 and highest during run 8.

There was no rainfall during the field period and none within the previous 7 days.

DATA: Data are summarized graphically on Figure A.18.1. Summary statistics on a run-by run basis are provided in Table A.18.1. Runs are shown on Figure A.18.2. Temperature and SC anomalies are highlighted on Figure A.18.3.

ANOMALIES: Anomalies of 0.28-0.52 °C were noted in the field during runs 8-12. Subsequent review of the data revealed a total of 44 anomalies

in all runs except run 2. Anomalies are summarized in Tables A.19.1 and A.19.2. Most are minor anomalies with slight, though discernible temperature or SC change. The largest anomalies were noted during runs 10 and 11 along the southwest shore along the Mascot-Kingsport contact in relatively shallow water above the channel edge. This is also an area where a number of ephemeral seeps and springs have been identified along the shoreline, suggesting this is an area of concentrated though diffuse groundwater discharge. Those anomalies encountered along the north shore are located either right along the channel edge or on the shallow shoulder in water depths <3 m. Anomaly 314R09-3 occurs coincident with an anomaly identified on march 13, 1996 (313R06-1). Similarly, anomalies noted on run 7 (314R07-1) and run 8 (314R08-1) appear to roughly coincide, indicating a corroborated point of groundwater discharge under these conditions.

Table A.18.1. Summary of field data for March 14, 1996.

				TEMPERATURE (°C)			SC (uS/cm)				ANOMALIES			
RUN	DIRXN	TIME	RECORDS	MIN	MAX	MEAN	MIN	MAX	MEAN	DEPTH (m)	Class I	Class II	Class III	Class IV
1	DS	11:41-11:55	537	8.01	8.24	8.08	215	224	218.2	3.35-5.79			1	1
2	DS	12:05-12:23	530	7.89	7.97	7.93	211	224	217.3	6.10-7.62				
3	DS	13:04-13:17	338	7.89	7.97	7.94	207	224	215.8	6.40-7.92				
4	US	13:22-13:36	430	7.97	8.07	8.02	210	223	216.5	6.10-8.23				3
5	DS	13:41-14:06	936	7.97	8.09	8.04	210	224	216.6	6.40-8.53				
6	US	14:21-14:43	551	8.04	8.12	8.08	212	222	217.1	4.27-7.32				
7	DS	14:48-15:20	1227	8.06	8.22	8.10	212	223	217.6	2.74-7.01				
8	US	15:26-15:52	1094	8.09	8.61	8.23	214	222	217.6	1.22-4.88		1	1	6
9	DS	16:06-16:32	1031	8.19	8.56	8.32	216	221	217.9	3.96-7.32		1	1	1
10	US	16:43-17:12	1179	8.38	8.66	8.53	216	222	218.6	3.66-5.49			6	1
11	DS	17:23-17:53	1007	8.70	9.07	8.86	217	221	219.4	0.91-2.44		3	7	3
12	US	18:07-18:14	174	8.32	8.84	8.44	215	219	216.5	0.91-2.44	1			

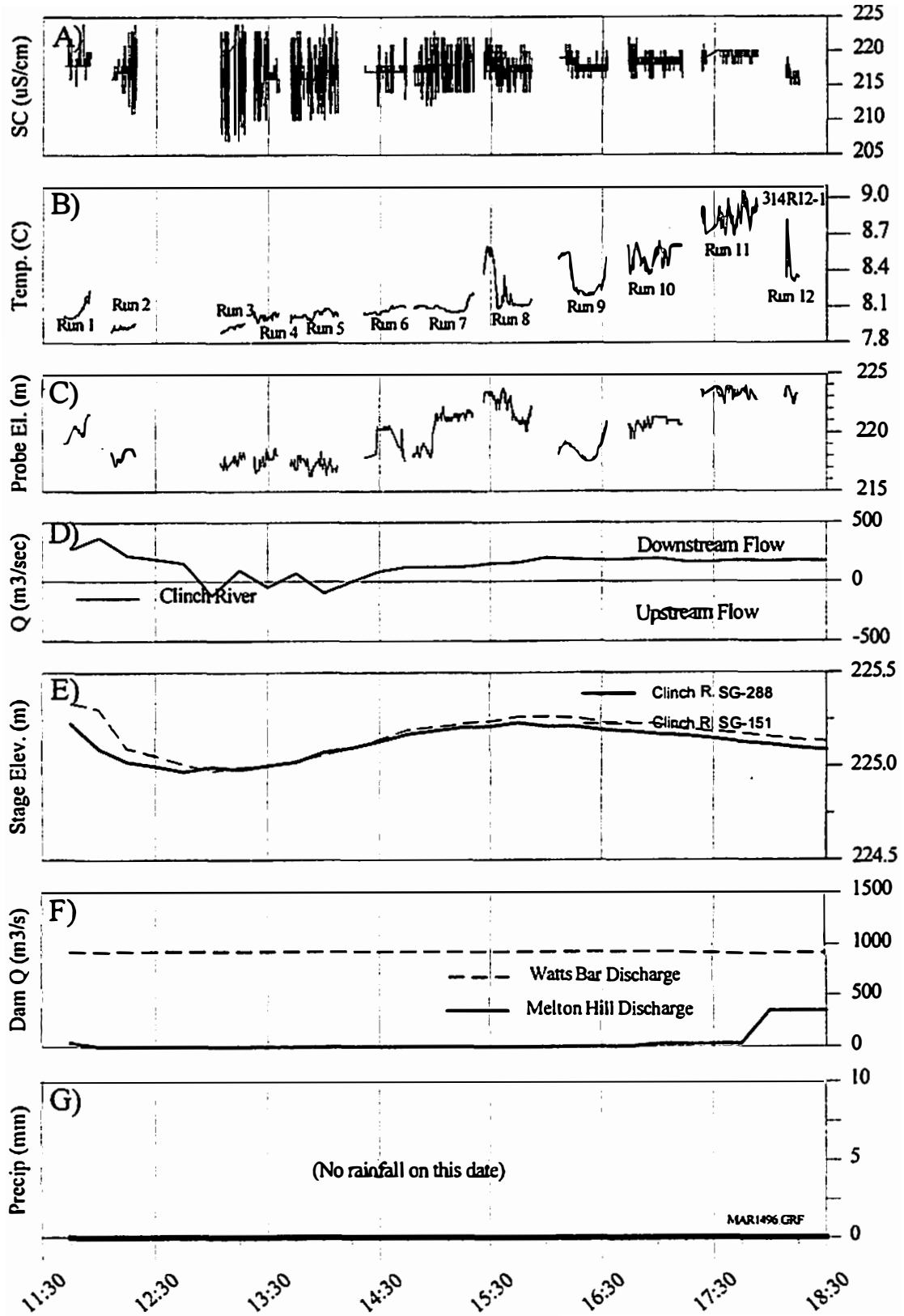


Figure A.18.1. Survey data and ambient hydrologic conditions, March 14, 1996.

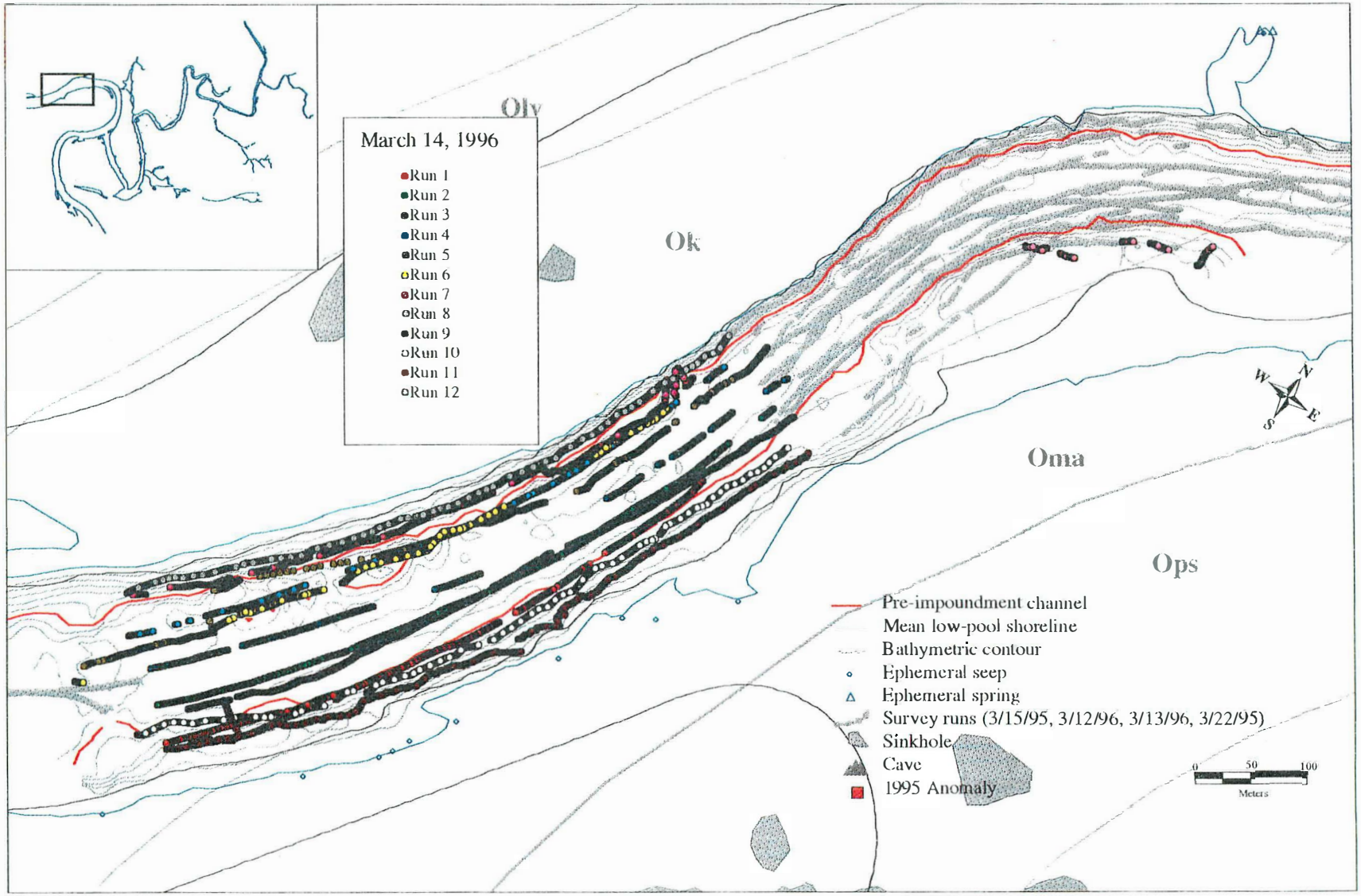


Figure A.18.2. Survey location map, March 14, 1996.

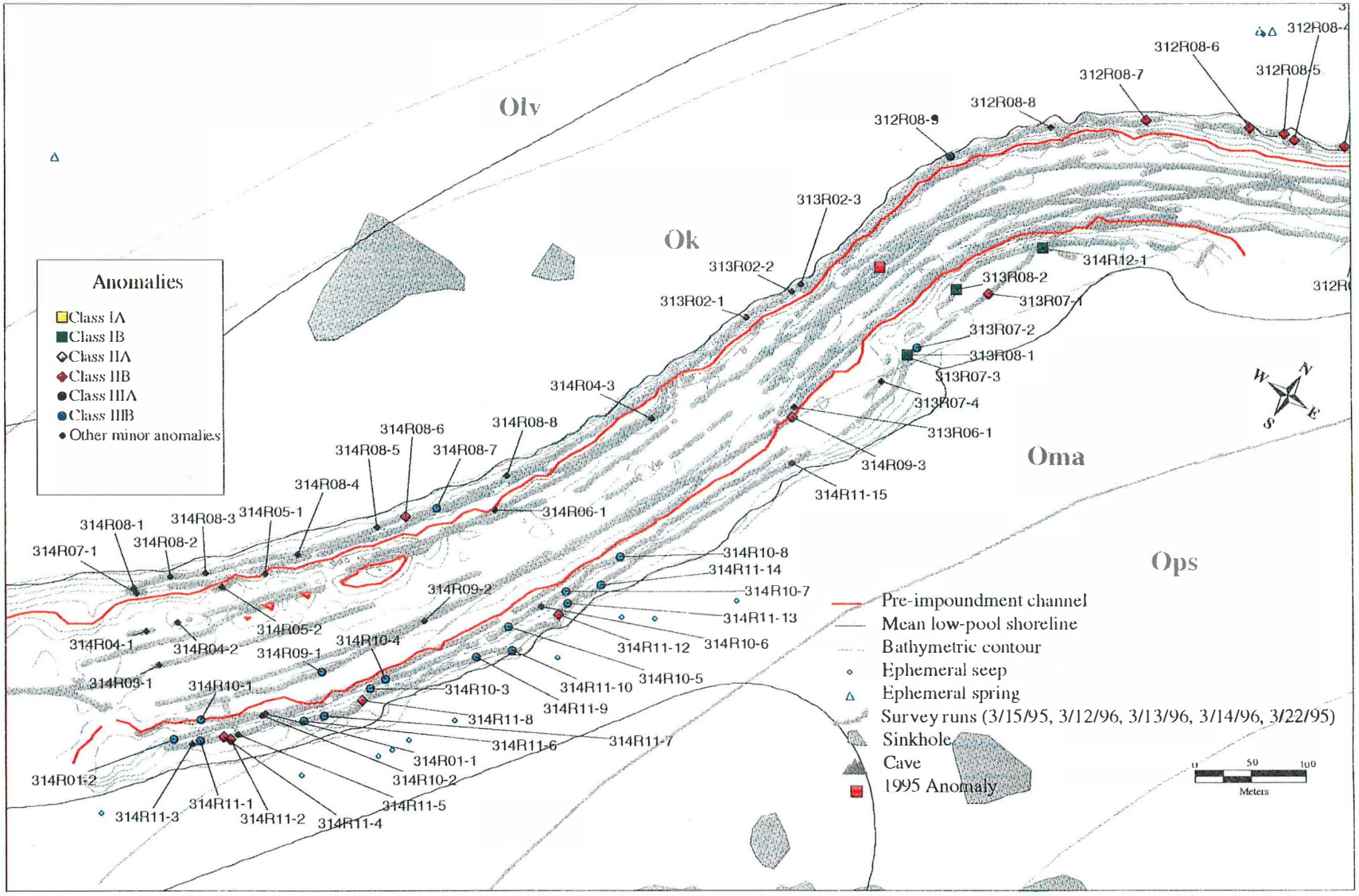


Figure A.18.3. Anomaly location map, March 14, 1996.

APPENDIX A.19

Anomaly Summary Tables

Table A19.1 Anomaly summary information, sorted by class

			Peak Location		Temperature (C)				Specific Conductance (uS/cm)				
Anomaly	Water Body	Class	X	Y	To	Tmax	Tt	dT	SCo	SCmax	SCt	dSC	Depth (m)
215R04-1	PC	IIIB	13912.1422	41756.9080	7.99	8.09	7.99	0.10	188	189	187	2	1.37
219R02-1	PC	V	13820.6102	41821.4240	5.78	5.82	5.78	0.04	211	211	211	0	2.83
219R04-1	PC	IVB	13767.7217	41815.0699	5.78	5.83	5.78	0.05	211	212	211	1	4.24
219R05-1	PC	V	13892.7819	42007.5260	5.82	5.83	5.82	0.01	210	212	212	2	3.51
220R07-1	PC	IA	18262.0554	40780.3242	8.47	9.06	8.42	0.64	219	226	188	38	2.41
220R08-1	PC	IIA	18051.9995	40249.9924	8.45	8.60	8.45	0.15	187	196	188	9	1.46
220R08-2	PC	IVA	17952.5334	39009.8564	8.58	8.63	8.58	0.05	193	196	192	4	1.40
220R10-1	PC	IVB	17929.5260	38754.8139	8.96	9.01	8.96	0.05	205	206	204	2	1.89
220R10-2	PC	IVA	17931.4019	38752.1236	8.97	9.04	8.97	0.07	207	207	204	3	2.01
221R01-1	PC	IVB	9899.6141	38331.3885	8.76	8.81	8.76	0.05	192	193	192	1	1.86
221R02-1	PC	IVB	9891.4312	38335.1586	8.83	8.86	8.81	0.05	192	192	192	0	3.35
221R07-1	PC	IVB	10390.5718	38678.5812	9.17	9.24	9.19	0.07	190	191	191	1	4.72
222R13-1	PC	V	10451.1710	36755.3599	9.94	9.96	9.94	0.02	193	193	192	1	2.56
222R13-2	PC	V	10516.8457	36508.6689	9.94	9.96	9.94	0.02	193	193	193	0	1.46
222R14-1	PC	IVA	10465.2674	36695.5179	9.89	9.94	9.89	0.05	190	193	190	3	2.35
226R01-1	PC	IVB	10633.7831	35732.6940	11.50	11.50	11.43	0.07	204	204	204	0	1.52
226R01-2	PC	V	10621.3675	35473.2557	11.42	11.45	11.42	0.03	204	205	204	1	4.05
226R02-1	PC	IIB	10652.4603	35634.4746	11.17	11.32	11.25	0.15	205	205	205	0	2.59
226R02-2	PC	IIIB	10655.1641	35463.4280	11.19	11.29	11.22	0.10	205	205	205	0	2.74
226R02-3	PC	V	10583.6566	34875.0386	11.19	11.22	11.19	0.03	205	205	205	0	2.59
226R03-1	PC	IVB	10660.4879	35569.5150	11.19	11.25	11.19	0.06	205	205	204	1	2.01
226R03-2	PC	IVB	10566.3188	34722.9475	11.17	11.24	11.17	0.07	206	207	206	1	1.71
226R03-3	PC	IVB	10546.1826	34599.8636	11.19	11.24	11.19	0.05	206	207	206	1	1.52
226R03-4	PC	IIIB	10476.7789	34315.1774	11.20	11.32	11.32	0.12	206	208	207	2	1.40
226R04-1	PC	IVB	10431.1829	34181.0342	11.27	11.35	11.27	0.08	206	207	206	1	1.40
226R04-2	PC	IIB	10415.2330	34137.9337	11.17	11.38	11.25	0.21	205	208	206	3	1.40
226R05-1	PC	IVB	10474.5509	34357.3755	11.12	11.19	11.12	0.07	206	206	205	1	1.43
226R05-2	PC	V	10415.1763	34161.3530	11.12	11.16	11.12	0.04	205	205	205	0	1.55
226R06-1	PC	IIIB	10277.9049	33932.4926	11.89	12.01	11.99	0.12	206	207	205	2	3.11

Table A19.1 Continued

Anomaly	Water Body	Class	Peak Location		Temperature (C)				Specific Conductance (uS/cm)				Depth (m)
			X	Y	To	Tmax	Tt	dT	SCo	SCmax	SCt	dSC	
226R07-1	PC	IVB	10325.8730	34061.0555	11.99	12.04	11.99	0.05	206	206	205	1	3.35
226R08-1	PC	IVB	10207.4581	33871.9805	11.98	11.98	11.91	0.07	206	206	206	0	2.99
226R09-1	PC	IVB	10327.6676	34137.7127	11.68	11.73	11.68	0.05	205	206	206	1	2.56
226R09-2	PC	IVB	10192.9215	33871.3603	11.68	11.75	11.75	0.07	205	206	206	1	2.56
226R11-1	PC	IIB	10282.4269	34141.9044	11.80	12.12	11.80	0.32	206	207	206	1	1.52
226R12-1	PC	IIB	10139.6829	33670.6032	11.75	12.08	12.03	0.33	207	207	208	0	2.01
226R12-2	PC	IIB	9957.6134	33400.7150	11.98	12.19	11.99	0.21	208	207	206	1	1.52
227R01-1	PC	IVB	9290.8881	33775.5242	12.45	12.47	12.42	0.05	205	205	205	0	2.80
227R01-2	PC	V	9387.3680	33902.2883	12.40	12.44	12.40	0.04	205	205	204	1	1.68
227R02-1	PC	IVB	9116.7374	33689.3885	12.34	12.42	12.34	0.08	206	206	207	0	1.68
227R03-1	PC	IIB	9388.5507	33828.3367	12.04	12.31	12.17	0.27	207	206	206	0	5.55
227R04-1	PC	IIIB	9395.3486	33790.2131	12.21	12.27	12.17	0.10	206	207	206	1	6.34
227R05-1	PC	IIB	9375.9933	33727.4028	12.14	12.31	12.17	0.17	207	207	207	0	3.02
227R05-2	PC	IVB	9428.1231	33772.0492	12.17	12.22	12.17	0.05	207	207	207	0	3.47
227R06-1	PC	V	9475.0039	33824.2409	12.42	12.44	12.42	0.02	207	207	207	0	1.86
227R07-1	PC	IIB	13394.2562	39172.2279	12.60	12.83	12.65	0.23	208	210	210	2	1.28
227R07-2	PC	IIB	13357.9822	39072.2650	12.65	12.88	12.59	0.29	209	210	209	1	1.28
227R07-3	PC	IIB	13247.3062	38745.2201	12.67	12.93	12.73	0.26	210	211	210	1	1.37
227R07-4	PC	IIB	13247.0760	38757.4943	12.73	12.93	12.82	0.20	210	211	211	1	1.37
227R07-5	PC	IIB	13242.8214	38741.0079	12.87	12.93	12.65	0.28	212	212	211	1	1.34
229R01-1	PC	IVB	13248.1358	38735.4012	12.09	12.14	12.09	0.05	209	211	209	2	0.85
229R02-1	PC	IIIB	13340.6665	39052.1270	11.98	12.08	11.98	0.10	207	208	207	1	1.86
229R03-1	PC	V	13208.2108	38658.1970	11.94	11.98	11.96	0.04	206	207	207	1	1.86
229R03-2	PC	IVB	13264.7592	38841.4934	11.91	11.96	11.94	0.05	207	207	207	0	1.83
229R04-1	PC	IIIB	13085.8000	38404.5880	11.99	12.09	12.01	0.10	207	207	207	0	1.83
229R04-2	PC	IIIB	13010.4679	38279.9259	12.01	12.14	12.14	0.13	207	207	207	0	0.61
229R05-1	PC	IIIB	12900.1983	38180.1596	12.14	12.24	12.14	0.10	207	207	207	0	2.80
229R05-2	PC	IIIB	12883.7269	38175.7789	12.14	12.27	12.16	0.13	207	207	207	0	2.87
229R05-3	PC	IIB	12788.3314	38077.1358	12.11	12.31	12.14	0.20	207	207	207	0	2.19

Table A19.1 Continued

Anomaly	Water Body	Class	Peak Location		Temperature (C)				Specific Conductance (uS/cm)				Depth (m)
			X	Y	To	Tmax	Tt	dT	SCo	SCmax	SCt	dSC	
229R05-4	PC	IIB	12483.2778	37818.9679	12.14	12.37	12.14	0.23	206	208	207	2	0.76
229R05-5	PC	IIB	12244.8500	37705.2795	12.16	12.32	12.14	0.18	207	209	207	2	1.52
229R05-6	PC	IIB	11987.4413	37653.8864	12.24	12.40	12.19	0.21	208	212	207	5	0.64
229R05-7	PC	IIIB	11907.4959	37652.0024	12.19	12.31	12.21	0.12	207	209	207	2	1.22
229R05-8	PC	IIIA	11682.9563	37759.9591	12.22	12.34	12.29	0.12	208	212	210	4	0.94
229R06-1	CR	IVB	8968.5035	40254.6695	9.06	9.06	8.99	0.07	262	262	260	2	2.47
229R06-2	CR	V	8938.8393	40353.5649	9.01	9.01	8.99	0.02	260	260	260	0	2.23
229R07-1	CR	IA	8970.4208	40253.8024	8.99	9.42	9.04	0.43	259	274	260	15	1.43
304R09-1	CR	V	6267.2215	37494.2327	8.58	8.60	8.58	0.02	248	250	249	2	4.94
304R10-1	CR	V	7196.8607	37455.6619	8.56	8.60	8.56	0.04	249	249	249	0	7.68
304R10-2	CR	IVB	6297.1929	37379.4818	8.56	8.61	8.56	0.05	249	249	248	1	7.77
304R11-1	CR	V	7383.6660	37529.8461	8.56	8.60	8.58	0.04	249	249	249	0	7.53
304R11-2	CR	IVB	5239.1887	37193.4186	8.61	8.66	8.65	0.05	248	249	248	1	7.19
311R01-1	CR	IVB	5219.9577	37313.4049	7.81	7.84	7.78	0.06	242	242	242	0	2.01
311R02-1	CR	IIIB	5171.3627	37265.0290	8.12	8.22	8.12	0.10	242	241	241	0	2.07
311R02-10	CR	IA	7014.9609	37535.0123	7.42	8.19	8.09	0.77	223	235	234	12	0.94
311R02-2	CR	IVB	5555.3483	37524.1890	7.94	7.99	7.94	0.05	242	242	242	0	2.19
311R02-3	CR	IVB	6036.9160	37568.0508	7.83	7.91	7.83	0.08	242	243	243	1	1.95
311R02-4	CR	IVB	6176.1788	37530.7664	7.84	7.89	7.84	0.05	242	242	242	0	1.92
311R02-5	CR	IIA	6359.2034	37461.4527	7.30	7.58	7.33	0.28	219	229	212	17	2.44
311R02-6	CR	IIIA	6362.0676	37463.0243	7.33	7.45	7.35	0.12	218	220	214	6	1.98
311R02-7	CR	IIA	6349.6046	37455.0006	7.37	7.46	7.30	0.16	215	223	213	10	2.01
311R02-8	CR	IIB	6399.6579	37492.9075	7.53	7.84	7.58	0.31	225	234	225	9	2.19
311R02-9	CR	IA	6599.7557	37502.4955	7.12	7.65	7.27	0.53	206	228	208	22	1.62
311R03-1	CR	IVA	6445.7874	37454.3892	7.17	7.19	7.14	0.05	215	216	211	5	4.63
311R03-2	CR	IIA	6336.7664	37458.2497	7.14	7.55	7.45	0.41	209	226	221	17	6.74
311R03-3	CR	IIB	6298.2164	37476.6147	7.51	7.60	7.42	0.18	225	229	221	8	6.89
311R03-4	CR	IVA	6119.3976	37527.6488	7.43	7.51	7.46	0.08	225	229	226	4	3.38
311R03-5	CR	IVA	5972.0668	37555.2207	7.58	7.61	7.55	0.06	231	232	229	3	4.24

Table A19.1 Continued

Anomaly	Water Body	Class	Peak Location		Temperature (C)				Specific Conductance (uS/cm)				Depth (m)
			X	Y	To	Tmax	Tt	dT	SCo	SCmax	SCt	dSC	
311R03-6	CR	IVA	5685.2646	37547.2754	7.51	7.60	7.55	0.09	230	233	231	3	4.57
311R03-7	CR	IIIB	5520.1165	37490.9345	7.73	7.79	7.65	0.14	234	233	234	0	5.15
311R03-8	CR	IIIB	5340.7135	37387.6901	7.68	7.81	7.69	0.13	234	233	236	0	6.07
311R03-9	CR	IIIB	5252.0100	37314.6750	7.69	7.79	7.68	0.11	236	237	235	2	5.88
311R04-1	CR	IVB	7838.6147	37819.2737	7.20	7.27	7.20	0.07	216	216	216	0	2.38
311R04-2	CR	IIB	7945.5773	37890.7574	7.63	7.65	7.48	0.17	221	221	219	2	2.23
311R04-3	CR	IVB	8152.2166	38052.1558	7.88	7.97	7.88	0.09	225	226	224	2	1.77
311R04-4	CR	IVA	8273.6793	38147.9392	7.88	7.96	7.89	0.08	226	231	229	5	1.52
311R05-1	CR	IIIB	8009.6739	37932.0953	7.74	7.88	7.79	0.14	223	225	223	2	2.38
311R05-2	CR	IIIA	8060.0653	37974.9573	7.79	7.88	7.74	0.14	223	225	222	3	2.62
311R06-1	CR	IVB	7853.7673	37817.4551	7.74	7.81	7.74	0.07	221	222	221	1	2.77
311R06-2	CR	IVB	7966.6646	37886.8319	7.74	7.81	7.74	0.07	220	222	222	2	3.05
311R06-3	CR	IIIB	8144.3285	38013.3413	7.96	8.09	7.96	0.13	226	226	224	2	3.32
311R06-4	CR	IVB	8259.8815	38092.4512	7.96	8.04	7.96	0.08	224	224	223	1	4.94
311R06-5	CR	IIIB	8326.3407	38153.9716	7.96	8.06	8.06	0.10	223	223	223	0	4.48
311R06-6	CR	IVB	8374.8053	38196.9492	7.79	7.84	7.76	0.08	221	221	222	0	4.42
312R01-1	CR	IVB	8969.9556	40268.8824	7.60	7.68	7.61	0.08	227	229	228	2	2.74
312R01-2	CR	IIIB	8902.6304	40435.7725	7.61	7.71	7.69	0.10	228	230	229	2	1.83
312R01-3	CR	IVB	8623.4256	40668.7561	7.61	7.68	7.63	0.07	230	230	230	0	1.52
312R01-4	CR	IIIB	8356.5551	40806.0755	7.60	7.73	7.61	0.13	230	230	230	0	0.79
312R01-5	CR	IIIB	8338.0062	40811.4578	7.61	7.71	7.61	0.10	230	229	230	0	1.68
312R01-6	CR	IVB	8251.8261	40841.1623	7.60	7.66	7.60	0.06	230	230	230	0	2.26
312R01-7	CR	IVB	7989.2878	40898.4112	7.61	7.68	7.61	0.07	230	230	230	0	1.22
312R02-1	CR	IIIB	8884.8115	40452.9952	7.55	7.65	7.60	0.10	230	230	230	0	3.57
312R02-2	CR	IVB	8856.9414	40489.6335	7.60	7.68	7.61	0.08	230	230	230	0	3.44
312R02-3	CR	IIB	8612.7743	40672.0557	7.65	7.83	7.66	0.18	230	232	230	2	3.32
312R03-1	CR	V	8712.8620	40567.6450	7.69	7.73	7.69	0.04	231	230	230	0	6.77
312R03-2	CR	V	8752.8867	40538.5797	7.71	7.74	7.71	0.03	231	231	230	1	6.64
312R03-3	CR	IVB	8830.6129	40495.6949	7.76	7.81	7.76	0.05	231	231	231	0	6.37

Table A19.1 Continued

Anomaly	Water Body	Class	Peak Location		Temperature (C)				Specific Conductance (uS/cm)				Depth (m)
			X	Y	To	Tmax	Tt	dT	SCo	SCmax	SCt	dSC	
312R03-4	CR	IVB	8888.5963	40353.4646	7.78	7.86	7.78	0.08	231	231	231	0	8.17
312R03-5	CR	IIIB	8953.8519	40252.1045	7.83	7.96	7.96	0.13	231	232	232	1	7.38
312R04-1	CR	IVB	8803.8328	40433.3187	7.79	7.81	7.76	0.05	231	231	232	0	7.38
312R04-2	CR	IVB	8879.8969	40319.9582	7.83	7.91	7.88	0.08	232	232	232	0	9.24
312R05-1	CR	IVB	7861.3326	40898.6651	7.58	7.65	7.60	0.07	231	231	231	0	3.72
312R05-2	CR	IVB	7622.7741	40936.6940	7.74	7.83	7.76	0.09	231	231	231	0	3.14
312R05-3	CR	IVB	7277.9515	40937.0090	7.86	7.92	7.89	0.08	232	232	232	0	1.86
312R05-4	CR	IVB	7172.2694	40966.3980	7.76	7.83	7.83	0.07	232	232	232	0	2.74
312R06-1	CR	IVB	7133.9085	40971.6358	7.94	7.94	7.86	0.08	232	232	232	0	3.26
312R07-1	CR	IVB	8157.7563	40875.5882	7.92	8.01	7.96	0.09	232	232	232	0	1.86
312R07-10	CR	IIB	7212.8481	40971.7664	8.35	8.37	7.99	0.38	231	231	231	0	1.10
312R07-11	CR	IIB	7139.7638	40982.8451	7.97	8.25	8.22	0.28	231	230	231	0	0.91
312R07-2	CR	IIB	8127.5185	40896.3040	7.96	8.14	8.07	0.18	232	232	231	1	1.22
312R07-3	CR	IIB	8068.6430	40901.1249	8.09	8.29	8.17	0.20	231	232	231	1	0.79
312R07-4	CR	IIIB	8023.5241	40896.9798	7.97	8.07	7.99	0.10	232	231	231	0	1.55
312R07-5	CR	IVB	7950.8922	40912.2649	7.97	8.02	7.97	0.05	232	232	231	1	1.71
312R07-6	CR	IIIB	7941.4635	40907.9003	7.99	8.07	7.96	0.11	232	231	231	0	1.77
312R07-7	CR	IIB	7737.3835	40933.4247	7.88	8.15	7.96	0.27	231	231	230	1	1.01
312R07-8	CR	IIB	7555.5878	40930.5820	7.92	8.09	7.92	0.17	231	231	232	0	1.01
312R07-9	CR	IIB	7307.2001	40962.7047	7.94	8.15	7.94	0.21	231	231	231	0	0.82
312R08-1	CR	IIB	7127.3090	40977.4603	8.55	8.56	8.37	0.19	232	231	231	0	1.68
312R08-2	CR	IIB	7069.5558	40999.4535	7.91	8.29	7.92	0.39	232	230	231	0	1.10
312R08-3	CR	IIB	7027.6520	41001.5998	7.94	8.25	8.20	0.31	232	231	230	1	0.76
312R08-4	CR	IIB	6882.7767	41019.3503	7.88	8.11	8.11	0.23	233	231	231	0	1.19
312R08-5	CR	IIB	6852.3582	41037.0181	7.97	8.33	8.06	0.36	231	231	231	0	0.82
312R08-6	CR	IIB	6752.4797	41055.5807	8.06	8.40	7.99	0.41	232	227	230	0	0.82
312R08-7	CR	IIB	6454.6990	41076.9529	8.24	8.43	8.33	0.19	231	231	230	1	1.25
312R08-8	CR	IVB	6174.9461	41056.7212	7.84	7.91	7.84	0.07	232	232	232	0	1.40
312R08-9	CR	IIIA	5884.9046	40972.5575	8.07	8.15	8.01	0.14	231	234	232	3	0.91

Table A19.1 Continued

Anomaly	Water Body	Class	Peak Location		Temperature (C)				Specific Conductance (uS/cm)				Depth (m)
			X	Y	To	Tmax	Tt	dT	SCo	SCmax	SCt	dSC	
313R02-1	CR	IVB	5286.4651	40510.4674	8.32	8.43	8.33	0.09	229	229	229	0	1.01
313R02-2	CR	IVB	5417.4112	40584.1862	8.32	8.40	8.35	0.08	229	229	229	0	2.71
313R02-3	CR	IVB	5444.3980	40605.8778	8.35	8.40	8.35	0.05	229	229	229	0	2.32
313R06-1	CR	IVB	5423.5746	40251.2145	8.47	8.48	8.42	0.06	230	231	229	2	5.55
313R07-1	CR	IIB	5992.6121	40578.0195	8.55	8.93	8.55	0.38	232	231	231	0	0.73
313R07-2	CR	IIIB	5784.1511	40422.9909	8.53	8.63	8.60	0.10	231	231	230	1	2.29
313R07-3	CR	IVB	5757.8428	40395.9885	8.60	8.66	8.61	0.06	230	231	231	1	2.29
313R07-4	CR	IVB	5680.3387	40325.4701	8.61	8.65	8.58	0.07	231	231	231	0	3.08
313R08-1	CR	IB	5756.4703	40401.3320	8.88	9.20	8.73	0.47	232	231	231	0	1.04
313R08-2	CR	IB	5899.2050	40589.5245	8.66	9.24	8.78	0.58	231	231	231	0	0.98
314R01-1	CR	IVB	3877.8291	39360.5812	8.14	8.20	8.15	0.06	218	220	219	2	3.17
314R01-2	CR	IIIB	3611.1669	39286.0348	8.14	8.24	8.24	0.10	218	220	220	2	3.20
314R04-1	CR	IVA	3531.2489	39599.7059	8.02	8.07	8.02	0.05	214	217	218	3	6.68
314R04-2	CR	IVA	3622.7114	39625.0006	8.01	8.02	7.97	0.05	214	223	210	13	7.25
314R04-3	CR	IVB	5008.8481	40218.6298	8.04	8.07	8.02	0.05	216	217	216	1	5.73
314R05-1	CR	V	3877.6931	39767.0123	8.06	8.09	8.07	0.03	217	220	217	3	6.55
314R05-2	CR	IVA	3752.4902	39729.0412	8.07	8.09	8.04	0.05	217	221	217	4	7.41
314R06-1	CR	V	4549.4049	39953.4557	8.09	8.12	8.09	0.03	217	221	218	4	4.05
314R07-1	CR	V	3501.4852	39710.8026	8.20	8.22	8.20	0.02	218	221	217	4	3.29
314R08-1	CR	IVB	3493.7304	39726.2306	8.42	8.47	8.43	0.05	220	220	218	2	1.95
314R08-2	CR	IVB	3601.8624	39758.8812	8.58	8.61	8.56	0.05	219	219	219	0	1.37
314R08-3	CR	IVB	3705.0641	39769.3344	8.53	8.60	8.53	0.07	219	221	220	2	1.28
314R08-4	CR	IVB	3973.1310	39823.0890	8.15	8.22	8.14	0.08	220	220	219	1	2.47
314R08-5	CR	IVB	4202.8747	39902.1119	8.12	8.20	8.14	0.08	218	218	217	1	1.52
314R08-6	CR	IIB	4288.2054	39933.1339	8.20	8.37	8.20	0.17	217	217	217	0	0.73
314R08-7	CR	IIIB	4378.6009	39957.3948	8.20	8.27	8.15	0.12	218	219	219	1	1.46
314R08-8	CR	IVB	4583.9430	40052.4077	8.14	8.22	8.15	0.08	217	217	217	0	2.01
314R09-1	CR	IIIB	4042.0109	39480.3723	8.55	8.56	8.45	0.11	219	221	219	2	5.46
314R09-2	CR	IVB	4341.0911	39629.7580	8.24	8.27	8.22	0.05	218	219	220	1	5.70

Table A19.1 Continued

			Peak Location		Temperature (C)				Specific Conductance (uS/cm)				
Anomaly	Water Body	Class	X	Y	To	Tmax	Tt	dT	SCo	SCmax	SCt	dSC	Depth (m)
314R09-3	CR	IIB	5417.6861	40222.6200	8.33	8.52	8.52	0.19	217	219	219	2	4.15
314R10-1	CR	IIIB	3690.2677	39343.1224	8.45	8.53	8.43	0.10	217	219	220	2	4.42
314R10-2	CR	V	3868.5809	39355.4328	8.61	8.65	8.61	0.04	219	219	219	0	4.24
314R10-3	CR	IIIB	4182.0644	39432.4096	8.48	8.53	8.43	0.10	217	219	218	2	3.66
314R10-4	CR	IIIB	4227.5320	39459.1200	8.43	8.50	8.40	0.10	219	220	218	2	3.75
314R10-5	CR	IIIB	4588.2438	39611.6285	8.50	8.60	8.53	0.10	218	219	219	1	3.23
314R10-6	CR	IVB	4683.7313	39671.1985	8.53	8.61	8.56	0.07	218	219	219	1	3.20
314R10-7	CR	IIIB	4755.0686	39715.0744	8.55	8.66	8.60	0.11	218	219	219	1	3.20
314R10-8	CR	IIIB	4913.7338	39815.4940	8.48	8.60	8.47	0.13	219	219	218	1	3.23
314R11-1	CR	IIIB	3687.9497	39282.7734	8.86	8.94	8.84	0.10	219	218	220	0	0.76
314R11-10	CR	IIIB	4598.0273	39543.4714	8.84	8.89	8.79	0.10	219	220	219	1	1.37
314R11-12	CR	IIB	4732.2857	39647.9327	8.91	9.07	8.96	0.16	220	220	219	1	1.10
314R11-13	CR	IIIB	4759.4568	39680.0390	8.93	9.06	8.93	0.13	220	220	220	0	1.10
314R11-14	CR	IIIB	4857.6571	39734.0070	8.91	9.01	8.91	0.10	220	220	220	0	0.73
314R11-15	CR	IVB	5416.8835	40088.0602	8.93	9.01	8.93	0.08	219	220	220	1	1.52
314R11-2	CR	IIB	3776.5002	39287.2412	8.84	8.94	8.73	0.21	219	220	220	1	0.94
314R11-3	CR	IVB	3664.4662	39272.7257	8.86	8.94	8.86	0.08	220	220	220	0	0.94
314R11-4	CR	IIB	3756.8845	39293.4212	8.76	8.89	8.76	0.23	220	220	219	1	1.40
314R11-5	CR	IVB	3798.8916	39300.3497	8.76	8.81	8.76	0.05	220	220	220	0	1.16
314R11-6	CR	IIIB	3990.4008	39339.3585	8.91	9.01	8.89	0.12	220	220	220	0	0.88
314R11-7	CR	IIIB	4048.2686	39353.1620	8.86	8.94	8.83	0.11	220	220	220	0	0.88
314R11-8	CR	IIB	4157.7636	39399.2344	8.79	8.86	8.70	0.16	220	219	219	0	0.88
314R11-9	CR	IIIB	4493.9187	39523.3993	8.84	8.96	8.86	0.12	218	220	219	2	1.16
314R12-1	CR	IB	6150.1892	40709.0481	8.35	8.84	8.45	0.49	217	219	217	2	0.91

Table A19.2 Summary of hydrogeologic information for anomalies

			Flow Conditions (m3/sec)					
Anomaly	Water Body	Class	Q -MH	Qr	Qs -calc	Qr:Qs	Formation	Remarks
215R04-1	PC	IIIB	268	10	**0.15**	67	Ok	At "M" bend, bank springs
219R02-1	PC	V	268	14	**0.06**	219	Ok	At "M" bend, bank springs; positions unreliable
219R04-1	PC	IVB	268	12	**0.07**	175	Ok	At "M" bend, bank springs; positions unreliable
219R05-1	PC	V	268	10	**0.01**	873	Ok	At "M" bend, bank springs; positions unreliable
220R07-1	PC	IA	265	17	*1.68*	10	Oma	At/near Ock-Och contact; DS of EFPC confluence
220R08-1	PC	IIA	265	16	*0.39*	41	Om	
220R08-2	PC	IVA	265	16	**0.13**	124	Olb	Just US of thrust fault
220R10-1	PC	IVB	265	15	**0.13**	114	Ok	on thrust sheet; coincides w/ 220R10-2
220R10-2	PC	IVA	265	15	*0.18*	81	Ok	on thrust sheet; coincides w/ 220R10-1; noted in field
221R01-1	PC	IVB	302	17	**0.15**	115	Oca	Along deformation zone, peak dT @ sl. Shallowing
221R02-1	PC	IVB	268	17	**0.15**	115	Oca	Along deformation zone
221R07-1	PC	IVB	271	14	*0.18*	76	Olb	
222R13-1	PC	V	271	15	**0.07**	230	Ocn-Ocy	Coincides w/ 222R14-1 along syncline axis
222R13-2	PC	V	271	15	**0.07**	230	Ocn-Ocy	
222R14-1	PC	IVA	271	16	*0.17*	93	Ocn-Ocy	Coincides w/ 222R13-1 along syncline axis
226R01-1	PC	IVB	0	29	*0.64*	45	Ocn/Ocy/Oh	@ fm contact
226R01-2	PC	V	0	28	*0.27*	105	Oca	On strike w/ 226R02-2 in upper Oca; shallowing
226R02-1	PC	IIB	0	26	*1.16*	22	Oh	
226R02-2	PC	IIIB	0	25	*0.74*	34	Oca	On strike w/ 226R01-2 in upper Oca
226R02-3	PC	V	0	23	*0.21*	112	Oca	Adj. To K-1007 pond
226R03-1	PC	IVB	169	15	*0.26*	58	Oh	
226R03-2	PC	IVB	169	16	*0.32*	50	Oca	
226R03-3	PC	IVB	169	16	*0.23*	70	Oca	EOL anomaly; along axis of map scale anticline
226R03-4	PC	IIIB	169	5	*0.17*	29	Oca	Along axis of map scale anticline
226R04-1	PC	IVB	169	12	*0.28*	42	Oca	
226R04-2	PC	IIB	169	11	*0.68*	16	Oca/Oh	@ fm contact
226R05-1	PC	IVB	268	9	*0.18*	49	Oca	Along axis of map scale anticline
226R05-2	PC	V	268	6	**0.07**	86	Oca	
226R06-1	PC	IIIB	268	20	*0.81*	25	Oh	Temp increases with increasing depth.

Table A19.2 Continued

Anomaly	Water Body	Class	Flow Conditions (m3/sec) Q -MH	Qr	Qs -calc	Qr:Qs	Formation	Remarks
229R05-4	PC	IIB	265	4	*0.38*	11	Oh/Ocn-Ocy	@ fm contact and axis of minor anticline in def. zone
229R05-5	PC	IIB	265	7	*0.52*	14	Ocn-Ocy	
229R05-6	PC	IIB	265	9	*0.77*	12	Ocn-Ocy	
229R05-7	PC	IIIB	265	9	*0.44*	20	Ocn-Ocy	
229R05-8	PC	IIIA	175	8	*0.39*	20	Ocn-Ocy	Peak dT/dSC @ shallowest point (0.3 m shallower)
229R06-1	CR	IVB	0	15	*0.19*	80	Ops	Along edge of former channel; @ 229R07-1
229R06-2	CR	V	0	17	0.06	280	Ops	Along edge of former channel; near K901 outfall
229R07-1	CR	IA	0	14	*1.09*	13	Ops	Along edge of former channel; with 229R06-1
304R09-1	CR	V	0	41	0.00	-	Om	EOR anomaly; coincides w/ 311R03-3
304R10-1	CR	V	0	91	*0.66*	139	Ord	Along axis of map scale syncline
304R10-2	CR	IVB	0	106	*0.96*	111	Om	
304R11-1	CR	V	0	138	*1.00*	139	Olb	Along axis of map scale syncline near contact w/ Ord
304R11-2	CR	IVB	0	160	*1.44*	111	Om	Highest temp along run; just DS of Om/Ops contact
311R01-1	CR	IVB	0	96	*0.85*	112	Om/Ops	@ fm contact, coincides w/ 311R03-9
311R02-1	CR	IIIB	0	153	*2.07*	74	Om/Ops	@ fm contact
311R02-10	CR	IA	0	110	*11.48*	10	Ord	End of run anomaly; shallow water
311R02-2	CR	IVB	0	115	*0.78*	148	Om	
311R02-3	CR	IVB	0	120	*1.30*	92	Om	
311R02-4	CR	IVB	0	139	*0.94*	148	Om	
311R02-5	CR	IIA	0	142	*5.39*	26	Ord/Om	@ fm contact
311R02-6	CR	IIIA	0	145	*2.36*	62	Ord/Om	@ fm contact
311R02-7	CR	IIA	0	154	*3.34*	46	Ord/Om	@ fm contact
311R02-8	CR	IIB	0	166	*6.97*	24	Ord/Om	@ fm contact
311R02-9	CR	IA	0	178	*12.78*	14	Ord	
311R03-1	CR	IVA	0	171	*1.16*	148	Ord	
311R03-2	CR	IIA	0	175	*9.70*	18	Om	
311R03-3	CR	IIB	0	179	*4.35*	41	Om	Coincides w/ 304R09-1
311R03-4	CR	IVA	0	191	*2.06*	93	Om	
311R03-5	CR	IVA	0	194	*1.57*	123	Om	

Anomaly	Water Body	Class	Flow Conditions (m3/sec) Q -MH	Qr	Qs -calc	Qr:Qs	Formation	Remarks
226R07-1	PC	IVB	268	23	*0.43*	53	Oh	
226R08-1	PC	IVB	268	22	*0.52*	42	Oh	Near contact w/ Ocn-Ocy; coincides w/ 226R09-2
226R09-1	PC	IVB	268	19	*0.32*	59	Oca/Oh	@ fm contact & fault, coincides w/226R10-1, 226R11-1
226R09-2	PC	IVB	268	19	*0.45*	42	Oh	Near contact w/ Ocn-Ocy; coincides w/ 226R08-1
226R11-1	PC	IIB	268	16	*1.72*	9	Oca/Oh	@ fm contact & fault, coincides w/226R09-1, 226R10-1
226R12-1	PC	IIB	265	15	*1.77*	8	Ocn-Ocy	
226R12-2	PC	IIB	265	16	*1.20*	13	Ocn-Ocy	
227R01-1	PC	IVB	271	20	*0.47*	42	Oh/Ocn-Ocy	Along fm contact
227R01-2	PC	V	271	19	*0.33*	57	Oh	Near mapped reverser fault
227R02-1	PC	IVB	271	16	*0.52*	31	Oh/Ocn-Ocy	Along fm contact
227R03-1	PC	IIB	271	15	*1.65*	9	Oh	In deep "hole"
227R04-1	PC	IIIB	271	10	*0.40*	25	Oh/Ocn-Ocy	Along fm contact
227R05-1	PC	IIB	271	13	*0.84*	15	Ocn-Ocy	
227R05-2	PC	IVB	271	14	*0.27*	52	Oh/Ocn-Ocy	Along fm contact
227R06-1	PC	V	271	5	0.04	121	Oh/Ocn-Ocy	Along fm contact
227R07-1	PC	IIB	271	16	*1.83*	9	Ord	
227R07-2	PC	IIB	271	16	*2.31*	7	Ord	
227R07-3	PC	IIB	271	12	*1.55*	8	Olb	Coincides w/ 227R07-5, 229R01-1; field observed
227R07-4	PC	IIB	271	12	*1.19*	10	Olb	
227R07-5	PC	IIB	271	12	*1.67*	7	Olb	Coincides w/ 227R07-3, 229R01-1, 227R07-4
229R01-1	PC	IVB	265	14	*0.28*	49	Olb	Coincides w/ 227R07-5, 229R07-3; noted shallowing
229R02-1	PC	IIIB	265	12	*0.47*	26	Ord	Near 227R07-2; peak @ shallowest point
229R03-1	PC	V	265	11	*0.16*	67	Olb/Oca	Straddles fm contact
229R03-2	PC	IVB	265	11	*0.20*	54	Olb	
229R04-1	PC	IIIB	265	9	*0.33*	27	Oca	
229R04-2	PC	IIIB	265	8	*0.39*	21	Oca	At mapped fault within 'deformation' zone; EOR
229R05-1	PC	IIIB	265	4	*0.16*	24	Oca	
229R05-2	PC	IIIB	265	3	*0.16*	19	Oca	
229R05-3	PC	IIB	265	1	0.08	12	Oca	

Table A19.2 Continued

Anomaly	Water Body	Class	Flow Conditions (m3/sec) Q -MII	Qr	Qs -calc	Qr:Qs	Formation	Remarks
311R03-6	CR	IVA	0	190	*2.31*	82	Om	
311R03-7	CR	IIIB	0	187	*3.54*	53	Om	
311R03-8	CR	IIIB	0	184	*3.23*	57	Om	
311R03-9	CR	IIIB	0	182	*2.71*	67	Om/Ops	@ fm contact; coincides w/ 311R01-1
311R04-1	CR	IVB	0	182	*1.71*	106	Oca/Olb	"deformation zone near fault, spr, @ fm contact
311R04-2	CR	IIB	0	165	*3.78*	44	Oca	Along "deformation zone near fault
311R04-3	CR	IVB	0	160	*1.94*	83	Oca	Along "deformation zone near fault
311R04-4	CR	IVA	0	159	*1.71*	93	Oca	Along "deformation zone near fault
311R05-1	CR	IIIB	0	149	*3.02*	49	Oca	Along "deformation zone near fault
311R05-2	CR	IIIA	0	149	*3.02*	49	Oca	Along "deformation zone near fault
311R06-1	CR	IVB	0	155	*1.60*	97	Oca	Along "deformation zone near fault
311R06-2	CR	IVB	0	157	*1.62*	97	Oca	Along "deformation zone near fault
311R06-3	CR	IIIB	0	158	*3.03*	52	Oca	Along "deformation zone near fault
311R06-4	CR	IVB	0	160	*1.89*	85	Oca	Along "deformation zone near fault
311R06-5	CR	IIIB	0	161	*2.38*	68	Oca	Along "deformation zone near fault
311R06-6	CR	IVB	0	162	*1.91*	85	Oca	Along "deformation zone near fault
312R01-1	CR	IVB	0	148	*1.70*	87	Ops	Along edge of former channel; near ephem. bank sp.
312R01-2	CR	IIIB	0	118	*1.69*	70	Ops	Along edge of former channel
312R01-3	CR	IVB	0	112	*1.12*	100	Oma	Along edge of former channel; @ 312R02-3
312R01-4	CR	IIIB	0	98	*1.83*	54	Oma	Along edge of former channel
312R01-5	CR	IIIB	0	98	*1.41*	70	Oma	Along edge of former channel
312R01-6	CR	IVB	0	93	*0.80*	116	Oma	Along edge of former channel
312R01-7	CR	IVB	0	87	*0.87*	100	Oma	Along edge of former channel
312R02-1	CR	IIIB	0	95	*1.36*	70	Ops	Along edge of former channel
312R02-2	CR	IVB	0	97	*1.11*	88	Ops/Oma	@ OCk-Och contact; along edge of former channel
312R02-3	CR	IIB	0	114	*2.93*	39	Oma	Along edge of former channel; @ 312R01-3
312R03-1	CR	V	0	151	*0.87*	174	Oma	
312R03-2	CR	V	0	153	*0.66*	231	Oma	
312R03-3	CR	IVB	0	157	*1.13*	139	Ops/Oma	@ OCk-Och contact; along edge of former channel

Table A19.2 Continued

Anomaly	Water Body	Class	Flow Conditions (m3/sec) Q -MH	Qr	Qs -calc	Qr:Qs	Formation	Remarks
312R03-4	CR	IVB	0	166	*1.91*	87	Ops	On strike w/ deepest hole in Clinch
312R03-5	CR	IIIB	0	170	*3.18*	53	Ops	On strike w/ 229R07-1 but in channel
312R04-1	CR	IVB	0	180	*1.29*	140	Ops	
312R04-2	CR	IVB	0	179	*2.05*	87	Ops	
312R05-1	CR	IVB	0	172	*1.73*	100	Oma	
312R05-2	CR	IVB	0	172	*2.22*	77	Oma/Ok	Fm contact, on strike with 312R07-8
312R05-3	CR	IVB	0	172	*1.97*	87	Ok	On strike with 312R07-9
312R05-4	CR	IVB	0	173	*1.74*	100	Ok	
312R06-1	CR	IVB	0	178	*2.05*	87	Ok	
312R07-1	CR	IVB	0	162	*2.16*	75	Oma	
312R07-10	CR	IIB	0	159	*8.96*	18	Ok	
312R07-11	CR	IIB	0	158	*6.56*	24	Ok	
312R07-2	CR	IIB	0	155	*4.14*	37	Oma	
312R07-3	CR	IIB	0	155	*4.60*	34	Oma	
312R07-4	CR	IIIB	0	155	*2.30*	67	Oma	
312R07-5	CR	IVB	0	155	*1.15*	135	Oma	
312R07-6	CR	IIIB	0	160	*2.61*	61	Oma	
312R07-7	CR	IIB	0	171	*6.85*	25	Oma/Ok	Fm contact, on strike with 312R05-2, 312R07-8
312R07-8	CR	IIB	0	174	*4.39*	40	Oma/Ok	Fm contact, on strike with 312R05-2
312R07-9	CR	IIB	0	175	*5.45*	32	Ok	On strike, near 312R05-3
312R08-1	CR	IIB	0	161	*4.49*	36	Ok	
312R08-2	CR	IIB	0	155	*8.86*	17	Ok	
312R08-3	CR	IIB	0	152	*6.91*	22	Ok	
312R08-4	CR	IIB	0	146	*4.92*	30	Ok	
312R08-5	CR	IIB	0	146	*7.71*	19	Ok	
312R08-6	CR	IIB	0	146	*8.78*	17	Ok	
312R08-7	CR	IIB	0	146	*4.07*	36	Ok	
312R08-8	CR	IVB	0	146	*1.50*	97	Ok	
312R08-9	CR	IIIA	0	148	*3.04*	49	Ok	

Table A19.2 Continued

			Flow Conditions (m3/sec)					
Anomaly	Water Body	Class	Q -MH	Qr	Qs -calc	Qr:Qs	Formation	Remarks
313R02-1	CR	IVB	0	95	*1.37*	70	Ok	Strike parallels shoreline; shallow water above channel
313R02-2	CR	IVB	0	93	*1.19*	78	Ok	Strike parallels shoreline; shallow water above channel
313R02-3	CR	IVB	0	92	*0.73*	125	Ok	Strike parallels shoreline; shallow water above channel
313R06-1	CR	IVB	0	196	*1.90*	103	Oma/Ok	Along fm contact
313R07-1	CR	IIB	0	167	*10.27*	16	Ok	
313R07-2	CR	IIIB	0	168	*2.72*	62	Oma/Ok	Along fm contact
313R07-3	CR	IVB	0	168	*1.63*	103	Oma/Ok	Along fm contact
313R07-4	CR	IVB	0	168	*1.90*	88	Oma/Ok	Along fm contact
313R08-1	CR	IB	0	170	*13.16*	13	Oma/Ok	Along fm contact
313R08-2	CR	IB	0	170	*16.24*	10	Ok	
314R01-1	CR	IVB	17	325	*3.00*	108	Ok	
314R01-2	CR	IIIB	15	332	*5.12*	65	Ok	On shallow channel shoulder
314R04-1	CR	IVA	0	29	*0.22*	131	Ok	In channel
314R04-2	CR	IVA	0	19	0.15	131	Ok	In channel
314R04-3	CR	IVB	0	25	*0.19*	131	Ok	In channel
314R05-1	CR	V	0	87	*0.40*	218	Ok	At channel edge
314R05-2	CR	IVA	0	98	*0.75*	131	Ok	At channel edge
314R06-1	CR	V	0	101	*0.47*	215	Ok	At former channel edge
314R07-1	CR	V	0	132	*0.41*	322	Ok	Proximal to 314R08-1
314R08-1	CR	IVB	0	144	*1.12*	128	Ok	Proximal to 314R07-1
314R08-2	CR	IVB	0	147	*1.15*	128	Ok	
314R08-3	CR	IVB	0	151	*1.65*	92	Ok	
314R08-4	CR	IVB	0	153	*1.91*	80	Ok	
314R08-5	CR	IVB	0	154	*1.92*	80	Ok	
314R08-6	CR	IIB	0	155	*4.11*	38	Ok	
314R08-7	CR	IIIB	0	156	*2.92*	53	Ok	
314R08-8	CR	IVB	0	157	*1.96*	80	Ok	Strike parallels shoreline; shallow water above channel
314R09-1	CR	IIIB	0	191	*3.33*	57	Ok	In channel
314R09-2	CR	IVB	0	188	*1.49*	126	Ok	In channel

Table A19.2 Continued

Anomaly	Water Body	Class	Flow Conditions (m3/sec) Q -MH	Qr	Qs -calc	Qr:Qs	Formation	Remarks
314R09-3	CR	IIB	0	182	*5.48*	33	Oma/Ok	Along fm contact
314R10-1	CR	IIIB	2	188	*3.07*	61	Ok	At former channel edge
314R10-2	CR	V	5	189	*1.24*	153	Ok	
314R10-3	CR	IIIB	12	191	*3.12*	61	Oma/Ok	Along fm contact
314R10-4	CR	IIIB	12	191	*3.12*	61	Oma/Ok	Along fm contact
314R10-5	CR	IIIB	18	193	*3.15*	61	Oma	
314R10-6	CR	IVB	20	193	*2.21*	87	Oma	
314R10-7	CR	IIIB	23	192	*3.45*	56	Oma	
314R10-8	CR	IIIB	23	188	*3.99*	47	Oma	
314R11-1	CR	IIIB	23	165	*2.84*	58	Ok	Field observed anomaly
314R11-10	CR	IIIB	23	165	*2.84*	58	Oma	
314R11-12	CR	IIB	23	167	*4.61*	36	Oma	
314R11-13	CR	IIIB	23	169	*3.79*	45	Oma	
314R11-14	CR	IIIB	23	169	*2.91*	58	Oma	
314R11-15	CR	IVB	23	172	*2.37*	73	Oma	
314R11-2	CR	IIB	23	172	*6.23*	28	Ok	
314R11-3	CR	IVB	23	174	*2.40*	73	Ok	
314R11-4	CR	IIB	23	176	*6.98*	25	Ok	
314R11-5	CR	IVB	23	177	*1.53*	116	Ok	
314R11-6	CR	IIIB	23	179	*3.70*	48	Ok	Field observed anomaly
314R11-7	CR	IIIB	44	178	*3.38*	53	Ok	
314R11-8	CR	IIB	65	178	*4.91*	36	Oma/Ok	Along fm contact
314R11-9	CR	IIIB	173	176	*3.64*	48	Oma	
314R12-1	CR	IB	344	176	*13.95*	13	Ok	Field observed anomaly in shallows, inside meander

APPENDIX B

CLINCH RIVER AND POPLAR CREEK FLOW CALCULATIONS

APPENDIX B LIST OF FIGURES

Figure	Title	Page
B.1	Cross -sectional area changes with increasing stage; Clinch River at SG-288.	248
B.2	Rating curve: Area (A) as a function of stage, Clinch River section @ SG-288	249
B.3	Rating curve: "R" as a function of stage (dH), Clinch River at SG-288.	249
B.4	Cross -sectional area changes with increasing stage, lower Poplar Creek at SG-287.	251
B.5	Rating curve: Area (A) as a function of stage, Poplar Creek at SG-287.	252
B.6	Rating curve: "R" as a function of stage (dH), Poplar Creek at SG-287	252
B.7	Cross -sectional area changes with increasing stage, upper Poplar Creek at SG-282.	254
B.8	Rating curve: Area (A) as a function of stage, Poplar Creek at SG-282	255
B.9	Rating curve: "R" as a function of stage (dH), Poplar Creek at SG-282	255

APPENDIX B LIST OF TABLES

Table	Title	Page
B.1.	Calculated cross-sectional area and R-values as a function of stage, Clinch River section at SG-288.	247
B.2.	Calculated cross-sectional area and R-values as a function of stage, lower Poplar Creek section at SG-287.	250
B.3.	Calculated cross-sectional area and R-values as a function of stage, upper Poplar Creek section at SG-282.	253
B.4	Summary of rating functions for A and R as a function of stage (dH).	256
B.5.	Summary statistics for Clinch River and Poplar Creek flows during the field effort, 1/1/96 - 4/1/96.	257

APPENDIX B

CLINCH RIVER AND POPLAR CREEK FLOW CALCULATIONS

Subaqueous spring discharge and the ability to observe these are in part, a function of the ambient stage and flow conditions within the receiving water bodies. In order to evaluate the role of ambient flow conditions during the time of the surveys on potential heat transfer and thus, the ability to detect temperature anomalies, it was necessary to quantify the flow rates in both the Clinch River and Poplar Creek. Since there are no flow gaging stations on Poplar Creek or the Clinch River, this was done using bathymetric data obtained during this research, concurrent continuous recording stage data from site stage gages, and application of the Manning equation for channel flow. The Manning equation relates hydraulic gradients to the cross-sectional area of flow by:

$$Q = [(1.49)(R^{0.66})(s^{0.5})(A)]/n$$

where:
- Q = discharge (L^3/T)
- s = hydraulic gradient (dimensionless)
- A = cross-sectional area (L^2)
- n = roughness factor, (0.029 - 0.035)
- R = hydraulic radius, = (A/wetted perimeter)

Based upon field observations and supported by the stage data, the river and creek stage fluctuates as much as 0.6 m one or more times throughout the day. Greater stage fluctuations were observed in response to rainfall. Seasonally, stage ranges from 224.03 m to 225.86 m during TVA controlled low and high pool stage conditions, respectively. Flow was also observed in the field to be quite variable over short periods of time, with both strong downstream flow and strong upstream backflow, depending on reservoir operations at upstream Melton Hill Dam (principally) and downstream Watts Bar Dam. Consequently, while hydraulic gradients could be determined at any point in time from the continuous stage data, the actual discharge rate at any time is both a function of

gradient *and* cross-sectional area, the latter of which changes in relation to stage increases or decreases. To address this, detailed river/creek cross-sections were developed for key locations representative of Clinch River and Poplar Creek flow conditions, and a rating curve developed relating stage height changes (dH) to cross-sectional area (A) and wetted perimeter (WP), both of which are required to apply the Manning equation.

Bathymetric data obtained during the field effort were used to construct a bathymetric contour map of the reaches of the Clinch River and Poplar Creek within the bounds of the study area. The bathymetric map, in conjunction with point data was used to develop detailed cross sections of the river/creek. Section locations were biased towards stage gage locations where the bathymetric control was greatest and the channel form less complex. Sections were constructed at stage gage SG-288 along the Clinch River downstream of the confluence with Poplar Creek, at stage gage SG-287 located near the mouth of Poplar Creek, and at SG-282, representing the upper reaches of Poplar Creek within this study area. Profiles were constructed digitally, with area and wetted perimeter determined for each incremental stage increase of approximately 0.3 m within the normal range of fluctuation (224.03 - 225.86 m). Values for R were calculated based upon measured values for A and WP for each stage increment. These data area tabulated for each section in tables B.1 through B.3. Cross-sectional plots are shown as figures B.1, B.4 and B.7; these plots graphically demonstrate the change in cross-sectional area and wetted perimeter associated with incremental increases in stage (dH), above a base flow stage of 224.03. Further, both A and R were plotted against dH (figures B.2, B.3, B.5, B.6, B.8 and B.9), the data fitted with a line and the equation of the line used to relate changes in stage to each of the two primary Manning equation parameters. In general, the plots indicate a linear relationship between R and dH such that a simple linear regression was appropriate. In some cases, the area was shown to change exponentially with dH, and an exponential curve fitting algorithm was used. The rating curves for A and R as a function of dH for the three locations are summarized in Table B.4. Flow rates were then calculated via spreadsheet using the continuous stage data, resultant hydraulic gradient data, and the rating curves. All of the above calculations and

plots were performed using U.S. units (i.e., ft, cfs), and with resulting discharges later translated into metric units. Flow statistics for the Clinch River and Poplar Creek are summarized in Table B.5.

Given the resolution of the data used to determine A and dH, the main source of potential error lies in the selection of the appropriate value of *n* to be used in the Manning equation. The *n* term in the equation is used to describe the channel form, and since Q is inversely proportional to *n*, an error of 0.001 in *n* yields a potential difference of about 3% in Q. Values of *n* for natural channels range form 0.029 for clean, straight, full stage channels without pool to 0.112 for sluggish, weedy channels with pools (Linsley, Kohler, Paulhus, 1958). A constant value of $n = 0.029$ was used in these calculations since the river/creek bottom is comprised of predominantly bare bedrock outcrops and few to no pools. Further, the cross-sectional areas selected for these calculations are free of weeds or other restricting channel features.

Table B.1. Calculated cross-sectional area and R-values as a function of stage, Clinch River section at SG-288.

Stage		Wetted Perimeter		Area		dH		
ft	m	ft	m	ft^2	m^2	ft	m	R
741	225.86	354.60	108.08	8462	786	6	1.83	23.8635
740	225.55	349.90	106.65	8159	758	5	1.52	23.3181
739	225.25	344.50	105.00	7756	720	4	1.22	22.5138
738	224.95	339.30	103.42	7483	695	3	0.92	22.0542
737	224.64	334.30	101.90	7183	667	2	0.61	21.4867
736	224.34	329.00	100.28	6818	633	1	0.31	20.7234
735	224.03	323.90	98.73	6529	607	0	0	20.1575

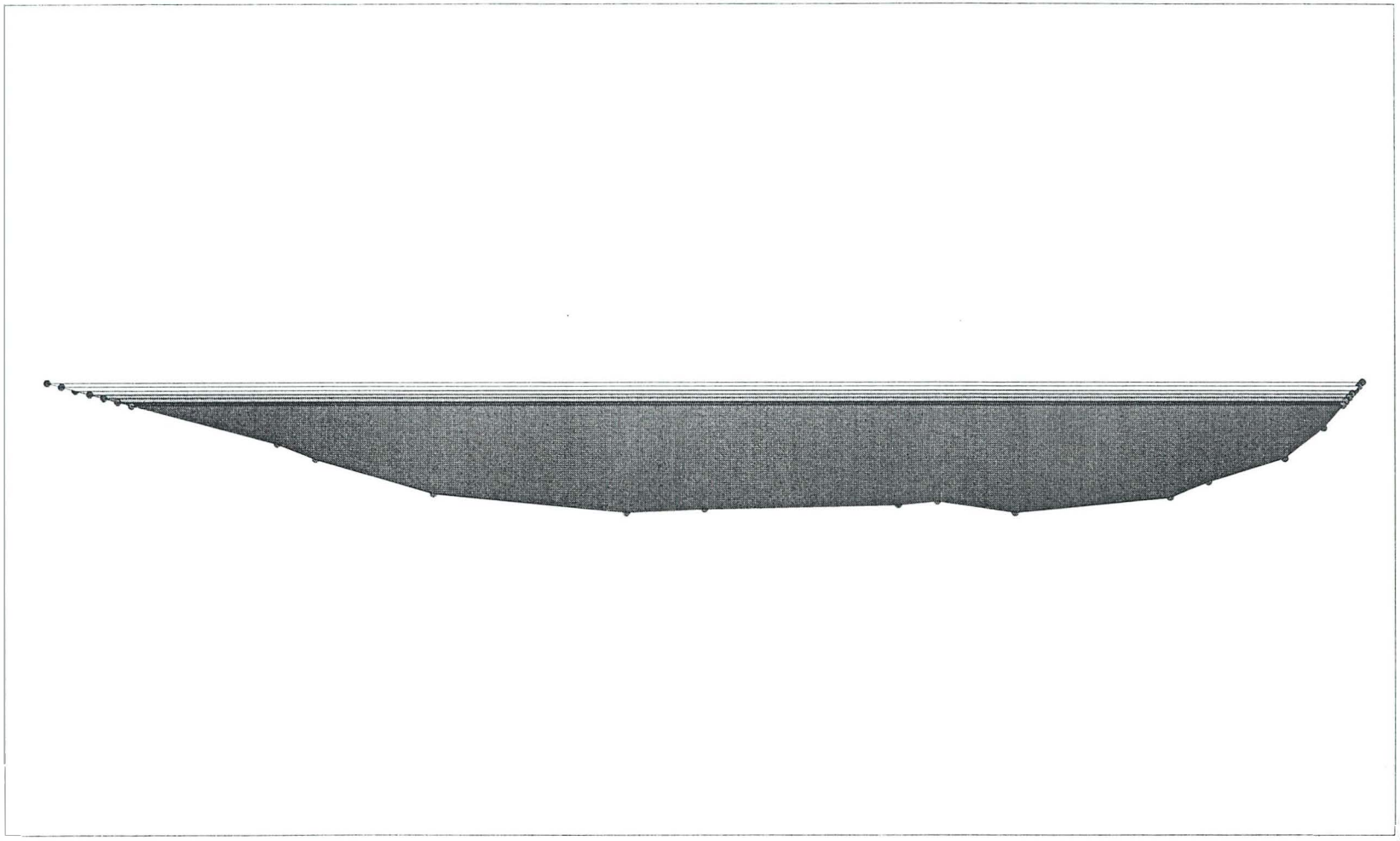


Figure B.1. Cross -sectional area changes with increasing stage; Clinch River at SG-288.

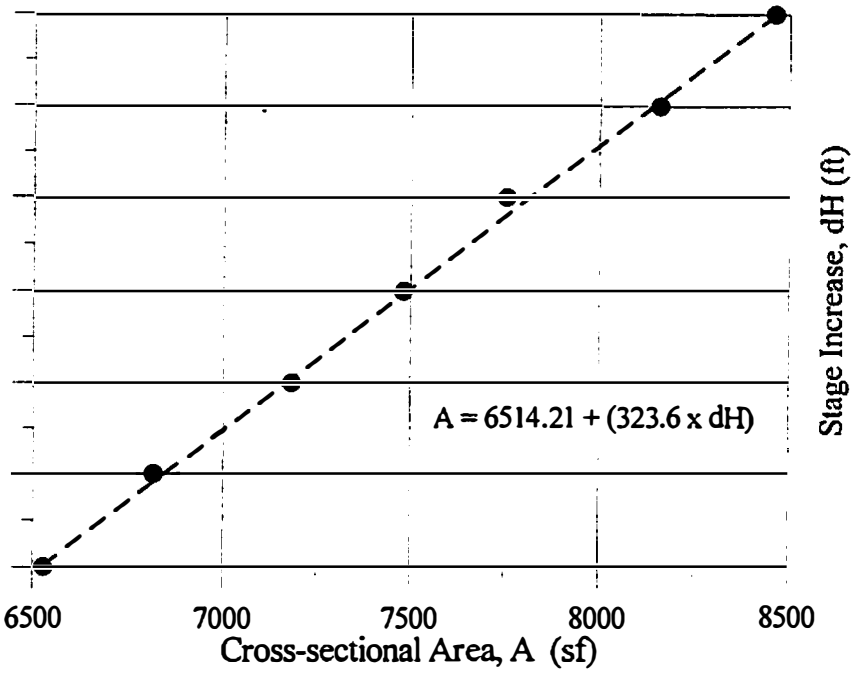


Figure B.2. Rating curve: Area (A) as a function of stage, Clinch River section @ SG-288

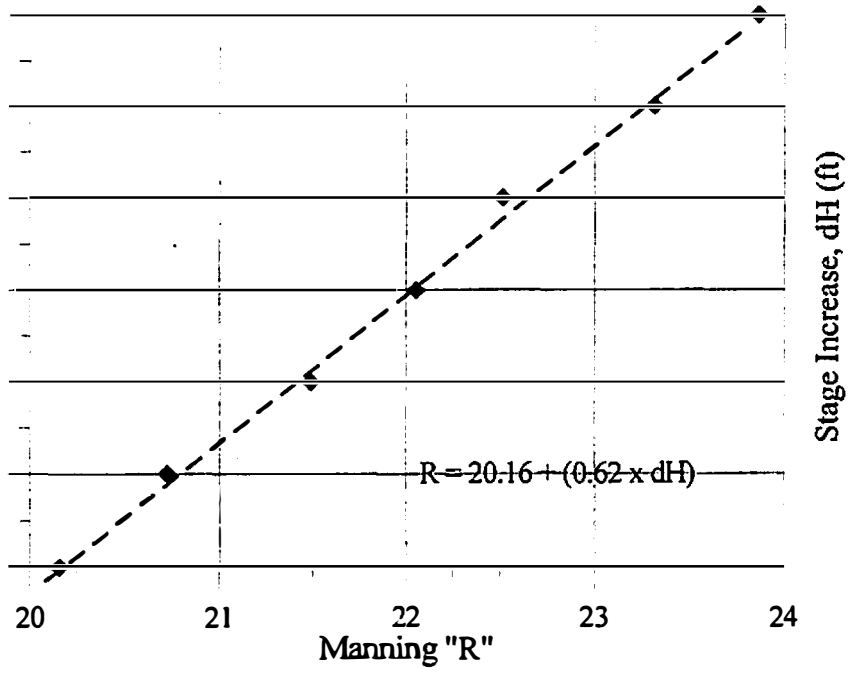


Figure B.3. Rating curve: "R" as a function of stage (dH), Clinch River at SG-288.

Table B.2. Calculated cross-sectional area and R-values as a function of stage, lower Poplar Creek section at SG-287.

Stage		Wetted Perimeter		Area		dH		
ft	m	ft	m	ft^2	m^2	ft	m	R
741	225.86	317	97	2359	219	6	1.83	7.4416
740	225.55	289	64	2009	187	5	1.52	9.6124
739	225.25	262	80	1767	164	4	1.22	6.7443
738	224.95	234	71	1519	141	3	0.92	6.4915
737	224.64	222	68	1297	120	2	0.61	5.8423
736	224.34	207	63	1078	100	1	0.31	5.2077
735	224.03	195	59	885	82	0	0	4.5385

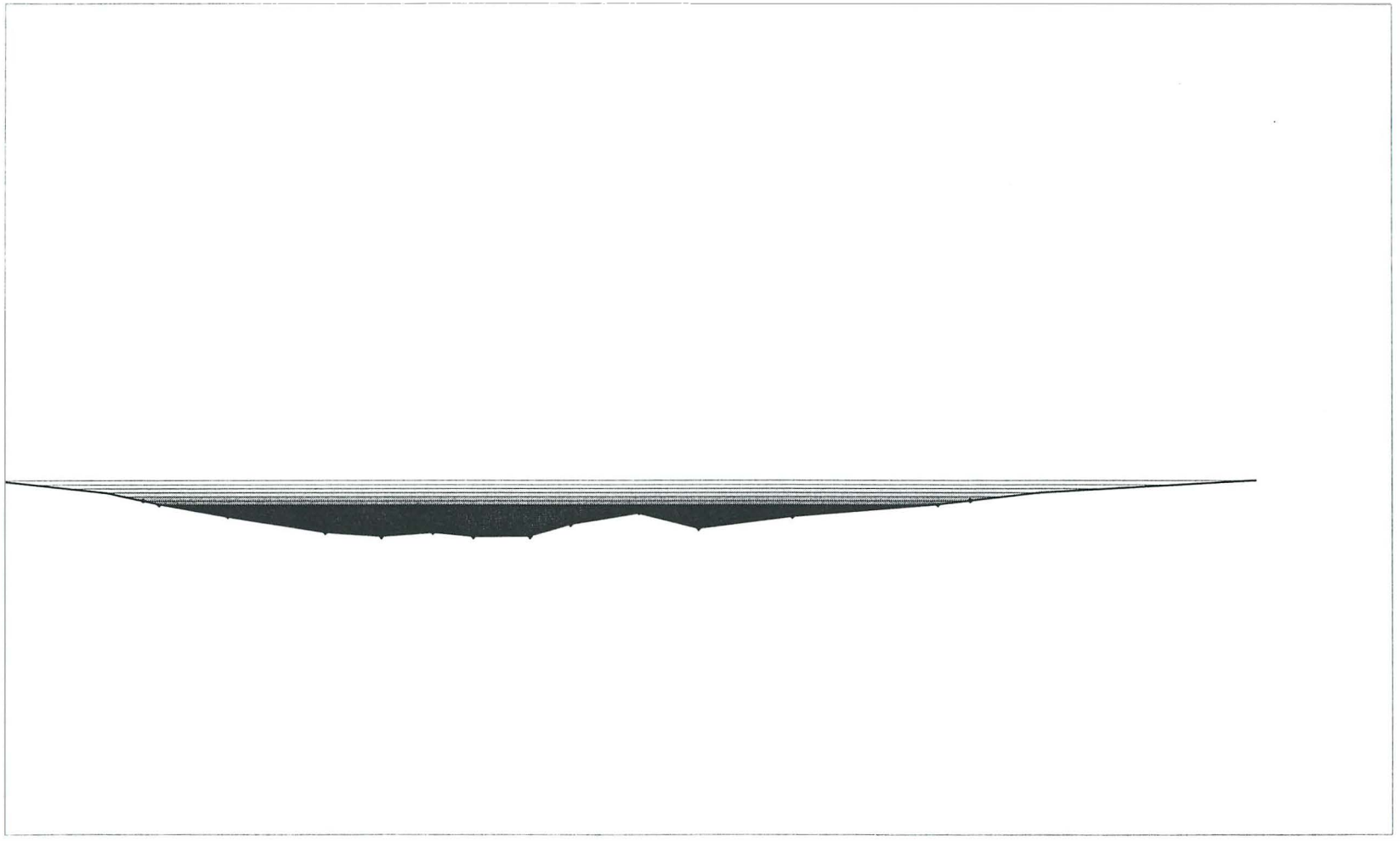


Figure B.4. Cross -sectional area changes with increasing stage, lower Poplar Creek at SG-287.

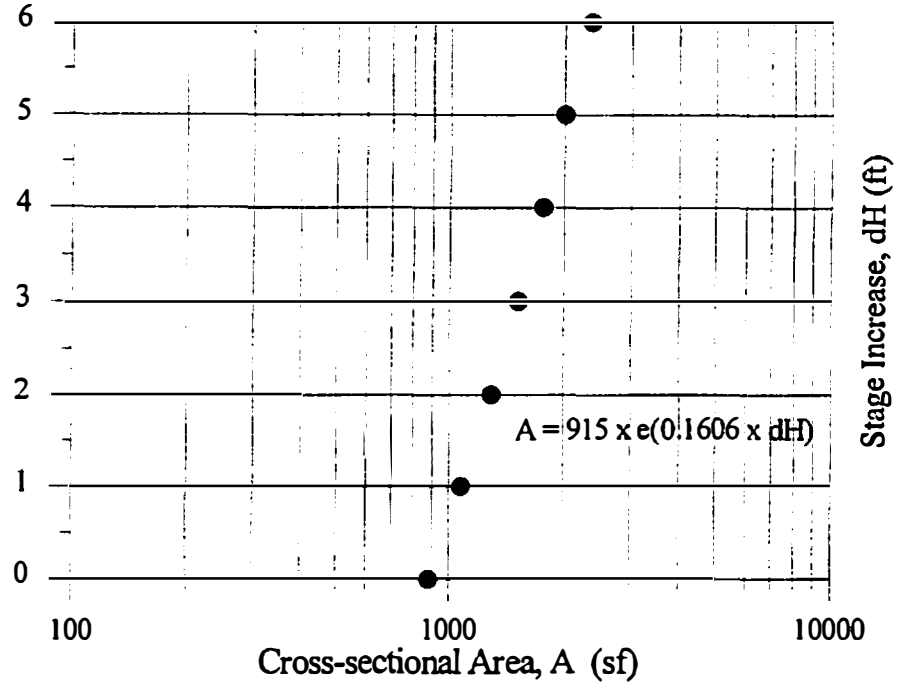


Figure B.5. Rating curve: Area (A) as a function of stage, Poplar Creek at SG-287.

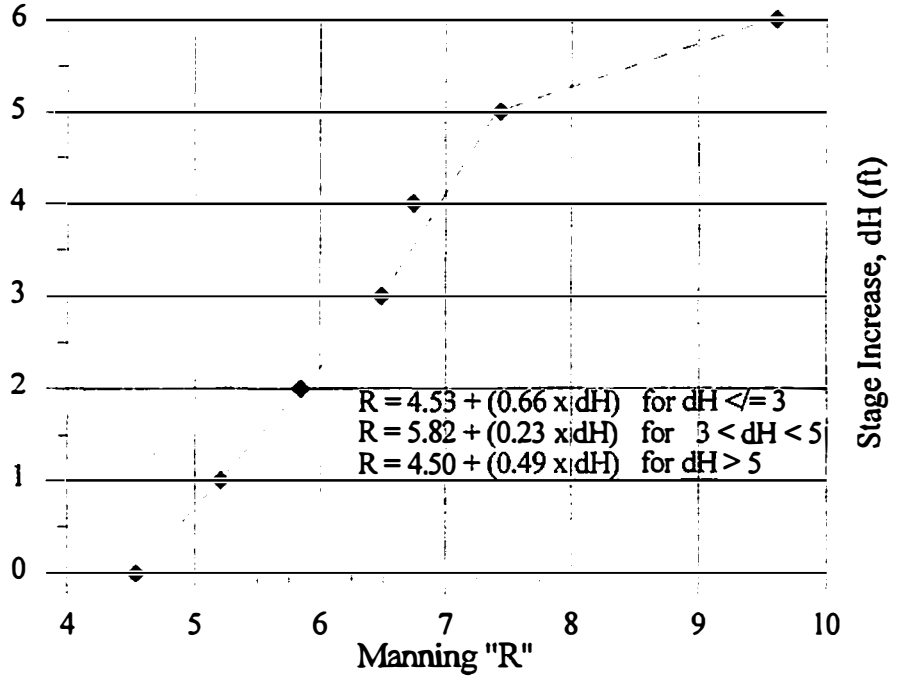


Figure B.6. Rating curve: "R" as a function of stage (dH), Poplar Creek at SG-287.

Table B.3. Calculated cross-sectional area and R-values as a function of stage, upper Poplar Creek section at SG-282.

Stage		Wetted Perimeter		Area		dH		
ft	m	ft	m	ft^2	m^2	ft	m	R
741	225.86	125.1	38.1	1309	122	6	1.83	10.4636
740	225.55	119.8	36.5	1199	111	5	1.52	10.0083
739	225.25	114.2	34.8	1091	101	4	1.22	9.5534
738	224.95	107.4	32.7	988	92	3	0.92	9.1993
737	224.64	103.1	31.4	892	83	2	0.61	8.6518
736	224.34	97.7	29.8	801	74	1	0.31	8.1986
735	224.03	92.2	28.1	714	66	0	0	7.7440

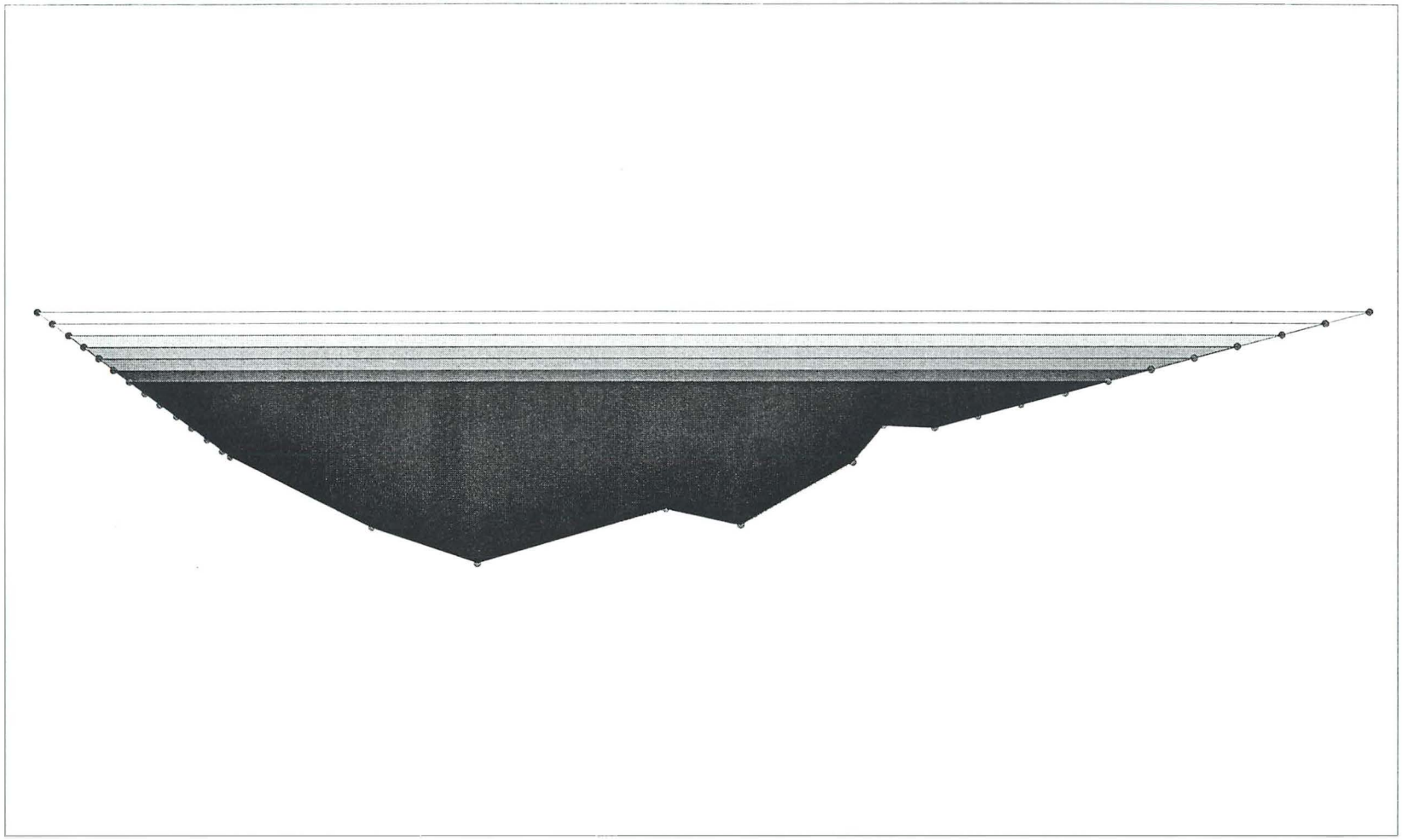


Figure B.7. Cross -sectional area changes with increasing stage, upper Poplar Creek at SG-282.

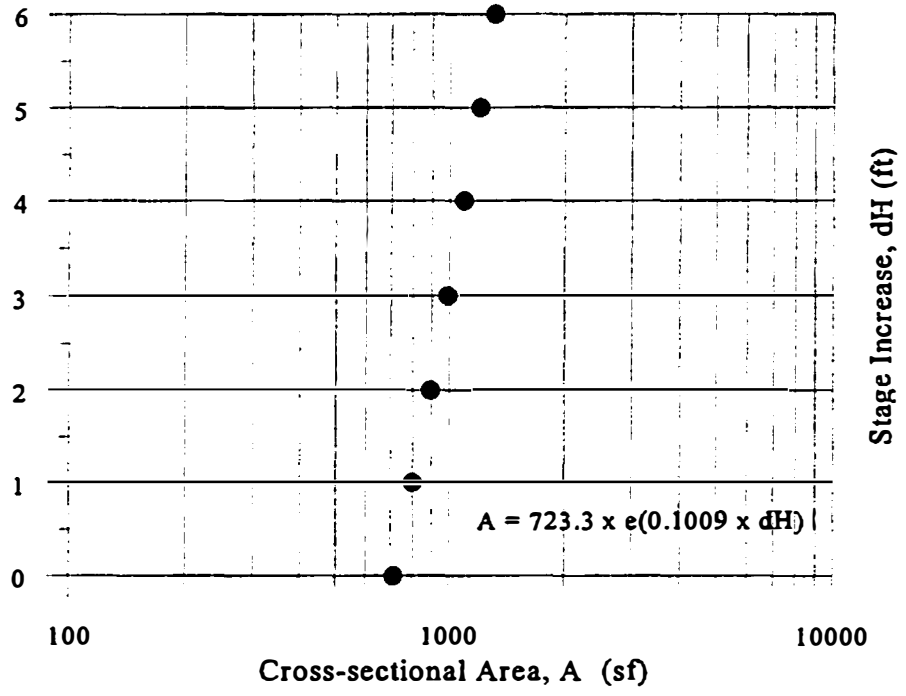


Figure B.8. Rating curve: Area (A) as a function of stage, Poplar Creek at SG-282

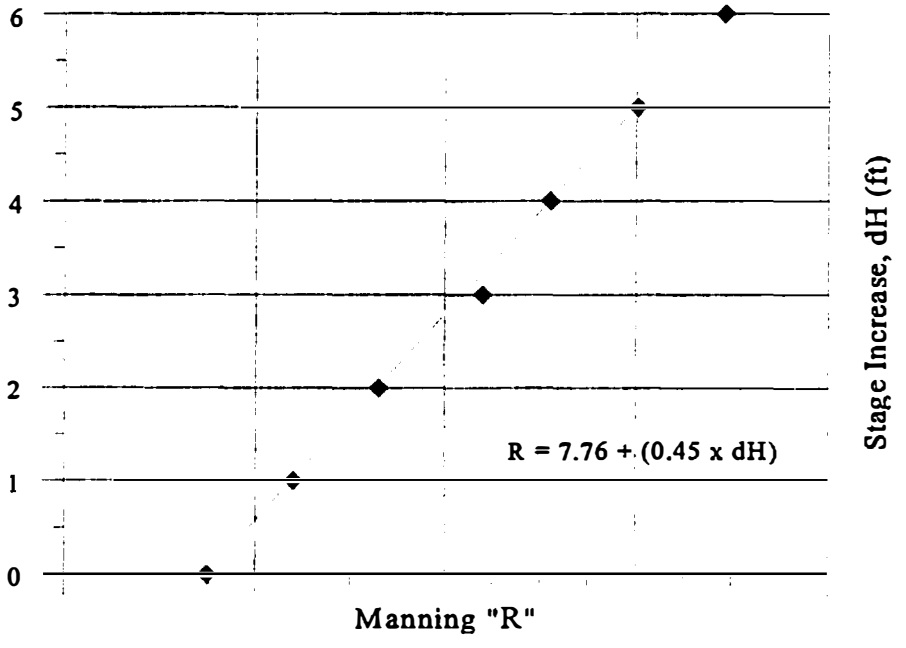


Figure B.9. Rating curve: "R" as a function of stage (dH), Poplar Creek at SG-282.

Table B.4 Summary of rating functions for A and R as a function of stage (dH).

Location	Cross-sectional Area (A)	Hydraulic Radius (A/WP)	Conditions
Clinch River @ SG-288	$A = 6514.21 + (323.6 \times dH)$	$R = 20.16 + (0.62 \times dH)$	-
		$R = 4.531 + (0.66 \times dH)$	dH</= 3 ft
Poplar Creek @ SG-287	$A = 915 \times e^{(0.1606 \times dH)}$	$R = 5.82 + (0.23 \times dH)$	3 < dH < 5 ft
		$R = 4.50 + (0.49 \times dH)$	dH > 5 ft
Poplar Creek @ SG-282	$A = 723.3 \times e^{(0.1009 \times dH)}$	$R = 7.76 + (0.45 \times dH)$	-

Note: dH (ft) = (stage elevation in feet - 735)

Table B.5. Summary statistics for Clinch River and Poplar Creek flows during the field effort, 1/1/96 - 4/1/96.

	Discharge (Q)							
	Minimum		Maximum		Median		Mean	
Location	m^3/sec	cfs	m^3/sec	cfs	m^3/sec	cfs	m^3/sec	cfs
Clinch River below confluence with Poplar Creek (@ SG-288)	-435	-15,361	474	16,714	200	7,045	196	6,933
Poplar Creek near mouth (@ SG-287)	-67	-2,366	92	3,251	21	729	27	952
upper Poplar Creek below confluence with East Fork Poplar Creek (@ SG-282)	-64	-2,258	53	1,864	12	405	13	449
Melton Hill Dam[1]	0	0	596	21,033	263	9,270	228	8,063
Watts Bar Dam[1]	0	0	1,287	45,455	1,211	42,764	1,037	36,615

NOTE: Negative values (e.g., -435) pertain to upstream backflow conditions while positive values represent normal downstream flow conditions.

1 - Based upon hourly discharge data provided by TVA.

VITA

Thomas Zondlo, a native of New Jersey, graduated with a Bachelor of Science degree (geology) from Rutgers University in 1978. After a brief period as a graduate student at the University of Tennessee in 1979, he entered the workforce and has been employed as a professional geologist for the past 20 years, involved in petroleum exploration and hydrogeologic/environmental consulting. In 1993 he re-entered the graduate program at the University of Tennessee as a part-time student seeking a Masters of Science degree in geology (hydrology focus) while employed full time as a research staff hydrogeologist at the Oak Ridge National Laboratory in Oak Ridge, Tennessee. The Masters degree was received in June, 1998. He is still serving on the research staff of the Environmental Sciences Division at Oak Ridge National Laboratory where he is engaged in applied hydrogeologic research in support of the environmental restoration efforts at the Department of Energy Oak Ridge Reservation facilities. Principal research interests include aqueous geochemistry, karst hydrology, and groundwater-surface water interactions.